Exploring functional mechanisms underlying tumor initiation, EMT and cell migration

Inauguraldissertation

zur
Erlangung der Würde eines Doktors der Philosophie
vorgelegt der
Philosophisch-Naturwissenschaftlichen Fakultät
der Universität Basel

von

Dorothea Cornelia Gruber

aus Gießen, Deutschland

Basel, 2012

Originaldokument gespeichert auf dem Dokumentenserver der Universität Basel
edoc.unibas.ch

Dieses Werk ist unter dem Vertrag „Creative Commons Namensnennung-Keine kommerzielle Nutzung-Keine Bearbeitung 2.5 Schweiz“ lizenziert. Die vollständige Lizenz kann unter
creativecommons.org/licences/by-nc-nd/2.5/ch
eingesehen werden.

Namensnennung-Keine kommerzielle Nutzung-Keine Bearbeitung 2.5 Schweiz

Sie dürfen:

das Werk vervielfältigen, verbreiten und öffentlich zugänglich machen

Zu den folgenden Bedingungen:

Namensnennung. Sie müssen den Namen des Autors/Rechteinhabers in der von ihm festgelegten Weise nennen (wodurch aber nicht der Eindruck entstehen darf, Sie oder die Nutzung des Werkes durch Sie würden entlohnt).

Keine kommerzielle Nutzung. Dieses Werk darf nicht für kommerzielle Zwecke verwendet werden.

Keine Bearbeitung. Dieses Werk darf nicht bearbeitet oder in anderer Weise verändert werden.

- Im Falle einer Verbreitung müssen Sie anderen die Lizenzbedingungen, unter welche dieses Werk fällt, mitteilen. Am Einfachsten ist es, einen Link auf diese Seite einzubinden.

- Jede der vorgenannten Bedingungen kann aufgehoben werden, sofern Sie die Einwilligung des Rechteinhabers dazu erhalten.
- Diese Lizenz lässt die Urheberpersönlichkeitsrechte unberührt.

Die gesetzlichen Schranken des Urheberrechts bleiben hiervon unberührt.

Die Commons Deed ist eine Zusammenfassung des Lizenzvertrags in allgemeinverständlicher Sprache: http://creativecommons.org/licenses/by-nc-nd/2.5/ch/legalcode.de

Haftungsausschluss:
Die Commons Deed ist kein Lizenzvertrag. Sie ist lediglich ein Referenztext, der den zugrundeliegenden Lizenzvertrag übersichtlich und in allgemeinverständlicher Sprache wiedergibt. Die Deed selbst entfaltet keine juristische Wirkung und erscheint im eigentlichen Lizenzvertrag nicht. Creative Commons ist keine Rechtsanwaltsgesellschaft und leistet keine Rechtsberatung. Die Weitergabe und Verlinkung des Commons Deeds führt zu keinem Mandatsverhältnis.

Quelle: http://creativecommons.org/licenses/by-nc-nd/2.5/ch/ Datum: 3.4.2009

Genehmigt von der Philosophisch-Naturwissenschaftlichen Fakultät
auf Antrag von

Prof. Dr. Gerhard Christofori
Prof. Dr. Markus Affolter

Basel, den 18. September 2012

Prof. Dr. Jörg Schibler
Dekan

Summary

Cancer is one of the leading causes of death. A primary tumor forms when cells start to proliferate in an uncontrolled way and stop reacting to restraining signals. Tumors that reach a critical volume induce angiogenesis, a vascular remodeling process that provides nutrients and oxygen to the degenerated cell mass. Upon further tumor progression to a malignant cancer, cells acquire the ability to invade the surrounding tissue. In order to do so, formerly epithelial tumor cells undergo an epithelial to mesenchymal transition (EMT). This process of cell-cell detachment, breaching through the basement membrane and gaining migratory capabilities is the first step of the metastatic cascade. Metastasis is a process that allows tumor cells to leave the primary lesion and disseminate via the vascular system to secondary sites. Metastases, as the fatal feature of cancer, lead in most of the cases to patients' death.

Furthermore, metastasis, as the end stage of malignant disease, until now is incurable. This is due to the fact that metastases are spread systemically throughout the body and are often multifocal. Moreover, they even can establish from a disseminated tumor cell months after the primary tumor has already been surgically removed. Another barely controllable feature of cancer is tumor relapse. Even after a thorough surgery with the aim to completely remove the primary tumor and eventual draining lymph nodes combined with chemotherapy, patients relapse redeveloping cancerous lesions. Resistance to chemotherapy and establishment of metastases has both been accounted for to the abundance of cancer stem cells (CSC) within the tumor mass. These CSCs are endowed with the ability to evade chemotherapeutic drugs, they are mesenchymal in nature, migratory and invasive, and, most importantly, they are able to establish cancer and metastasis *de novo*.

The work of my thesis has been dedicated to investigate the process of metastasis and the function of cancer initiation. Tumor initiation has recently been associated with EMT. To understand the functional circumstances how EMT cells gain the ability to form tumors, I used cellular murine breast cancer models. These model systems allowed me to study cells' behavior before and after EMT *in vitro* and *in vivo*. *In vitro* experiments validated the observation of others that EMT cells indeed resemble cancer stem cells by being able to form hollow spheres and being susceptible to the CSC-specific drug salinomycin. *In vivo* studies revealed that EMT cells initiate tumors with a much earlier onset and with a higher efficiency when limited amounts of cells were injected orthotopically into mice compared to their epithelial counterpart. Moreover, EMT cell-generated cancers are highly vascularized already in the early phase of tumor establishment. Knockdown studies of the main pro-angiogenic factor VEGF-A revealed that it is required for early tumor onset. Thus, tumor angiogenesis is not only an effect of early and fast EMT-tumor progression. Further supporting this notion are limiting dilution experiments, which suggest that tumor initiation in EMT cells is a multifactorial event. This concept was validated by the observation that 10 EMT cells could initiate a tumor, whereas VEGF-A knockdown cells could not. Hence, EMT-induced tumor initiation is achieved by the ability of promoting angiogenesis.

EMT can be induced by the cytokine TGFβ. Normally, cells that experience TGFβ signaling become quiescent or die due to induction of apoptosis. Cancer cells can overcome these effects and react to TGFβ by undergoing EMT. As part of my thesis, I could show that the transcription factor Dlx2 is an important switch that allows cells to react to TGFβ by undergoing EMT without facing apoptosis induction. Dlx2 exerts its anti-apoptotic, pro-survival function by directly reducing TGFβRI expression and inducing the expression of the epidermal growth factor receptor ligand betacellulin.

Another feature of EMT is the gain of cell motility. Cell migration is extremely important for cancer cells in order to leave their primary site and to disseminate. I have found ephrinB2 expression upregulated during EMT. EphrinB2 is a member of the Eph-ephrin signaling network that is known to be crucial for cell-cell communication. Thereby, cells that do not belong to the same entity repulse each other, restricting intermingling of tissue. Furthermore, ephrinB2 is required for neuronal axon guidance and angiogenesis. In my thesis, I showed that EMT cells need ephrinB2 to efficiently migrate. As an explanation for this phenotype I described that a knockdown for ephrinB2 led to an over-stabilization of focal adhesions. Cells normally use focal adhesions to hold on to an extracellular matrix (ECM) surface. Over-stabilization of focal adhesions attaches cells too firmly to the ECM and, hence, cells cannot retract their rear-end anymore which decreases cell motility.

In summary, I succeeded in gathering further insights into tumor initiation, EMT, and with this, the metastatic process.

Table of contents

Summary

Table of contents

1 General Introduction 1

1.1 Cancer 1

1.1.1 Hallmarks of cancer 2

1.2 Breast cancer 6

1.2.1 Classical and immunopathological classification of breast cancer 7

1.2.2 Molecular classification of breast cancer 7

1.2.3 Mouse models of breast cancer 9

1.3 Tumor angiogenesis 9

1.3.1 The mechanism of angiogenesis 10

1.3.2 Anti-angiogenic therapy 12

1.3.3 Clinical data 13

1.4 Epithelial to Mesenchymal Transition 14

1.4.1 The three types of EMT 14

1.4.2 Breakdown of cell-cell junctions 15

1.4.3 Cytoskeleton rearrangement 16

1.4.4 Invasion by basement membrane degradation 17

1.4.5 Gain of motility 17

1.4.6 Resistance to apoptosis 18

1.4.7 EMT inducing signals 19

1.5 Metastasis 20

1.5.1 The linear versus the parallel progression model 20

1.5.2 The invasion-metastasis cascade 20

1.6 Cancer stem cells 23

1.6.1 The concept of cancer stem cells 24

1.6.2 The origin of cancer stem cells 25

1.6.3 The stromal progression model 26

1.6.4 Cancer stem cells and EMT 26

2 Aim of the study 29

3 Results 31

3.1 VEGF-mediated angiogenesis links EMT-induced cancer stemness to tumor initiation 31

3.1.1 Abstract 32

3.1.2 Results 32

3.1.3 Discussion 41

3.1.4 Material & Methods 42

3.1.5 Supplementary data 44

3.1.6 Supplementary Methods 52

3.2 The functional role of ephrinB2 in mesenchymal cell migration 57

3.2.1 Abstract 57

3.2.2 Introduction 57

3.2.3 Results 63

3.2.4 Discussion 77

3.2.5 Material and Methods 79

3.3 The two faces of TGFβ: tumor suppressor and metastasis promoter 87

3.3.1 The modes of action of TGFβ signaling 87

3.3.2 The main outcome of TGFβ signaling 90

3.3.3 What goes wrong with TGFβ signaling in cancer 94

3.3.4 From tumor suppressor to tumor promoter 95

3.3.5 How to use the knowledge about TGFβ for cancer therapy 103

3.3.6 Conclusive remarks 104

3.4 Transcription factor Dlx2 protects from TGFβ-induced cell-cycle arrest and apoptosis 105

4 General conclusions and outlook 123

5 References 125

6 Curriculum Vitae 139

7 Acknowledgements 141

1 General Introduction

1.1 Cancer

The term cancer summarizes a large group of diseases with common features but different origins, locations, behaviors and outcomes. A tumor is defined by a cell mass that proliferates uncontrolled and its associated microenvironment. When a tumor becomes malignant by leaving the tissue it originated from, it is called cancer. These cancer cells invade the surrounding tissue and leave their primary site via blood or lymphatic vessels to initiate a tumor at secondary site, i.e. metastasis. Metastatic spread is in most cases the fatal event of the disease. While the best cure of a tumor is surgery, predominantly metastases are often not removable due to their multiplicity and their hiding nature. The most recent therapeutic strategy, in addition to removal of the primary tumors, is systemic treatment by targeted therapy and by chemotherapy that is meant to hit the residual cancer cells and more importantly the ones that already have left the primary site.

Cancer, starting with an uncontrolled proliferation of cells, can occur in every tissue. Mostly, tumors arise from epithelial cells forming carcinoma when progressing to invasive forms. Cancer can originate from other tissues than epithelium: melanomas from melanocytes, sarcomas from supporting tissues like bone, muscle and vessels, leukemias from the blood, lymphomas from lymph glands and gliomas from nerve tissue. Summing up all cancers worldwide, the World Health Organization (WHO) reported 7.6 million deaths of cancer in the year 2008, which makes cancer the leading cause of death (13 % of all deaths). Furthermore, the WHO states that an avoidance of the key risk factors like tobacco use, obesity, unhealthy diet, lack of physical activity, alcohol abuse, pollution, UV-exposure and viral infections, together with an early diagnosis of cancer could reduce cancer deaths worldwide by 30 %. Directly linking tobacco use being a high risk factor is the notion that lung cancer is the leading cause of cancer deaths (1.77 million), followed by stomach (736,000), liver (695,000), colorectal (608,000), breast (458,000) and cervical cancer (275,000) (*1*).

While avoiding certain types of cancer risk factors like smoking can be achieved relatively easily, early recognition is not. Early lesions and often even big and far progressed ones are mostly not hurting or disturbing patients, which often leads to late diagnosis of the disease. To counteract this fatal feature of cancer, screening methods are of high relevance to eradicate a tumor early and to avoid spreading of malignant cells. Additionally, research is constantly trying to understand cancer better with its different forms and stages in order to improve treatments.

1.1.1 Hallmarks of cancer

Leaders in the cancer biology field, Hanahan and Weinberg, describe in a review the hallmarks of cancer, features every cancer has to fulfill in order to be able to establish, progress and metastasize (*2*). These hallmarks will be summarized briefly in the following section.

Sustained proliferative signaling and evading growth suppressors

A tumor starts to evolve by an uncontrolled growth of abnormal, mutated cells that go through the cell cycle and proliferate, even though no further cells have to be generated for the normal homeostasis of the organ. Normally, cells are under the tight control of growth promoting and growth restricting signals only allowing them to enter the cell cycle when there is a need for increased cell numbers or cell turnover. Cancer cells uncouple these normally well-dosed growth stimuli mostly by mutations of so-called oncogenes or tumor suppressor genes, which leads to hyperproliferate.

In most cases sustained proliferation is achieved by gain of function mutations of the key mitotic pathways, e.g. B-Raf mutations are found in about 40 % of melanomas driving the mitogen-activated protein (MAP)-kinase pathway. In many tumors the protein kinase B (PKB) effector is artificially kept active by mutations of the catalytic subunit of the phosphoinositide 3-kinase (PI3K). Also upstream receptors of mitogenic stimuli can be overexpressed or activated in an uncontrolled manner making the receptors either more responsive to growth stimuli or even dispensable. Growth factors themselves can be overproduced stimulating the cancer cell not only in an autocrine loop but also acting on neighboring cells in a paracrine manner.

But even mitogenic signals can be too excessive forcing cells into senescence by so-called oncogenic stress. Cells avoid this stress by uncoupling oncoproteins from their senescence activity or counteract the mitotic proteins up to a certain point.

Cancer cells fueling themselves with mitogenic stimuli are not enough to sustain proliferation. Factors that inhibit mitogenic signals or their transduction have to be mutated or downregulated as well. Upon these, the tumor suppressor *PTEN* is one of the most famous silenced genes. PTEN's missing direct counteraction of PI3K leads to a mitotic brake loosening. Two other proto-typical tumor suppressor genes opposing directly the cell cycle entry and progression and being often found mutated are *TP53* and the retinoblastoma-associated (*RB*). Whereas Rb integrates signals mostly from outside the cell and halts the cells before entering the cell cycle, p53 senses stresses and damages form inside the cells not only inducing cell cycle inhibitory proteins but also being able to force cells into apoptosis. As exemplified, cells have various ways to control cell proliferation.

Resisting cell death

Every cell is able to commit suicide by programmed cell death, the so-called apoptosis. Apoptosis is a tool of multi-cellular organisms to balance cell numbers and to eradicate old or damaged cells in a physiological way. The integrity of the whole organ or organism is favored over the fate of an individual cell. In cancer this principle is lost. As mentioned above, aberrant cell stress like DNA damage leads to an induction of cell death in normal cells. Again, p53, the main player to sense unbearable DNA abnormalities and to force apoptosis, is mutated or inhibited in a lot of tumors, which allows cancer cells to survive. But also other proteins either pro- or anti-apoptotic are found changed in cancers making cells resistant or less sensitive to cell death. Further upstream, survival signals, very much like proliferation signals, help cells to tip the balance more to the survival side than to the apoptotic one. Transforming growth factor beta (TGFβ) is one example of a protein influencing both apoptosis and survival and is rendered to the more survival activity site in cancer. More details on how TGFβ function changes during cancer progression will be discussed below (3.3).

Enabling replicative immortality

Cells have an intrinsic cell-division counter, the telomeres. Telomeres are DNA repeats on each chromosome that are shortened with every replication cycle. After a certain amount of DNA duplications the telomeres become too short and cells go into replicative senescence or even apoptosis. This phenomenon can be observed when primary cells are taken into culture. After limited passages, cells first go into senescence and then into crisis. Only few cells overcome this crisis and become immortalized mostly by activating the telomere-prolonging enzyme telomerase. A similar way of infinite proliferation is believed to be gained by cancer cells. However, neoplasms with critically shortened telomeres have been observed in patients. Here chromosomal endjoinings of theses short telomeres of different chromosomes have occurred without an induction of senescence or apoptosis. In this case, where possibly p53-sensed chromosomal damage could not be translated into apoptosis, oncogenic chromosomal translocation of the genome could even favor further malignant mutations. A later reacquisition of telomerase activity would then stabilize the corrupted genome and thereby the cancer cell.

Inducing angiogenesis

Every tissue needs to be supplied with oxygen, nutrients and the possibility to evacuate metabolic waste and carbon dioxide in order to survive. This need is especially high in proliferating, energy consuming cells like tumor cells. The mechanism of tumor angiogenesis and its possible relevance in tumor initiation will be further discussed in the introductory section 'tumor angiogenesis' (1.3) and the results part 'VEGF-mediated angiogenesis links EMT-induced cancer stemness to tumor initiation' (3.1).

Activating invasion and metastasis

As mentioned above, dissemination of tumor cells and colonization at secondary sites can rarely be cured. Cancer cells gain the ability to detach themselves from the epithelial network and invade as single cells or in sheets the surrounding tissue. This process has to be accompanied by resistance to apoptosis and the capability to actively migrate. The epithelial to mesenchymal transition orchestrates all these features of single cell invasion that allows cancer cells not only to invade but also to intravasate into blood or lymphatic vessels. EMT will be described in more detail below (1.4).

In order to metastasize it is not enough to invade and intravasate. The survival in the foreign surroundings (blood stream and secondary site) and the capacity to establish a new tumor are challenging tasks for cancer cells. The reverse process of EMT, the mesenchymal to epithelial transition (MET), is favoring the latter. It has become clear that cancer cells alone are not able to achieve all the metastatic process in an autonomous way but need the stromal compartment in the primary and secondary site as well. Fortunately, the metastatic process is full of obstacles making it a rare event. The metastatic process will be discussed in more detail below (1.5).

Enabling hallmarks: Genome instability and mutation and tumor-promoting inflammation

Genomic instability is a feature of a lot of cancer cells. In normal cells DNA damages activate repair mechanisms and if too dramatic they lead to cell senescence or death (already mentioned in the example of telomeres). Cancer cells seem to acquire resistance to genomic guardian molecules like p53 and thereby tolerate genomic changes. Genomic instability can lead to oncogenic translocations like *BCR-ABL* or *AML1-ETO* and to loss of function mutations of tumor suppressor genes *(3,4*). Rendering the genome more instable by inactivating maintenance molecules gives tumor cells the opportunity to adapt and evolve to their needs faster.

An inflammatory surrounding can cause malignancy. This notion depicts already that factors released by immune cells can not only supply cancer cells with growth factors but also generate malignant cancer cells to begin with. The interaction with inflammatory cells and cancer cells can be visualized in highly infiltrated cancers. Nowadays, the supportive action of the immune system to cancer is well established, although cancer cells can also be recognized and attacked by the immune system.

Emerging hallmarks: Evading immune destruction and reprogramming energy metabolism

As mentioned above, cancer cells can be detected by the immune system as degenerated and with this to be cleared from the body. This line of defense against cancer is particularly effective in virus-induced cancer types. To evade the destruction by an anti-tumoral immune response cancer cells are selected for being as least immunogenic as possible or being able to suppress an immune reaction, for instance by TGFβ secretion. If a tumor can escape immune surveillance the cancer cells can use inflammatory cells and their cytokines for their profit.

Reflecting the unstable supply of oxygen to tumor cells due to chaotic angiogenesis and uncontrolled proliferation of cells, the metabolism of cancer cells changes. It has been described that most cancer cells switch to the rather inefficient aerobic glycolysis, a phenomenon called the Warburg effect. To gain enough energy, mainly relying on glucose as an energy donor, cancer cells upregulate the expression of e.g. glucose transporters. The switch of cancer cells to aerobic glycolysis as the main metabolic pathway has been described repeatedly but the exact reason for this phenomenon still remains elusive.

1.2 Breast cancer

The breast is a gland comprised of different cell types. Mammary stem cells (MaSC) give rise to different mammary epithelial cells thereby originating the mammary gland. MaSCs differentiate via committed progenitor states into myoepithelial cells and into luminal cells that can be further subdivided into ductal and alveolar luminal epithelial cells. Apart from the importance of MaSCs during the development of the mammary gland, MaSCs also maintain the tissue homeostasis. Upon other cells, adipocytes, ECM, fibroblasts, immune cells and vasculature surround the epithelial glandular structure (Fig. 1). Since the breast is an organ that is under constant change during a female lifetime due to huge hormonal alteration (i.e. puberty, pregnancy, nursing and weaning), MaSCs have to rebuilt mammary epithelium very often. The intrinsic ability of mammary cells to invade the mammary fat tissue, to remodel and reconstruct constantly the mammary gland structure makes the breast epithelium particularly prone to cancerous events (*5*).

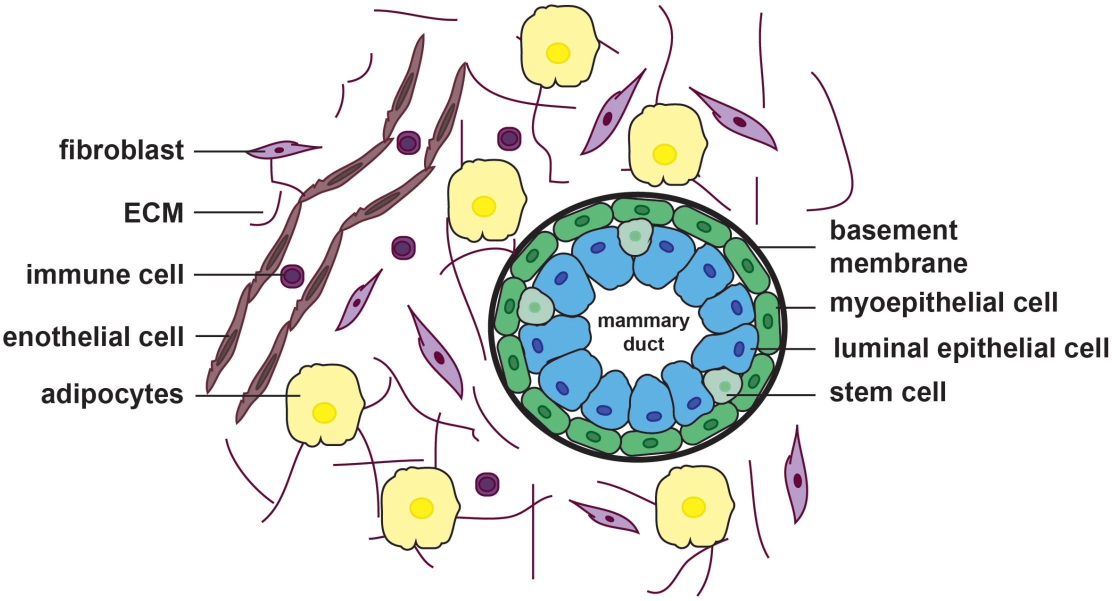

Figure 1: Schematic depiction of a mammary duct.
Mammary ducts are comprised of the different indicated epithelial cells that are surrounded by a basement membrane. Around the glandular structures extracellular matrix and stromal cells are resident.

The WHO declares breast cancer the most common cancer in the female population *(1)*. But as pointed out before also breast cancer is a heterogeneous disease and has to be identified and treated accordingly.

1.2.1 Classical and immunopathological classification of breast cancer

Breast cancer can be classified with different methods. The two most common classical pathology categories are based on morphology and structural organization. They are invasive ductal carcinoma, not otherwise specified (IDC NOS) with about 75 % and invasive lobular carcinoma (ILC) with about 10 % of cases of all breast cancers. The residual categories are comprised of types like metaplastic, neuroendocrine, medullary, tubular breast cancer and many others. While structural classifications are subdividing the different breast cancer kinds, more important for an adequate treatment are immunopathological classifications that use the main markers: estrogen receptor (ER), progesterone receptor (PR) and human epidermal receptor 2 (HER2). For clinicians the ER-status is of great relevance since ER-positive patients can be treated with anti-estrogen therapy although breast cancer that exceeds only 1 % ER-positive cells is referred to as ER-positive already. HER2-positive breast cancer can be treated with targeted therapy, a monoclonal antibody against HER2 (trastuzumab). Not surprisingly, $ER^+/HER2^-$ tumors have the best prognosis due to effective treatment against ER-signaling. With the targeted therapy against HER2-positive tumors those cancers have an intermediate prognosis, which is true for triple-positive ($ER^+PR^+HER2^+$) as well as for HER^+/ER^- breast cancer types. The worst prognosis has a triple-negative tumor ($ER^-/PR^-/HER2^-$) where none of the above-mentioned therapies can be applied. Extensive research to find treatments also for this type of breast cancer is ongoing (*6*).

1.2.2 Molecular classification of breast cancer

Another way to categorize breast cancer is by gene expression profiling (*7*). So far, six major molecular subtypes could be determined by gene expression profiling: luminal A, luminal B, basal-like, claudin-low, HER2-overexpressing and normal-breast-like (*8*). The titles of the subtypes already indicate that they are named after the normal breast cells they resemble and might have originated from. Among the luminal subtype, which is the most common type of invasive ductal and invasive lobular carcinomas, HER2 overexpression is associated with poor overall survival. The luminal A and B subtypes express the estrogen receptor and have a good prognosis. The basal-like subtype of breast cancer is the most aggressive one and shows high intratumoral heterogeneity. Indicative for a basal-like subtype is the lack of expressing hormone receptors (ER and PR) and HER2. The claudin-low subtype of breast cancer is triple-negative as well but in addition is alike normal stem cells in gene expression profile and is enriched for cancer stem cells. Furthermore, the claudin-low subtyped cancer cells rather have a mesenchymal morphology and they resemble EMT cells in shape and gene expression. The normal-breast-like subtype is similar to the normal gland and usually has a good prognosis (*5,6)*.

It is widely believed that the various subtypes of breast cancer have originated by transformation from their cognate cell type named after. But there is also the possibility that transformed mammary stem cells can transform and give rise to more differentiated breast cancer subtypes. One could further speculate that cells from the triple-negative basal-like breast cancer subtype or others could have undergone an EMT after transformation to become cancer stem cell-like. Notably, a generation of cancer stem cell-like cells by induction of EMT in normal cancer cells was reported (*9*). This matter will be further discussed in the cancer stem cell section 1.6.4.

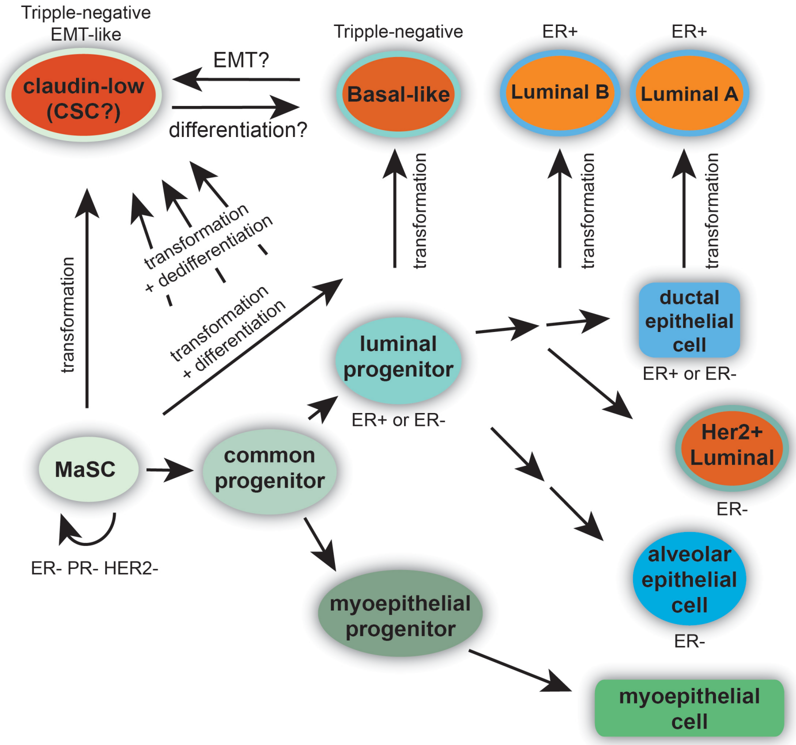
Tripple-negative
EMT-like
claudin-low
(CSC?)
EMT?
differentiation?
Tripple-negative
Basal-like
ER+
Luminal B
ER+
Luminal A
transformation
transformation
transformation
transformation
transformation
+ dedifferentiation
transformation
+ differentiation
luminal
progenitor
ER+ or ER-
ductal
epithelial
cell
ER+ or ER-
Her2+
Luminal
ER-
MaSC
common
progenitor
ER- PR- HER2-
myoepithelial
progenitor
alveolar
epithelial
cell
ER-
myoepithelial
cell

Figure 2: Hierarchy of a normal breast and their according molecular breast cancer subtypes. Mammary stem cells (MaSC) are capable to self-renew and to differentiate along the arrow to the right into progenitor and differentiated cells that compose the mammary ducts and alveoli. The according subtypes of breast cancer either arise by transformation from the depicted epithelial cells or directly from the MaSC or its transformed equivalent, the cancer stem cell (CSC) by partial differentiation. The opposite could be true for the

CSC that either arises from a transformed MaSC or from a more differentiated cancer subtype by undergoing EMT.
Additional to the molecular subtypes the predominant immunopathological classifications by ER, PR and HER2 status are indicated as an attempt to combine both classification parameters.

1.2.3 Mouse models of breast cancer

Although the human mammary gland has some morphological differences to the mouse mammary gland, the development of both tissues underlies the same hierarchy. Many studies in mouse models to mimic breast cancer have helped to understand the human disease better. To study the progression of breast cancer and the molecules playing a role in it, a big cohort of transgenic mice has been generated. One of the most used promoters to study genes specifically in the breast is the mouse mammary tumor virus LTR promoter (MMTV). The MMTV-Neu model, where the rat homolog of activated Neu/ErbB2/HER2 protein is expressed specifically in the mammary gland, reflects about 20 % of human breast cancers with *ERBB2* gene amplifications. These mice develop multifocal adenocarcinoma accompanied with lung metastasis (*10*). Another breast cancer mouse model, used later in this thesis, is the expression of polyoma-middle-T antigen (PyMT) under the control of the MMTV promoter (MMTV-PyMT). PyMT mainly transforms cells by activating Src, PI3K and protein kinase C. These mice develop multifocal mammary adenocarcinomas with lymph node and lung metastases after short latency (*11*). The resemblance of this breast cancer model to human breast cancer can be exemplified by the gradual loss of the estrogen and progesterone receptor as well as by an overexpression of ErbB2 in late-stage metastatic cancer (*10*).

Transplantation of tumor cells into the mammary fat pad (comprised of fibroblasts, adipocytes, endothelial cells and macrophages) is an easy tool to study cancer in an orthotopic site (*10*).

1.3 Tumor angiogenesis

In order to be supplied with nutrients and oxygen cells have to be in the proximity of blood vessels. In cancer where cells proliferate uncontrolled forming a bigger and bigger cell mass, the use of existing vessels is not sufficient anymore and the diffusion range to blood vessels becomes a limiting factor for cancer cell survival. Therefore, big tumor parts that are too distant from blood supply either die, forming necrotic regions, or adapt their microenvironment by inducing angiogenesis. The latter way of action is called the angiogenic switch (*12-14*).

1.3.1 The mechanism of angiogenesis

Angiogenesis is a process in which pre-existing endothelial cells are reacting to signals that turn them into active endothelial cells that will originate new vasculatures. The most prominent way of angiogenesis is the sprouting of vessels. Active endothelial cells remodel vessels by first loosening cell-cell adhesions to neighboring cells. The endothelial cell at the sprouting point of the vessel, the tip cell, starts migrating following a gradient of pro-angiogenic signals. The endothelial cells adjacent to the tip cell, the stalk cells, divide to elongate the stalk of the sprouting vessel. Finally, the newly formed tube is stabilized by the recruitment of perivascular cells, pruned and matures to become fully remodeled and functional (*15*). This classical way of angiogenesis in which pre-existing vessels grow and remodel themselves, is supported by the presence of bone marrow-derived cells. These cells can trans-differentiate into endothelial cells thereby contributing to the structure of the vessel as well. This generation of new endothelial cells by precursor cells is called vasculogenesis in the adult. Even tumor cells were reported to be able to trans-differentiate into endothelial cells or imitate vascular structures, a phenomenon named vascular mimicry (*16*).

Tumor cells that are located too far away from vessels experience hypoxia. Thus, tumor cells react by stabilization of hypoxia-induced factor 1 alpha (HIF1α). HIF1α in turn, activates the expression of the main angiogenic factor, vascular endothelial growth factor (VEGF) (*17*). VEGF is secreted by tumor cells and reaches quiescent endothelial cells that express the corresponding VEGF receptor (VEGFR) and promptly react to the VEGF gradients with angiogenesis. Upon hypoxia together with the release of VEGF the production of other factors, including platelet-derived growth factor (PDGF), fibroblast growth factor (FGF), angiopoietins and stromal cell-derived factor 1 (SDF1) are stimulated. This cytokine cocktail additionally recruits myeloid cells to the tumor further releasing pro-angiogenic factors and stimuli. These factors help increasing angiogenesis and tumor cell invasion (*18*).

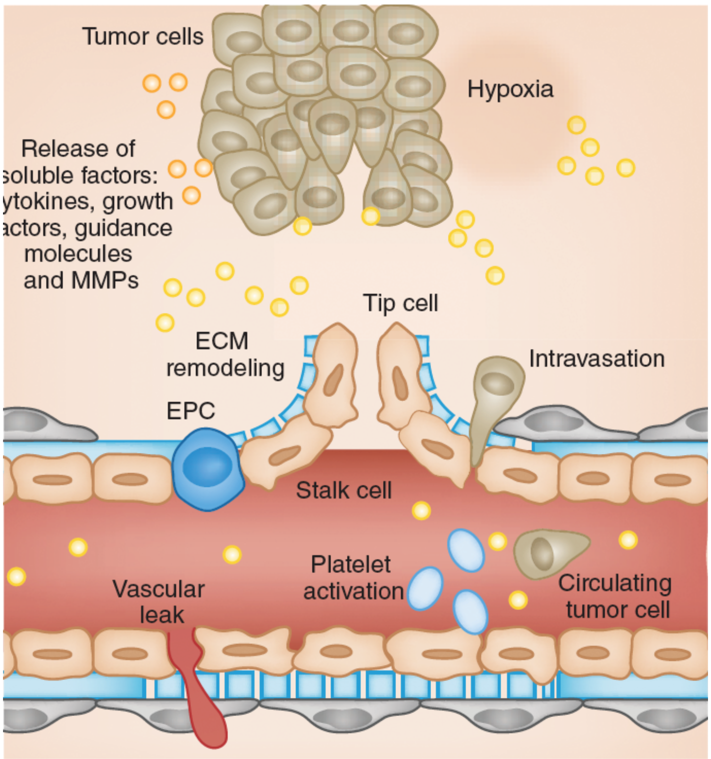
Tumor cells
Hypoxia
Release of
soluble factors:
ytokines, growth
actors, guidance
molecules
and MMPs
Tip cell
ECM
remodeling
Intravasation
EPC
Stalk cell
Platelet
activation
Vascular
leak
Circulating
tumor cell

Figure 3: Sprouting tumor angiogenesis.
Tumor cells that experience hypoxia secrete various angiogenic factors. These factors activate endothelial cells. The tip cell leads the sprouting vessel towards the hypoxic tumor whereas the neighboring stalk cells proliferate. Sprouting of an existing vessel is accompanied by pericyte detachment, ECM remodeling and platelet activation. Endothelial progenitor cells (EPC) can further contribute to the vessel formation. Due to the leakiness of tumor vessels, tumor cells can intravasate more easily and use the blood circulation to disseminate (*15*).

In more detail, when vessels sense angiogenic factors released by various sources (inflammatory or tumor cells), matrix metalloproteinases (MMP) are secreted and degrade the basement membrane shared by endothelial cells and pericytes. Pericytes detach from endothelial cells. Upon loosening of cell-cell junctions vessels dilate and become permeable to plasma proteins, which deposit an extracellular matrix bed suitable for vessel sprouting. This permeability increases by VEGF signaling. Further molecules of VEGF and FGF get released and made accessible by proteases from the ECM, further increasing the pool of angiogenic factors. In the tip cell, VEGF-A binds to VEGFR2 and to its Neuropilin co-receptors (Nrp) that in turn upregulate the Notch ligands Dll4 and Jag1. In this way, the tip cell senses guidance cues like ephrins and semaphorins with their filopodia that allows them to start to migrate directionally. On the other hand, stalk cells expressing the notch receptor, react to the exposed Dll4 on the tip cell. The Notch signaling leads to a downregulation of the main VEGF-A receptor, VEGFR2 and an upregulation of VEGFR1. By expressing mainly the VEGFR1 receptors and less VEGFR2, the stalk cell is less sensitive to VEGF but rather reacts to Wnt, PlGF and FGF signaling by proliferating and forming a prolonged tube behind the tip cell. In order to be fully matured after sprouting, the vessel needs to get covered by pericytes and new ECM has to be deposited (*19*).

1.3.2 Anti-angiogenic therapy

Angiogenesis is often not properly controlled and coordinated when tumors initiate it to get enough blood supply. An overproduction of VEGF and other angiogenic factors by tumor cells, cancer associated fibroblasts, immune cells and platelets leads to inefficient hyper-proliferation of endothelial cells. Without restricting signals that regulate for instance pruning, this unbalanced mixture of angiogenic factors gives rise to immature, leaky blood vessel resembling a wound rather than a proper vascularized tissue (*20*).

Angiogenesis could be an ideal drug target for anti-cancer therapy because blood supply is a limiting step in tumor development and also the highway for dissemination of tumor cells to distant organs (*21*). Additionally, the structure of tumor vessels is different compared to vessels in normal tissue. Tumor vessels are often chaotically branched, originating a tortuous blood flow and are leaky. This has advantages and disadvantages for a tumor. A disadvantage would be the inefficient perfusion due to immature vessels. A clear advantage instead would be the reduced accessibility to chemotherpeutics and the increased ability of disseminating cells to enter the blood stream.

One of the classical mouse models used to study angiogenic effectors and various anti-angiogenic treatments is the insulinoma model Rip1Tag2. In this model of multi-step carcinogenesis, the angiogenic switch from a pre-vascular hyperplasia to a highly vascularized and invasive tumor occurs in a defined manner (*22*). Extensive studies either overexpressing or knocking out different *VEGFs*, as well as treatments with inhibitors or interference with auxiliary factors like MMP9 gave a lot of insights on how tumor angiogenesis is modulated (*14*). For instance, blockage of VEGF-A signaling has led to a normalization of tumor blood vessels, not only with a reduction of vessel numbers but also the presence of less fenestrated and less sprouted vessels and a better coverage by pericytes. As a consequence, the tumor volume in treated mice decreased (*23*). Overall, VEGF-A and its bioavailability has been revealed to be the most important factor for tumor angiogenesis, however compensatory effects by FGF were shown (*14,24,25*).

1.3.3 Clinical data

The main task for cancer research it to translate results from experiments in animal models into clinical applications. VEGF signaling, being the most important pro-angiogenic factor, is used as a therapeutic target in cancer patients. However, anti-VEGF antibody therapy has been proven effective only in a limited number of cancer types. Initially, a study with untreated metastatic colorectal cancer patients showed an improved progression-free and overall survival when chemotherapy was supplemented with a humanized monoclonal anti-VEGF antibody (bevacizumab) (*26*). However, in an recent adjuvant therapy against stage II and III colon carcinoma bevacizumab combined with chemotherapy only shortly prolonged disease free-survival and did not show benefit after 3 years when compared to chemotherapy alone (*27*). As a consequence of these and other studies, bevacizumab treatment is only approved for metastatic colorectal cancer. In studies for metastatic breast cancer the addition of bevacizumab to paclitaxel (mitosis inhibitor, chemotherapeutic) as a first line therapy increased the progression free survival but had barely any effect on overall survival of patients (*28*). Nonetheless, bevacizumab is used for metastatic breast cancer in Europe, whereas the US Food and Drug Administration (FDA) has withdrawn its approval for this cancer type. These few examples already show that the type of cancer as well as the stage of the cancer has to be taken into account to predict whether bevacizumab treatment would be effective. Furthermore, the exact mode of treatment and the interpretation of clinical trials depending on the different endpoints defined have to be considered carefully to be able to draw a conclusion from a clinical trial (*29*). To date, bevacizumab has been approved by the FDA for the treatment of metastatic colorectal cancer and metastatic non-squamous non-small-cell lung cancer in association with chemotherapy. In recurrent glioblastoma multiforme bevacuzimab is used as a single therapy and in metastatic renal cell carcinoma in association with interferon-α (*19*).

Having observed resistance development against bevacizumab alone (*30*), multi-target receptor tyrosine kinase inhibitors like Sunitinib (blocking VEGFR, PDGFR) have been tested with the hypothesis that in this way both the endothelial cells and the pericytes would be attacked. As a result, the detachment of pericytes would render endothelial cells more sensitive to VEGF-A inhibition, because they lose their proximate VEGF-source (*20*). Sunitinib has proven to be a superior therapy for metastatic renal-cell carcinoma than interferon-α (*31*).

In conclusion, it turns out that a targeted therapy against angiogenesis in most cases is not as effective as hoped. Several questions about anti-angiogenic treatment remain to be solved: how do resistance mechanisms occur, which other factors apart from VEGF-A should be targeted and with which treatment schedule? Furthermore, the highly debated question whether anti-angiogenic therapy leads to more aggressive tumors has to be answered.

1.4 Epithelial to Mesenchymal Transition

An epithelial to mesenchymal transition (EMT) is a process in which epithelial cells lose their epithelial morphology and properties and gain mesenchymal, fibroblastoid ones. The process of EMT is characterized by high plasticity allowing cells to completely or partially change their cellular characteristics and even to reverse from the mesenchymal state back to the epithelial one (mesenchymal to epithelial transition, MET) (Fig. 4).

1.4.1 The three types of EMT

One can distinguish three kinds of EMT: the type I developmental EMT, type II wound healing/fibrotic EMT and type III oncogenic EMT. All different types of EMT follow very similar molecular changes and resemble each other on the cellular level. Major differences between these EMTs are of temporal nature and their functional outcome.

As the name already states, developmental EMT (type I) occurs during the development of an organism. One early example is when primitive epithelial cells change into mesenchymal cells in order to migrate to their designated place to form the primary mesenchyme. At the new site, these EMT cells can undergo the reverse process of EMT, i.e. MET, and form a new epithelium. This example can be observed during the developmental process of the kidney.

When an epithelium gets injured, cells at the edge of the wound undergo EMT (type II) in order to migrate into it, pulling the epithelial sheet behind to close the lesion. Constant wounding and associated inflammation of tissue can induce fibrosis.

Fibrosis is comprised of many fibroblasts and cells that had undergone EMT and stay in this state without complete repair of the tissue into a normal epithelium. Inflammation and fibrosis have been shown to be potent inducers of neoplastic lesions.

Oncogenic type III EMT is used by carcinoma cells to leave the tumor mass, break through the basement membrane, invade the surrounding tissue and ultimately seed metastasis. The resistance to anoikis, gain of motility and the breakdown of ECM are essential features of EMT allowing cells to disseminate. In most of the cases, carcinoma cells that have undergone EMT and have reached a secondary site undergo MET to establish metastases (*32*,*33*).

1.4.2 Breakdown of cell-cell junctions

An epithelial layer is composed of individual cells that are in tight contact to their basement membrane via integrins in hemidesmosomes and in close association to their neighboring cell via desmosomes, adherens (AJ) and tight junctions (TJ). These structures allow a high organization of an epithelium with a clear separation of basolateral and apical areas. An early sign of EMT is the resolution of these cell-cell junctions and with this the loss of epithelial polarity. As a component of adherens junctions E-cadherin is the most important epithelial marker. During the first steps of EMT, E-cadherin gets displaced from AJs, which initiates their collapse. Apart from the decrease of E-cadherin levels during EMT, also catenins and proteins of tight junctions, like ZO-1, occludins and claudins get displaced from AJs and TJs. (*34*). β-catenin, which is both a protein of the adherens junction complex and the effector of Wnt signaling is not only displaced from the cell membrane but is with this more abundant for Wnt signaling in the cytoplasm and nucleus. Nuclear β-catenin is one of the invasiveness markers in tumors since it modulates expression of potent mitogenic factors such as c-Myc and CyclinDs but also other migration and metastasis proteins like fibronectin, MMP-7 and S100A4, respectively (*35*).

E-cadherin is the main marker for epithelial cells and its downregulation seems to be crucial for EMT. It has been shown in various model systems that the sole repression of E-cadherin expression can trigger EMT. *In vivo*, the loss of E-cadherin could be observed in a panel of carcinomas where the loss of E-cadherin expression correlates with a bad prognosis. This notion is further underlined with the observation that forced sustained E-cadherin expression leads to more differentiated and less invasive carcinomas (*36,37*).

Not surprisingly, cells have many means by which E-cadherin expression can be modulated. Transcriptional repression of E-cadherin can either be accomplished by direct binding to its promoter by e.g. snail1, snail2, ZEB1, ZEB2, E47 and KLF8 or indirectly by e.g. twist, goosecoid and FoxC2. The different transcriptional repressors, although all regulating E-cadherin as their main target to induce EMT, distinguish from each other by modulating additional processes like cell polarity or survival as well. In diverse tissues and cancers, different E-cadherin repressors may be of importance (*38*). To sustain repression of E-cadherin expression its promoter can be hypermethylated or the gene (*CDH1*) can be lost or mutated, a phenomenon often found in human cancer. Additionally, E-cadherin can be modified post-translationally. A hyperactivation of tyrosine kinases like c-Met, Src or EGFR leads to phosphorylation of E-cadherin which results in its proteosomal degradation. But also cleavage of E-cadherin and a subsequent dislocation from adherens junction by e.g. MMPs, ADAMs or caspases has been reported (*39*).

While the loss of epithelial characteristics during EMT are reasonably well understood, the knowledge about the gain of expression of mesenchymal markers like N-cadherin, as well as the upregulation of extracellular matrix components and the intermediary filament vimentin is by far less profound (*40*).

1.4.3 Cytoskeleton rearrangement

Epithelial cells are motile but within the restriction to their epithelial layer. In contrast, mesenchymal cells can detach and move freely by different modes of migration. A very striking phenotypic difference between cells before and after an EMT are the aforementioned changes in cell shape and polarization. These changes in morphology go along with drastic cytoskeleton rearrangements. While epithelial cells have actin filaments organized cortically like a belt under the plasma membrane and express cytokeratins, mesenchymal cells have a fibroblastoid shape and exhibit highly dynamic actin cables within the cytoplasm (called stress fibers) and the intermediate filament vimentin (*34*).

1.4.4 Invasion by basement membrane degradation

Epithelial cells are separated from adjacent tissue by the basement membrane (BM). Without contact of epithelial cells to the BM, epithelial cells undergo anoikis (*41*). Furthermore, epithelial cells can only move laterally along the BM. The integrity of a BM, supported by ECM or other cells (like myoepithelial cells in the mammary gland) has been shown to be crucial to impede invasion (*42*). To overcome this border and to invade the neighboring tissue EMT cells secrete metalloproteinases (MMP). The upregulation and activation of MMPs in EMT cells does not only allow them to dissolve the BM to migrate though ECM but also unleashes ECM-bound growth factors making them bioavailable for cancer cells (*43*). Conversely, some MMPs have been shown to be able to induce EMT themselves (*38*).

1.4.5 Gain of motility

Whereas epithelial cells migrate only in 2 dimensions on the basement membrane, mesenchymal cell movement has to cope with the complexity of 3 dimensions. Migration through ECM instead of on ECM can be accomplished by different means. Neoplastic cells adopt already known migration mechanisms used by other cell types for example by fibroblasts or during morphogenesis.

Cells either migrate in a single cell mode or collectively. In the collective cell migration mode cell-cell junctions remain intact allowing a whole sheet, tube, strand or cluster of cells to move concertedly. The collective cell migration mode is predominantly found in squamous cell carcinomas where finger-like structures invade the surrounding tissue and even intravasate and disseminate as a cohort (*35*).

Single cell migration instead, can be further subdivided into a mesenchymal and an amoeboid version, both used by cancer cells. In the amoeboid cell migration mode the rapid movement of round cells is achieved by cytoplasmic streaming which allows squeezing through the ECM. In contrast, the mesenchymal cell migration mode is rather slow and uses in a highly coordinated way the ECM as strings to pull and slide on by attaching on it with focal adhesions. Adaptation or interchange between cell migration modes to upcoming obstacles or cues is possible (*44*).

Displacement of E-cadherin and thereby the adhesion junction’s disintegration initiates migration. p120-catenin, for instance, normally bound to the intracellular part of E-cadherin is released and thus can either bind N-cadherin or translocate to the cytoplasm where it indirectly activates the RhoGTPase family members Cdc42, Rac1 and represses RhoA. These GTPases are the key modulators of actin cytoskeleton remodeling and induce filopodia, lamellipodia and stress fiber formation, respectively (*35*).

Cells that have undergone EMT mostly use the proteolytic, mesenchymal cell migration mode. Here, a poorly polarized, sessile cell within extracellular matrix gets stimulated to move in a certain direction. Stimuli can be of various natures e.g. hypoxia or gradients of growth factors. The migration cycle begins with the formation of a protrusion at the leading edge, i.e. pseudopod. The pseudopod forms by actin polymerization and filament assembly in the direction of movement. Small filopodia within the pseudopod sense the micronenvironment. Focal contacts, integrin-rich structures connected to the actin cytoskeleton, attach the cell to the ECM substrate firmly, pulling and realigning ECM fibers. Cells use proteases to cleave ECM that is in the way of the cell soma. Having generated enough space to traverse the ECM, the cortical actin cytoskeleton helps the cell to push and branch confining ECM. To finally move the whole cell, actomyosin filaments contract and the rear end of the cell retracts. Due to the firmer attachment of adhesions in the leading edge than in the trailing one a cell moves directional. A new path is left behind allowing more cells to follow (*44*).

1.4.6 Resistance to apoptosis

As mentioned above, epithelial cells that lose contact to the basement membrane undergo anoikis (*41*). Since a hallmark of EMT is specifically to lose connection to the basement membrane, cells have to be able to resist anoikis. How this tolerance is achieved has not been completely understood, but it is likely that active PI3K signaling accompanying EMT plays a major role. Besides resistance to anoikis, EMT cells are also more resistant to apoptosis, chemotherapy and oncogene-induced senescence. The evasion from chemotherapy can be monitored when carcinomas are treated with various cytotoxic agents. After treatment in fact, the surviving cells show a relative enrichment of a mesenchymal gene signature (*40*). Again, factors that induce EMT by repressing E-cadherin expression can antagonize apoptosis mechanism as well. The same is true for oncogene-induced senescence where for example ZEB1 has been shown to downregulate p63 and p73 that in turn cannot induce the main cell cycle inhibitors and senescence inducers p21 and proteins of the Ink4 locus, respectively, anymore (*45*). How TGFβ exhibits its anti-apoptotic function will be discussed in more detail later (3.3).

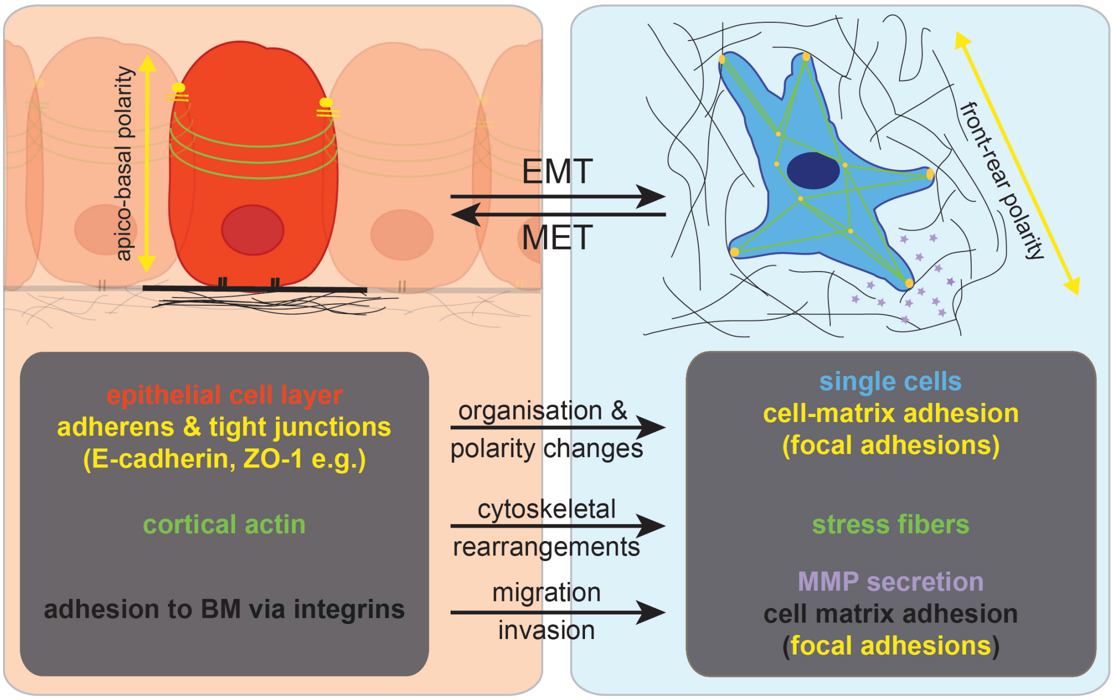
apico-basal polarity
EMT
MET
front-rear polarity
epithelial cell layer
adherens & tight junctions
(E-cadherin, ZO-1 e.g.)
cortical actin
adhesion to BM via integrins
organisation &
polarity changes
cytoskeletal
rearrangements
migration
invasion
single cells
cell-matrix adhesion
(focal adhesions)
stress fibers
MMP secretion
cell matrix adhesion
(focal adhesions)

Figure 4: Schematic representation of epithelial and mesenchymal cells.
Epithelial cells reside with an apico-basal polarity in a layer of epithelial cells. Adherens and tight junctions and a cortical organization of actin filaments stabilize this polarity. Upon EMT, these junctions are resolved, the apico-basal polarity is lost and a rear-front polarity emerges. Instead of cortical actin filaments mesenchymal cells show stress fibers. While epithelial cells are attached to the BM via Integrins, mesenchymal cells are able to migrate and invade by the secretion of MMPs that opens the ECM and by cell-matrix adhesions like focal adhesions that allows efficient migration. Colors in the scheme correspond to colors in the notes of the figure.

1.4.7 EMT inducing signals

EMT can be initiated by several different factors, among these are HGF, EGF, Wnt, NOTCH, VEGF, extracellular matrix proteins, TGFβ and many more. Often, different stimuli complement each other in inducing EMT. The signaling cascades activated by all these factors have in common that they converge on targeting E-cadherin expression. As a shortcut to extracellular signals, overexpression of transcriptional repressors of E-cadherin are sufficient to induce EMT in cells. The same is true for the genetic loss of CDH1, showing again the central role of the loss of E-cadherin during EMT (*38*).

1.5 Metastasis

Metastatic spread of cancer, considered as stage IV tumor, marks the disease as largely incurable and results in poor prognosis and short overall survival. Systemic spreading and resistance to existing therapy explains why more than 90 % of mortality from cancer is associated with metastases (*46*).

1.5.1 The linear versus the parallel progression model

There is a great debate going on whether dissemination of cancer cells that form metastases occurs late, after progression of cancer to full malignancy (linear progression model), or at early stages of tumor progression (parallel progression model). The latter model assumes a development of disseminated tumor cells (DTC) into metastatic lesions independent of the primary tumor. Indications for both phenomena have been found in patients. Very early during tumorigenesis, DTC can be found already in the bone marrow of patients (*47*). But it has been shown that these cells, that reside in the bone marrow, do not form metastases for a long time, if at all (*42*). Also, metastatic spread correlates best with tumor size. Final proof for both theories has not been achieved because early DTC could stay dormant and never establish a metastasis. On the other hand, metastases arise often long after the primary tumor has been surgically removed favoring the hypothesis that DTC had to leave the primary tumor before. Assuming that parallel progression indeed happens, even more effort should be made to understand DTC and their development at the secondary site. In this case early surgery of tumors would not be preventive for metastatic disease (*47*).

1.5.2 The invasion-metastasis cascade

The invasion-metastasis cascade describes the stepwise process cancer cells have to follow to be able to seed metastases at secondary sites (*48*). Cells have to be extremely plastic and adaptable in order to achieve all steps. This makes metastatic spread a rather inefficient process. It has been estimated that less than 0.01 % of cells that enter the systemic circulation are able to establish macrometastases (*49*).

First, an established epithelial tumor has to acquire the ability to breach through mechanical restrains like the basements membrane in order to be able to invade locally. In a sheet of invading epithelial cells the association to their neighboring cell is kept, whereas when single cells invade also these junctions have to be broken. The EMT process, as mentioned above, would provide the requirements for these first steps of metastasis (*40*).

Cells that have left their epithelial embedding and breached the basement membrane have to be able to actively migrate to traverse the surrounding stroma. Again cells that have undergone EMT have gained this capability. Invading cells can also use amoeboid type of cell migration instead of the mesenchymal cell motility mode mentioned above, that is dependent on proteases, stress-fibers and integrins. This type of migration, as the name already indicates, resembles amoebae that squeeze through ECM rather than degrade it or use it to pull themselves through the ECM fibers. That is why the amoeboid mode is independent of proteases, stress-fibers and integrins but Rho/Rock-dependent. Reacting to microenvironmental cues cells can switch between different modes of migration (*50*).

Within the stromal compartment, cancer cells experience the presence of other cell types like fibroblasts, immune cells and endothelial cells. These cells react to the cancerous surrounding by becoming activated. Activated stromal cells in turn influence cancer cells by promoting invasiveness (*51*).

Cancer cells that have infiltrated the surrounding tissues have to use systemic routes to disseminate throughout the body. For this purpose cancer cells take advantage of the lymphatic or blood vascular system. In order to do so, intravasation in vessels has to be accomplished. Entrance into vessels is favored by both the invasive property of cancer cells themselves and by the leaky structure of tumor-associated vessels.

Circulating tumor cells (CTC) have to cope with several stress sources within the bloodstream. Among these is the deprivation from ECM, which induces anoikis in epithelial cells, shear forces applied by blood flow and immune attacks mostly accomplished by natural killer cells within the blood. To overcome these obstacles cancer cells co-opt mechanisms of blood coagulation by shielding themselves with platelets and forming microemboli (*42*).

It has been noted for a long time already that certain types of cancer disseminate to specific secondary sites. Whereas breast cancer cells seed to lung, liver, bone and brain, other cancer types might show another metastatic tropism. The metastatic target organ is certainly directed by accessibility, such as organs with more easily exited vessels like bone and liver due to their fenestrated sinusoid. Moreover, specific signatures within cancer cells that target distinct organs could be discovered. Additional to the decision on where to home, cancer cells have to extravasate the vessels to be able to reach the secondary tissue. To extravasate, cancer cells can secrete factors making the vessel permeable to pass through. Angiopoietin-like 4 (Angptl4), as an example, is secreted already by the primary tumor in order to make lung capillaries less tight. Angptl4 favors specifically the lung as secondary site, because its effect on the vasculature seems to be specific for lungs endothelial cells (*52*).

CTC that have reached a secondary site have to interact with the organ tissue by either staying dormant for a while or by starting to build up a metastasis. It has been shown that the establishment of new tumors at secondary sites is facilitated by the formation of the so-called premetastatic niche. The premetastatic niche, a metastasis favorable microenvironment, is induced by tumor cells that are believed to secrete factors like VEGF, PlGF, TGFβ and TNFα which in turn induces the expression of inflammatory proteins of the S100 family in the target organ. The following recruitment of bone marrow-derived hematopoietic cells prepares the advent of cancer cells and with this the formation of the premetastatic niche. More and more factors influencing homing and the niche preparation on the tumor site and on the niche site are being discovered (*53*). Just recently the group of David Lyden has published that not only secreted proteins induce a premetastatic niche but that also exosomes, small membrane vesicles shed by tumors, can educate bone marrow progenitor cells to help establish metastases (*54*).

Metastases often resemble their primary tumor although DTC must have gone through a lot of adaptation steps in order to be able to reach secondary sites. In most of the cases heterogeneous carcinomas give rise to heterogeneous metastases comprising of well-differentiated and less differentiated parts. Because disseminating cell are rather dedifferentiated, EMT-like when reaching the metastatic site, these cells have to undergo an MET to form an epithelial secondary cancer. Thus gene expression changes favoring an EMT phenotype in the primary tumor have to be reversible which is indeed often the case for example by epigenetic silencing of CDH1 (*55*). Whether all cells undergo MET and restart EMT-MET cycles when disseminating further or whether some cells stay in their EMT and more cancer stem cell-like state has not been answered yet.

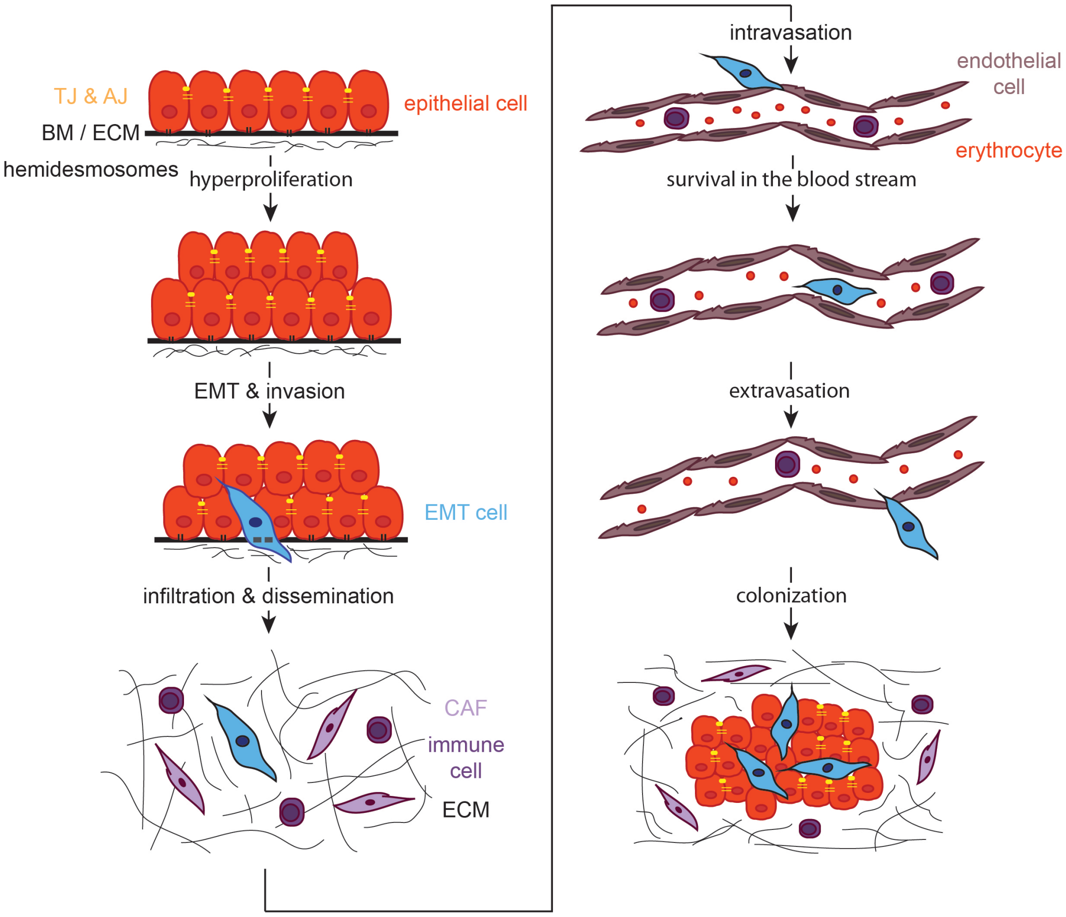
TJ & AJ
BM / ECM
hemidesmosomes
epithelial cell
hyperproliferation
EMT & invasion
EMT cell
infiltration & dissemination
CAF
immune cell
ECM
intravasation
endothelial cell
erythrocyte
survival in the blood stream
extravasation
colonization

Figure 5: Schematic representation of tumor progression and metastasis.
In an epithelial layer, cells (red) are connected to each other by tight junctions (TJ, yellow), adherens junctions (AJ, yellow) and desmosomes. Furthermore, cells adhere to their basement membrane (BM, black) with hemidesmosomes (black). Upon an oncogenic event, epithelial cells start to hyperproliferate. Some cells of this hyperplasia become invasive by undergoing an EMT (blue). The EMT cells resolve the BM and infiltrate the surrounding tissue depicted here by extracellular matrix (ECM, black) with cancer-associated fibroblasts (CAF, purple) and immune cells (purple). In order to disseminate further, EMT cells intravasate into vessels (here blood vessels in brown, with erythrocytes in red and immune cells in purple). Circulating tumor cells have to survive in the blood stream and extravasate at the site of secondary tumor growth. To establish a metastasis, EMT cells undergo an MET (red) but some might stay dormant in a mesenchymal state (blue).

1.6 Cancer stem cells

It has been known for a long time that organs are composed of a hierarchy of cells, where stem cells at the apex of the hierarchy would be the ones being able to divide asymmetrically to self-renew but also to give rise to progenitor cells and ultimately originate the whole organ. This concept is now being expanded to cancer, recognizing cancer as an organ as well. In cancer, the stem cell is not necessarily the cell originating the tumor in the first place but rather the driving force to fuel growth, progression and metastasis (*56*).

1.6.1 The concept of cancer stem cells

The progression of cancer has been described to occur via the clonal evolution model. In this model, successive mutations giving proliferative and survival advantages let individual cell clones overgrow the rest of the cells. Thereby, tumors evolve constantly and become highly heterogeneous (*57*). This concept of tumor cells being under continuous selection for the 'fittest', most adapted cell is now being integrated in the hierarchical model of somatic stem cells (*58*). After a long discussion on whether cancer stem cells (CSC) really exist, the CSC idea is now accepted for many cancer types after having been described originally in acute myeloid leukemia (*59,60*).

Cancer stem cells are defined by being able to self-renew by asymmetric cell division and by being able to reconstitute the phenotypic complexity of the tumor they had originated from. Additionally, *in vitro* CSCs should have the ability to form spheres from a single cell when cultured in non-adherent conditions and for infinite passages (*61*). These characteristics support the idea that only a specific proportion of tumor cells have the potential to propagate a tumor in a recipient mouse, which would be the tumor initiating cells (TIC).

Additionally, CSCs are drug-resistant because of their highly debated slower proliferation and their capacity to actively shuttle drugs out of their cell body. Furthermore, CSCs have been reported to be more efficient in DNA repair mechanisms helping to cope with radiation therapy. Resistance to therapeutic agents makes CSC not only the tumor propagating cells, but also the most potent cells to survive cancer treatment and to cause relapse (*56*). In contrast to the drug resistance feature of cancer stem cells, it has been found that CSCs and also EMT cells are more susceptible to salinomycin (*62*), an antibiotic acting by inhibition of the Wnt pathway (*63*). Along theses lines, treatments that induce differentiation of cancer (stem) cells would allow targeting cells that are otherwise difficult to target. All these observations fit very well with the notion that undifferentiated cancers are in most cases associated with poor prognosis and relapse, arguing that these cancers would comprise more CSCs than differentiated cancers do (*64*).

Great effort has been spent to identify CSCs by specific combinations of surface marker expression, but only limited success for some cancer types could be achieved, because the markers identified are very much dependent on the cancer subtype. Furthermore, the expression of markers is not exclusive for CSCs, making it difficult to isolate a pure CSC population rather than enriching for CSCs only. To sort CSCs by surface marker expression seems to be even more unreliable in mouse cells or cultured cell lines. However, the gold standard to identify a proportion of CSCs or better tumor initiating cells (TIC) is by serial transplantation of cells into recipient animals (*65*). Thereby, it is of great importance to transplant the suspected CSC/TIC into the adequate surrounding which would be an orthotopic site in either syngeneic or immunocompromised animals to effectively validate this concept (*66*). The drawback of using immunocompromised mice is the ignorance of the immune system on cancer progression, as mentioned above (1.1.1). However, human cells injected into mice will never trigger the same immune reaction as cancer cells that arise spontaneously within a patient (*64*).

In breast cancer, as the first solid cancer, a cancer stem cell-enriched population could be sorted out of primary human tumors by the surface marker combination $CD44^{+}$ $CD24^{-/low}$ ESA^{+} $Lineage^{-}$ which gave rise to tumors when only 200 cells were injected, a 50 fold higher tumorigenicity as compared to the unsorted cell population (*67*). But again, proving this marker combination useful for several human tumors, there are still high variations between patients, murine tumor models and even cell lines in expressing those markers (*64*).

1.6.2 The origin of cancer stem cells

The origin of CSCs is still controversial and a subject of constant discussion. There are formally two possibilities how CSCs originate. The first is transformation of somatic stem cells rendering the stem cell more proliferative. The second possibility is a gain of self-renewal capacity and de-differentiation of a progenitor or even a more differentiated cancer cell. Both ways of sources of cancer stem cells have been described and are still heavily debated (*68,69,59*). In any case, it is very likely that the microenvironment surrounding a CSC plays an important role. For instance it has been reported that the proximity to blood vessels is a microenvironmental cue that helps brain cancer stem cells to maintain their self-renewing capabilities (*70*).

1.6.3 The stromal progression model

The stromal progression model has been proposed as a combination of the clonal evolution model, the cancer stem cell theory and also including the relevance of microenvironmental cues (*71*). This model not only explains tumor initiation but also metastatic progression of cancer. In the stromal progression model the importance of cancer cells to activate and interact with stromal cells and their secreted factors is stressed. The origin of the CSC that could either arise by mutation from a somatic stem cell or by dedifferentiation of ‘normal’ cancer cell is not distinguished. Here, the CSC is not only dependent on the surrounding signals to stay in its stem cell-like state but can also be generated through cues coming from the stroma. In addition to CSCs, all cancer cells are dependent on the microenvironment. While cancer is progressing from adenoma to carcinoma and finally to metastases, tumor cells experience different stromal compartments which influence each other. In order to be able to seed metastasis efficiently and to grow out at secondary sites, tumor cells either have to be able to modify the microenvironment at arrival or have to educate it via cytokines beforehand. Cells that are not being welcomed by the target stroma either die or stay dormant until the necessary signals are being provided. Moving the microenvironment in the focus of tumor progression and anticipating that plasticity of CSCs could make it difficult to eradicate them without allowing other cells to dedifferentiate to form new CSCs, the microenvironment could be a potential drug target. Disturbing the cancerous microenvironment would prevent CSCs to find or create their niche needed for efficient tumor progression and metastatic spread.

1.6.4 Cancer stem cells and EMT

The Weinberg lab was the first to integrate EMT and the cancer stem cells theory with each other, even arguing that EMT cells would be cancer stem-like cells (*9*). EMT, an important process during development where a lot of cell plasticity is required, is co-opted by epithelial cancer cells to invade and metastasize. Now, studies have shown that cells that have undergone EMT are not only important for that step of tumorigenicity but also for the maintenance of a tumor by serving as a sub-population of cancer stem cells shown by the overlapping claudin-low gene signature (*72*). Furthermore, it has been found that relapsed tumors after either endocrine therapy (letrozol) or chemotherapy (docetaxel) show a claudin-low characteristic signature. Whether the relative increase in CSCs is generated by selection of resistant cells or by pushing cells into an EMT is not clear yet. However, these residual cells could give rise to an even more aggressive relapsed tumor (*73*). The notion that cancer stem cells in the breast have a mesenchymal gene signature like cells that have undergone EMT holds also true for normal breast stem cells. This observation argues rather for a general mesenchymal phenotype of stem cells in which epithelial cells can transit into by EMT (*74*).

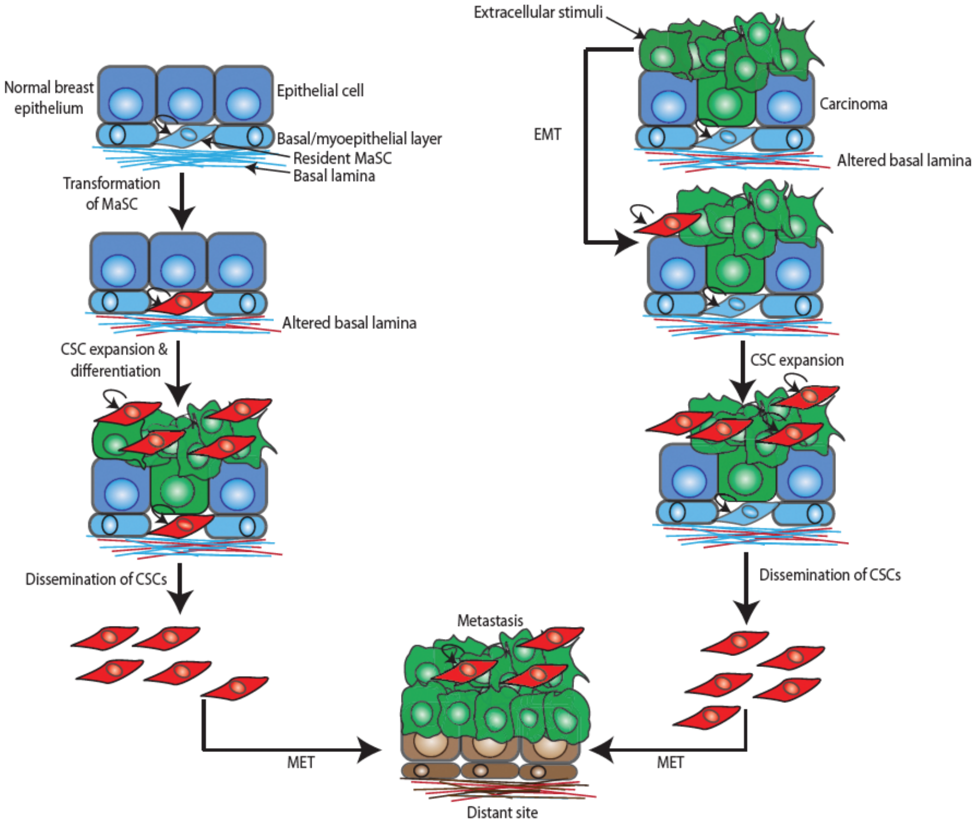
Extracellular stimuli
Normal breast epithelium
Epithelial cell
Basal/myoepithelial layer
Resident MaSC
Basal lamina
Transformation of MaSC
Altered basal lamina
CSC expansion & differentiation
Dissemination of CSCs
EMT
Carcinoma
Altered basal lamina
CSC expansion
Dissemination of CSCs
Metastasis
MET
MET
Distant site

Figure 6: EMT and cancer stem cells during breast cancer development.
The mammary gland is composed of epithelial cells and the basal/myoepithelial compartment. In the latter, the mammary stem cells (MaSC) are located in. One model describes that cancer stem cells (CSC) develop upon mutation and transformation of normal MaSCs: upon transformation, MaSCs start to proliferate, divide asymmetrically and migrate into the epithelial compartment and seed to secondary sites (left panel). Another way how CSCs could arise is through an EMT of carcinoma cells induced by extracellular stimuli. These newly formed CSC would expand and disseminate to secondary sites as well (right panel). At the metastatic site some of the mesenchymal CSC undergo an MET to grow out (*74*).

The possibility of the acquisition of a cancer stem cell phenotype by differentiated cancer cells forced to undergo EMT *in vitro* has been shown by the gain of the breast cancer stem cell specific surface markers $CD44^{+}CD24^{-/low}$, the ability to efficiently form mammospheres and the initiation of tumors when 1000 cells were injected into mice. Additionally, the opposite is true: freshly isolated human breast or breast tumor cells sorted for $CD44^{+}CD24^{-/low}$ were shown to be the breast (cancer) stem cell sub-population revealing a mesenchymal gene expression pattern like cells that had undergone EMT (*9*). Anyhow, the existence of cancer stem cells and their association to EMT cells is still controversially debated in the field (*71,75*). With my PhD thesis work, I hope to have generated new insights into this important topic to better understand tumor-initiating cells.

2 Aim of the study

Epithelial to mesenchymal transition (EMT) is a cellular process of cancer cells that aims to invade the surrounding tissue and to metastasize. TGFβ is one of the major signals that can stimulate EMT. Furthermore, TGFβ can induce apoptosis in non-transformed cells. Another hallmark of EMT is the gain of cell motility, which cancer cells use to migrate into surrounding tissues and to disseminate. Apart from these classical EMT-associated features EMT has also been implicated in tumor initiation and cancer stemness.

During the course of my study, several questions concerning EMT and its features *in vitro* and *in vivo* have been addressed:

I. Are cells that underwent EMT cancer stem cell-like? More importantly, which mechanism would lead to increased tumorigenicity?

II. What factors are generally important for EMT and for which part of EMT would they be relevant?

III. Which factors influence cells to undergo TGFβ-induced EMT instead of apoptosis?

3 Results

3.1 VEGF-mediated angiogenesis links EMT-induced cancer stemness to tumor initiation

Anna Fantozzi [1 *], Dorothea C. Gruber [1 *], Chantal Heck [1], Laura Pisarsky [1], Akiko Kunita [1 $], Mahmut Yilmaz [1 #], Ulrike Hopfer [1 ∞], Nathalie Meyer-Schaller [1] and Gerhard Christofori [1].

[1] Institute of Biochemistry and Genetics, University of Basel, Switzerland

Present addresses: [$] Department of Pathology, Graduate School of Medicine, The University of Tokyo, 113-0033 Tokyo· Japan; [#] CNIO Centro Nacional de Investigaciones Oncologicas, E-28029 Madrid, Spain; [∞] Novartis Pharma AG, CH-4002 Basel, Switzerland

[*] These authors contributed equally to this work

—paper manuscript—

3.1.1 Abstract

Tumor progression and metastatic spread are associated with the ability of cancer cells to gain invasiveness and migrate to secondary organs. Epithelial to mesenchymal transition (EMT), the mechanism determining the malignancy switch of tumor cells, is associated with enrichment of cancer stem cells (CSC) and increased tumorigenicity (*9*). The ultimate hallmark of cancer stemness and of metastatic cells is their capability to initiate *de novo* tumors (*65*). Moreover, once the tumor is established CSCs promote tumor growth through their self-renewal and differentiation ability. However, the mechanism underlying the increased tumorigenicity of mesenchymal tumor cells remains unsolved. We show that upon EMT, breast cancer cells increase their ability to be propagated as organized mammospheres and gain sensitivity to the CSC-specific drug salinomycin. EMT confers stem cell-like behaviors and characteristics and ultimately results in an increase in tumor initiation potential associated with induced angiogenesis. In our models, EMT-induced angiogenesis occurs through upregulation of the pro-angiogenic factor VEGF-A. In addition, inhibition of VEGF-A in the tumor initiating cells (TIC) is associated with loss of tumorigenicity. We propose a novel interpretation of the cancer stemness feature by introducing EMT-induced angiogenesis as the connecting mechanism between cancer stemness and tumor initiation. Tumor initiating cells, cancer stem cells with angiogenic properties, drive the early stages of tumorigenicity. In this perspective we envisage opportunities of therapeutic intervention: targeting VEGF-A in the appropriate cancerous cellular sub-population, i.e. the TIC, would result in inhibition of tumor growth.

3.1.2 Results

Tumor progression is associated with EMT that converts epithelial cells into migratory tumor cells and sets the stage for metastatic spread. Recent evidence demonstrates that EMT is associated with the generation of cancer stem cells and increased tumorigenicity (*9*). This prompted us to investigate this hypothesis in breast cancer using three defined *in vitro* models of EMT and *in vivo* orthotopic transplantations. The MTflECad cell line, established from a mammary tumor of an

MMTV-Neu;fl/flECad transgenic mouse undergoes EMT by Cre-mediated genetic ablation of the E-cadherin gene (MTΔECad) (*76*). To trigger EMT we treated Py2T cells, derived from a mammary gland tumor of an MMTV-PyMT transgenic mouse, as well as NMuMG cells with TGFβ. Gene expression profiling of MTflECad cells undergoing EMT showed that, in addition to the activation of cellular motility and adhesion pathways, EMT induced the expression of genes belonging to the angiogenesis and development network (Fig. 7a). The most relevant genes in these pathways were validated by qRT-PCR (Supplementary Fig. 1a). EMT also conferred stem cell-like properties to MTflECad, NMuMG, and Py2T cells by inducing the formation of organized hollow mammospheres compared to the epithelial ones (Fig. 7b, d, e), that could be reduced by culturing conditions that excluded cell aggregation (Fig. 7c) (*61*). N-cadherin was present at the cell-cell contacts in MTΔECad cells spheroids, while MTflECad spheres expressed E-cadherin and low levels of N-cadherin as expected for mesenchymal and epithelial cell respectively (Fig. 7d). Sequential spheroid passagings induced a cadherin switch at the cell-cell contacts in the MTflECad mammospheres (Supplementary Fig. 1c).

In addition, EMT conferred increased sensitivity to the cancer stem cell specific drug salinomycin, supporting the hypothesis that EMT would enrich the cancer stem cell population (Fig. 7f) (*62*).

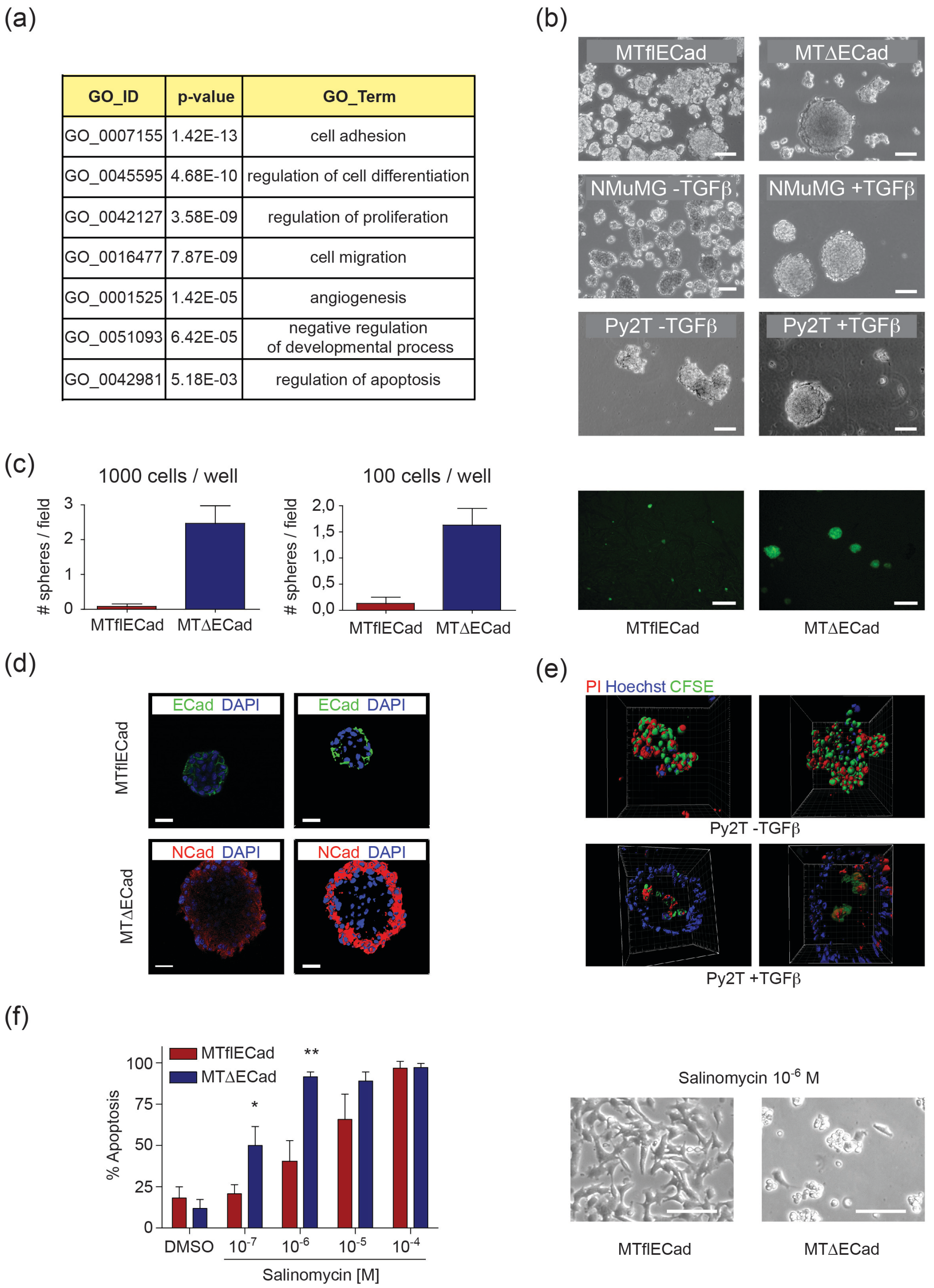

GO_ID	p-value	GO_Term
GO_0007155	1.42E-13	cell adhesion
GO_0045595	4.68E-10	regulation of cell differentiation
GO_0042127	3.58E-09	regulation of proliferation
GO_0016477	7.87E-09	cell migration
GO_0001525	1.42E-05	angiogenesis
GO_0051093	6.42E-05	negative regulation of developmental process
GO_0042981	5.18E-03	regulation of apoptosis

Figure 7: Cancer stem cell properties of cells undergoing EMT.
(a) Gene expression profiling by micro array analysis of MTflECad and MTΔECad cells was performed using R. Genes differentially regulated at least two fold in MTΔECad cells compared to MTflECad cells were analyzed for their gene ontology by GO_term analysis tool. Selected GO_terms are listed with their corresponding adjusted p-value.
(b) MTflECad/MTΔECad, NMuMG -/+ TGFβ and Py2T cells -/+ TGFβ were cultured over two passages in non-adherent, mammosphere conditions. Representative light microscopic pictures of the different epithelial and mesenchymal counterpart cell lines cultured in 3D as mammospheres are shown. Scale bars, 100 μm.
(c) Either 100 or 1000 MTflECad and MTΔECad cells expressing GFP were plated in methylcellulose containing media to rule out cell aggregation instead of sphere formation out of single cells. Quantification and representative light microscopic pictures of mammospheres grown for 4 days are depicted. Scale bars, 200 μm.

(d) Confocal analysis of M2 mammospheres stained for E-cadherin (green), N-cadherin (red) and DAPI (blue). The left pictures show one focal plane of the spheres, the right picture shows a surface rendering. Scale bars, 30 μm.
(e) 3D reconstruction of epithelial (-TGFβ) and mesenchymal (+TGFβ) Py2T cells grown for two passages in mammosphere conditions. Nuclei are stained with Hoechst (blue), PI (red) stains the dead cells and CFSE (green) as membrane dye of the cells that are slowly proliferating.
(f) MTflECad and MTΔECad cells were treated for 72h with the indicated concentrations of salinomycin. The percentage of apoptotic cells was measured by Annexin V FACS. Mean of three independent experiments with SEM are displayed, using paired Students t-test for significance evaluation with * $p < 0.05$ and ** $p < 0.01$. One representative micrograph of MTflECad and MTΔECad cells treated for 72 hours with 10^{-6} M salinomycin is shown. Scale bar, 100 μm.

To identify CSCs a panel of surface markers proven valid in experimental primary tumors and human cellular systems was tested (Supplementary Table I) (*77-83*). In our system these markers were not suitable to identify an EMT-induced sub-population, supporting a controversial debate on the validity of this approach (*56*). The tumorigenicity potential of unsorted MTflECad and MTΔECad cells, the defining feature for EMT-induced cancer stem cells, was therefore assayed with *in vivo* orthotopic transplantation experiments in BALB/c Rag2$^{-/-}$;commonγ$^{-/-}$ (RG) mice. Histological examination of tumor sections showed a distinctive morphology. MTflECad cells, belonging to the normal-like subtype of tumor cells, gave rise to tumors with epithelial morphology, defined borders and central necrotic areas (Fig. 8a). Tumors that were originated from the mesenchymal lineage, with the claudin-low signature (MTΔECad), showed an invasive phenotype, fibroblast-like appearance and absence of necrosis (Fig. 2a), in line with published data (*72*). Additionally, the tumors arose with a different growth kinetic depending on their epithelial or mesenchymal origin. *In vivo* limiting dilution experiments showed that when cells were cultured in 2D prior to transplantation, MTΔECad cells had a higher tumor take rate than MTflECad cells (Fig. 8b). When cells were cultured as mammospheres before injection, this pattern became more obvious, revealing an inefficient tumor take rate for MTflECad. Strikingly, as few as 10 TIC-enriched MTΔECad cells could efficiently grow as tumors (Fig. 8c).

In conclusion, EMT generated a better tumor initiating capability, which could be further increased via TIC's enrichment (mammosphere culturing). Tumors and cell lines were characterized at the protein level and upon EMT several genes involved in tumorigenicity were found to be upregulated (TIMP-1, galectin-1, MMPs, P-selectin); (Supplementary Table II)(*84-87*). Orthotopically transplanted mesenchymal cells form bigger metastases than their epithelial counterparts (Fig. 8d-f). Consistent findings were obtained in a metastasis formation assay where a distinctive lung colonization phenotype was observed: MTflECad cells gave rise to many small metastases, while MTΔECad cells gave rise to few but bigger ones (Fig. 8g, h). This phenotype, observed independently of the pre-culturing conditions of cells (data not shown), was partially explained by the strong vascularization present in the MTΔECad metastases (Fig. 9d) as well as by the reduced levels of apoptosis in the mesenchymal metastases (Supplementary Fig. 2a, b). Because we observed no differential ability of tumor cells to be able to persist in the blood stream and/or home to the lungs (Supplementary Fig. 2c) we hypothesized that the difference in amount of metastases could be due to the genetic impairment of MTΔECad cells to undergo MET.

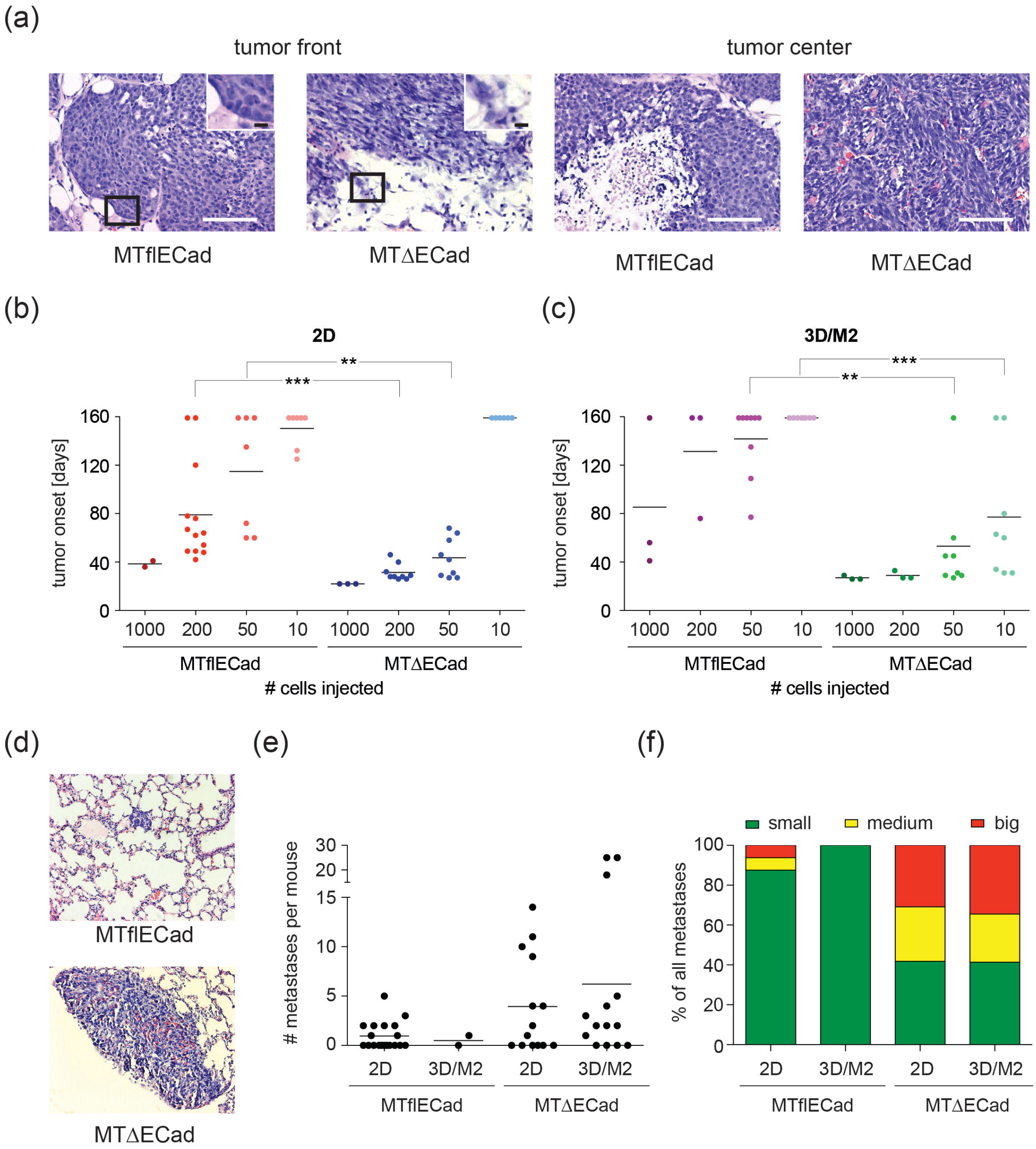

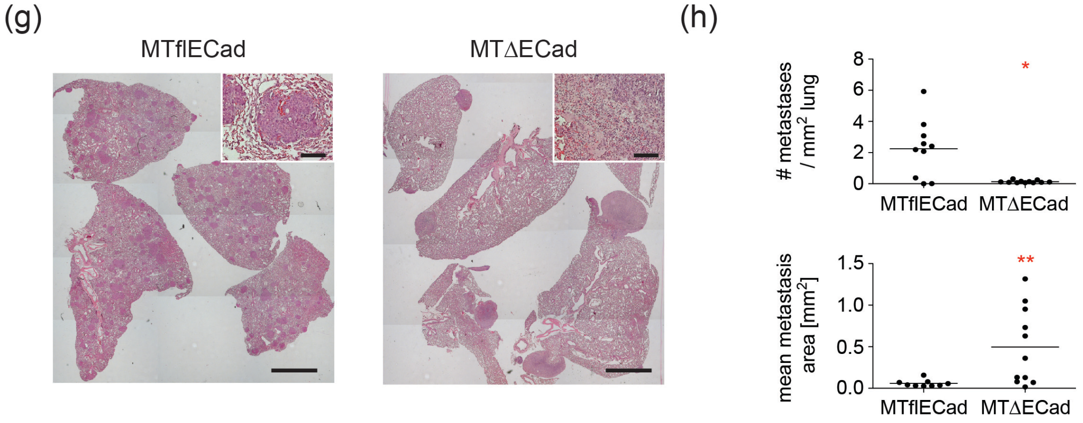

Figure 8: EMT cells have a higher tumor initiation potential accompanied by bigger metastases to the lung.
(a) MTflECad and MTΔECad cells were transplanted in PBS into the 9th mammary fat pad of female RG mice. Tumors were taken out individually when they reached the size of 1.5 cm^3. H&E staining of the tumor front (left) or tumor center (right) are shown. Black squares indicate which part of the picture is depicted in a higher magnification in the upper right corner. Scale bar, 100 *µ*m or *µ*10 m in the zoomed picture.
(b) 2D cultured MTflECad and MTΔECad cells were transplanted in limiting dilutions into the mammary fat pad of RG mice (x-axis shows the amount of cells injected). The tumor onset of individual mice is plotted. The experiment was finally terminated 160 after injection, mice that had not developed tumors until then are recorded with a tumor onset of 160 days. MTflECad cells gave rise to tumors in 100, 84.6, 57.1 and 28.6 % of the cases when 1000, 200, 50 and 10 cells were injected, respectively. MTΔECad cells gave rise to tumors in 100 % of the cases when 1000, 200 or 50 cells were injected, whereas 0 % of tumor take was monitored when only 10 MTΔECad cells had been injected.
(c) Mammosphere cultured MTflECad and MTΔECad cells were transplanted in limiting dilutions into the mammary fat pad of RG mice (x-axis shows the amount of cells injected). The tumor onset of individual mice is plotted. The experiment was finally terminated 160 after injection, mice that had not developed tumors until then are recorded with a tumor onset of 160 days. Here, MTflECad cells gave rise to tumors in 66.6, 33, 37.5 and 0 % of the cases when 1000, 200, 50 or 10 cells were injected, respectively. MTΔECad cells gave rise to tumors in 100 % of the cases when 1000 or 200 cells were injected and in 85.7 and 75 % of the cases when only 50 or 10 cells had been injected, respectively.
(d) The above-mentioned mice were individually sacrificed when the tumors had reached the size of about 1.5 cm^3. Tumors and lungs were taken out for analysis. Representative H&E pictures of metastases seeded by MTflECad and MTΔECad tumors to the lung are shown. Scale bars, 100 *µ*m.
(e) The amount of metastases in the lung per mouse was plotted per genotype and per pre-culturing condition of the tumor cells injected.
(f) Size distribution of metastases in the lung in proportion to all metastases seeded per genotype and per pre-culturing condition is shown (MTflECad 2D: N = 19, M2: N = 2; MTΔECad 2D: N = 14; M2: N = 14 mice).
(g) Representative H&E staining of lung sections 3 weeks after injection of 10^6 MTflECad and MTΔECad cells into the tail vein of 8 weeks old MMTV-Neu mice. Scale bars, 2 mm and 100 *µ*m in the zoomed pictures.
(h) Experimental metastases were quantified for the amount per lung and their mean size.
Statistical significances were calculated using Mann-Whitney U test with * $p < 0.05$ ** $p < 0.01$ and *** $p < 0.001$. The 10-cell comparison was statistically evaluated using a Fisher's exact test with *** $p < 0.001$.

In vivo, EMT induced active angiogenesis in the mesenchymal tumors and metastases explaining the difference in tumor takes, onset and metastasis size as an advantage mechanism for tumor cell colonization and survival (Fig. 9a-d, and Supplementary Fig. 3a). Vessels within the tumors and metastases were functional (Supplementary Fig. 3b). Consistent with these findings, in a spontaneous model of pancreatic cancer, loss of E-cadherin in the β-cells of the pancreatic tumor islets (Rip1Tag2;ΔECad) (*76*) also correlated with induced angiogenesis (Supplementary Fig. 3c). Furthermore, in contrast to mesenchymal tumors, epithelial tumors had strong hypoxic areas distant to vessels and showed big internal areas of necrosis associated with high levels of apoptosis, probably due to the lack of vascularization (Fig. 9e and Supplementary Fig. 3d, e). This phenotype correlated with high levels of VEGF-A protein and mRNA produced by MTΔECad cells at time of injection (Fig. 9a-d and f-g). Mammosphere culturing caused a further increase in VEGF-A levels in the mesenchymal cells (Fig. 9g). VEGF-A upregulation upon EMT was also validated in another cellular system (Supplementary Fig. 3f).

In line with these findings, barely palpable mesenchymal tumors were highly vascularized, in comparison to their epithelial counterpart, stressing the relevance of angiogenesis in the early events of tumor growth (Supplementary Fig. 3g). Moreover, the elevated levels of VEGF-A in epithelial tumors argued in favor of a slow adaptation to their need of VEGF-A in order to achieve tumor initiation. Additionally, hypoxia, as a potent inducer of VEGF-A expression should not be neglected (Fig. 3e, h and Supplementary Fig. 5b) (*17*).

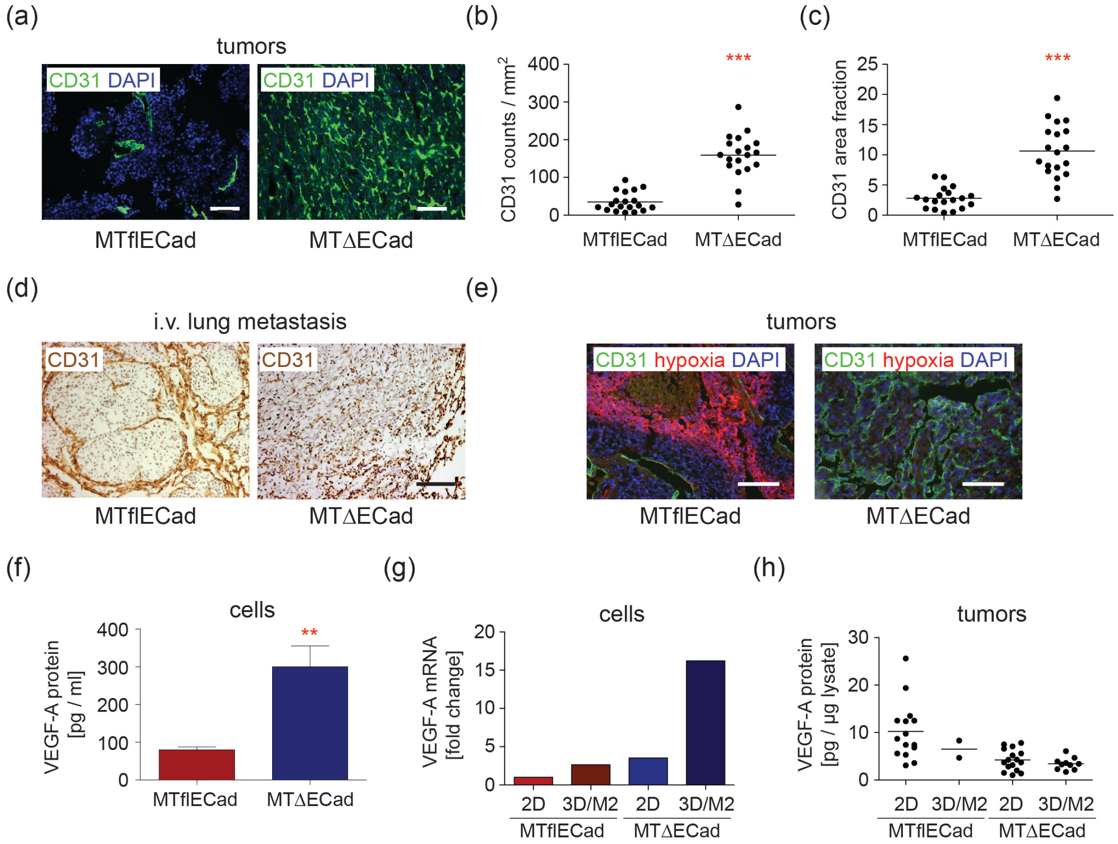

Figure 9: Tumors formed by mesenchymal cells are highly vascularized.
(a) Tumor sections of MTflECad and MTΔECad cells were stained for the endothelial marker CD31 (green) and DAPI (blue) by immunofluorescence.

(b, c) CD31-positive counts per area (b) and the area fraction (c) of CD31 staining were quantified using ImageJ software. N = 6 mice; Statistical significance was calculated using Mann Whitney U test with ** $p < 0.01$ and *** $p < 0.001$.
(d) Metastases formed after intravenous injection of MTflECad and MTΔECad cells were stained immunohistochemically for CD31 (brown) and counterstained with hematoxylin (purple). Representative pictures of both conditions are shown.
(e) Hypoxia in MTflECad and MTΔECad tumors was visualized by injecting pimonidazole into mice before sacrificing them and staining by immunofluorescence for its adducts (red), CD31 (green) and DAPI (blue) was performed. Representative pictures of both types of tumors are shown.
(f) Analysis of secreted VEGF-A protein in the supernatant of MTflECad and MTΔECad cells by ELISA. The mean of 3 independent measurements is plotted with the SEM. Statistical significances were calculated using Students t-test with ** $p < 0.01$.
(g) qRT-PCR of MTflECad and MTΔECad cells cultured in 2D or in 3D mammosphere conditions were analyzed for their relative expression of VEGF-A. Fold changes to MTflECad 2D cultured cells are plotted.
(h) VEGF-A protein abundance was measured in tumor lysates by ELISA.
Scale bars, 100 μm.

To determine the importance of VEGF-A in tumor angiogenesis and tumor onset, shVEGF-A MTΔECad were orthotopically transplanted into RG mice and compared to MTΔECad cells expressing a non-targeting shRNA (MTΔECad shCtr) (Fig. 4a, b and Supplementary Fig. 4a). While MTΔECad shCtr cells gave rise to tumors after 30 days, no tumors were palpable at this time in mice transplanted with MTΔECad shVA #1 or MTflECad expressing a non-targeting shRNA. The epithelial MTflECad shVA #1 tumor onset was slightly delayed compared to the MTflECad cells. Additional small hairpins against VEGF-A were used to validate the results obtained with shVA #1 (Fig. 4c, d, Supplementary Fig. 4b). Tumors lacking VEGF-A expression exhibited significantly reduced angiogenesis compared to the MTΔECad and the vascularization extent was comparable to the one of MTflECad tumors (Fig. 4e-g), showing that reduced VEGF-A levels impaired angiogenesis and delayed tumor onset. These results showed that VEGF-A is required for EMT-induced angiogenesis in the early events of tumor initiation, in line with results in skin and brain (*88-90*).

No difference was instead observed in the vasculature of MTflECad cells upon depletion of VEGF-A (Fig. 4b and also Fig. 2). VEGF-A knockdown was effective in MTflECad and MTΔECad cells and slightly affected cell growth (Supplementary Fig. 4c). High VEGF-A levels, necessary for tumor initiation and incidence, were proven essential in the TIC-enriched population. Strikingly, TICs relied on the presence of VEGF-A for their tumorigenic properties as shown in Fig. 4h where 10 mammosphere-cultured shVEGF-A MTΔECad cells were no longer able to originate tumors when orthotopically transplanted.

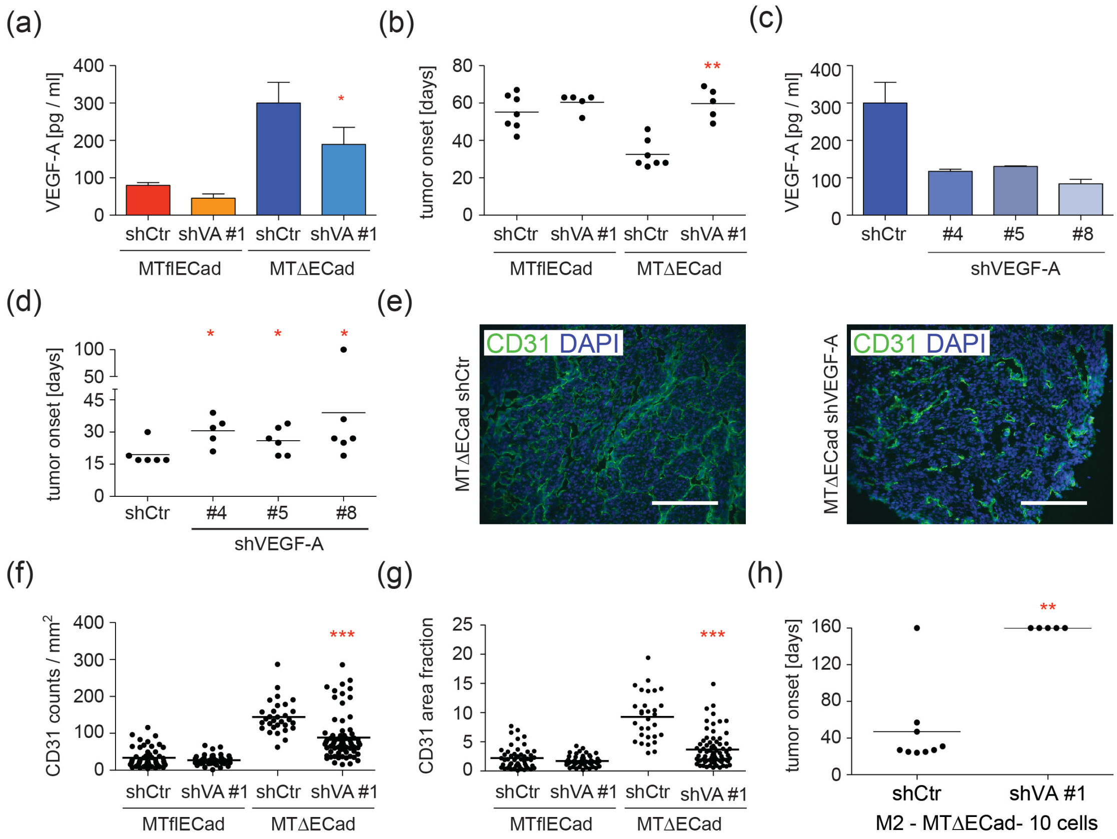

Figure 10: Tumor cell-derived VEGF-A is required for early tumor onset and tumor angiogenesis.
(a) Secreted VEGF-A protein levels in the supernatant of MTflECad and MTΔECad cells that have been infected with a non-targeting short hairpin (shCtr) or one against VEGF-A (shVA #1), were assessed by ELISA. The mean of 3 independent measurements is plotted with the SEM. Statistical significances were calculated using paired Students t-test with * $p < 0.05$.
(b) 200 knockdown cells for VEGF-A (shVA #1) and their controls (shCtr) were injected into the mammary fat pad of RG mice. The onset of the different tumors was plotted and the knockdown tumors were compared to their control by Mann Whitney U test with ** $p < 0.01$.
(c, d) Additional small hairpins against VEGF-A (shVA #4, shVA #5, shVA #8) were used to validate the result from shVEGF-A #1. The knock down-efficiency was tested by assessing the levels of VEGF-A in the cell supernatant by ELISA. The mean of 3 independent measurements is plotted with the SEM (c). The onset of these tumors was determined (d).
(e) The vascularization of MTΔECad shCtr and shVEGF-A #1 tumors was analyzed by CD31 (green) immunofluorescence staining. Representative pictures are shown. Scale bars, 100 μm.
(f, g) The degree of vascularization was quantified by counting the amount of CD31-positive vessels per area (f) and the area fraction of vessels (g). Statistical analysis of the quantifications was performed by Mann Whitney U test with *** $p < 0.001$ with N = 4 mice.
(h) MTΔECad cells infected with a control shRNA (shCtr) or one against VEGF-A (shVA #1) were cultured for 2 passages as mammospheres. After dissociation of the spheres, 10 cells were injected in PBS into the 9th fat pad of RG mice. The tumor onset was monitored and plotted. The experiment was finally terminated 160 after injection, mice that had not developed tumors until then are recorded with a tumor onset of 160 days. Statistical analysis of the quantifications was performed by Fisher's exact test wit * $p < 0.05$.

Having established a crucial role of VEGF-A in EMT-associated increased tumorigenicity we investigated the role of the other VEGF members in cell lines and tumor extracts and found them to be upregulated upon EMT. (Supplementary Fig. 5a, b). However, knockdown experiment of VEGF-C showed no differential tumor growth *in vivo* (Supplementary Fig. 5c-f).

Mesenchymal tumor cells showed a five-fold induction of VEGFR1 mRNA expression both in 2D and M2 conditions that was associated with upregulation of the Nrp1 and Nrp2 co-receptors not excluding a potential role of the VEGF-VEGFR1-Nrp2 loop in stemness and tumor take (Supplemental Fig. 6a).

In mice, transplanted with MTflECad or MTΔECad cells, treatment with the VEGFR inhibitor PTK787/ZK222584 (PTK) significantly impaired vascularization and tumor growth of both tumor types showing the essential role of angiogenesis during tumor progression (Supplementary Fig. 6b, c). However, *in vitro* cells were insensitive to PTK treatment (Supplementary Fig. 6d).

Overexpression of VEGF-A in MTflECad (Supplementary Fig. 7a, b) significantly increased tumor vessel number and area without resulting in induced tumor onset (Supplementary Fig. 7e) and proved VEGF-A not to be sufficient to enhance tumor initiation alone (Supplementary Fig. 7d). In these tumors apoptosis was decreased to values comparable to the MTΔECad ones while no difference in the proliferation rate was detected (Supplementary Fig. 7f, g). Other factors were therefore necessary to complete the induction. MMP abundance was found increased in MTΔECad tumors possibly allowing a higher bioavailability of VEGF-A in these tumors compared to MTflECad tumors (Supplementary Table II). *In vitro* data also showed that while MTΔECad cells conditioned medium supported HUVEC growth, MTflECad conditioned media could not (Supplementary Fig. 8). Accordingly, VEGF-A overexpression in MTflECad cells restored, whereas VEGF-A knockdowns in MTΔECad cells decreased HUVEC survival.

3.1.3 Discussion

Standardized assays for stemness evaluation were used to explain the mechanism underlying EMT-induced tumorigenicity. While some of the CSC hallmarks were revealed, other assays (surface markers, ALDH+ side population and general drug resistance, data not shown) were proven unsuitable to properly address this question. However, *in vivo* tumorigenicity assay successfully proved the principle of EMT-induced stemness. Indeed we could show that EMT increased tumor initiation ability and that EMT-induced angiogenesis, the mechanism by which this occurred, was crucial for early tumor onset. Moreover, upon EMT the enrichment of TIC enabled 10 cells to effectively initiate tumors with increased angiogenesis, a capacity that was abrogated in the absence of VEGF-A. Tumor initiation required the presence of TICs within the correct and permissive microenvironment (*88,89*). A central role for VEGF-A in tumor progression has emerged from our studies and was supported by recent findings (*91-97*). We speculated that EMT-induced VEGF-A created an optimal microenvironment for TICs to establish and grow as a highly vascularized tumor.

The calculated CSC frequency of MTΔECad (1:14.2 in M2 and 1:33.4 in 2D) and of MTflECad cells (1: 691.7 in M2 and 1: 81.4 in 2D) could not be statistically verified. On the basis of the ELDA function, the single hit hypothesis was rejected ($p = 0.0072$ for M2 and $p = 0.02$ for 2D in MTΔECad cells, and $p = 0.76$ in M2 and $p = 0.68$ in 2D in MTflECad) (*98*). The values obtained indeed supported a multi-hit event, where TIC achieved tumor initiation in a concerted action with other factors, such as VEGFA-induced angiogenesis. All together our data showed that increased tumor take rate was a phenomenon that could not be simply described by the presence of one tumor initiating cell (single hit hypothesis) and we concluded that activation of angiogenesis was one of the additional required events. In the absence of VEGF-A mammosphere formation ability was not abrogated indicating angiogenesis and stemness as separate events. We propose a novel interpretation of the cancer stemness features by introducing the angiogenesis event as a link between the two phenomena.

3.1.4 Material & Methods

For *in vitro* mammospheres culturing an adapted version of previously described protocol was used (*61*). For *in vivo* experiments mammospheres were collected after M2 and a single cell suspension was obtained by trypsinization. Cells resuspended in PBS were transplanted into the 9th mammary gland of 7-10 weeks old females BALB/c Rag2$^{-/-}$;common$\gamma^{-/-}$ (a kind gift from T. Rolink). Tumor growth was monitored and measured with the caliper. Tumor volume was obtained by the formula $L \times l^2 \times 0.543$ (with L = biggest measure, l = shortest measure). Mice were checked routinely and individually sacrificed when tumors reached 1500 mm^3. Mammospheres stainings were performed upon 4 % PFA fixation, with permeabilization 0.1 % Triton X-100, and over night stainings for N-cadherin (33-3900 Zymed) and E-cadherin

(13-1900 Zymed). Confocal sequential images were acquired using the Leica SP5 confocal microscope and 3D images were generated using IMARIS software.

MMTV-Neu mice were injected intravenously with 10^6 MTflECad and MTΔECad cells resuspended in PBS. After 3 weeks mice were sacrificed, H&E stained lungs paraffin-embedded sections were analyzed for lung metastasis. For the trap assay, 10^6 GFP-tagged cells were inoculated i.v. into MMTV-Neu mice, GFP-positive cells were scored in lung sections 3 days after injections.

Cryosections and paraffin sections were prepared as described previously (*76*). 7 μm cryostat sections of tumor samples were permeabilized with 0.1 % Triton-X100 in PBS, blocked with 5 % goat serum or BSA for 1 hour at RT, stained over night at 4°C with primary antibodies against CD31 (1:50; 440274, BD Pharmigen) followed by fluorescent-conjugated secondary antibodies (Alexa-Fluor, Invitrogen), nuclei were counterstained with DAPI. To measure hypoxia mice were injected i.p. with 60 mg/kg hypoxyprobe for 30 min before sacrifice and OCT sections were processed according to manufactory instructions (Hypoxyprobe^{TM} -1 Kit, HPI, USA). Immunofluorescence pictures were acquired with a Leica DMI 4000. ImageJ was used for processing and analysis of the signal intensity. Apoptosis was measured after 72 hours of salinomycin treatment by Cy5-Annexin V (559934, BP Pharmigen) staining following the manufactory protocol.

3.1.5 Supplementary data

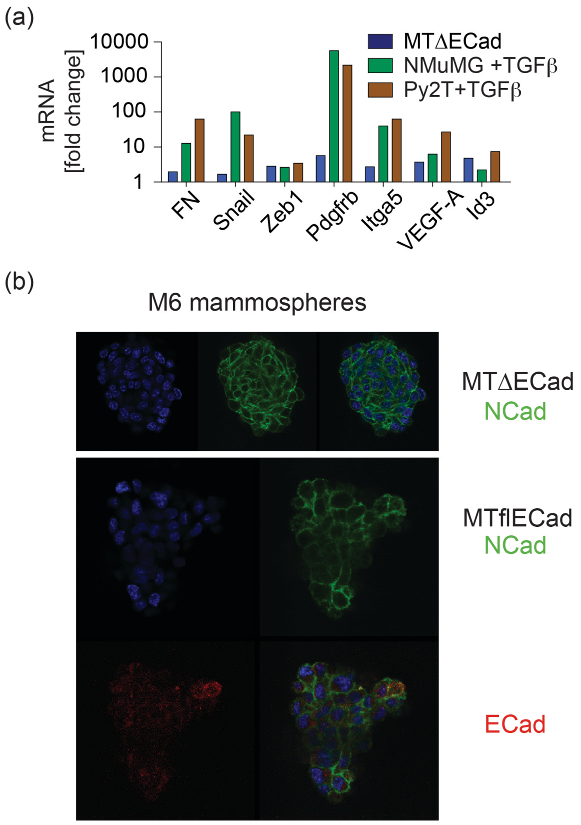

Supplementary Figure 1: Validation of genes within each GO_term in all three cellular EMT systems and the cadherin switch in late-passage MTflECad mammospheres.

(a) Differentially expressed genes representative for each GO_term were validated in the three EMT systems MTflECad/MTΔECad, NMuMG -/+ TGFβ and Py2T -/+ TGFβ by qRT-PCR. Fold changes of gene expression in the mesenchymal cells relative to their epithelial counterparts are indicated.

(b) Representative picture of passage 6 mammospheres (M6) cultured MTflECad and MTΔECad cells stained for DAPI (blue), E-cadherin (red) and N-cadherin (green). E-cadherin staining in MTΔECad cells is not shown due to the deletion of *CDH1* in these cells.

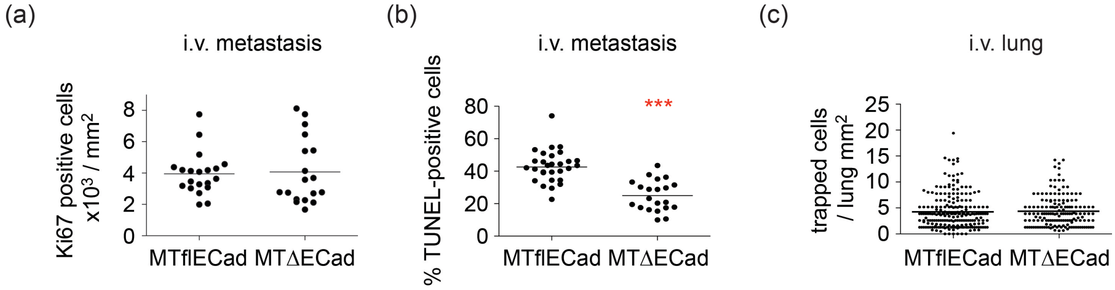

Supplementary Figure 2: Characterization of experimental metastases.

(a) Proliferating cells within the metastases were analyzed by staining for Ki67 (N = 6 mice).

(b) Apoptotic cells were visualized by TUNEL staining and counted within the lung metastases (N = 6 mice).

(c) 10^6 MTflECad-GFP and MTΔECad-GFP cells were injected into the tail vein of 8-week old MMTV-Neu mice. 3 days after injection, lungs were taken out and the amount of GFP-positive cells per lung section was quantified (N = 2 mice).

One datapoint represents one field of view. Statistical analysis of the quantifications was performed by Mann Whitney U test with *** $p < 0.001$.

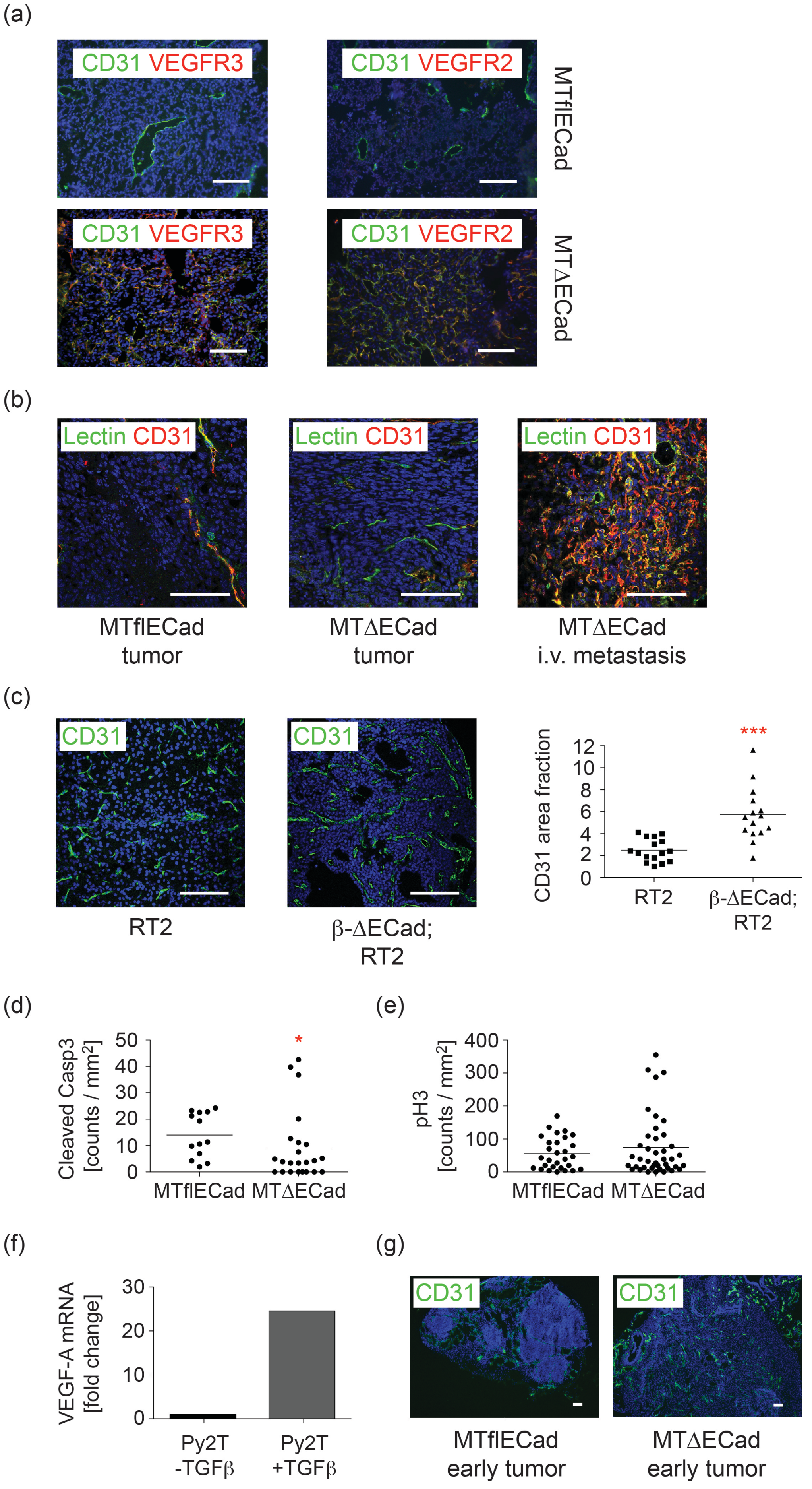
(a)
CD31 VEGFR3
CD31 VEGFR2
MTflECad
CD31 VEGFR3
CD31 VEGFR2
MTΔECad
(b)
Lectin CD31
Lectin CD31
Lectin CD31
MTflECad tumor
MTΔECad tumor
MTΔECad i.v. metastasis
(c)
CD31
CD31
RT2
β-ΔECad; RT2
CD31 area fraction
0
2
4
6
8
10
12
***
RT2
β-ΔECad; RT2
(d)
Cleaved Casp3 [counts / mm²]
0
10
20
30
40
50
*
MTflECad
MTΔECad
(e)
pH3 [counts / mm²]
0
100
200
300
400
MTflECad
MTΔECad
(f)
VEGF-A mRNA [fold change]
0
10
20
30
Py2T -TGFβ
Py2T +TGFβ
(g)
CD31
CD31
MTflECad early tumor
MTΔECad early tumor

Supplementary Figure 3: Active angiogenesis in further EMT models.

(a) Blood vessels induced by MTΔECad tumors are active, visualized by co-staining of CD31 (green) to indentify vessels and the angiogenic receptors VEGFR2 (red) and VEGFR3 (red).

(b) Perfusion of vessels was visualized by injecting FITC-Lectin into mice prior to sacrifice. Co-staining of the endothelial marker CD31 (red) and Lectin (green) shows functionality of the blood vessels in MTflECad and MTΔECad tumors as well as in experimental metastases of MTΔECad cells.

(c) Representative CD31 staining and quantification of control Rip1Tag2 (RT2) tumors and Rip1Tag2 tumors with a β-cell specific *CDH1* knockout (β−ΔECad;RT2). One datapoint represents one mouse.

(d, e) MTflECad and MTΔECad tumors were analyzed for apoptosis (d) and proliferation (e) by immunofluorescence staining for cleaved Caspase3 and pHistone3, respectively (N = 4 mice).

(f) qRT-PCR analysis of the cellular EMT model Py2T showing an upregulation of VEGF-A expression in the mesenchymal Py2T +TGFβ cells.

(g) MTflECad and MTΔECad cells were injected into RG mice. When the first tumors were just palpable all mice were sacrificed and mammary glands were taken out for analysis. CD31 staining revealed that already very small MTΔECad tumors (about 2 mm in diameter) are highly vascularized.

Scale bars, 100 μm. Statistical analysis of the quantifications was performed by Mann Whitney U test with *** $p < 0.001$.

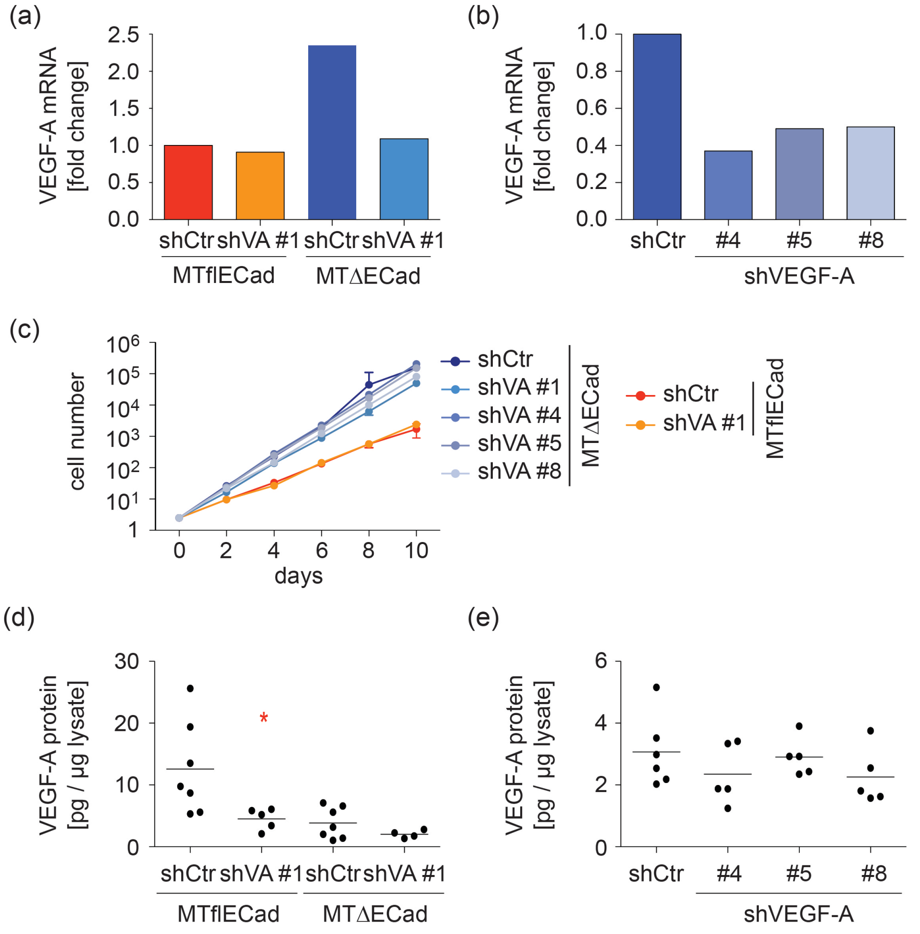

Supplementary Figure 4: *In vitro* and *in vivo* characterization of VEGF-A signaling interference.

(a) The knockdown efficiency of the shRNA against VEGF-A (shVA #1) was monitored by qRT-PCR. The MTflECad shCtr sample was used as reference to set the fold change. Notably, the knockdown of VEGF-A in MTflECad cells is not effective in cells, which changes *in vivo* (d).

(b) The knockdown efficiency of the further shRNA against VEGF-A (shVA #4, #5, #8) was monitored by qRT-PCR. The MTΔECad shCtr sample was used as reference to set the fold change.

(c) Growth curves for MTflECad and MTΔECad cells with or without knockdown of VEGF-A (N = 2 experiments).

(d, e) VEGF-A protein abundance was measured in tumors by ELISA. Statistical significance was calculated using Mann Whitney U test with * $p < 0.05$.

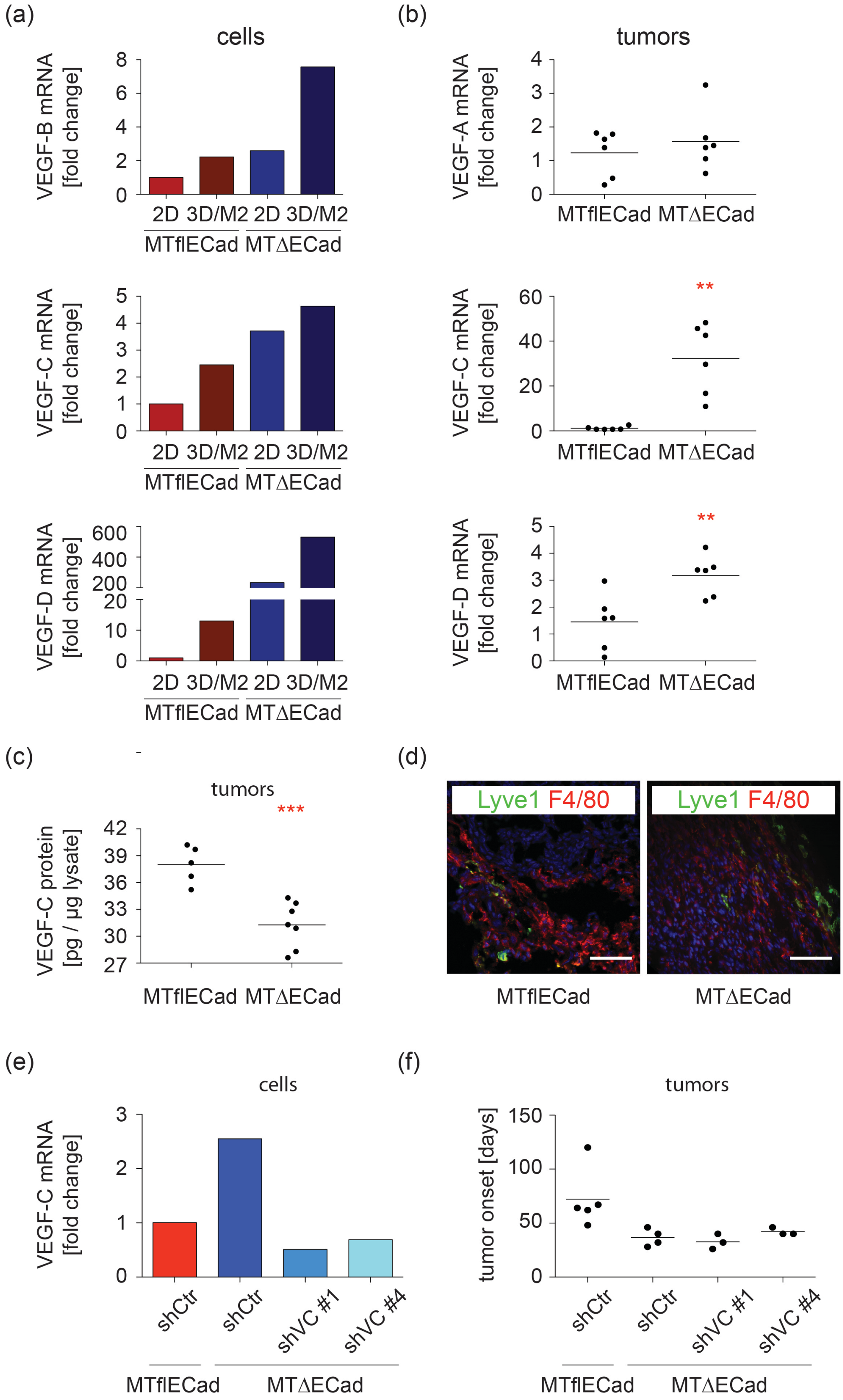

Supplementary Figure 5: Angiogenic factors are upregulated in MTΔECad cells and tumors but are not necessary for early tumor onset.
(a) Expression analysis by qRT-PCR reveals an upregulation of the angiogenic factors VEGF-B, VEGF-C and VEGF-D in MTΔECad cells when compared to MTflECad cells (2D MTflECad cells set to fold 1).

(b) Expression analysis by qRT-PCR of tumor samples shows an increased expression of VEGF-C and VEGF-D in MTΔECad originated tumors compared to MTflECad tumors. No change in VEGF-A mRNA expression levels could be observed. mRNA expression levels are plotted as fold changes using the mean of MTflECad tumor as the reference.
(c) MTflECad and MTΔECad tumors were analyzed for their VEGF-C protein levels by ELISA which do not reflect the mRNA expression levels of VEGF-C (Supplemental Fig. 4).
(d) Both, MTflECad and MTΔECad tumors show barely any lymphatic vessels visualize by Lyve1 staining (green). Most Lyve1-positive cells are also F4/80-positive indentifying them as macrophages.
(e) qRT-PCR was performed in order to assess the knockdown efficiency of the 2 small hairpins against VEGF-C (shVC #2 and shVC #4). MTflECad cells were set to fold 1.
(f) 200 cells were transplanted orthotopically into RG mice and the tumor onset was measured.
Scale bars, 100 μm. Statistical significances were calculated by Mann-Whitney U test with ** $p < 0.01$, *** $p < 0.001$.

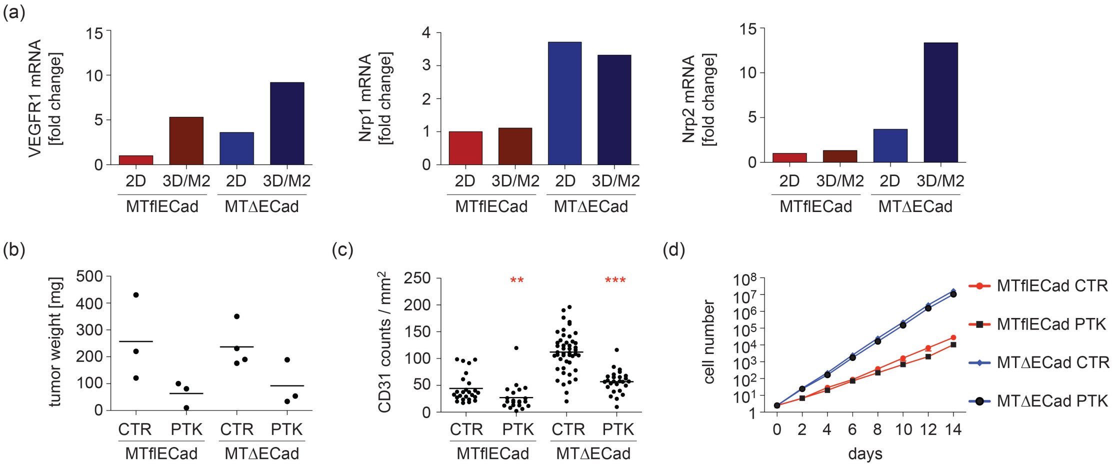

Supplementary Figure 6: Tumor growth is impaired open VEGFR inhibitor treatment *in vivo*.
(a) Expression analysis by qRT-PCR reveals an upregulation of VEGFR1, Nrp1 and Nrp2 in MTΔECad cells when compared to MTflECad cells (2D MTflECad cells set to fold 1). VEGFR2 and VEGFR3 are not expressed in either of the cells (data not shown).
(b, c) RG mice were injected with 10^5 MTflECad or MTΔECad cells and treated daily *per os* with the solvent polyethylene glycol (CTR) or with 75 mg/kg of the pan VEGFR inhibitor PTK787/ZK222584 (PTK). The experiment was terminated after 15 day of treatment. The tumor weight was measured (b) and the microvessel density was assessed (c) (N = 3 mice). Statistical significances were calculated by Mann-Whitney U test with ** $p < 0.01$ and *** $p < 0.001$.
(d) Growth curves of MTflECad cells and MTΔECad cells treated with solvent polyethylene glycol (CTR) or 5 µM PTK were performed twice.

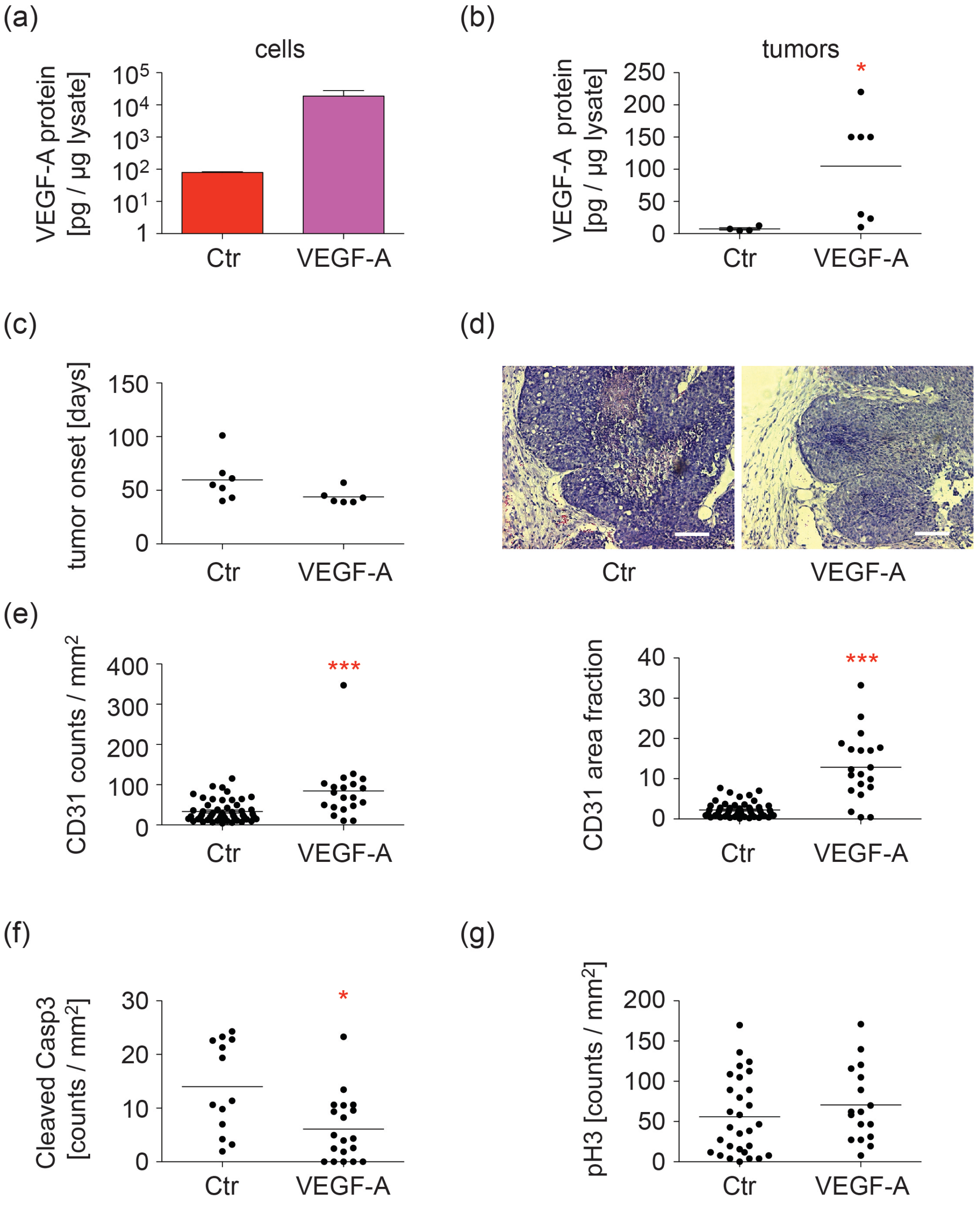

Supplementary Figure 7: VEGF-A overexpression in MTflECad cells is not sufficient to induce an early tumor onset.
200 MTflECad cell either overexpressing a control vector (Ctr) or VEGF-A were injected orthotopically into RG mice. Mice were sacrificed when the tumors reached the volume of 1.5 cm^3.
(a, b) ELISA of secreted VEGF-A in MTflECad cells (a) or in their formed tumors (b) reflects the overexpression of VEGF-A.
(c) Tumor onset of MTflECad cells overexpressing VEGF-A or not (Ctr) was monitored and mice were sacrificed when the tumor reached the volume of 1.5 cm^3.
(d) H&E stained light microscopic pictures of these tumors show less necrotic areas within the tumors but otherwise no morphological change.
(e) The angiogenic effect of the overexpression of VEGF-A was quantified by CD31 staining. VEGF-A overexpressing MTflECad tumors have more vessels and a higher CD31 area fraction (N = 4 mice).
(f, g) MTflECad tumors overexpressing a control vector or VEGF-A were analyzed for apoptosis (f) and proliferation (g) by immunofluorescence staining for cleaved Caspase3 and pHistone3, respectively (N = 4 mice).
Scale bars, 100 μm. Statistical significances were calculated by Mann-Whitney U test with * $p < 0.05$ and *** $p < 0.001$.

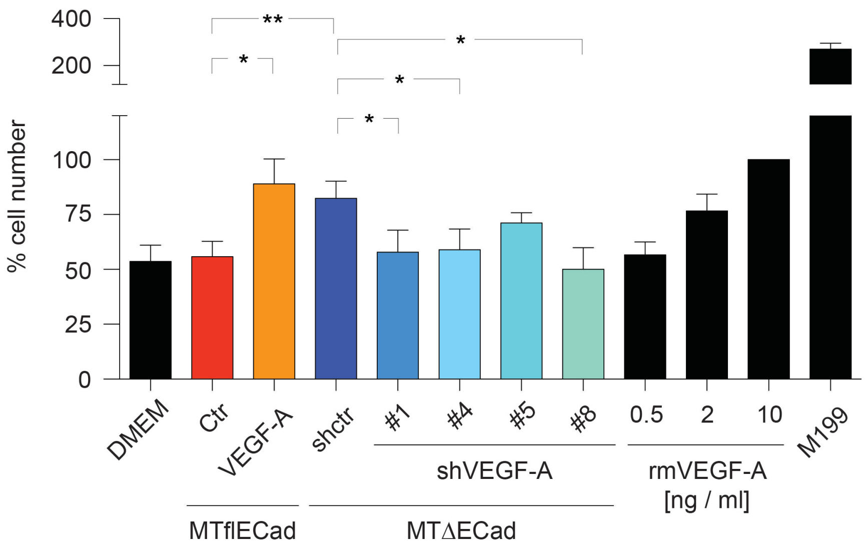

Supplementary Figure 8: MTΔECad supernatant enables endothelial cells to grow *in vitro*.
(a) Human umbilical vein endothelial cells (HUVEC) were grown in conditioned media of MTflECad cells with VEGF-A overexpression (VEGF-A) or without (Ctr) or in conditioned media of MTΔECad cells expressing the different shVEGF-A constructs as indicated. Conditioned media were refreshed 2 days after plating and after 5 days of cultivation the vital HUVEC cells were counted with a Neubauer chamber by trypan blue exclusion. As a negative control unconditioned media of MTflECad and MTΔECad cells and as a positive control HUVEC media (M199) was used. To determine the effect of VEGF-A alone, unconditioned media was supplemented with 10, 2 and 0.5 ng/ml recombinant murine VEGF-A (rmVEGF-A). Cell numbers are represented as % of cells of HUVECs treated with 10 ng/ml rmVEGF-A. Mean values of 4 different experiments are plotted with the SEM. Statistical significances where calculated by paired Student's t-test with * $p < 0.05$, ** $p < 0.01$.

CD24+	**adherent**	**M1**	**M2**	**M3**
MTflECad	76.5% (+/- 8.2)	63.1% (18.9)	51.5% (43.9)	50.1%(36.6)
MTΔECad	94.3% (+/- 3.2)	74.0% (7.5)	78.1% (10.0)	74.9% (23.2)
Py2T	87.3% (+/- 5.3)	98.5%	91%	82.3%
Py2T LT	95.7% (+/- 1)	97.7%	93.7%	96.6%
E9	97.8% (+/- 2.6)	99.1% (0.4)	98.7% (1.0)	97.6% (1.6)
E9 LT	99.1% (+/- 1.4)	91.7% (1.8)	91.6% (0.1)	99.1% (0.9)

CD29+	**adherent**	**M1**	**M2**	**M3**
MTflECad	99.8% (+/-0.2)	99.7% (0.5)	99.8% (0.1)	99.9% (0)
MTΔECad	99.9% (+/-0.2)	63.1% (0.2)	99.9% (0.1)	99.9% (0.1)
Py2T	99.8% (+/-0.1)	100%	99.9%	99.9%
Py2T LT	99.9% (+/-0.1)	100%	99.8%	100%
E9	99.9% (+/-0.1)	99.5% (0.3)	99.3% (0.9)	98.9% (1.4)
E9 LT	99.8% (+/-0.2)	99.4% (0.4)	99.6% (0.1)	100% (0)

CD49f+	**adherent**	**M1**	**M2**	**M3**
MTflECad	96.8% (+/-2)	99.4% (0.2)	99.5% (0.4)	99.9% (0.1)
MTΔECad	98.6% (+/-1.1)	99.8% (0.1)	99.7% (0.3)	99.9% (0.1)

Supplementary Table I: cancer stem cells surface marker expression.
Cancer stem cells surface marker expression analysis evaluated by FACS of epithelial and mesenchymal cells. Values represent the percentage of positive cells per each staining. Cells analyzed were either cultured in 2D or 3D in three sequential passages (M1-3). 2 or 3 replicates with standard deviation in parenthesis are shown.

	Cells: MTΔECad/MTflECad
IGF-II	6.84
VCAM-1	5.19
GAS1	4.91
Axl	4.56
CTACK	2.92
IL-4	2.78
IL-12 p70	2.73
GM-CSF	2.65
P-selectin	2.62
IL-2	2.61
fractalkine	2.55
galectin1	2.53
sTNFRII	2.53
IL-3	2.51
BLC	2.47
PF-4	2.46
eotaxin	2.43
IGFBP-3	2.36
CXCL16	2.35
IFNγ	2.32
SDF-1α	2.30
L-selectin	2.27
MIP-3β	2.27
MCP1	2.23
IL-10	2.22
MIP-2	2.20
IL-1β	2.20
IL-12 p40/p70	2.18
IL-1α	2.17
IL-13	2.16
Timp-1	2.13
TPO	2.12
VEGF	2.04
KC	1.98
lymphotactin	1.95
TCA-3	1.94
IL-3Rβ	1.92
MIP-1g	1.88
bFGF	1.86
EGF	0.47
JAM-A	0.47
neprilysin	0.40
MAdCAM-1	0.37
HAI-1	0.32
osteopontin	0.22
MFG-E8	0.14
IL-1rα/IL1F3	0.13
E-cadherin	0.03

	Tumors: MTΔECad/MTflECad
Pro-MMP-9	6.34
GAS2	5.62
MIP-1γ	3.85
bFGF	3.46
VCAM-1	3.06
4-1BB	2.76
thymus CK1	2.43
galectin	2.39
MMP-3	2.02
CYCL16	1.94
JAM-A	1.91
sTNFRI	1.82
FcγRIIB	1.82
cardiotropin-1	0.53
osteopontin	0.35
E-cadherin	0.19

Supplementary Table II: protein array.
Lysates from MTflECad and MTΔECad cells and tumors were compared for expression of 144 proteins. Ratios between MTΔECad and MTflECad lysates are shown.

3.1.6 Supplementary Methods

Antibodies

Antibodies: VEGFR2 (R&D Systems, AF644), VEGFR3 (R&D Systems, AF743), cleaved Caspase3 (1:100, Asp175, 9664, Cell Signaling), pHistone3 (1:200, 06-570, Millipore), Lyve1 (1:200, 103-PA50S/0412P02-2, ReliaTech), F4/80 (1:100, MCAO497, Serorec), Ki-67 (1:50, clone Tec3 DAKO), CD31 for IHC (clone ER-MP12, Bachem, T-2001), TUNEL (in situ death detection kit, Roche, 1684817)

Cell lines and reagents

A subclone of NMuMG cells (NMuMG/E9; hereafter NMuMG) expressing E-cadherin has been described earlier (*99*). MTflECad and MTΔECad cells were previously described from our lab (*76*). Py2T cells were established from an MMTV-PyMT mammary gland tumor (*100*). Py2T, NMuMG, MTflECad and MTΔECad cells were cultured in DMEM supplemented with glutamine, penicillin, streptomycin and 10 % FCS (Sigma-Aldrich). NMuMG and Py2T, cells were treated with 2 ng/ml TGFβ (R&D Systems) without serum deprivation and replenished every three days. MTflECad and MTΔECad cells received 10^{-4}-10^{-7} mM salinomycin (Sigma-Aldrich) for 72 hours. HUVECs were cultured in M199 supplemented with 40 μg/ml bovine pituitary gland extract, 80 U/ml Heparin, 20 % FCS, glutamine, penicillin and streptomycin.

Mammospheres formation assay

Cells were grown in non-adherent ULA-plates (Cornig) in DMEM/F12 (SIGMA) supplemented with B27 (GIBCO), 20 ng/ml EGF (Invitogen), 20 ng/ml bFGF (Invitrogen), 1 U/ml Heparin (Roche), glutamine, penicillin, streptomycin and 1 nM estradiol (Sigma), seeded at 200,000 cells/ml (M1) and passaged every seven days by trypsin dissociation and subsequent re-plating at clonal density of 50,000 cells/ml (from M2 onwards) (*61*). One fourth of fresh medium was added every second day. To avoid aggregates formation 1 % methylcellulose (SIGMA) was added to the medium.

RT-qPCR

To evaluate transcripts relative expression levels, RNA was isolated using TriReagent (Sigma-Aldrich), reverse transcribed with MMLV reverse transcriptase (Promega, Wallisellen, Switzerland), and cDNA was quantified by qPCR (StepOne

Plus, Applied Biosystems) using Mesa Green pPCR MasterMix plus (Eurogentec). The following primers have been used:

mRNA	**Forward primer (5’-3’)**	**Reverse primer (5’-3’)**
Rpl19	ctcgttgccggaaaaaca	tcatccaggtcaccttctca
VEGF-A	actggaccctggctttactg	tctgctctccttctgtcgtg
Nrp1	cccggaggaatgttctgtc	ccaatgtgagggccaactt
Nrp2	atggctggacacccaattt	atggttaggaagcgcaggt
VEGFR1	acctccgtgcatgtgtatga	catggacagccgataggac
fibronectin	cccagacttagtgtggcaatt	aatttccgcctcgagtctga
Snail1	ctctgaagatgcacatccgaa	ggcttctcaccagtgtgggt
ZEB1	gccagcagtcatgatgaaaa	tatcacaatacgggcaggtg
Pdgfrb	acctgcagagacctcaaaaggtg	ctgatcttcctcccagaaagtcaca
Itga5	caccaccattcaatttgacagca	gctcctctcccttggcactgta
Id3	gaggagcttttgccactgac	gctcatccatgccctcag
VEGF-B	cccagccaccagaagaaa	acattgcccatgagttccat
VEGF-C	aacacacagaagtgcttcctt	ttcgcacacggtcttctgta
VEGF-D	gcacctcctacatctccaaacag	ggcaagcacttacaacccgtat

Rpl19 was always used for normalization (ΔCt). Results are presented as fold change of the normalized (ΔΔCt).

Viral infections:

Lentiviral shRNA constructs were purchased from Sigma-Aldrich: (Mission Non-Targeting shRNA control vector, SHC002; shVEGF-A #1: TRCN0000066818, #4: TRCN0000304451, #5: TRCN0000310985, #8: TRCN0000316047). Retroviral pAMFG-mVEGF-A_IRES_CD8 expression vector was a kind gift from A. Banfi, University of Basel.

Viral expression plasmids were transfected into packaging cell lines (Plat-E for retroviruses, HEK293T for lentiviruses) using FugeneHD (Roche). HEK293T cells were additionally transfected with the packaging vector pR8.92 and the envelope encoding plasmids pVSV. One day conditioned virus-containing supernatant was harvested, filtered with a 0.45 μm pore filter, supplemented with 8 ng/ml polybrene and added to the target cells. The target cells were centrifuged with the viral supernatant for 90 min, 1000 xg, 30 °C, followed by 3 hours incubation at 37 °C and 5 % CO_2 afterwards cells were given fresh medium.

ELISA

Cell culture supernatants and tumor lysates were analyzed for the presence of mVEGF-A (Quantikine ELISA kit; R&D MMV00) and mVEGF-C (Platinum ELISA kit from eBioscience), following the manufacturer's instructions.

FACS staining

For FACS analysis of surface receptors we have used the following antibodies: CD24-Biotin (553260, BD Pharmigen), CD44-PE (553143, BD Pharmigen), CD49f-biotin (MCA699BT, Serotec), CD90 (Thy1.1), EPCAM (347197 BD), and mammospheres cultured cells were stained for 1hr at RT with combinations of different antibodies, followed by secondary antibody coupled to fluorochromes, PI stained, and analyzed at the FACSCanto II, population was gated for living cells and doublets were excluded.

Histological analysis

Rip1Tag2;ΔECad mice carrying a deletion of the E-cadherin gene specifically in the β-islets of Langerhans were previously described by us (*76*). BALB/c $Rag2^{-/-}$;$common\gamma^{-/-}$ mice were kindly provided by T. Rolink.

The preparation of histology samples and cryo-samples was done as described before (*76*).

Trap assay

10^6 GFP-labeled MTflECad or MTΔECad cells were injected i.v. into MMTV-Neu mice. 3 days after injection, mice were sacrificed and lungs were embedded in OCT. Each lung was cut through with 35 μm sections, stained with DAPI and analyzed for GFP-positive cells per field.

Lectin perfusion

To detect vessels permeability mice were injected i.v. with 100 μl of 1 mg/ml fluorescein-conjugated lycopersicon esculentum lectin (FL-1171, Vector Laboratories) followed by PFA perfusion after 2 min.

PTK treatment

To block VEGF signaling mice were treated daily p.o. with 75 mg/kg PTK787/ZK222584 for 14 days starting one day after tumor cells transplantation.

Statistical analysis

Statistical analysis and graphs were generated with the help of GraphPad Prism software (GraphPad Sofware Inc, San Diego, CA) using the indicated methods.

Microarray processing and data analysis

RNA was isolated from MTflECad and MTΔECad cells using TriReagent (Sigma-Aldrich) and RNA quality and quantity evaluated with the Agilent 2100 Bioanalyzer (Agilent Technologies). The RNA was processed to cDNA according to Affymetrix protocols and analyzed on the Affymetrix 430a2 mouse array. Raw microarray data were normalized with Robust Multi-Array (RMA) and analyzed using R software (www.r-project.org). Microarray probesets were annotated to mouse Refseq IDs with the brainarray annotation package (http://brainarray.mbni.med.umich.edu/Brainarray/). Differentially expressed genes between MTflECad and MTΔECad were determined using linear modeling with limma and Empirical Bayes Statistics. Probesets were considered differentially expressed if they showed a least 2-fold change in expression, an average log expression of at least 3 and logOdds of at least 0. Differentially expressed genes were analyzed for GO term enrichment in R. GO categories with an adjusted p-value of 0.01 or smaller (by Benjamini & Hochberg), containing between 1000 and 200 genes per category to avoid getting too general or too specific pathways, are reported. R version R2.13.0 and the packages limma_3.8.2 and GO.db_2.5.0 were used.

3.2 The functional role of ephrinB2 in mesenchymal cell migration

3.2.1 Abstract

Cancer and its progression to metastatic disease is one of the leading causes of death. The invasive phenotype of cancer cells and metastatic spread is often associated with epithelial to mesenchymal transition (EMT). The hallmarks of the EMT process are the loss of epithelial cell polarity and cell-cell adhesions, accompanied by *CDH1* silencing and a gain of migratory and invasive capabilities (*32*).

In order to investigate factors changing upon EMT, three independent cellular model systems were investigated on their gene expression level. Upon others, the expression of ephrinB2 was found to be commonly upregulated. EphrinB2 is a member of the Eph-ephrin cell-cell communication system, which allows cells to react upon binding to each other by Eph-mediated forward and ephrin-mediated reverse signaling. Eph-ephrin signaling predominantly uses the actin cytoskeleton to conduct its output, which is mostly cell repulsion.

I show that in NMuMG cells that underwent EMT, as well as in mesenchymal MTΔECad cells, siRNA-mediated knockdown of ephrinB2 reduces the cells' general migratory capability. This effect on migration is carried out by an over-stabilization of focal adhesions, not allowing cells to retract they rear end. In this way, ephrinB2 knockdown cells, when plated on a thin line of substrate, rather elongate than move forward independent of cell-cell contacts. Investigating the role of ephrinB2 in breast cancer, a knockout of *efnb2* in breast epithelial cells could not reveal a critical role of ephrinB2 for tumor growth or metastasis.

3.2.2 Introduction

3.2.2.1 The Ephrin system

The ephrin system is comprised of Eph receptors (Eph) and Eph receptor interacting ligands (ephrins). Eph receptors form the largest group of receptor tyrosine kinases (RTK). Their extracellular part is composed of a globular ligand-binding domain, a cysteine-rich region, and two fibronectin type III repeats. Their intracellular parts comprise a juxta-membrane region, a tyrosine kinase domain, a sterile α motif (SAM) protein-protein interaction domain, and a C-terminal PDZ-binding site (Fig. 11). Eph receptors include members of the EphA subclass (EphA1-8, 10) and members of the EphB subclass (EphB1-4, 6), however, EphA10 and EphB6 lack kinase activity. The subdivision into A and B categories can be attributed to the ligands they bind to. Whereas the ephrinA ligands (ephrinA1-5) are proteins that are attached to the plasma membrane via glycosylphosphatidylinositol (GPI) anchors, ephrinB ligands (ephrinB1-3) are transmembrane proteins with a C-terminal intracellular part. This intracellular part can be bound by Src-homology-2 (SH2) domain adaptor proteins and by proteins carrying a PDZ-motif. Despite the preferential binding of class A and B receptors and ligands within their group, high promiscuity allows even binding across subclasses, although with lower affinities (*101*).

Eph-ephrin expression pattern

Ephrins and their receptors are classically expressed on opposing cells allowing contact-depending communication between them. The main output of such a contact between different cells is repulsion mediated by actin cytoskeleton remodeling. Other examples for Eph-ephrin signaling outputs are modulations in morphology, migration, invasion and cell adhesion.

Ephrins' and Eph receptors' most prominent function is their role during neuronal development by axon guidance and during vasculogenesis and angiogenesis. Being essential for arterious and venous endothelial cell determination, ephrinB2 and EphB4, respectively, mark exclusively their subtype of blood vessels. Along this line, the Eph-ephrin system is extremely important for tissue pattern formation. The differential expression of ligands and receptors on cell surfaces leads to repulsion as soon as different cells come in contact to each other. This repulsive effect restricts the mixture of cell types that are not supposed to intermingle (*102*). The importance of segregation of cell types has been shown in various tissue examples such as the intestine (*103*). Eph-ephrin system components are also expressed in lymphoid organs and lymphocytes where direct communication between cells is crucial for positive and negative selection of lymphocytes (*104*).

Eph-ephrin signaling

Eph-ephrin signaling is extremely complex. Apart from the promiscuity of ligands and receptors, both entities are able to transduce signals in their cells. So-called forward signaling by Eph receptors stimulates intracellular signals. In contrast to classical RTK signaling, Eph receptors are poor Ras-MAPK and PI3K-PKB pathway activators and rather induce RhoGTPase signaling. Ephrins, on the other side, lack intrinsic kinase activity and thus use members of the non-receptor tyrosine kinase family, i.e. src family kinase proteins, to conduct so-called reverse signaling (Fig. 11). Apart from signaling via phosphorylation, Eph receptors and ephrinB ligands additionally have C-terminal PDZ domain-binding sites (*101*). The importance of the PDZ domain-binding sites has been demonstrated by its removal in the ephrinB2 protein, leading to major developmental defects in the lymphatic system and during angiogenesis when conditionally expressed in endothelial cells (*105,106*).

Another level of complexity for Eph-ephrin signaling is introduced by the fact that receptor/ligand dimers have to bind to other Eph/ephrin dimers to form tetramers which further cluster laterally to achieve full signaling strength. The amount of lateral clustering within cells decides how strong a signal is. The signal could be even inhibitory if only few clusters are formed or if unclustered soluble ligands are applied to receptor expressing cells. In the case where receptors and ligands are expressed on the same cell, it is not totally clear which effect is predominant, but it has been found that interaction of receptors and ligands *in cis* would mask rather than stimulate signaling. Apart from reacting with each other *in cis*, Eph receptors and ephrins can also act in parallel being located in different subcellular membrane patches (*107*).

Upon trans-binding of receptors and ligands and further lateral clustering, the whole cell-cell interaction complex is internalized by the cell. This often occurs together with the surrounding plasma membrane patches allowing repulsion of cells. This effect can be realized by cleavage of either the Eph receptor or the ligand e.g. by ADAM10 (a disintegrin and metalloproteinase domain 10) (Fig. 11). Internalization of Eph-ephrin complexes results in their destruction and ultimately leads to signal termination. While strong kinase-dependent Eph signaling mainly results in repulsion, weaker signaling by less clustering or strong phosphatase activity leads to cell adhesion. The association of Eph-ephrin clusters with E-cadherin further favors adhesion (*108*).

Uncoupling the function of the Eph-ephrin system, single molecules of ligands and receptors can act independently of each other though crosstalk with various signaling systems. These include epidermal growth factor receptor (EGFR), fibroblast growth factor receptor (FGFR) and Wnt signaling. Like most signal transducers, also the Eph-ephrin system can be influenced by other pathways, thus being embedded into the whole cellular signaling network (*109*).

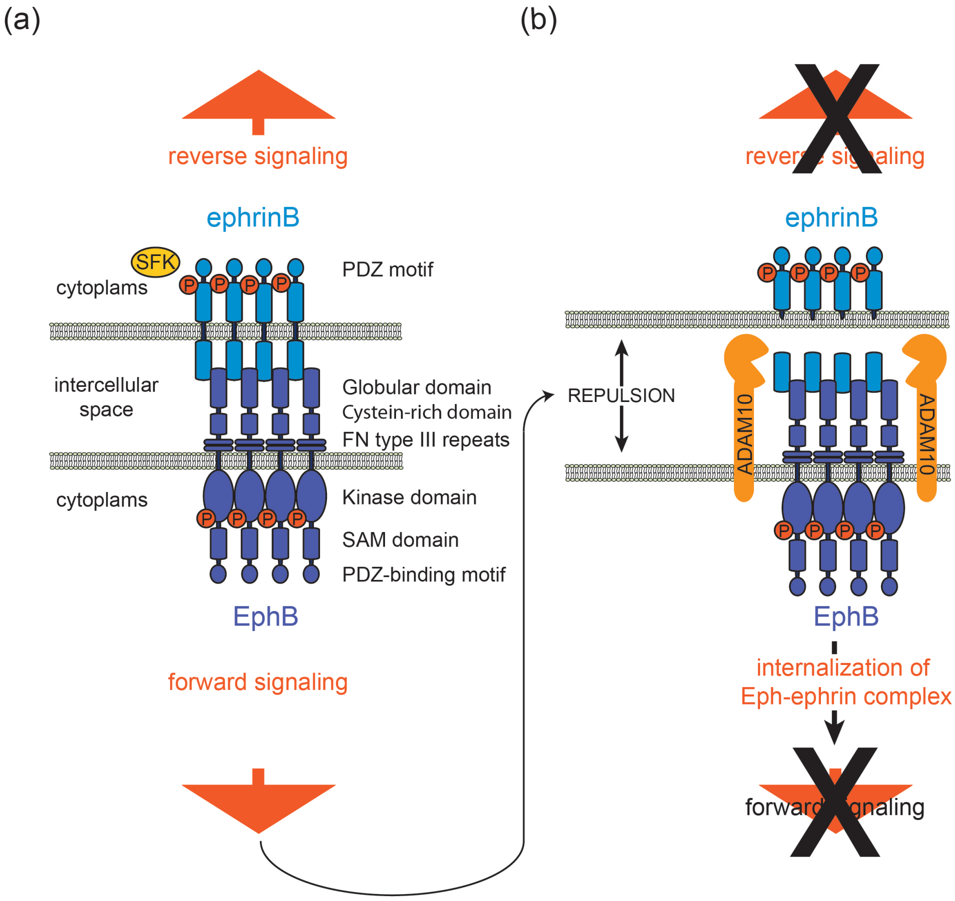
(a)
(b)
reverse signaling
ephrinB
SFK
cytoplams
P
PDZ motif
intercellular space
Globular domain
Cystein-rich domain
FN type III repeats
cytoplams
Kinase domain
SAM domain
PDZ-binding motif
EphB
forward signaling
reverse signaling
ephrinB
REPULSION
ADAM10
ADAM10
EphB
internalization of Eph-ephrin complex
forward signaling

Figure 11: Schematic representation of Eph-ephrin signaling.
(a) EphB receptors (dark blue) with there indicated domains bind with the globular domain to ephrins (light blue) expressed by opposing cells. Upon receptor-ligand binding, Ephs cross phosphorylate (P) each other leading to active forward signaling. In the opposing cells clustering of ephrins leads to e.g. recruitment of src family kinases (SFK), which phosphorylate ephrins. Phosphorylated ephrins conduct reverse signaling.
(b) Repulsion of opposing cells can be carried out when ADAM10 or other proteolytic enzymes cut the whole Eph-ephrin complex which leads to its internalization, segregation of cells and consequently to termination of Eph-ephrin signaling.

The Eph-ephrin system in cancer

Ephrins and Eph receptors have been found both up- and downregulated in cancer. EphA2, for instance, is upregulated in many cancers and correlates with cancer progression and poor clinical outcome. More specifically, in breast cancer EphA2 expression is predominant in the more aggressive basal subtype. Another example for an association with cancer malignancy is EphB4 expression. On the other hand, several proteins of the Eph-ephrin system, such as EphA1, EphA5, EphB4 and EphB6, have been found downregulated in advanced cancers, arguing for anti-cancerous effects of these factors, at least in specific cancer types. Speaking for a more general tumor-suppressive function is the notion that Eph receptors seem to have a remarkable ability to oppose oncogenic signaling pathways like H-Ras or PI3K. Again, the complexity of the system allows different members of the Eph-ephrin network to be pro- or anti-tumorigenic. Most likely, the combination and amount of Ephs and ephrins expressed, as well as the signaling network they are embedded in, play a major role in determining the significance that each molecule would have during tumor development (*109*).

Interestingly, the expression of Eph-ephrin molecules on cancer cells alone might not decide whether tumor growth is promoted or repressed. The surrounding tissue, expressing the matching ligand or receptor, could keep tumor cells from invading by conducting repulsive effects. In addition to the confinement by neighboring cells, an overactivation of the Eph-system can lead to tight adhesion of cells within the tumor. As an example, ephrinB2 is present in endothelial cells and adjoining smooth muscle cells and pericytes (*109*).

EphrinB2

EphrinB2, encoded by the *Efnb2* gene, serves as a ligand for the Eph receptors EphB2, EphB3, EphB4 and EphA4 (*110*). The crystal structure of ephrinB2 binding to EphB2 has been solved to get deeper insight into the nature of this association (*111*).

During vascular development, as mentioned above, arterial endothelial cells express ephrinB2 while venous endothelial cells are marked by EphB4. The relevance of ephrinB2 expression during vascular development is strengthened by the observation that *Efnb2* knockout mice die early (E11.5) due to a failure to properly remodel the embryonic vasculature (*112*). The differential expression of ephrinB2 and its receptors does not only lead to boundary formation within the capillary endothelial cells but is also important for communicating with surrounding mesenchymal cells to form a mature vasculature (*113*).

The mechanistic role of ephrinB2 during angiogenesis has recently been unraveled. EphrinB2 has been shown to be essential for VEGFR2 internalization and activity, allowing tip cell filopodia extension in angiogenic vessels (*106*). Similar results could be demonstrated during angiogenic and lymphangiogenic growth, where ephrinB2 was necessary for VEGFR3 internalization and signaling (*114*). Along theses lines, an antibody targeting ephrinB2 reduces endothelial cell migration *in vitro* and the number of blood and lymphatic vessels as well as tumor growth *in vivo* (*115*).

On the cell biology level, human umbilical vein endothelial cells (HUVECs) react to ephrinB2 overexpression by increased random migration associated with repeated contraction-expansion cycles. This motility phenotype is independent of receptor binding but dependent on ephrinB2's C-terminal PDZ-motif (*116*). EphrinB2-deficient smooth muscle cells show defective focal adhesion formation, poor spreading, non-polarized lamellipodia and increased non-directional motility (*117*).

In the mammary gland, ephrinB2 expression is limited to luminal epithelial cells, whereas EphB4, ephrinB2's cognate receptor, is predominantly expressed by myoepithelial cells. The expression of both proteins is highly dependent on estrogen abundance (*118*). Overexpression of ephrinB2 within the mammary gland, using the MMTV promoter, leads to a delayed mammary gland development. During pregnancy and lactation, overexpression of ephrinB2 results in precocious differentiation. The transgenic expression of an ephrinB2 variant that is unable to perform reverse signaling (ephrinB2ΔC) delays epithelial differentiation (*119*). In two models of mammary carcinogenesis, the Wap-Ras and Wap-Myc transgenic mice, ephrinB2 expression was lost upon tumor progression (*118*). Additionally arguing for reverse signaling opposing tumor progression is the finding that ephrinB2ΔC transgenic expression in mice leads to shorter tumor latency and increased metastasis in an MMTV-Neu breast cancer model. However, the overexpression of wild type ephrinB2 has no effect on tumor latency or metastasis (*119*).

A full knockout of *Efnb2* results in embryonic lethality around E11 (*112*). Therefore, conditional alleles of *Efnb2* have been generated (*120*). A conditional knockout of *Efnb2* in the mammary gland under the control of the wap-cre promoter (active at the 13th day of pregnancy) causes a disturbed architecture of the mammary gland that is not able to properly produce milk. Additionally, less E-cadherin staining between epithelial cells was observed, resulting in an instable mammary gland epithelium, associated with cell death (*121*). On the other hand, embryonic stem cells that are deficient for the E-cadherin gene show increased levels of ephrinB2 expression, which can be rescued by re-expressing E-cadherin in these cells (*122*).

Although it is clear that ephrinB2 is crucial during angiogenesis and migration of cells, not a lot is known about its function in cancer cells. Studies of ephrinB2 in melanoma cells have found that stimulation with ephrinB2 induces EphB4 forward signaling that increases RhoA activity and cell migration (*123*). Along this line, overexpression of ephrinB2 in B16 melanoma cell leads to activation of focal adhesion kinase (FAK), increased β1-integrin-mediated adhesion to laminin and fibronectin and cell migration (*124*). Similar results have been found in glioma cells (*125*). In contrast to these observations, stimulation of breast cancer cells with ephrinB2 leads to Ephb4-dependent inhibition of proliferation, migration and invasion (*126*). In patients, positive correlations between ephrinB2 expression in melanoma, glioma, oesophageal squamous carcinoma, uterine endometrial, uterine cervical and ovarian cancer and tumor progression have been found (*107*). These correlations not necessarily need to reflect a pro-tumorigenic function of ephrinB2 in tumor cells but could also result from its function in tumor-associated angiogenesis and with this its expression in blood vessels.

3.2.3 Results

3.2.3.1 EphrinB2 is upregulated in EMT cellular systems

In order to study what drives EMT in a comprehensive manner, three different cellular systems of EMT were used to evaluate the differential gene expression profile between epithelial cells and their mesenchymal counterparts. These three cellular EMT systems comprise a human breast cancer cell line, MCF7 cells, that upon a stable knockdown of E-cadherin become mesenchymal (*76*). The second cell line is the normal murine mammary gland, NMuMG that can be triggered to undergo EMT by addition of recombinant TGFβ (*99*). And the third system is the MTflECad cell line that had been established from an MMTV-Neu tumor in which the E-cadherin gene is flanked by LoxP sites. *In vitro*, upon Cre-recombinase infection these cells excise the E-cadherin gene and thereby become the mesenchymal cell line MTΔECad (*76*) (Fig. 12a). Using these three systems and comparing the gene expression differences identified by microarray analysis, ephrinB2 was found to be commonly upregulated upon EMT (Fig. 12b).

This upregulation of ephrinB2 during EMT could be validated both on protein level (Fig. 12c) and on mRNA expression level (Fig. 12d, e). Evaluating whether possible receptors for ephrinB2 would be present to stimulate its reverse signaling activity, qRT-PCR analysis revealed that EphB2, EphB3, Ephb4 and EphA4 are all expressed in the NMuMG and in the MTflECad/MTΔECad system. EphB2 expression is upregulated during EMT in both models (Fig. 12f).

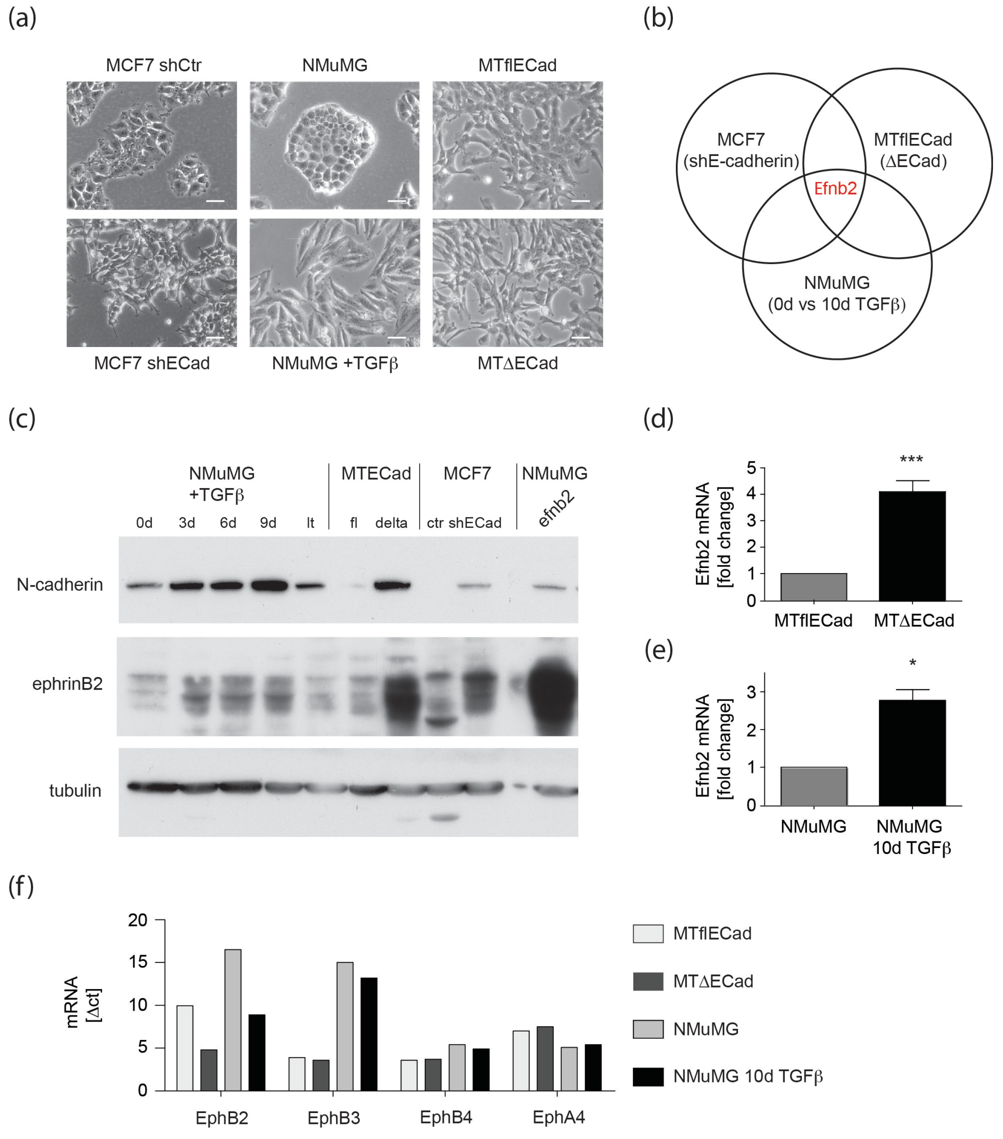

Figure 12: EphrinB2 is upregulated during EMT.
(a) Light microscopic pictures of the three different EMT systems (NMuMG cells without or with TGFβ for at least 20 days (NMuMG +TGFβ), MTflECad versus MTΔECad cells and MCF7 shCtr versus shE-cadherin cells) used for gene expression profiling. Scale bars, 100 μm.
(b) Gene expression profiling by cDNA microarray was performed for all three EMT systems. Gene expression changes of 2 fold were taken into account for comparing the systems in a Venn diagram.
(c) Immunoblotting was performed in order to verify the upregulation of ephrinB2 in all three systems on protein level. NMuMG cells were treated for the indicated days with TGFβ or had been with TGFβ for at least 20 days, considering them long term treated (NMuMG/lt). MTflECad (fl) cells were compared to MTΔECad (delta) cells and MCF7 cells infected with a control shRNA (shCtr) to shE-cadherin (shECad) infected cells. NMuMG cells overexpressing ephrinB2 were used as positive control for the ephrinB2 immunoblot. N-cadherin serves as control to verify the change from the epithelial state cells to the mesenchymal ones. Tubulin was used as a loading control.
(d, e) qRT-PCR analysis of the murine EMT systems shows the differential expression of ephrinB2 between the epithelial and the mesenchymal cell.
(f) qRT-PCR analysis of the different Eph receptors, expressed in the indicated cell lines. Relative mRNA expression is depicted as Δct values.

3.2.3.2 Neither overexpression nor ablation of ephrinB2 affects EMT

The NMuMG cellular system is ideal to monitor the actual transition from the epithelial to the mesenchymal cell state over time (*99*). This transition is accompanied by changes of marker proteins. Upon others, the mesenchymal proteins N-cadherin and NCAM are gained during the TGFβ-treatment, whereas the epithelial E-cadherin gets downregulated (*76*). To investigate whether an overexpression of ephrinB2 (Fig. 13a) or a knockdown of ephrinB2 (Fig. 13b) would interfere with the EMT process, NMuMG cells were stably infected with an EphrinB2 overexpression construct or a small hairpin RNA (shRNA) against ephrinB2. These modified cells were then treated with TGFβ over time and the lysates were evaluated for changes in protein levels. Neither gain of function experiments (Fig. 13a) nor loss of function experiments (Fig. 13b) had a striking effect on the EMT process in NMuMG cells. Also the levels of phosphorylated focal adhesion protein kinase (pFAK) did not change by miss-expression of ephrinB2. Additionally, the range of ephrinB2 overexpression could be documented in Figure 13a, whereas the admittedly weak knockdown is barely visible on the immunoblot but could be verified by qRT-PCR analysis (Fig. 13c).

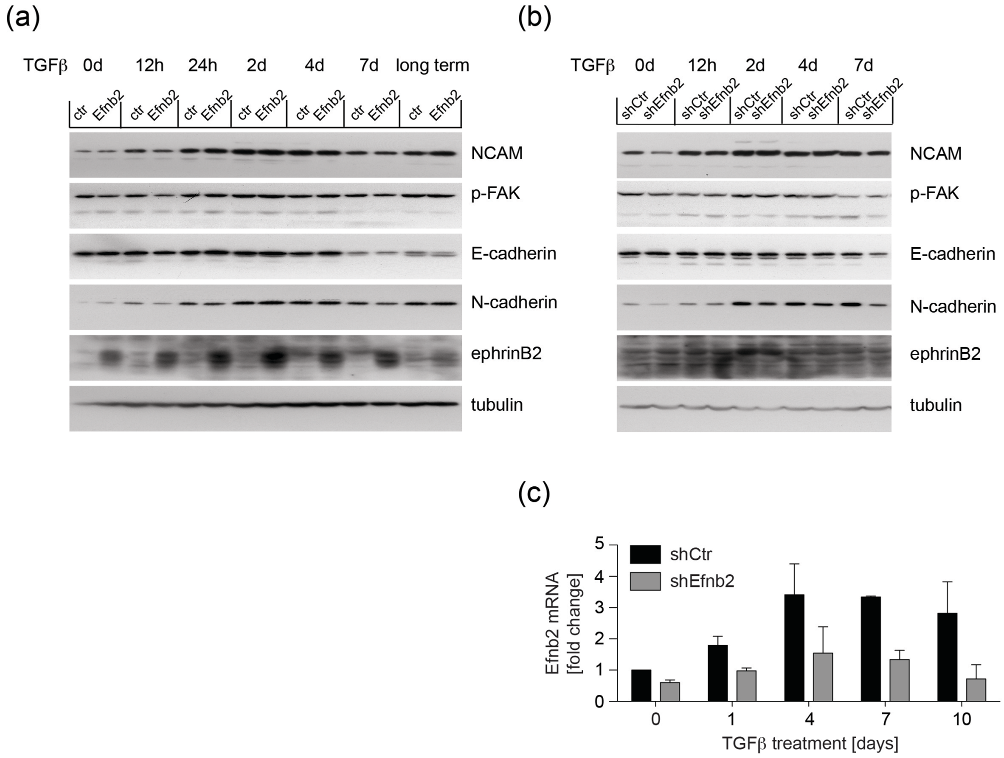

Figure 13: Neither overexpression nor ablation of ephrinB2 affects EMT.
(a, b) Immunoblotting of NMuMG cells either overexpressing **(a)** or with a knockdown of ephrinB2 **(b)** during TGFβ treatment. Lysates of cells treated with TGFβ for the indicated time points were loaded on a gel and protein levels of the different EMT markers, as indicated, were assessed. Tubulin serves as a loading control.
(c) To evaluate the knockdown efficiency of the shRNA against ephrinB2, qRT-PCR analysis of two independent time courses of NMuMG cells treated with TGFβ was performed. Untreated NMuMG cells that express the control shRNA were use as reference and set to fold 1. Mean values with SEM are shown.

3.2.3.3 Mesenchymal cells are more motile than their epithelial counterparts.

Another hallmark of EMT, apart from the marker changes, is to gain migratory capacity in contrast to immobile epithelial cell (*35*). As a tool to investigate the role of ephrinB2 in the mesenchymal cells, the MTΔECad cells as well as long term TGFβ-treated NMuMG cells (NMuMG/lt) were used as a model system to study cell migration. This gain of motility in mesenchymal cells compared to their epithelial counterpart was validated in a transwell migration assay (Fig. 14a, b) where the cells squeeze through pores following an increasing gradient of serum and by tracking nuclei of cells that randomly move in an un-stimulated way (Fig. 14c, d).

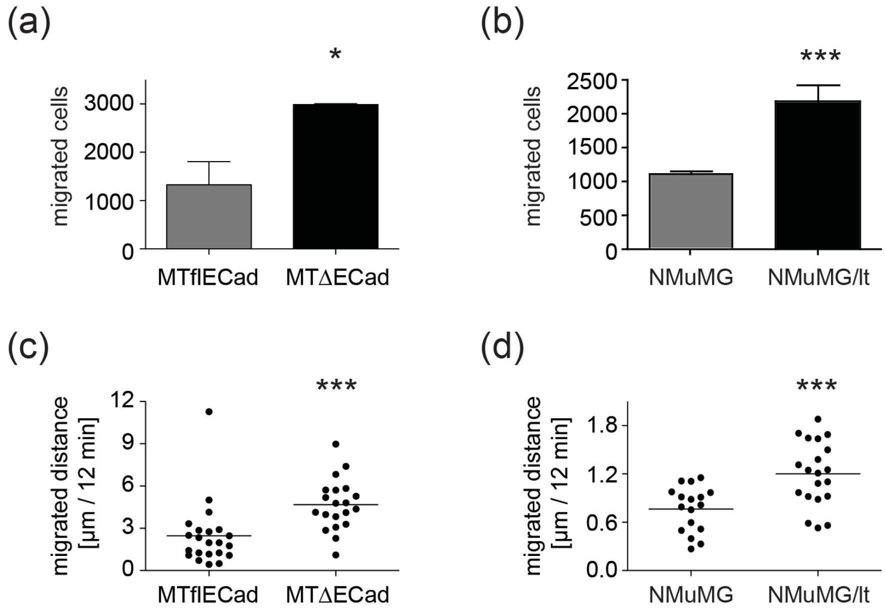

Figure 14: Mesenchymal cells are more motile than their epithelial counterparts.
(a, b) Cells were plated on Boyden chamber inserts using a gradient of FBS as an attractant to move through the pores of the insert. After 16 hours all cells were fixed and cells that had migrated through the pores were stained with DAPI for their nuclei and counted.
(c, d) In order to track cells that randomly move, cells were seeded sparsely on cover slips, put in a Ludin chamber and monitored for 16 hours every 12 minutes by live cell microscopy. To be able to track cells, nuclei were stained with Hoechst and this nuclear staining was used to quantify cell movement using MetaMorph software. To visualize cell viability DIC images were taken. Each dot represents one cell.

3.2.3.4 siRNAs against ephrinB2 efficiently reduce its expression levels.

I discovered that ephrinB2 is upregulated in the more motile cells that had undergone EMT. Since ephrinB2 is implicated in cell motility, I decided to knockdown EphrinB2 in the mesenchymal state cells and assessed whether ephrinB2 plays a role in this gain of motility upon EMT (*116,117,123-125*).

To first determine whether siRNA-mediated knockdown would be effective, mesenchymal cells were transfected with two different siRNAs against ephrinB2 (siEfnb2 #1 and siEfnb2 #3 in MTΔECad cells; siEfnb2 #1 and siEfnb2 #2 in NMuMG/lt cells) and always compared to a control siRNA (siCtr). Observing the morphology of the cells after siRNA transfection, only in the mesenchymal NMuMG/lt cells a slight increase in a rounded-up shape, accompanied by a decrease in protrusions could be monitored (Fig. 15a). This observation pointed towards a more epithelial, less spread morphology and with this a less migratory phenotype of the cells. To evaluate the efficacy of the siRNAs transfected against ephrinB2, qRT-PCR analysis was used documenting a reproducible knockdown of ephrinB2 mRNA levels in MTΔECad cells (Fig. 15b) as well as in NMuMG/lt cells (Fig. 15c).

The efficient reduction of ephrinB2 protein level was additionally shown by immunoblotting (Fig. 15d, e).

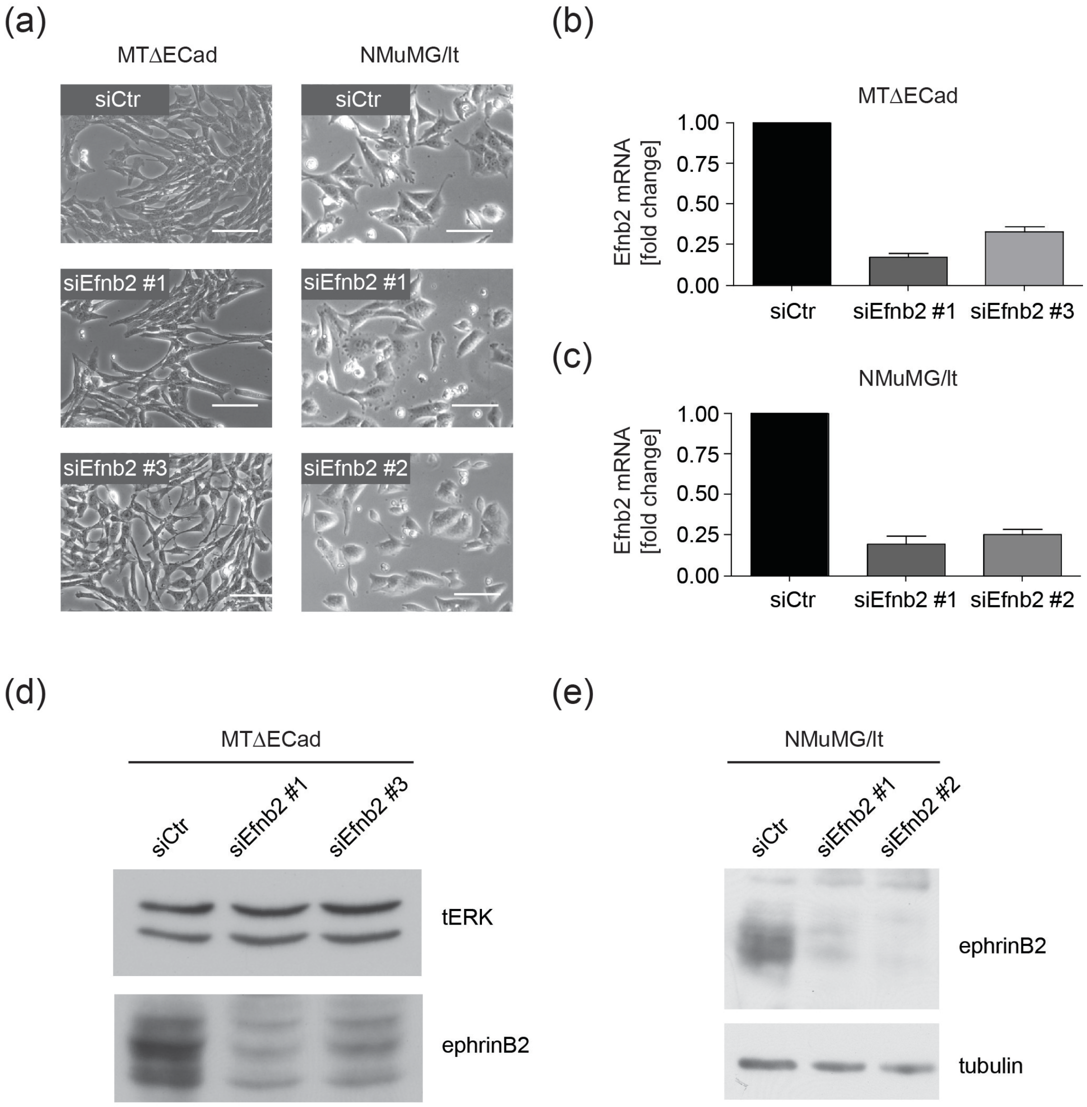

Figure 15: siRNAs against ephrinB2 efficiently reduce its expression levels.
(a) Light microscopic pictures of MTΔECad and NMuMG/lt cells transfected with a control siRNA (siCtr) or with different siRNAs against ephrinB2. Scale bars, 100 µm.
(b, c) qRT-PCR of ephrinB2 expression in MTΔECad (b) and NMuMG/lt cells (c), setting the siCtr value to fold 1.
(d, e) Immunoblotting of ephrinB2 in control siRNA and ephrinB2 knockdown cells in MTΔECad cells using total Erk protein (tErk) as a loading control (d) and in NMuMG/lt cells using tubulin as a loading control (e).

3.2.3.5 EphrinB2 is important in mesenchymal cell motility.

Knowing that ephrinB2 expression levels can effectively be reduced by siRNA-mediated knockdown, mesenchymal cell lines were transfected with two different siRNAs against ephrinB2 in order to investigate whether this would have an influence on cell migration as suggested from literature (*116,124,125*). Cells were plated in a Boyden chamber and their migration towards a gradient of fetal bovine serum (FBS) was measured. MTΔECad cells (Fig. 16a) as well as NMuMG/lt cells (Fig. 16b) react to a knockdown of ephrinB2 with a decrease in their motility. Another assay to assess motility is the scratch wound closure assay. In this assay cells are monitored while closing a gap, scratched in a confluent cell monolayer, as opposed to the transwell migration assay or the tracking assay where single cells migrate. Also under this condition MTΔECad cells migrate slower, resulting in a delayed wound closure (Fig. 16c). NMuMG/lt cells were imaged while moving randomly on a cover slip in a Ludin chamber in complete absence of a given stimulus. By tracking the Hoechst-stained nuclei I could retrieve the reduced distance that cells with an EphrinB2 knockdown moved over time (Fig. 16d).

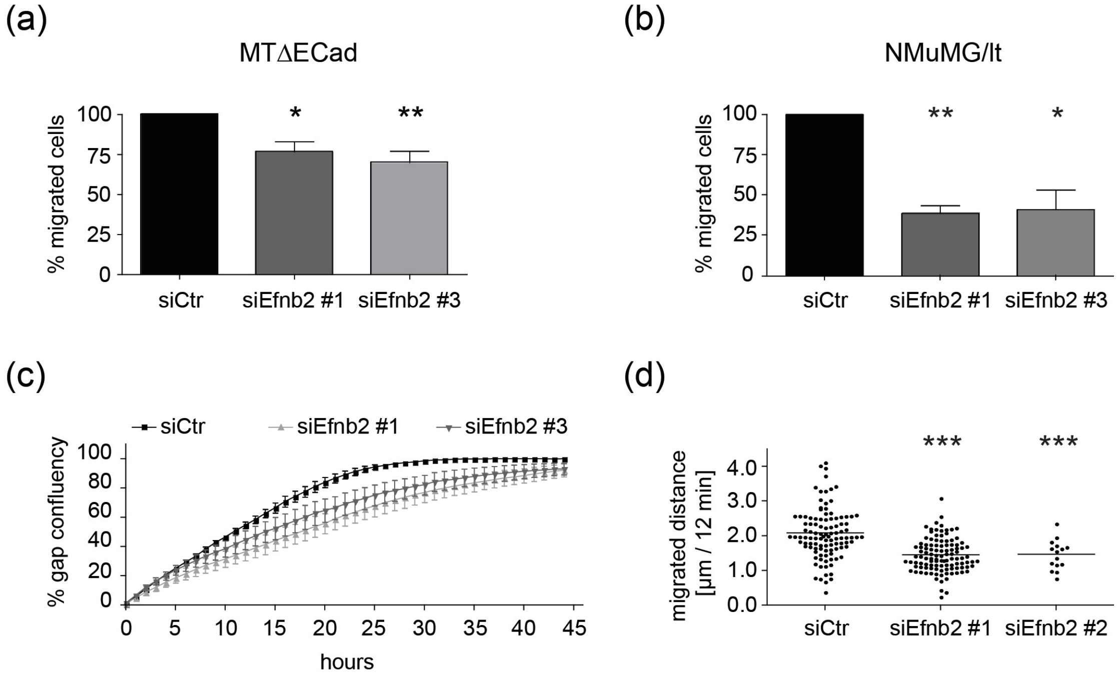

Figure 16: Knockdown of ephrinB2 in mesenchymal cells slows down their motility.

(a, b) Boyden chamber transwell migration assays of MTΔECad (a) and NMuMG/lt cells (b) were performed using 2 different siRNAs against ephrinB2. The amount of migrated siCtr cells were set to 100 %. The mean value of 6 (a) and 3 (b) independent experiments with the SEM is shown.

(c) MTΔECad cells were seeded to confluency in a 24 well dish. The wound closure of a scratch applied to the monolayer of cells was monitored every 30 minutes. The percentage of wound closure, setting the initial wound area to 0 %, is plotted against the time. The mean value of 3 independent experiments with the SEM is shown.

(d) NMuMG/lt cells were seeded sparsely on a cover slip, stained with Hoechst and put into a Ludin chamber. Images were taken every 12 minutes and nuclei were tracked afterwards using MetaMorph software. Each data point represents one cell.

3.2.3.6 Decreased motility is not caused by activity changes in the small GTPases Rac1, RhoA or Cdc42

Having assessed that ephrinB2 is needed for cells that have undergone EMT to effectively migrate, I investigated the mechanism by which the cell migration capacity is affected.

The main remodelers of the actin cytoskeleton, the migratory machinery of a cell, are small GTPases. Among these, the most famous ones involved in cell migration are RhoA, Rac1 and Cdc42 (*50*). In order to assess whether their activity would be changed by an ephrinB2 knockdown that could explain the reduction in velocity of the cells, GTPase activity pulldown assays were performed. Lysates of cells transfected with a control siRNA or siRNAs against ephrinB2 (siEfnb2 #1, siEfnb2 #3 or a mixture of both siRNAs) was used to pull down either the GTP-bound, active forms of Cdc42, Rac1 or RhoA. The immunoprecipitates were then loaded on an immunoblot to determine the amounts of active Cdc42 and Rac1 (Fig. 17a) or the active form of RhoA (Fig. 17b). EphrinB2 knockdown cells did not show changes in Rac1 and Cdc42 activity, only for RhoA activity a minor change for only one siRNA could be measured repeatedly, leading to the conclusion that these prominent small GTPases do not play a role in ephrinB2's way of action on cell migration.

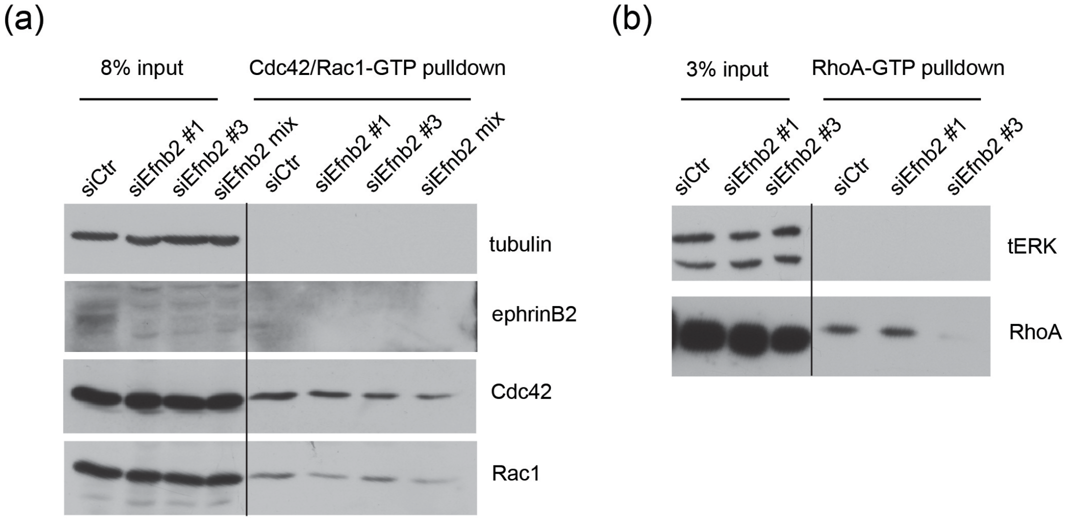
(a)
8% input
Cdc42/Rac1-GTP pulldown
siCtr
siEfnb2 #1
siEfnb2 #3
siEfnb2 mix
siCtr
siEfnb2 #1
siEfnb2 #3
siEfnb2 mix
tubulin
ephrinB2
Cdc42
Rac1
(b)
3% input
RhoA-GTP pulldown
siCtr
siEfnb2 #1
siEfnb2 #3
siCtr
siEfnb2 #1
siEfnb2 #3
tERK
RhoA

Figure 17: Decreased motility is not caused by activity changes in the small GTPases Rac1, RhoA or Cdc42. **(a, b)** MTΔECad cells were transfected with a control siRNA (siCtr) or with siRNAs targeting ephrinB2 (siEfnb2 #1, siEfnb2 #3 or a mixture of both). Lysates of these cells were used to pull down the active GTP-bound versions of Cdc42, Rac1 (a) or RhoA (b). Both input samples and pulldown samples were loaded on a gel and the levels of Cdc42, Rac1 and RhoA were determined by immunoblotting. Tubulin **(a)** and total Erk **(b)** serve as a loading control. Both experiments are representative of two independent pulldown experiments performed.

3.2.3.7 EphrinB2 knockdown cells over-stabilize their focal adhesions

Since the small GTPases do not change with a knockdown of ephrinB2 and also the actin cytoskeleton seems to be normal in shape (Fig. 18a) I focused my attention on the focal adhesions of the cells. A cell uses its focal adhesions (FA) to make contact to the surface on which it holds on in order to move forward (*44*). Plating MTΔECad cells on cover slips and staining for the focal adhesion marker pFAK revealed that the focal adhesions in ephrinB2 knockdown cells are bigger in size but less in number, especially in the body of the cells (Fig. 18a). Having observed this phenomenon, I quantified the size and abundance of focal adhesions of the cells (Fig. 18b). Surprisingly, quantification only partially coincided with the results obtained by stainings, most likely due to the high variations in shape of the MTΔECad cells in general.

To decrease the amount of diversity within the cell population, minimizing the different cell shapes and sizes observed upon 2D culturing conditions, I plated the cells on 10 μm thin lines of poly-L-lysine. This technique of patterning a surface in order to restrict cell spreading on a thin, 1D-like, line was done in collaboration with the Pertz group (University of Basel). Since focal adhesion dynamics are at least as important as their abundance and size (*50*), I stably infected cells with a construct for paxillin-GFP, a component of focal adhesions (*127*). Following paxillin-GFP by live imaging microscopy allowed me to monitor focal adhesions while cells were moving (*128*). To investigate whether ephrinB2 plays a role in focal adhesion dynamics, MTΔECad cells were transfected with siRNAs against ephrinB2 and a control siRNA and plated on the 10 μm lines coated with poly-L-lysine. After spreading on the lines and being adherent over night, cells were monitored by live imaging microscopy. A picture of the focal adhesions depicted by paxillin-GFP and a DIC picture for general cell shape was taken every 5 minutes. Showing an image of the cells every 100 minutes elucidates that control cells mostly stabilize and destabilize their focal adhesions while they are moving forward. In contrast, ephrinB2 knockdown cells tend to stick to their distal focal adhesions, over-stabilizing them and making it difficult for them to move in one direction (Fig. 18c). The phenomenon to be stuck with the focal adhesions, but still trying to move, is accompanied by the cell becoming longer and longer over time. To quantify the differences in length of the cells on the lines, cells were fixed and stained with phalloidin in order to visualize the whole cell. As observed already in the movies, cells with a knockdown of ephrinB2 are consistently longer than their control cells (Fig. 18d).

Focal adhesion over-stabilization explains the decrease of cell migration in ephrinB2 knockdown cells. Repulsion, being the main output of Eph-ephrin signaling, could additionally have an effect on cell migration behavior. To investigate whether repulsion between cells was changed upon ephrinB2 knockdown, differently labeled cells were transfected with siRNAs, mixed and monitored by live cell imaging microscopy. Quantifying the time cells adhered to each other, revealed a decrease of cell repulsion when ephrinB2 knockdown cell were confronted with each other (Fig. 18e).

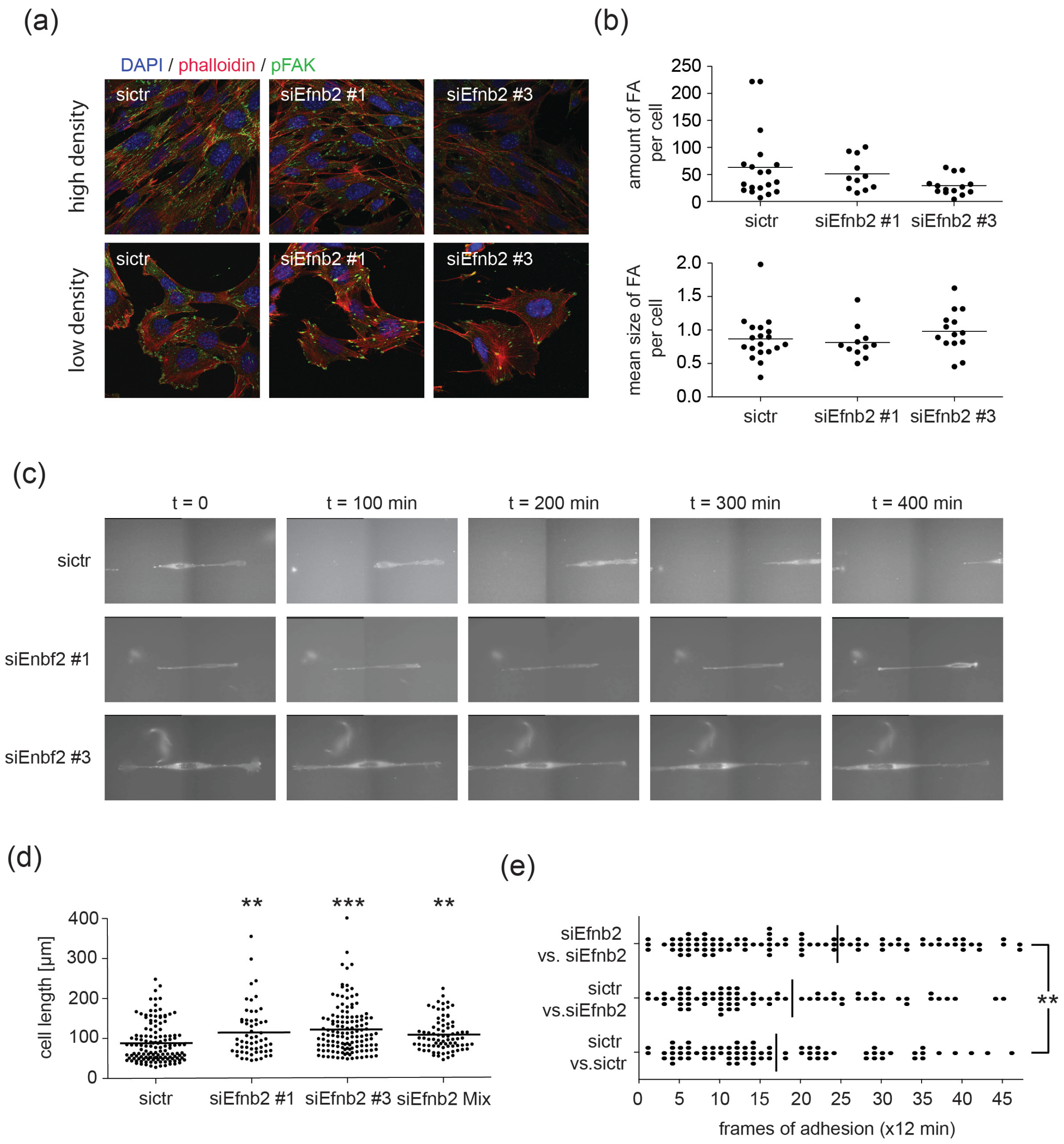

Figure 18: EphrinB2 knockdown cells over-stabilize their focal adhesions and stretch.
(a) Immunofluorescence staining of MTΔECad cells transfected with control siRNA (siCtr) or siRNAs against ephrinB2 (siEfnb2 #1, siEfnb2 #3). Cells were labeled by marking their actin cytoskeleton with phalloidin (red) and their focal adhesions with an antibody against pFAK (green). The nuclei are labeled with DAPI (blue). The upper panel shows cells in close cell-cell contact, whereas the lower panel shows cells in sparse conditions.
(b) 2D cultured cells were stained for their focal adhesions. Pictures of single cells where acquired in high resolution to be able to quantify positive signals with ImageJ software. The amount of focal adhesions per cell and the mean size of focal adhesions per cell are shown. Every data point represents one cell.
(c) MTΔECad cells with an ephrinB2 knockdown were seeded on 10 *μ*m thin lines coated with poly-L-lysine. Every 5 minutes pictures of the cells (DIC) and of the focal adhesions (paxillin-GFP) were taken. Single pictures in a 100 min time interval are shown for each condition.
(d) MTΔECad cells spread on 10 μm lines coated with poly-L-lysine with or without an ephrinB2 knockdown were fixed and stained with phalloidin. Images where taken and the length of each cell was measured by MetaMorph software.
(e) MTΔECad-GFP or MTΔECad-mCherry cells were transfected with a control siRNA or with siEfnb2 #1. The indicated cells were mixed, imaged with live cell microscopy and the duration of adhesion was quantified.

3.2.3.8 EphrinB2 ablation in the polyoma-middle-T breast cancer model does neither change tumor growth nor lung metastases.

Since ephrinB2 seems to play a role in cell migration, I wanted to figure out whether a decrease of cell motility by a knockout of *Efnb2* would affect tumor growth or, more importantly, metastasis. An elegant way to study breast cancer is a mouse model where breast epithelial cells express the viral oncogene polyoma-middle-T (PyMT) under the control of the mouse mammary tumor virus LTR promoter (MMTV) (*129*). To first examine whether breast tumors of this model would express ephrinB2, I stained tumor sections for ephrinB2 by immunhistochemistry. Indeed, breast tumors originating in MMTV-PyMT mice (Mpy) show positive staining for ephrinB2 in cells mainly at the edges of the tumors (Fig. 19a, left panel), whereas the center of the tumor lacks ephrinB2 (Fig. 19a, middle and right panel).

Since the mice carrying the *Efnb2* gene that is flanked by loxP sites (*Efnb2* fl/fl) were in a C57BL/6 background (*120*), these mice were backcrossed for 6 generations into FVB/N mice. Taking advantage of the Mpy breast cancer model system in FVB/N background, I crossed Mpy mice with *Efnb2* fl/fl mice. To compare mice that carry the knockout or not, the resulting Mpy;*Efnb2* fl/fl mice were further crossed with a mouse expressing a breast specific *Cre*-recombinase transgene (MMTV-Cre) (*130*). To validate the effectiveness of the knockout, RNA was isolated from tumor pieces and the expression levels of ephrinB2 were examined by qRT-PCR. Only a marginal overall reduction of ephrinB2 expression in fl/fl;Mpy;Mcre mice could be monitored (Fig. 19b). The observation that total tumor RNA did not show a decrease in ephrinB2 levels does not exclude a functional knockout in the mammary epithelial cells of these mice, since the knockout is a conditional one and tumors are composed of many more cells than the actual cancer cells. Further arguing for a ‘contamination’ of the total tumor mRNA result is the notion that cells like endothelial cells and mural cells express ephrinB2 as well (*106,114,116,117*). To analyze the tumorigenicity of the mice, the whole mammary gland, mostly composed of cancerous tissue, was taken out and weighted after sacrificing mice at 12.5 weeks of age. No difference in tumor weight could be observed, comparing mice, which should have a full *Efnb2* knockout in the breast epithelium to mice that have only one *Efnb2* allele floxed or mice that do not even express the *Cre*-recombinase (Fig. 19c).

Since EMT and cell migration is rather implicated in metastasis than in tumor growth itself, I analyzed the lungs of tumor-bearing mice for metastases. In order to do so, lungs were sectioned, stained with H&E and then screened by light microscopy to count metastases (Fig. 19d). Additionally, the metastases were scored for their size to see whether there would be growth differences (Fig. 19e). Unexpectedly, there is neither a difference in the amount of lung metastases nor in their size distribution between the compared genotypes.

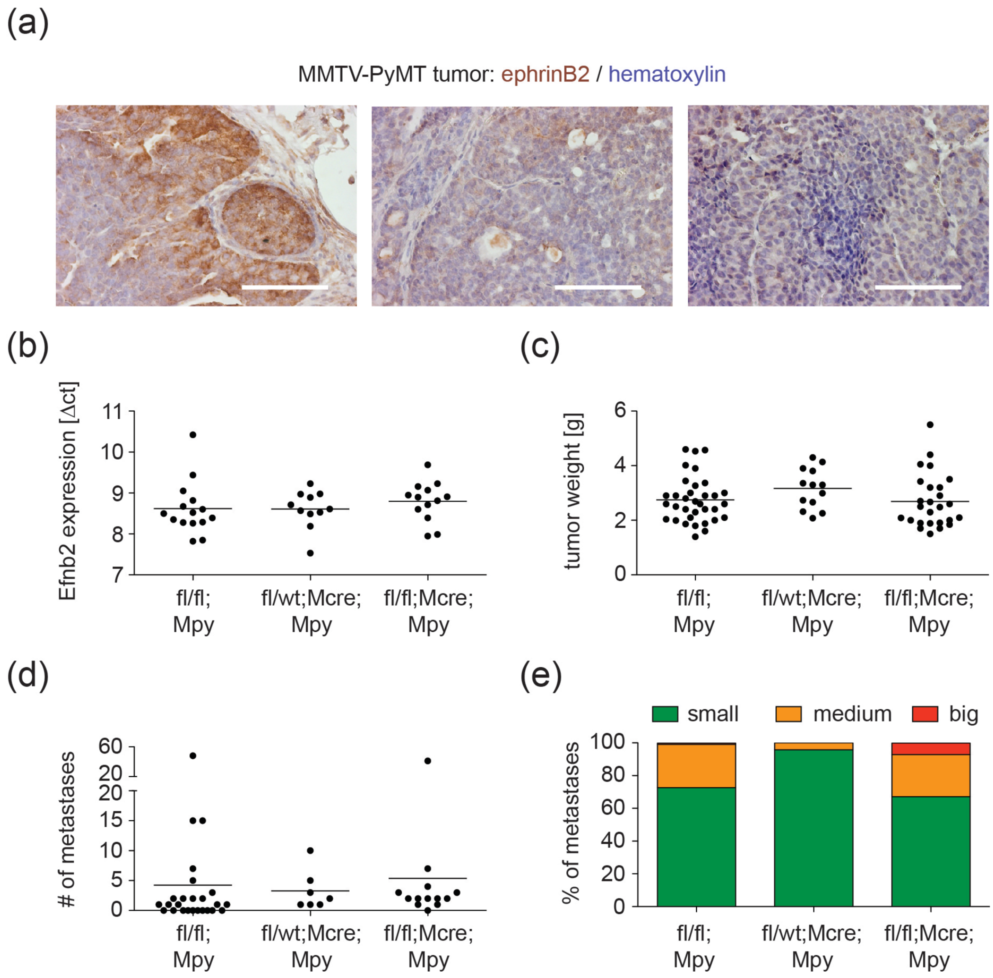

Figure 19: *Efnb2* ablation in a polyoma-middle-T breast cancer model does neither change tumor growth nor lung metastasis.
(a) Immunhistochemistry staining of ephrinB2 (brown) in MMTV-PyMT tumors. Nuclei were counterstained by hematoxylin (blue). The left panel represents the tumor edge towards the stroma whereas the middle and right panels depict the central tumor mass. Scale bars, 100 μm.
(b) qRT-PCR analysis of RNA isolated from MMTV-Polyoma-middle-T (Mpy) mice which carry either two floxed alleles of *efnb2* (fl/fl) or only one (fl/wt) and express MMTV-Cre (Mcre) or not. The y-axis shows Δct values.
(c) After 12.5 weeks, tumor-bearing mice with the indicated genotypes were sacrificed and all mammary glands with tumors were weighted.
(d, e) Lungs of tumor-bearing mice were taken out, sectioned, stained with H&E and metastases were counted and scored for their size. The amount of metastases per mouse, represented by 4 sections per mouse, is shown in panel **(d)** whereas the size distribution is depicted in panel **(e)**.

3.2.3.9 *Efnb2* ablation in the MMTV-Neu-IRES-Cre breast cancer model does neither change tumor growth nor lung metastases.

Another breast cancer model that has a longer progression time and is less aggressive than the Mpy model is the MMTV-Neu mouse model (*11*). Here, an activated version of the Neu protein is specifically expressed in the mammary gland and leads, after a delay of about 5 months, to breast cancer. Immunohistochemical staining for ephrinB2 in these tumors barely showed any expression of ephrinB2 and if so only the invasive front of the tumor was positive (Fig. 20a). This observation is not surprising and would fit nicely to the hypothesis that only invasive cells in the tumor that have undergone EMT would upregulate ephrinB2 in contrast to the epithelial bulk of the tumor cells.

To use the MMTV-Neu model for a conditional knockout of *Efnb2* in the breast epithelium a modified version of the MMTV-Neu, the MMTV-Neu-IRES-Cre (NIC) mouse model, was used (*131*). In this mouse model, cells that express the activated form of the Neu oncogene also express the Cre-recombinase on the same transcript making sure that the tumor cells have recombined their DNA for having a knockout of the gene of interest, in this case *Efnb2*, that is flanked by LoxP sites. Since ephrinB2 could barely be detected on protein level in the Neu-induced breast tumors, I relied on qRT-PCR analysis for the expression of ephrinB2 and an inside on the knockout efficiency. Not surprisingly, no difference in ephrinB2 expression in the tumor carrying one or both *Efnb2* floxed alleles could be detected (Fig. 20b). Notably, the Δct values obtained from Mpy tumors as well as from NIC tumors are very similar, despite the observation that ephrinB2 was much more abundant in Mpy tumors visualized by immunhistochemistry stainings (Fig. 19a, b and Fig. 20a, b). Again, the knockout effect of *Efnb2* could have been masked by non-mammary epithelial cells within the tumor that express ephrinB2. Without knowing the efficiency of the conditional *Efnb2* knockout in this breast cancer model, I anyway investigated the tumor mass of mice after 23 weeks of age. For these tumors where the penetrancy of tumor formation is not equal to all mammary glands, only the ones having a tumor, the glands 2, 3, 4, 7, 8 and 9 were taken out with their tumors and weighted. No difference in tumor weight between NIC;fl/fl and NIC;fl/wt mice could be detected (Fig. 20c). The more relevant analysis of the lung metastases also revealed no difference in the amount of metastases (Fig. 10d). The size distribution of the lung metastases which are in general much bigger than the ones found in the Mpy-system rather gave the opposite tendency of having less small sized metastases in the *Efnb2* knockout mice compared to mice that still carry one intact *Efnb2* allele (Fig. 20e).

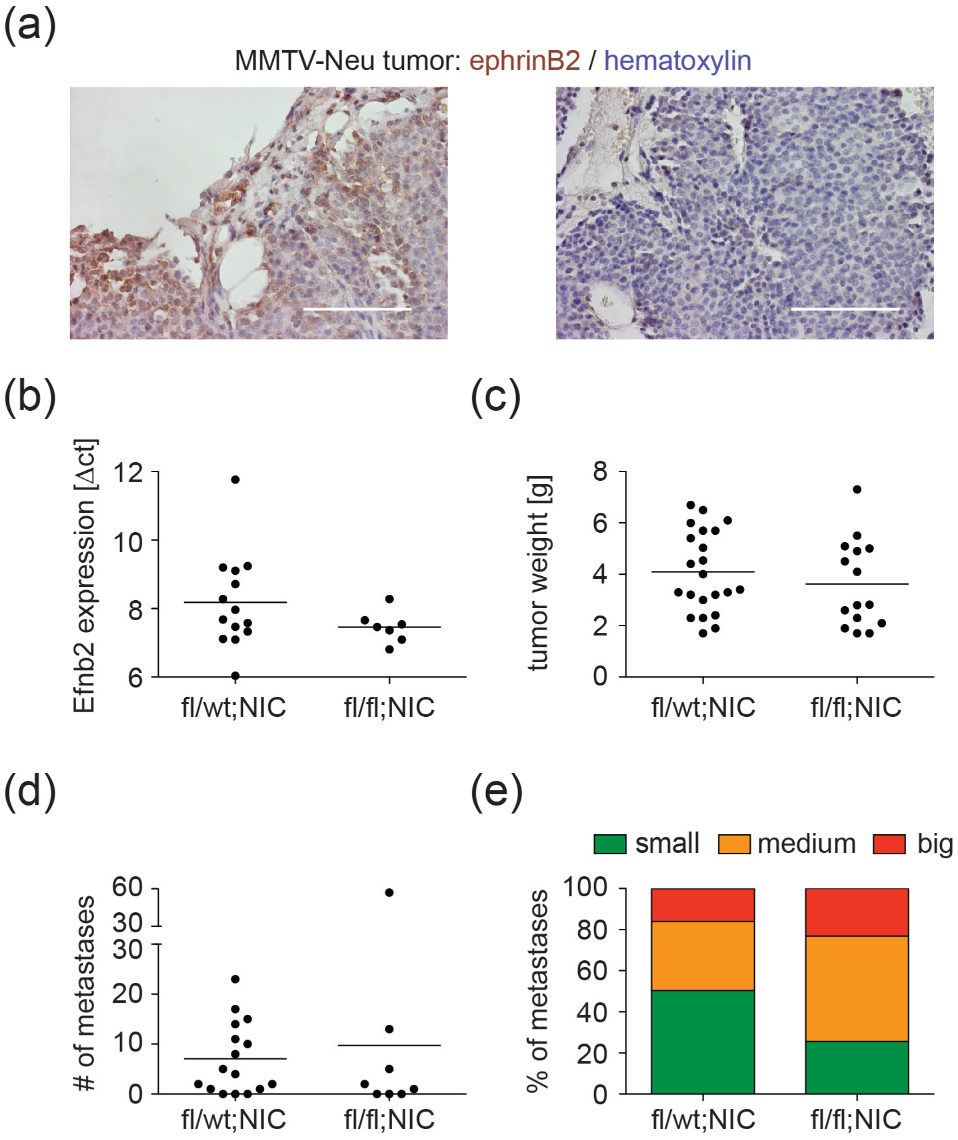

Figure 20: *Efnb2* ablation in an MMTV-Neu_IRES-Cre breast cancer model does neither change tumor growth nor lung metastasis.
(a) Immunhistochemistry staining of ephrinB2 (brown) in MMTV-Neu tumors. Nuclei were counterstained by hematoxylin (blue). The left panel represents the tumor edge towards the stroma whereas the right panel depicts the central tumor mass. Scale bars, 100 μm.
(b) qRT-PCR analysis of RNA isolated from MMTV-Neu-IRES-Cre (NIC) mice, which carry either two floxed alleles of *Efnb2* (fl/fl) or only one (fl/wt). The y-axis shows Δct values that are normalized to Rpl19.
(c) After 23 weeks tumor-bearing mice with the indicated genotypes were sacrificed and mammary glands 2, 3, 4, 7, 8, 9 with tumors were weighted.
(d, e) Lungs of tumor-bearing mice were taken out, sectioned, stained with H&E and metastases were counted and scored for their size. The amount of metastases per mouse represented by 3 sections per mouse is shown in panel **(d)** whereas the size distribution is depicted in panel **(e)**.

3.2.4 Discussion

The ability of cells, to move not only within the tumor but also away from the bulk of the primary tumor cells, is a hallmark of EMT and one of the causes of live threatening metastatic disease (*46*). To study the molecular mechanisms underlying this gain of motility in cells that have undergone EMT, I have searched for genes commonly regulated in different cellular EMT systems and found ephrinB2 consistently upregulated. EphrinB2's implication on cell motility has long been known but never put in association to the process of EMT (*116,117,123-125*).

In the present study, I demonstrated that a reduction of ephrinB2 levels in cells that have undergone EMT leads to a decrease in cell migration. This phenomenon was validated in two independent EMT model systems. The generality of impairment of cell motility was shown, using three different migration assays. This allows concluding that the effect of ephrinB2 knockdown holds true for directed cell migration towards a gradient or to close a gap, as well as random cell migration. Cell migration speed is further reduced by diminished cell repulsion in the case when ephrinB2 knockdown cells get in contact with each other.

The investigated cellular EMT systems express various Eph receptors ephrinB2 could use to interact with, either on its own cell or coming in contact with another cell. Arguing for a reverse signaling effect of ephrinB2 knockdown on cell migration is the notion that also single cells show a reduction of motility (cell tracking assay), excluding a cell-cell contact dependent Eph-ephrin signaling output in this case. An impact of ephrinB2 reverse signaling on cells' morphology and motility independent of Eph-receptor binding has been shown before (*115,117*). Here, the PDZ binding motif plays an important role (*116*). To elucidate also in our system whether the reduction in migration is due to less reverse signaling of ephrinB2 or due to less activation of ephrin's receptors, further studies would be required. One approach to follow up this question would be an attempt to rescue the ephrinB2 knockdown by a version of ephrinB2 that lacks its C-terminus. This mutant should only rescue the lack of receptor activation but not the reduction in reverse signaling. A similar experiment would be the rescue of the knockdown phenotype by addition of clustered recombinant ephrinB2 to cells, which would directly activate receptor signaling.

A connection between focal adhesion turn over, motility and ephrinB2 has been made before (*117*). The authors explained this phenomenon by less focal adhesions in general and enlarged ones at the periphery. This defect in FA maturation and with this an unstable, undirected migration was further explained by a decreased activation of CrkII/CrKL p130 (CAS) by ephrinB2. Also in our mesenchymal cellular systems, I found less but bigger FAs especially at the protrusions of cells. In contrast to the aforementioned study, where these big FAs were immature and led to unstable lamellipodia, I found that enlarged FAs account for an over-stabilization, not allowing a cell to retract its rear end. Supporting our hypothesis that over-stabilized FAs lead to slower migration is the notion, that a limiting step in migration speed is the force of FAs attaching to a substrate and with this their turn-over rate (*50*). The results of my study are descriptive in nature and further quantification would be necessary using a more standardized assay. Forcing cells on thin lines as well as a powerful techniques like total internal reflection microscopy (TIRF) would allow a better space-resolved analysis of FAs.

Unexpectedly, my loss-of-function studies in two breast cancer models, has not shown any effect of ephrinB2 on tumor growth and metastatic seed. Studies in patients have revealed for numerous cancer types that ephrinB2 correlates with tumor progression (*107*). On the other hand, studies in murine breast cancer have stated the opposite (*118*). In this study, ephrinB2 expression was lost during breast cancer progression, however, overexpression of ephrinB2 had no effect on metastasis. In contrast, transgenic expression of a C-terminal deficient ephrinB2 protein (ΔC-ephrinB2) led to shorter tumor latency and more metastases. These contradictory results could be explained by a dominant-negative effect of the ΔC-ephrinB2 version blocking specifically reverse signaling. With my *Efnb2* knockout analyses in the different breast cancer models, I hoped to add another piece of information to this puzzle. Unfortunately, the lack of an effect of *Efnb2* knockout on metastasis without the important control of whether the excision of the *efnb2* gene really happened in the mice does not allow excluding an effect of ephrinB2 in breast cancer progression. Optimization of the ephrinB2 staining protocol is needed, since further staining attempts, apart form the initial ones characterizing the breast cancer models, remained unsuccessful. However, comparisons between patients' expression data that include all tumor cell types for analysis and mouse data where the transgene is expressed specifically in one type of cell, have to be done carefully.

Having generated data both agreeing and disagreeing with the literature, one always has to keep the immense complexity of Eph-ephrin signaling in mind. The fact that the whole system is highly promiscuous and that clustering is of great relevance in this pathway, together with the fact that forward, reverse and even receptor-independent signaling can take place has to be considered. These facts do not allow studying ephrins by focusing only on one factor and neglecting the complexity of the system.

In summary, I am confident to state that ephrinB2 plays a functional role during EMT, which is manifested by its effect on cell migration. Most likely, the need of ephrinB2 signaling during cell migration lies in its role in focal adhesion stabilization and turnover. However, whether this phenomenon of ephrin-modulated mesenchymal cell migration is of relevance during tumor progression needs to be further investigated.

3.2.5 Material and Methods

3.2.5.1 Reagents and antibodies

Antibodies

N-cadherin (1:2000; Takara, M142), E-cadherin (1:3000; Transduction Labs, 610182), ephrinB2 (1:500 for WB; 1:10 for IHC; R&D AF496), NCAM (1:2000; Sigma-Aldrich, OB11, #9672), pY297FAK (1:1000 for WB and 1:100 for IF; BD 611806), tubulin (1:6000, Sigma-Aldrich T-9026), tErk (1:10000; Sigma-Aldrich M7927), Cdc42 (1:250; active Cdc42 pull-down and detection Kit, Thermos scientific, 89857), Rac1 (1:1000, Transduction Lab; R56220), RhoA (1:200; Active Rho pull-down and detection Kit, Thermos scientific, 89854), paxillin (1:100; BD 610052), Alexa-Fluor 488 and 568 (1:200, Molecular Probes), *Reagents*

Recombinant human TGFβ1 (R&D #240-B), DAPI (Sigma-Aldrich), phalloidin Alexa-Fluor 568 (1:200; Molecular Probes, A12380), hematoxylin (Sigma-Aldrich), eosin (Sigma-Aldrich).

3.2.5.2 Cell lines and cell culture

Cell lines

A subclone of NMuMG cells (NMuMG/E9; hereafter NMuMG) expressing E-cadherin has been described earlier (*99*). MTflECad cells that were established from an MMTV-Neu-fl/fl-ECad mammary gland tumor and *in vitro* induced to undergo EMT by Cre-recombinase-mediated loss of *cdh1* (MTΔECad). Both, MTflECad/MTΔECad and MCF7 shE-cadherin have been described earlier (*76*).

Cell culturing

NMuMG, MTflECad, MTΔECad and MCF7 cells were cultured in Dulbecco's modified eagle medium (DMEM) supplemented with glutamine (2 nM), penicillin (100 U), streptomycin (0.2 mg/l) and 10 % FCS (all from Sigma-Aldrich).

For high resolution live imaging microscopy DMEM without phenolred was used (Sigma-Aldrich D1145).

Lenti viral infection and plasmids

cDNA encoding murine ephrinB2 (kindly provided by K. Nobes, Universitiy of Bristol, UK) was subcloned into a lentiviral expression vector pLenti-CMV-puro (kindly provided by M. Kaeser, University of Bern, Switzerland). The pLenty-CMV-puro paxillin-GFP vectors were kindly provided by Olivier Pertz (University of Basel, Switzerland). Expression vectors pLKO.1-puro for small hairpins were purchased from Sigma-Aldrich (shEfnb2: TRCN0000066494; Mission non-target shRNA control vector (shCtr): SHC002). In order to get lentiviral particles, a lentiviral expression plasmid was transfected into HEK293T cells together with the packaging vector pR8.92 and the envelope encoding plasmids pVSV using FugeneHD (Roche). The first day after transfection medium of HEK293T was changed. The second day, the virus-containing supernatant was harvested, filtered with a 0.45 μm pore filter, supplemented with 8 ng/ml polybrene and added to the target cells. The target cells were centrifuged with the viral supernatant for 90 min, 1000 xg, 30 °C, followed by 3 hours incubated at 37 °C and 5 % CO_2 and then cells were given fresh medium. Selection with 1 µg/ml puromycin (Sigma-Aldrich) was started 2 days after infection and stopped 3 days later.

Retroviral infection and plasmids

Retroviral expression plasmids (pGabe, pChabe (*132*)) were transfected using FugeneHD (Roche) into the retroviral packaging cell line PlatE (Cell Biolabs) (*133*). One day after transfection, medium was changed and retroviral supernatant was conditioned for 1 day. Retrovirus-containing supernatant was filtered through a 0.45 µm pore filter and added together with 8 ng/ml Polybrene to target cells. Target cells were centrifuged with the virus for 90 min, 30 °C, 1000 xg and incubated for 3 hours at 37 °C, 5 % CO_2 before the viral supernatant was exchanged with normal growth medium. FACS sorting was used to purify highly GFP or mCherry-positive cells.

siRNA transfection

siRNAs against ephrinB2 were purchased from Invitrogen (Stealth RNAi; #1: EFNB2MSS203804; #2: EFNB2MSS203805; #3: EFNB2MSS203806) and as a control the stealth siRNA negative universal control medium from Invitrogen was used (45-2001). For knockdown experiments 5 nM siRNA were reversely transfected into cells using LipofectAMINE RNAiMAX (Invitrogen) according to manufacture's instruction.

3.2.5.3 Migration assays

Transwell migration assay

Cells were trypsinized, washed in PBS and resuspended in medium containing 2 % FBS instead of the normal 10 %. After counting the cells and diluting them in the 2 % FBS containing medium, a cell suspension with the concentration of 1.5x 10^5/ml was prepared. 8 µm pore Boyden chambers (Falcon BD, Franklin Lakes, NJ) were put into a 24-well plate with 600 µl of medium containing 20 % FBS. 100 µl of the cells suspension was administered to the upper compartment. NMuMG/lt cells had all media supplemented with TGFβ. 16 hours after incubation at 37 °C and 5 % CO_2 the chambers were washed once with PBS and then fixed with 4 % Paraformaldehyde (PFA) for 15 min at room temperature. After washing the inserts again, cells on the upper part of the chamber were scratched away with a cotton stick. The remaining cells that had migrated through the pores on the lower side of the inserts' membrane were stained for 5 minutes with 0.5 μg/ml DAPI, washed again and then kept in PBS. To analyze the amount of migrated cells, Boyden chamber inserts were put on a slide and pictures were taken with a 10x objective. ImageJ software was used to quantify migrated cells.

Scratch wound assay

Cells were seeded on 24-well image lock plates (Essen Bioscience) and grown to a confluent monolayer. One scratch through the center of the well was applied with a 10 μl pipette tip using the scratch device from Essen Bioscience. The gap closure was monitored by sequential pictures taken every 30 minutes with the IncuCyte (Essen Bioscience). The initial gap was set to 0 % wound confluency and the IncuCyte software was used to calculate the gap confluency of each picture taken.

Tracking assay

Cells were seeded on 18 mm cover slips and stained with 3.3 μg/ml Hoechst (33342 Invitrogen) in full medium for 30 min, 37 °C, 5 % CO_2. After staining, cells were washed 5 times with medium and then put into a Ludin chamber (Life Imaging Services) filled with full medium. DIC and blue-fluorescent images of the cells were taken every 12 minutes with a 10x objective by a Leica DMI 6000 live imaging microscope by 37 °C within a Ludin box (Life Imaging services). Cell movements were measured by tracking the Hoechst-stained nuclei throughout the movie using MetaMorph software. Cell viability was monitored by DIC images.

Repulsion assay

GFP or mCherry-expressing MTΔECad cells were trypsinized, counted, mixed with equal numbers in a reaction tube and plated on 18 mm cover slips. After overnight incubation by 37°C, 5 % CO_2, cover slips were transferred into Ludin chambers and cells were imaged for 16 hours, taking a red, green and DIC picture every 12 minutes. The time of cell adhesion was quantified by analyzing the movies.

Line assay

In order to produce a 10 μm thin line pattern, tissue culture plates (μ-Dish$^{35mm,\ high}$, obliterate, ibidi 88156) were treated with plasma for 5 seconds, 100 % power in a plasma cleaner (Femto Science, model: CUTE-MP). To make the dish anti-adhesive, the surface was covered with 0.5 mg/ml PLL-PEG (SUSOS, Zürich) for 30 min at room temperature (RT), the dish was washed with 0.22 μm filtered ddH2O, dried and a PDMS line pattern was applied on the dish (kindly provided by K. Martin, group Pertz, University of Basel). To burn away the PLL-PEG on the unprotected culture dish surface, the plate was plasma treated for 2 min, 100 % power. The PDMS line pattern was removed and lines were coated with 0.02 % poly-L-lysine for 1 h at RT. The culture dish was washed with water, dried and silicone culture-inserta (ibidi, 80209) were placed into it. Cells were plated into these inserts, incubated over night at 37 °C, 5 % CO_2. Imaging of cells on lines was performed by 37 °C in a Nikon Ti-E live imaging microscope. This assay was done in collaboration with O. Pertz' group, University of Basel.

3.2.5.4 Quantitative RT-PCR

To evaluate transcripts relative expression levels, RNA was isolated using TriReagent (Sigma-Aldrich) following the protocol, reverse transcribed with MMLV reverse transcriptase (Promega, Wallisellen, Switzerland), and cDNA was quantified by quatitative PCR (qPCR) (Step One Plus, Applied Biosystems) using Mesa Green qPCR MasterMix plus (Eurogentec). Rpl19 was always used for normalization (ΔCt). Results are represented as fold change of the normalized ΔΔCt or as ΔCt-values. To determine mRNA expression levels, the following qPCR primers have been used:

mRNA:	**Forward primer (5'-3'):**	**Reverse primer (5'-3'):**
Rpl19	ctcgttgccggaaaaaca	tcatccaggtcaccttctca
ephrinB2	tctttggagggcctggat	ccagcagaacttgcatcttg
EphB2	tggactctacgacagcaacg	gtcgtagccgctcacctct
EphB3	ccactcaagctctactgcaatg	gctttgtaactcccaggagga
EphB4	actgggacatgagcaacca	tctgccaacagtccagcat
EphA4	aggtgtctgactttggcatgt	cagtccaccggataggaatc

3.2.5.5 Immunoblotting

Protein extracts were obtained by lysing cells with RIPAplus buffer (150 mM NaCl, 2 mM MgCl, 2 mM $CaCl_2$, 0.5 % NaDOC, 1 % NP40, 0.1 % SDS, 10 % Glycerol, 50 mM Tris pH 8.0, 2 mM Na_3VO_4, 10 mM NaF, 1 mM DTT, and a 1:200 dilution of stock protease inhibitor cocktail for mammalian cells (Roche)) directly on the culturing dish after having washed them with ice cold PBS. Lysing cells were transferred to a reaction tube and lysis could happen for 30 min on ice. Lysates were spined down and protein concentrations in cleared lysates were measured by DC Protein Assay (BioRad Laboratories). Equal amounts of protein were diluted in SDS-PAGE loading buffer (10 % glycerol, 2 % SDS, 65 mM Tris, 1 mg/100 ml Bromphenolblue, 1 % betamercaptoethanol) and resolved by SDS poly acrylamide gel electrophoresis (SDS-PAGE). Resolved proteins were transferred to polyvinylidene fluoride (PVDF) membranes (Millipore) by tank blotting, blocked with 5 % skim milk powder in Tris-buffered saline with 0.05 % Tween 20 (TBST) and incubated with the indicated antibodies. HRP conjugated antibodies were detected using enhanced chemiluminescence.

3.2.5.6 Immunofluorescence

Cells grown on cover slips were once washed with PBS and fixed for 15 min, RT with 4 % PFA. Cover slips were washed 3 times with PBS and permeabilized for 5 min in 0.5 % Nonidet P40 (Fluka) in PBS. Cells were blocked for 30 min in 3 % bovine serum albumine (BSA, Sigma-Aldrich) in PBS containing 0.01 % Triton-X-100 (Fluka Analytical) (PBS-T). After 3 washes with PBS-T, 1st antibodies, diluted in blocking solution, were incubated for 1.5 h at RT on the cover slips. After 2 washings with PBS-T, cells were incubated with 0.5 μg/ml DAPI in PBS-T for 10 min, washed again 2 times with PBS-T and then mounted with fluorescent mounting medium (Dako, S3023). Confocal imaged were taken with the confocal, Zeiss LSM 510 Meta microscope. Epi-fluorescent pictures were obtained with the Leica DMI 4000 microscope.

In order to evaluate the length of a cell, cells were plated on 10 μm lines as described above, fixed, stained with phalloidin Alexa 568 and imaged with the scan slide tool of MetaMorph software. MetaMorph software was further used to quantify the lengths of cells imaged.

3.2.5.7 Immunhistochemistry

For immunhistochemistry of ephrin-B2 the PerkinElmer TSA amplification was used following its instructions.

3.2.5.8 Mice

MMTV-PyMT (*129*), MMTV-Neu (*11*), MMTV-Cre (*130*), MMTV-Neu-IRES-Cre (both kindly provided by W. J. Muller, McGill University, Canada) (*131*) and

Efnb2 floxed mice (kindly provided by R. Adams, MPI Münster, Germany) (*120*) were all bred within FVB/N background.

For genotyping of mice the following primers were used:

mRNA:	**Forward primer (5'-3'):**	**Reverse primer (5'-3'):**
MMTV-PyMT	cggcggagcgaggaactgaggagag	tcagaagactcggcagtcttaggcg
Efnb2 floxed alleles	cttcagcaatatacacaggatg	tgcttgattgaaacgaagcccga
MMTV-NIC	cggtcgatgcaacgagtgatgagg	ccagagacggaaatccatcgctcg
MMTV-Neu	ggaagtacccggatgaggagggcatatg	ccgggcagccaggtccctgtgtacaagccg

3.2.5.9 Statistics

Statistical analysis and graphs were generated with the help of GraphPad Prism software (GraphPad Sofware Inc, San Diego, CA) using paired, two-sided t-tests with * $p < 0.05$ ** $p < 0.01$ and *** $p < 0.001$.

3.3 The two faces of TGFβ: tumor suppressor and metastasis promoter

— review manuscript —

The transforming growth factor beta (TGFβ) is a famous cytokine mostly studied in development and cancer. Its canonical signaling has been described many years ago, but other factors feeding in and additional non-canonical pathways are being more and more explored and complicate the picture of TGFβ's action. The dual role of TGFβ signaling, being lost in a variety of human cancers as a tumor suppressor yet on the other hand being able to promote tumor progression and metastasis, is controversially discussed. In this review, we describe the current state of research on TGFβ signaling combined with data of *in vivo* studies in mice and man. We explicitly stress controversial data in order to provide insights into the complexity of TGFβ signaling.

3.3.1 The modes of action of TGFβ signaling

3.3.1.1 Canonical TGFβ signaling

The most studied signaling cascade stimulated by TGFβ is the canonical TGFβ pathway using Smad proteins as signal transducers. The cytokine TGFβ binds to TGFβ receptor II (TGFβRII) which, upon interaction, hetero-tetramerizes with TGFβ receptor I (TGFβRI). The TGFβRIII can present TGFβ to the TGFβRII beforehand, thereby further facilitating ligand-receptor interaction. Ligand-bound TGFβRII acts as serine/threonine kinase that phosphorylates its partner TGFβRI. TGFβRI, a serine/threonine kinase as well, recruits the receptor Smads (R-Smads), Smad2 and Smad3, and phosphorylates them at their C-terminus. The phosphorylated complex of Smad2/3 binds Smad4, the common Smad, and together they translocate into the nucleus. In the nucleus, Smad2/3/4 can either transactivate or repress target gene expression. Only Smad3 and Smad4 directly bind to a specific DNA motif, the Smad binding element (SBE) (Fig. 21a). Because Smads alone are poor DNA binders, other transcriptional co-activators or co-repressors are needed for effective transcriptional regulation (*134*).

3.3.1.2 Non-canonical TGFβ signaling

The ligand-bound TGFβR complex activates not only the canonical Smad pathway but also several other non-canonical ones (*135*). TGFβR-complexes can stimulate c-Jun N-terminal kinase (JNK) signaling via map kinase kinase 4 (MKK4) which for instance, induces the expression of the extracellular matrix protein fibronectin and thereby is important for cell migration (*136*).

The mitogen activated protein kinase (MAPK) p38 is another non-canonical target of TGFβ signaling. p38 is induced after association of αvβ3-integrin, bridged by the focal adhesion kinase (FAK), with TGFβRII. Upon this interaction, Src phosphorylates TGFβRII on Tyr284. The created phospho-tyrosine site at the receptor can be bound by the adapter protein Grb2 which further downstream leads to an enhanced p38 activity (*137-139*). A different way to induce p38 and JNK signaling by TGFβ is the interaction of TGFβRI with TRAF6, which activates TGFβ activated kinase (TAK1) leading ultimately to p38 and JNK activation (*140*). The importance of p38 as a TGFβ output was shown in normal mammary gland cells. Here, the activation of p38 by a mutant TGFβRI that cannot activate Smads is sufficient to induce apoptosis. Furthermore, the activation of p38 is required for epithelial to mesenchymal transition (EMT) but not for arresting cells in the cell cycle (*141*). JNK and p38 can increase canonical TGFβ signaling by phosphorylating Smad3 in its linker region, which enhances its signaling activity (*142,143*).

Another non-canonical branch of TGFβ signaling leads to cell growth via PI3K, PKB, mTor and S6 kinase (S6K) (*144*). Additionally, TGFβ can affect S6K by the activation of the phosphatase PP2A, which dephosphorylates and thereby inactivates p70S6K leading to a cell cycle arrest in G1 (*145*).

To make TGFβ signaling even more complex, Lee *et al.* have reported that TGFβRI cannot only act as a serine/threonin kinase but also as a tyrosine kinase. Thus, the TGFβR complex can phosphorylate ShcA on a serine and a tyrosine residue which further downstream leads to an activation of the extracellular-signal regulated kinase (Erk) thereby mimicking signaling of receptor tyrosine kinases (RTKs) (*146*).

Apart from the classical cell survival, apoptosis and proliferation pathways discussed below, TGFβ has an impact on cell shape. Major changes in cell morphology are initiated by TGFβ. TGFβ phosphorylates the polarity complex protein Par6, which in turn recruits the ubiquitin ligase Smurf1 that targets the

GTPase RhoA for proteasomal degradation leading to tight junctions breakdown (*147*). On the other hand, TGFβ can activate RhoA and thereby its effector ROCK, inducing stress fibers, EMT and cell cycle arrest (*148*) (Fig. 21b).

The non-canonical signaling branches modulated by TGFβ have emerged to be of great relevance. Clearly, TGFβ-induced signaling is more complex than the single Smad pathway because it involves many non-canonical signaling branches as well.

3.3.1.3 Fine tuning of TGFβ signaling and negative feedback loops

To modulate TGFβ signaling the different players of the pathway can be positively or negatively modified. The inhibitory Smad7 is a direct target of TGFβ signaling and acts in a negative feedback mechanism on the TGFβR complex (*149*). Smad7 binds to and re-localizes Smad ubiquitin regulatory factors, Smurf1 and Smurf2, from the nucleus to TGFβRs. Smurfs are E3-ubiquitin ligases and their interaction leads to ubiquitination of TGFβRI and ultimately to its proteasomal degradation (*150,151*). In addition to the recruitment of ubiquitin ligases, Smad7 accompanies phosphatases to the TGFβR complex reverting their activation (*152*). Inhibiting the canonical pathway only, Smad7 competes with receptor Smads for binding to TGFβRI, thereby antagonizing signal transduction (*153*).

Another way to tune TGFβ signaling in a negative feedback loop is by transcriptionally repressing TGFβRII expression. The transcription factor Dlx2 is upregulated by canonical TGFβ signaling and directly represses the expression of TGFβRII (*154*).

The TGFβR complex is not only regulated negatively but also positively. Sumoylation of TGFβRI in an active TGFβR-complex increases its ability to recruit and phosphorylate Smad3 thereby enhancing Smad signaling (*155*). Activated TGFβ receptors are constitutively internalized. Endocytosis can lead to degradation of the TGFβR complex. However, when the receptors are internalized in clathrin-coated pits, SARA (Smad anchor for receptor activation) presents Smad2 to the receptors, thereby facilitating pathway activation. (*156,157*).

In addition to TGFβ receptors, Smads are an entity that can also be regulated in a variety of ways. The first step of TGFβ pathway activation, the recruitment of the R-Smads to the activated receptors, is facilitated by the interaction with SARA, cytoplasmic PML and Elf (*157-159*). Later on, the subsequent accumulation of active

Smad2/3/4 complexes in the nucleus depends on Taz (WWTR1), which binds and links it to the transcription machinery (*160*).

Apart from the localization of Smads, R-Smads can be covalently modified in various ways. Linking integrin signaling to TGFβ function, the adaptor protein p130Cas is phosphorylated upon adhesion or growth factor stimulation. Phosphorylated p130Cas binds to Smad3 and inhibits its phosphorylation and thereby its activity (*161*). The phosphatase PPM1A can remove the phosphorylation of R-Smads gained by the active TGFβRI. This leads to shuttling R-Smads out of the nucleus and reverts their activation (*162*). PPM1A can dephosphorylate RanBP3, a component of the nuclear export machinery. As a consequence, Smads are excluded from the nuclei in a higher efficiency, which further decreases their activity (*163*).

Smad4, on the other hand, is modified by monoubiquitination. Ubiquitination of Smad4 by Tif1γ prevents its binding to p-Smad2. This effect is opposed by the de-ubiquitinase FAM. Monoubiquitination of Smad4, regulating its binding ability to R-Smads, makes this modification the equivalent to phospho-modifications of the R-Smads (*164*).

Protein stability is yet another issue not only important for the TGFβ receptors but also for R-Smads. GSK3β phosphorylates inactivated Smad3, marking it for ubiquitination and further degradation. Thereby, Smad3 levels can become a limiting factor in canonical TGFβ signaling (*165*).

As exemplified by the different modifications on all TGFβ pathway components, TGFβ signaling can be influenced in various ways. For example, interfering with the stability, localization and availability of TGFβ receptors, R-Smads and Smad4, can modulate the TGFβ signaling strength.

3.3.2 The main outcome of TGFβ signaling

3.3.2.1 TGFβ induces cytostasis and differentiation

The main effect of TGFβ signaling, using the canonical Smad pathway, is to arrest cells in the G1-phase of the cell cycle (*166*). In order to do so, Smad3/4 uses the co-transcription factors E2F4/5 and C/EBPβ to repress the expression of the potent mitogenic transcription factor c-Myc (*167,168*). c-Myc function can additionally be indirectly repressed by TGFβ. Smad2/3, in certain cell types even without Smad4 binding, interacts with the inhibitory kappa kinase alpha (IKKα) and together induces the c-Myc antagonists Mad1, Mad2 and Ovol1 (*169*).

TGFβ signaling not only represses mitogenic factors such as c-Myc, but also induces the expression of cell cycle inhibitors. The most prominent ones are the cyclin-dependent kinase inhibitor genes *CDKN1A* and *CDKN2B*, which are transactivated by Smad complexes, using FoxO as co-transcription factor (*170,171*). Additionally, TGFβ can interfere with the recruitment of c-Myc to the *CDKN2B* promoter via Miz1 and thereby de-represses the expression of this cell cycle inhibitor (*172*). Smad transcription complexes directly activate another member of the cell cycle inhibitors of the Ink4 locus, i.e. p19Arf, yet its expression can additionally be dependent on p38 activity shown in MEFs and *in vivo* during mouse development. This stimulation is ancillary to p19Arf's prominent role as an oncogene sensor (*173*).

The classical Smad4 target gene plasminogen activator inhibitor 1 (PAI-1) is reported to be critical for TGFβ-induced cell cycle arrest in several cell types. The authors speculate that PAI-1's cytostatic activity is achieved by attenuating PI3K/PKB signaling (*174*). More globally, TGFβ signaling can decrease translation by increasing directly the expression of 4E-BP1, which sequesters the eukaryotic translation initiation factor-4F ultimately leading to G1 arrest (*175*).

To force cells not only into cell cycle arrest but also into differentiation, Smads directly repress the inhibitors of differentiation (Id1-3) (*176,177*).

Taken together TGFβ can provoke a G1-arrest by directly increasing the amount of cell cycle inhibitory proteins like p15, p21 and 4E-BP1 as well as by repressing mitogenic factors like c-Myc and Ids (Fig. 21c).

3.3.2.2 TGFβ induces apoptosis

TGFβ-activated signaling has many means by which it can force a cell into apoptosis (*178*). The canonical TGFβ pathway can directly influence the apoptotic machinery by upregulating the pro-apoptotic protein Bim (*179*) and DAPK, an inducer of the mitochondrial based apoptosis (*180*). Another target of canonical TGFβ signaling that propagates apoptosis is the inositol phosphatase SHIP. SHIP alters the intracellular pool of phospholipids and inhibits the survival factor PKB, thereby favoring cell death over survival (*181*).

Further prominent inducers of apoptosis are the stress kinases p38 and JNK (*182*). MAP-kinase p38 is not only a non-canonical target of TGFβ signaling, but is also induced via up-regulation of the stress-inducible protein Gadd45b by Smads (*183*). Interestingly, p38 can phosphorylate and thereby stabilize p53, which can then initiate its pro-apoptotic transcriptional program. This interaction is supported by Smad7's function as a scaffold for both proteins (*184*). TGFβRII binds to DAXX, a Fas-associated protein, which activates JNK, thus another way to induce apoptosis (*185*).

Furthermore, activation of the apoptosis-related protein in the TGFβ signaling pathway (ARTS), which activates caspase 3, is crucial for TGFβ-induced apoptosis in several cell types and can even restore the ability of TGFβ to induce apoptosis in normally TGFβ-insensitive cell lines (*186*) (Fig. 21d).

TGFβ can not only induce apoptosis but also inhibit it. It has been shown that in starved cells TGFβ can protect cells against apoptosis by phosphorylating Jun and inhibiting JNK (*187*). Another way to rescue cells from apoptosis is TGFβ's ability to induce EGFR signaling, thereby, shifting the balance from apoptosis to survival (*154,188*).

3.3.2.3 TGFβ induces Epithelial to Mesenchymal Transition (EMT)

EMT is a process that occurs physiologically during embryonic development and wound healing as well as in malignant cells in order to invade foreign tissue (*189*). A main inducer of EMT is TGFβ. Active Ras can further enhance this effect (*190*). Yang *et al* have shown in hepatocytes that the decision whether TGFβ induces apoptosis or EMT is made by the cell cycle state. Cells that are in G1/S-phase readily undergo EMT upon TGFβ stimulation whereas cells in G2/M-phase respond to TGFβ mostly with apoptosis (*191*). The induction of EMT is not only dependent on canonical TGFβ signaling but also on TGFβ's ability to induce p38 via the non-canonical route (*141*).

Loss of cell adhesion and polarity is a hallmark of EMT both induced by TGFβ. TGFβ leads to a loss of tight junctions by degrading RhoA in a non-canonical fashion as mentioned above. The loss of adherens junctions is mainly accomplished by transcriptional repression of the classical epithelial protein E-cadherin. The transcriptional repressor Snail is a direct target of canonical TGFβ signaling, which together with Smad3/4 represses *CDH1* gene expression, thereby inducing EMT (*147,192*).

TGFβ signaling is not only important for the induction of EMT but also for sustained EMT. In MCF10A breast cancer cells the DNA methyltransferase DNMT1 methylates the epithelial genes *CDH1*, *CGN*, *CLDN4* and *KLK10* upon which their expression is silenced in the cells that have undergone EMT. Withdrawal of TGFβ in mesenchymal cells reverts their EMT phenotype, accompanied by a loss of the methylation marks on the aforementioned genes (*193*) (Fig. 21e).

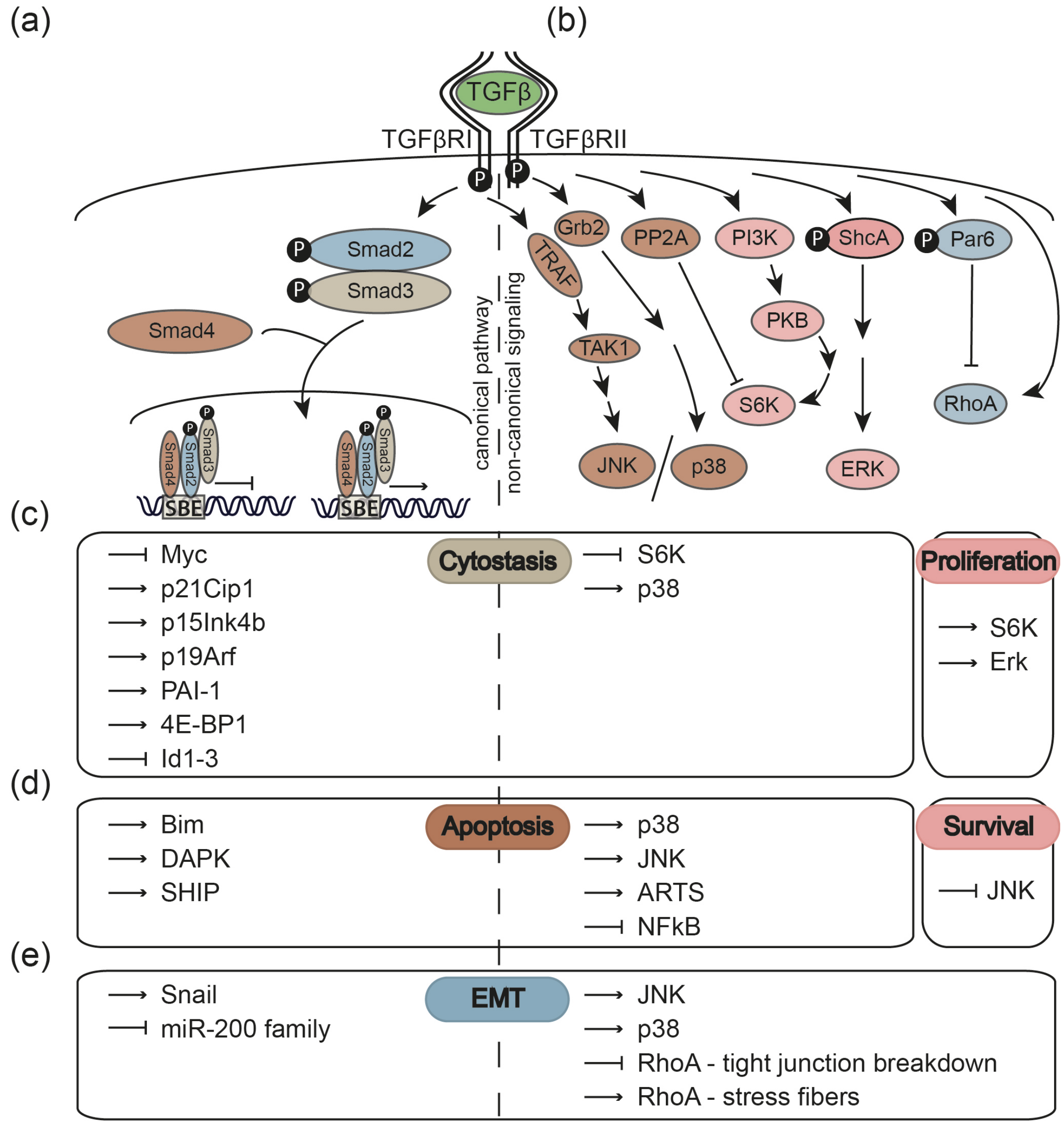
(a)
(b)
TGFβ
TGFβRI
TGFβRII
P
P
P Smad2
P Smad3
Smad4
Smad4 Smad2 Smad3
SBE
canonical pathway
non-canonical signaling
Grb2
TRAF
TAK1
JNK
p38
PP2A
PI3K
PKB
S6K
P ShcA
ERK
P Par6
RhoA
(c)
Myc
p21Cip1
p15Ink4b
p19Arf
PAI-1
4E-BP1
Id1-3
Cytostasis
S6K
p38
Proliferation
S6K
Erk
(d)
Bim
DAPK
SHIP
Apoptosis
p38
JNK
ARTS
NFkB
Survival
JNK
(e)
Snail
miR-200 family
EMT
JNK
p38
RhoA - tight junction breakdown
RhoA - stress fibers

Figure 21: An overview of canonical and non-canonical TGFβ signaling and the main outcomes.
(a) Upon binding to its receptors, TGFβ induces canonical Smad signaling. Smad complexes induce and repress transcription of target genes.
(b) TGFβ signaling additionally activates non-canonical pathways.
(c-e) The main outputs of TGFβ signaling are cytostasis (c), apoptosis (d) and EMT (e) but also proliferation and survival signaling can be stimulated. Here, the different genes activated or repressed by TGFβ signaling are depicted. The colors used for the pathway components reflect the colors of their main output.

3.3.3 What goes wrong with TGFβ signaling in cancer

3.3.3.1 Mutations

Loss-of-function mutations of TGFβ pathway components can be found in a lot of human cancers like colon, pancreas, head and neck, ovarian and gastric cancer and could be recapitulated by genetically engineered mice. Remarkably, other cancer types like breast, prostate, glioma, melanoma and hematopoietic cancer only seem to lose the tumor suppressive parts of the TGFβ pathway selectively and keep its tumor promotive function untouched (*194,195*).

TGFβ receptors

Loss-of-function mutations in the *TGFβRII* gene are often found in colon cancer with microsatellite instability. The *TGFβRII* gene has a poly-adenine repeat sequence, which is a hot spot for mutations when the cellular DNA repair mechanisms are impaired (*196*). The same mutations have been reported in replication error-positive glioma and gastric cancer (*197,198*). To prove the relevance of loss of TGFβRII in cancer, a genetic deletion of *TGFβRII* has been analyzed in mice. Conditional deletion of *TGFβRII* in the colon epithelium has revealed no significant histological changes. However, in combination with an oncogenic stimulus, loss of *TGFβRII* became overt by a more rapid onset and an increased number of neoplasms (*199*) as well as a higher grade of malignancy (*200*). Similar results have been found in murine models for pancreas cancer (*201*), head-and-neck squamous cell carcinoma (*202*), breast (*203*) and skin cancer (*204*).

The *TGFβRI* gene was found in human colorectal cancer to be either mutated (*TβR-I(6A)*) or germline allele-specific expressed which both leads to a decrease in function and, thereby, to a weakening of TGFβ signaling (*205,206*). Other point mutations or a loss of the *TGFβRI* gene have been found only rarely in some studies (*194*). A reduction in TGFβRI expression can be readily observed in gastric cancer where the *TGFβRI* locus is silenced by methylation (*207*). In order to mimic the decrease of TGFβ signaling, mice with a heterozygous deletion of *TGFβRI* have been generated. Deletion of one *TGFβRI* allele led to faster development and growth of tumors in a colorectal cancer model. Remarkably, the tumors kept the second allele of the *TGFβRI* gene, being still able to use TGFβ signaling but in a down-tuned manner (*208*).

The TGFβRIII's function is to present TGFβ to the TGFβRII increasing the probability of receptor complex formation. In renal cell carcinoma, *TGFβRIII* has been found mutated early in carcinogenesis, whereas a second hit in the *TGFβRII* gene was monitored later during malignant progression (*209*). Also in non-small cell lung cancer *TGFβRIII* was found mutated and the loss of TGFβRIII expression correlated with disease progression (*210*). Epigenetic silencing of *TGFβRIII* linked to advanced cancer progression has been described in ovarian and prostate cancer (*211,212*).

Summing up, all three TGFβRs can be found mutated in human cancer. Whereas the *TGFβRII* is the most commonly lost receptor, TGFβRI and TGFβRIII rather lose the functionality of one allele. Also the frequency of mutations in cancer is higher for TGFβRII than for the other two receptors.

Smads

Apart from mutations in the TGFβ receptors, which mostly block the whole TGFβ signaling, the canonical pathway components, the Smads, are found mutated in human cancers as well. So far, only one group has been able to report a loss of Smad3 expression in gastric cancer (*213*). Also for the other receptor Smad, Smad2, mutations are only rarely found (*214-216*).

The most prominent Smad, to be lost or mutated in several cancers and even called a tumor suppressor, is *DPC4* (*217*). Mutated versions of Smad4 proteins are usually unable to bind to R-Smads and thereby unable to carry out TGFβ-induced signaling (*218*). The role of Smad4 as a tumor suppressor has been validated in a conditional mouse model where *Dpc4* is deleted in the breast. Here, the sole loss of *DPC4* could induce hyperplasia and trans-differentiation of the mammary epithelium into squamous cell carcinoma accompanied by β-catenin stabilization (*219*). In combination with an additional oncogenic driver mutation *Dpc4* knockout mice are giving rise to more aggressive tumors than the oncogenic mutations alone (*220*).

3.3.4 From tumor suppressor to tumor promoter

3.3.4.1 TGFβ signaling: tumor suppressor and metastasis inducer

Dysregulation of the TGFβ pathway in humans, genetically recapitulated in mice, shows a higher risk for cancer in various organs hinting to a tumor suppressive role of TGFβ. Controversially, overactivation of the pathway seems to have a bad outcome as well. Several studies where TGFβ is overexpressed in a tumorigenic setting complement the aforementioned tumor suppressive role of the pathway. However, progressing tumors, that have overcome the tumor suppressive function of TGFβ, are more invasive and more metastatic, eventually accompanied by an EMT phenotype (*221,222*). Along this line, in experimental metastasis models in mice TGFβRI kinase inhibitors could reduce the number and size of metastases (*223*). The same is true when different TGFβ inhibitors were administered to tumor bearing mice (*224-226*). These examples hint to TGFβ being an early tumor suppressor but later during tumor progression a metastasis inducer.

Arguing against the role of TGFβ as a tumor suppressor are findings that loss of function mutations arise rather late during tumor progression (*227-229*). Having said that, it is most likely that other factors in the tumor influence the outcome of TGFβ signaling and thereby favor or select against genetic alterations in the TGFβ pathway. In most of the cases TGFβ seem to be a tumor suppressor but when this function is overcome, TGFβ increases the malignancy of cancer.

3.3.4.2 TGFβ stands for poor prognosis

That TGFβ does not only arrest cells in G1 or induces apoptosis is indicated by the observation that high TGFβ plasma levels in patients with cancer are predictive for a poor prognosis, especially after surgery (*194*). An additional indication for a poor prognosis is that TGFβ levels are increased in tumors that have metastasized compared to the ones that have not (*230*). A high deposition of TGFβ in cancer cells and in the surrounding extracellular matrix has been found at tumor fronts and in lymph node metastases of breast cancer patients (*231*). This has an effect on tumor development what has been shown in a mouse model overexpressing TGFβ1 in keratinocytes. These cells give rise to less tumors when challenged with carcinogenes but tumors that do arise are much more aggressive (*221*).

How do the notions that *TGFβRII* and *DPC4* are tumor suppressor genes and that high levels of TGFβ correlate with poor prognosis fit together?

3.3.4.3 Transcription cofactors conduct the output

Smad complexes are very poor transactivators, so they need additional transcription cofactors to enhance their ability to induce transcription. That is why the availability and activity of transcription cofactors plays a major role on the output of canonical TGFβ signaling. The transcription cofactors not only decide about the strength of transactivation but also about the genes to be targeted. Loss of transcription cofactors can down-modulate the tumor suppressive arm of TGFβ signaling, leaving the non-canonical pathway untouched (*195*). In the following section, transcription cofactors found underrepresented or overrepresented in human cancers will be addressed.

Runx3 normally binds to and helps Smad2/3 complexes to induce cell cycle arrest and apoptosis. Upon loss or mutation of *RUNX3*, which is often found in gastric cancer, TGFβ cannot fulfill its tumor suppressive role anymore (*232*). TSC2 is another tumor suppressor that binds to Smad2/3 and is important for TGFβ's ability to transcriptionally increase p21 and p27 levels in order to halt cells in G1-phase (*233*). Overrepresented in human gastric cancers are the two similar DNA-binding proteins Ski and SnoN which are able to interfere with Smad signaling by disrupting the Smad complex and recruiting transcriptional repressor complexes to target genes. Normally, TGFβ signaling itself can oppose this interference by helping the ubiquitin ligase Arcadia to target Ski and SnoN, leading to their degradation. In several cancer types Arcadia has been found downregulated, allowing SnoN to accumulate and repress canonical signaling by substituting Smad2/3 as partners for Smad4 (*234,235*). Another way to disturb Smad signaling is by an isoform change of C/EBPβ to its inhibitory version LIP. C/EBPβ is a transcriptional modulator that is required for Smad/FoxO complexes to activate transcription of the cell cycle inhibitor p15. It is also essential for Smad/E2F4/5 complexes to repress c-Myc expression. Both of this is critical for TGFβ's ability to arrest cells in the cell cycle. In metastatic breast cancer this action of TGFβ is selectively lost, most likely due to the expression of the c/EBPβ inhibitory form LIP (*168*).

Supporting TGFβ's tumor-promotive function, IKKα can bind to Smad3, facilitating Smad complex formation on promoters of the EMT-inducer like Snail and Slug and provoking tumor progression (*236*).

3.3.4.4 Shift from canonical to non-canonical signaling

Some *TGFβR* mutations affect only a branch of TGFβ signaling, so that TGFβRs are still able to activate non-canonical signaling pathways.

As mentioned above, p130Cas is able to inhibit TGFβR-mediated Smad2/3 phosphorylation. p130Cas, which is often upregulated in breast cancer, shifts the TGFβ signaling from the canonical, rather tumor suppressive pathway, to the non-canonical pathway (*237*). One of the strongest oncogenes, Ras, is able to induce phosphorylation of Smad2 and Smad3 via Erk, leading to their cytoplasmic retention, which makes them unavailable for TGFβ-induced canonical signaling. In normal epithelial cells, this inhibition of TGFβ signaling by Ras is just one way of fine-tuning the pathway. However, in cells that express oncogenic Ras or have a hyperactivated EGFR signaling, TGFβ-induced apoptosis is overridden by sequestration of the Smads (*238*). In a similar manner, the oncoprotein Raf is capable to induce TGFβ secretion, thereby synergizing with TGFβ to induce EMT. Here, TGFβ-mediated cell cycle arrest induction, could be transiently monitored, whereas the induction of apoptosis was inhibited. In this case, the selective action towards an EMT and not towards apoptosis was not due to inhibition of canonical TGFβ pathway, but rather to a general effect of the overstimulation of the MAPK pathway (*239*). Many researchers use cellular systems that are transformed by Ras or EGFR so that cells tolerate TGFβ treatment without having to deal with the apoptotic branch of TGFβ signaling of non-transformed cells. Acting on Smad4 to inhibit canonical TGFβ signaling, the transcription factor Dlx4 is able to sequester Smad4 from the R-Smads. Dlx4 is found upregulated in a number of cancers what could reflect its ability to specifically interfere with canonical TGFβ signaling, leaving the non-canonical untouched (*240*).

It has been described that TGFβ can even promote the expression of c-Myc in cancer, completely changing TGFβ's tumor suppressive function. This is achieved by inducing the expression of NFAT transcription factors in a calcineurin-dependent way. NFAT can replace the repressive canonical Smad3 complex on the c-Myc promoter leading to an upregulation of c-Myc and ultimately to cancer cell proliferation. This growth-promoting effect of TGFβ in cancer cells is specific for c-Myc expression (*241*). Summing up, c-Myc regulation by TGFβ seems to be a central event leading either to cytostasis or to cell proliferation. The outcome is depending on the contribution of other factors: the strength of the canonical signaling over the non-canonical effects of TGFβ and on the overall survival (e.g. Ras, EGFR) over apoptotic signals in cells.

3.3.4.5 Specific inhibition of tumor suppressive actions of TGFβ

In tumors where no TGFβ signaling components are mutated, the cytostatic and apoptotic functions of TGFβ have to be inhibited in another way. In this section, several mechanisms on how cells can evade the constraints by TGFβ will be highlighted.

A strong pro-survival and proliferation signal is mediated via the PI3K/PKB pathway. Yet, it is not only the pathway alone that leads to cell survival but also its interaction with the TGFβ pathway. PKB is able to bind and sequester not yet activated Smad3 out of the nucleus without using its kinase activity. Therefore, Smad3 is not available for signaling and for the induction of apoptosis. The ratio between Smad3 and PKB seems to be important for the sensitivity of cells to TGFβ-induced apoptosis (*242*).

Investigations of Smad2 and Smad have revealed their distinct roles. The adaptor protein DAB2 has been shown to specifically interfere with Smad2 phosphorylation leaving Smad3 unchanged. DAB2 is frequently epigenetically silenced in squamous cell carcinomas, which correlates with a poor patient prognosis. Thus, the loss of DAB2 leads to a de-repression of Smad2, upon which cancer cells have been described to become more motile and invasive without activating the tumor suppressive arm of TGFβ (*243*). Having described this phenomenon, it seems contradictory that a *Smad3* knockout in keratinocytes leads to resistance to chemically-induced carcinogenesis, whereas loss of *Smad2* had the contrary effect accompanied by cells undergoing EMT (*244*). Furthermore, in a breast cancer cell line a Smad3 knockdown has led expectedly to less Smad3-induced transcription, but the opposite is true for cells with a Smad2 knockdown. These differential roles of the R-Smads have been further underlined in a transplantation model. Here, Smad3 knockdown cells were less metastatic than their parental cell line, whereas Smad2 knockdown cells were even more metastatic (*245*). The existence of specific target genes for both Smads has been shown by selectively knocking them down, and also here only Smad3 seems to be necessary for TGFβ-induced cell cycle arrest (*246*). All in all, the normally described canonical TGFβ pathway seems to be oversimplified and further investigation of its modulators needs to be performed.

In contrast to the aforementioned non-canonical inhibition of NFϰB by TGFβ in non-transformed cells, TGFβ can also activate NFϰB in tumorigenic cells or cells that have undergone EMT. This activation is achieved by phosphorylation of the inhibitory protein IKK, via the TGFβ-activated kinase 1 (TAK1)-binding protein (TAB1), thus de-repressing NFϰB (*247,248*).

In general, TGFβ has been described to be able to increase the amounts of several receptor tyrosine kinases (*249*). The abundance of more RTKs makes the cell more accessible to pro-survival signals and thereby less sensitive to apoptosis induced by TGFβ. Recently, we have been able to describe that Dlx2, which is upregulated via canonical TGFβ signaling, down-modulates the TGFβRII in a negative feed back loop, thereby reducing its ability to transactivate p21. Furthermore, Dlx2 directly upregulates the EGFR ligand betacellulin supporting cells to overcome TGFβ-induced apoptosis (*154*). Similarly, Wendt *et al.* have shown that the induction of EGFR stability by TGFβ during EMT increases invasiveness (*250*).

As described above, c-Myc repression by TGFβ is a hallmark of TGFβ's ability to induce cytostasis. However, some tumor cells explicitly lose this reaction to TGFβ, without major changes in other target gene expression, allowing c-Myc to drive cells further through the cell cycle even in the presence of active TGFβ signaling (*251*). Sasaki *et al.* have described that the Wnt signaling transcription factor LEF1 in association with β-catenin transactivates c-Myc. Normally, TGFβ signaling can oppose Wnt-induced c-Myc transcription, which is conducted by the TCF4/β-catenin transcriptional activator complex. In the case of tumor cells, where β-catenin binds to LEF1 instead, TGFβ cannot interfere with Wnt signaling anymore and therefore cannot oppose the induction of c-Myc expression (*252*).

In gastric cancer miR-106b, miR-93 and miR-25 have been found overrepresented. These miRNAs are induced by E2F and target not only the S-phase-inducer E2F1 in a negative feedback loop, but they also affect the TGFβ-induced mRNA levels of the cytostatic protein p21 and of the pro-apoptotic protein Bim. Thereby TGFβ's tumor suppressive actions are selectively inhibited (*253*).

In summary, there are many ways a cell can selective lose only TGFβ's tumor suppressive functions without inhibiting TGFβ signaling completely. One way would be by modulation of single TGFβ signaling molecules, like the Smads. Another way is the activation of RTK-signaling that can override TGFβ's cytostatic and apoptotic function. Thus, the signaling environment TGFβ is embedded in plays a major role concerning the effect TGFβ can conduct in a cell.

3.3.4.6 TGFβ changes the microenvironment towards tumor growth and invasion

Tumors normally evolve in a hypoxic environment. The induction of angiogenesis by growing tumors is not only necessary in order to deliver enough nutrients and oxygen, but also for disseminating cells to leave the primary cancer site. TGFβ signaling induces angiogenesis in tumors. Together with Smad3, the hypoxia-induced factor 1 alpha (HIF1α) initiates the expression of vascular endothelial growth factor (VEGF) (*17,254*). In contrast, it has been shown for gallbladder tumors and hepatomas that TGFβ suppresses angiogenesis *in vivo* (*255,256*). Again, the consequences of TGFβ signaling on tumor angiogenesis are dependent on additional signals within cells and the environment.

Escape from the immune surveillance is a feature cancer cells have to acquire in order to establish a tumor. TGFβ has been described as a potent suppressor of immune reactions, which enables cancer cells to evade an attack by the immune system (*257*). An immuno-suppressive action is achieved when TGFβ induces expression and activation of IKK which interferes with survival signals conducted by NFϰB in lymphocytes. TGFβ's immunosuppressive function by reducing lymphocytes stands in contrast to TGFβ's ability to act tumor suppressive in lymphomas where the immune cells themselves are the threat (*247,258*).

Loss of TGFβ signaling is often found in colorectal cancer. This loss has been mimicked in a *Dpc4*-deficient mouse model of colorectal cancer. Here, the loss of TGFβ signaling in epithelial adenocarcinoma cells leads to secretion of CCL9 that in turn recruits myeloid derived suppressor cells (MDSC) (*259*). In mammary tumor models, the cytokines responsible for MDSC recruitment have been found to be CXCL5 and SDF-1. MDSCs facilitate invasion and metastasis via secretion of matrix metalloproteinases. Furthermore, MDSCs themselves secrete TGFβ that acts as a tumor suppressor in the microenvironment of cancer but has no effect on cancer cells in case of TGFβR loss (*260*). In this example, it is nicely shown how genetic loss of TGFβ signaling, together with TGFβ production within the tumor, synergizes to promote invasiveness and metastasis without affecting cancer cells directly. A similar phenomenon has been observed in humans, where high levels of TGFβ at the invasive front and high infiltration of MDSCs can be found (*230,260*).

Fibroblasts are another cell type that is susceptible to TGFβ signaling. Loss of TGFβ-responsiveness in fibroblasts by a *TGFβRI* knockout leads to hyperproliferation of activated fibroblasts accompanied by increased secretion of hepatocyte growth factor (HGF). This secreted HGF then stimulates epithelial cells, which surround fibroblasts and induces their proliferation, transformation and invasiveness (*261*).

In summary, TGFβ signaling has many means to influence the tumor microenvironment favoring tumor progression.

3.3.4.7 TGFβ as a mediator of metastatic spread

TGFβ signaling in cancer cells that have overcome its tumor suppressive function can promote metastasis. Rendering cancer cells mesenchymal via induction of EMT is one way TGFβ directly favors metastatic spread (*262*). Apart from the function of TGFβ within cancer cells, it plays an additional role in metastatic tropism. Cancer cell that disseminate in order to colonize secondary organs follow distinct metastatic patterns which can be influenced by TGFβ signaling (*52*).

An example for TGFβ signaling and its direct involvement in malignant colonization at secondary sites is breast cancer. The ER-negative subset of breast cancer, that shows a high TGFβ activity, primarily targets the lung for metastatic spread. TGFβ primes this cancer cells by inducing angiopoietin-like 4 (Angptl4) expression in a Smad-dependent manner. Angptl4 then helps the cancer cells to enter the lung parenchyma by loosening the endothelial cell-cell contacts, making the vasculature permeable for cancer cells' extravasation (*263*).

To attract disseminated cancer cells, also the future metastatic site can provide TGFβ. Bone, as secondary cancer target site, secretes TGFβ when it is being lysed by osteoclasts. The released TGFβ can activate the canonical TGFβ signaling within the cancer cells that have reached the bone, transactivating the metastasis genes IL11 and CTGF. IL11 and CTGF, in turn lead to maturation of osteoclasts and angiogenesis, respectively, which ultimately propagates osteolytic bone metastasis (*264,265*). In a study where a small molecule inhibitor of TGFβRI kinase (SD-208) was administered to mice, osteolytic bone metastasis were reduced (*266*). Supporting its clinical relevance, active TGFβ signaling has been shown by staining for p-Smad2 in breast cancer patients with bone metastases (*267*).

These examples demonstrate that TGFβ signaling can have a systemic effect to prepare sites of cancer cell dissemination. Therefore, TGFβ inhibition could be a potential therapeutic target to treat metastasis.

3.3.5 How to use the knowledge about TGFβ for cancer therapy

The TGFβ signaling status in sera of tumor patients is used as a biomarker to predict cancer aggressiveness and relapse (*194*). Mutations in TGFβ pathway components can be predictive but not meant to be targeted for therapy themselves. As an example, the integrity of the *DPC4* gene in colorectal cancer does not only stand for a better prognosis but also predicts a beneficial reaction of tumors against 5-fluoruracil-based adjuvant therapy (*268*). A very elegant study combines human sample analysis (histology and gene expression profiling) and combinatorial genetic modeling in mice. Using this method, the authors have shown that in a *PTEN*-negative tumor, often found in prostate intraepithelial neoplasia, loss of *DPC*4 leads to more advanced stages and metastatic tumors. Loss of *DPC4* was accompanied by the de-repression of the Smad4 target cyclinD1, and the invasion gene SPP1. Ding *et al.* have further shown that the status of these 4 factors (Smad4, cyclinD1, SPP1 and PTEN) can be used as a powerful marker for prostate cancer progression (*269*).

On the other hand, considering TGFβ as a pro-metastatic element rather than a tumor suppressor, the TGFβ ligand itself would be a possible drug target. Especially, since TGFβ seems to have a major impact not only on tumor cells by inducing EMT, but also on the microenvironment which helps tumor cells to evade immune responses, invade or colonize secondary organs. In order to block the auto- and paracrine function of TGFβ, soluble TGFβRII:Fc was administered to murine breast cancer models. Here, the sequestration of TGFβ could reduce invasiveness and metastases (*270*). Furthermore, transgenic expression of this TGFβ inhibitor in mammary epithelial cells did not lead to as severe phenotypes as seen in TGFβ knockout mice, despite a high concentration of inhibitor throughout the body. Therefore, TGFβ sequestration, in contrast to complete TGFβ depletion, does not diminish mice's lifespan and may be considered as an approach for human treatment as well (*271*).

The above-mentioned small molecule inhibitor of the TGFβRI kinase, SD-208, is suggested to be a potent inhibitor to block TGFβ signaling and thereby its pro-metastatic and immunosurveillance functions. Tumor bearing mice treated with SD-208 survived significantly longer than those treated with vehicle only (*272*). In order to avoid side effects of blocking TGFβ signaling systemically, Gorelik and Flavell suggest targeting TGFβ signaling only in T-cells. Hence, T-cells would be immune to TGFβ's immun-suppressive function and therefore able to effectively attack tumor cells (*273*).

3.3.6 Conclusive remarks

TGFβ is of major interest in cancer biology. However, the dissection of its bivalent functions, as a tumor suppressor and as metastasis inducer, remains a challenge. The complexity of TGFβ signaling, both canonical and non-canonical, that can be modulated by various ways has to be further investigated to get a more complete picture of TGFβ's functions. The cellular system and the animal models chosen to study TGFβ play an important role on the results being obtained. However, first great efforts to understand TGFβ's way of action have been made. Then recent notions that TGFβ is not only relevant during tumorigenicity in cancer cells but also in the microenvironment has highlighted new fascets of TGFβ signaling. Therefore, the hope that targeted therapy against TGFβ pathway components reach the clinics is justified.

The EMBO Journal (2011), 1–11 | © 2011 European Molecular Biology Organization | All Rights Reserved 0261-4189/11
www.embojournal.org

THE
EMBO
JOURNAL

Transcription factor Dlx2 protects from TGFβ-induced cell-cycle arrest and apoptosis

Mahmut Yilmaz[1,2], Dorothea Maaß[1], Neha Tiwari, Lorenz Waldmeier, Petra Schmidt, François Lehembre[3] and Gerhard Christofori*

Department of Biomedicine, Institute of Biochemistry and Genetics, University of Basel, Basel, Switzerland

Acquiring resistance against transforming growth factor β (TGFβ)-induced growth inhibition at early stages of carcinogenesis and shifting to TGFβ's tumour-promoting functions at later stages is a pre-requisite for malignant tumour progression and metastasis. We have identified the transcription factor distal-less homeobox 2 (Dlx2) to exert critical functions during this switch. Dlx2 counteracts TGFβ-induced cell-cycle arrest and apoptosis in mammary epithelial cells by at least two molecular mechanisms: Dlx2 acts as a direct transcriptional repressor of TGFβ receptor II (*TGFβRII*) gene expression and reduces canonical, Smad-dependent TGFβ signalling and expression of the cell-cycle inhibitor $p21^{CIP1}$ and increases expression of the mitogenic transcription factor c-Myc. On the other hand, Dlx2 directly induces the expression of the epidermal growth factor (EGF) family member betacellulin, which promotes cell survival by stimulating EGF receptor signalling. Finally, Dlx2 expression supports experimental tumour growth and metastasis of B16 melanoma cells and correlates with tumour malignancy in a variety of human cancer types. These results establish Dlx2 as one critical player in shifting TGFβ from its tumour suppressive to its tumour-promoting functions.

The EMBO Journal advance online publication, 6 September 2011; doi:10.1038/emboj.2011.319
Subject Categories: signal transduction; molecular biology of disease
Keywords: betacellulin; Dlx2; EGFR; metastasis; TGFβ

Introduction

Transforming growth factor β (TGFβ) plays a central role in various biological processes such as development, tissue homeostasis, fibrosis, and cancer. During gastrulation and neural crest cell migration, TGFβ induces cell motility and invasiveness, thus enabling cells to migrate to distant sites within the developing embryo. In contrast, in differentiated epithelial tissue, TGFβ primarily maintains tissue homeostasis by promoting growth arrest and apoptosis, thus exerting tumour suppressor function (Massague, 2008).

This ambivalent nature of TGFβ signalling also plays a critical role in cancer initiation and progression. At early stages of tumourigenesis, TGFβ functions as a tumour suppressor by promoting cell-cycle arrest and apoptosis. In contrast, during late stage tumourigenesis, TGFβ exerts malignant activities, such as inducing an epithelial–mesenchymal transition (EMT), supporting tumour angiogenesis, and suppressing anti-tumoural immune responses (Wakefield and Roberts, 2002; Siegel and Massagué, 2003; Pardali and Moustakas, 2007; Massague, 2008). The switch of TGFβ signalling from its tumour suppressor activity to a tumour-promoting factor is achieved by at least two major modifications: the attenuation of pro-apoptotic TGFβ signalling and the activation of phosphoinositide 3-kinase (PI3K) and mitogen-activated protein kinase (MAPK) signalling pathways (Huber *et al*, 2005). Tumour-suppressive TGFβ signalling is mediated by canonical, Smad-dependent TGFβ signalling. Upon ligand binding to TGFβ receptors I and II, the receptor-associated Smad proteins (Smad2/3) are phosphorylated, dissociate from the receptor complex, and translocate to the nucleus in association with Smad4, where they modulate the expression of specific target genes. Expression of genes encoding anti-proliferative and pro-apoptotic factors is induced, such as the cell-cycle inhibitors $p15^{INK4B}$ and $p21^{CIP1}$, while the expression of mitogenic factors like c-Myc is repressed (Massague, 2004). In tumours, canonical TGFβ signalling is often suppressed, and cell-cycle arrest and apoptosis are bypassed by reduced TGFβ receptor II (TGFβRII) expression or by mutational inactivation of Smad proteins (Massague, 2008). Yet, cancer cells utilize TGFβ to promote tumour progression and survival by non-canonical TGFβ signalling, which mainly results in the activation of the MAPK and the PI3K pathways (Gotzmann *et al*, 2002; Lee *et al*, 2007b). A total loss of TGFβ signalling impairs late stage tumour progression and metastasis formation, demonstrating a critical role of TGFβ signalling for cancer malignancy (Cui *et al*, 1996; Oft *et al*, 1998; Moustakas and Heldin, 2005). However, the molecular mechanisms underlying the switch from TGFβ's growth inhibitory functions to its tumour-suppressive activities are only poorly understood.

Here, we report that the transcription factor distal-less homeobox 2 (Dlx2) is upregulated upon TGFβ treatment and attenuates growth-suppressive TGFβ signalling in a negative feedback loop. Moreover, Dlx2 induces mitogenic epidermal growth factor receptor (EGFR) signalling by directly inducing the expression of the EGFR-ligand betacellulin. Together, these Dlx2 functions protect cells from TGFβ-induced cell-cycle arrest and apoptosis and supports primary tumour growth and metastasis of B16 melanoma cells. Finally, the clinical relevance of Dlx2 is underscored by the observation that its expression correlates with the malignant progression of various human cancer types.

---

*Corresponding author. Department of Biomedicine, Institute of Biochemistry and Genetics, University of Basel, Mattenstrasse 28, 4058 Basel, Switzerland. Tel.: +41 61 267 3562; Fax: +41 61 267 3566; E-mail: gerhard.christofori@unibas.ch

[1] These authors contributed equally to this work

[2] Present address: CNIO, Madrid, Spain

[3] Present address: Actelion Pharmaceuticals Ltd, Allschwil, Switzerland

Received: 7 April 2011; accepted: 8 August 2011

Results

Dlx2 expression is induced by canonical TGFβ signalling

We have employed the normal murine mammary gland (NMuMG) cells as an experimental system to dissect the molecular mechanisms that enable epithelial cells to switch TGFβ signalling from proliferation suppressive to pro-survival functions. These non-transformed, epithelial cells respond with cell-cycle arrest and, partially, apoptosis during the early phases of TGFβ treatment. However, with ongoing TGFβ treatment, NMuMG cells overcome growth-suppressive TGFβ signalling and undergo EMT (Gal *et al*, 2008). To identify genes critically required to overcome TGFβ-mediated growth suppression, NMuMG cells were treated with TGFβ, and changes in gene expression during TGFβ treatment were determined. Among a large number of genes changing in their expression during TGFβ treatment, Dlx2 mRNA was found increasingly expressed after 2 days, with highest levels after 6 days (Figure 1A), a time period during which TGFβ-induced cell-cycle arrest and apoptosis was most prominent. Amplified Dlx2 mRNA levels were accompanied by increased levels of Dlx2 protein as determined by immunoblotting analysis (Figure 1B). Notably, increased levels of Dlx2 were predominantly localized to the nucleus in TGFβ-treated cells (Figure 1C). That Dlx2 is a general target of TGFβ signalling was further confirmed in a murine breast cancer cell line established from a tumour of a MMTV-Polyoma Middle T (MMTV-PyMT) transgenic mouse and in B16 melanoma cells (Supplementary Figure S1A). Dlx2 mRNA expression was not significantly induced upon TGFβ treatment in NMuMG cells harbouring a stable knockdown of Smad4 (shSmad4-NMuMG) (Figure 1D; Deckers *et al*, 2006), indicating that *Dlx2* gene expression depended on canonical TGFβ signalling.

Dlx2 promotes cell survival and proliferation during TGFβ treatment

We next investigated whether Dlx2 function was required for cell survival during TGFβ treatment. NMuMG cells were transfected with siRNA against Dlx2 (siDlx2) or with control siRNA (siCTR) (Supplementary Figure S1B), and changes in proliferation and apoptosis were determined. The potential protective function of Dlx2 was analysed at 6 days of TGFβ treatment, when cell death and detachment of cells from the cell culture plate were most prominent. Notably, siDlx2-NMuMG cells exhibited reduced cell numbers as compared with control siRNA-transfected cells (Figure 1E).

To assess whether loss of Dlx2 function affected proliferation and/or apoptosis during TGFβ treatment, we compared the levels of proliferation (BrdU incorporation) and of apoptosis (Annexin V staining) between siCTR- and siDlx2-treated NMuMG cells upon TGFβ treatment. Proliferation was significantly reduced and apoptosis was significantly increased in the absence of Dlx2 upon TGFβ treatment (Figure 1F and G), explaining the reduced cell number in TGFβ-treated siDlx2-NMuMG cells. These results were confirmed by the diminished growth rate of TGFβ-treated NMuMG cells in which Dlx2 expression was ablated by stable expression of shRNAs against Dlx2 (shDlx2-NMuMG) as compared with control shRNA-transfected cells (shCTR-NMuMG) (Figure 1H; Supplementary Figure S1C).

Next, we analysed whether the forced expression of Dlx2 affected proliferation and/or apoptosis of NMuMG cells in the

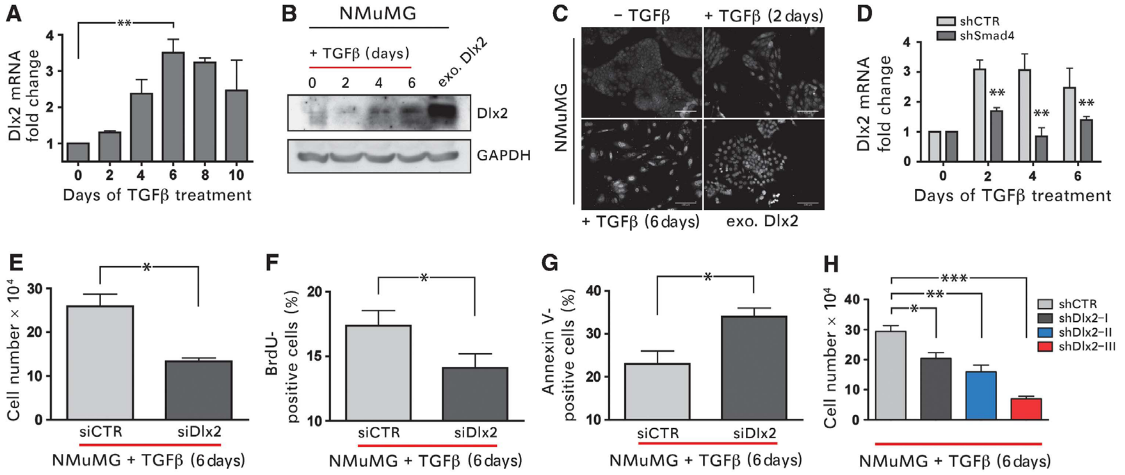

Figure 1 Dlx2 is a target of canonical TGFβ signalling and is critical for survival during TGFβ treatment of NMuMG cells. (**A**) Dlx2 mRNA levels were determined by quantitative RT–PCR in NMuMG cells treated with TGFβ for the days indicated. (**B**) Immunoblotting analysis of Dlx2 protein levels in NMuMG cells treated with TGFβ for the days indicated and of cells stably expressing Dlx2 is shown. GAPDH was used as loading control. (**C**) Subcellular localization of Dlx2 in NMuMG cells treated with TGFβ or stably expressing Dlx2 (exo. Dlx2) was determined by fluorescence microscopy. Scale bar = 100 μm. (**D**) Dlx2 mRNA levels were determined by quantitative RT–PCR in stable Smad4 knockdown (shSmad4) and control (shCTR) NMuMG cells treated with TGFβ for the days indicated. (**E–G**) Dlx2-depleted (siDlx2) and control (siCTR) NMuMG cells were treated with TGFβ (2 ng/ml) for 6 days. Viable cells were counted by trypan blue exclusion using a Neubauer cell counting chamber (**E**). Proliferation rates were determined by BrdU incorporation and flow cytometry (**F**). The rates of apoptosis were measured by Annexin V staining and flow cytometry (**G**). (**H**) NMuMG cells stably expressing three independent shRNAs against Dlx2 (shDlx2 I–III) or control shRNA (shCTR) were treated with TGFβ (1 ng/ml), and cell numbers were determined using a Neubauer counting chamber at day 6 of TGFβ treatment. Data are shown as mean ± s.d. and are representative of three independent experiments. Statistical values are calculated by using an unpaired, two-tailed *t*-test. $^{*}P \leqslant 0.05$; $^{**}P \leqslant 0.01$; $^{***}P \leqslant 0.005$.

©2011 European Molecular Biology Organization

presence or absence of TGFβ. We stably infected NMuMG cells with lentiviral vectors encoding HA-tagged, murine Dlx2 or firefly luciferase as control and used infected cell pools for further analysis. Dlx2 was exclusively expressed in the nucleus of stably infected NMuMG cells (Figure 2A). Dlx2-expressing NMuMG cells exhibited a significantly increased cell proliferation rate, as compared with control cells, and showed no sensitivity towards TGFβ-mediated growth inhibition (Figure 2B). Indeed, while control NMuMG cells ceased growing in the presence of TGFβ, Dlx2-expressing cells increased in numbers in the absence as well as in the presence of TGFβ. Annexin V staining and BrdU incorporation analysis revealed that, in comparison to control-transfected cells, Dlx2-expressing NMuMG cells exhibited decreased levels of apoptosis and proliferated at higher rates, respectively (Figure 2C and D).

Together, these gain and loss-of-function experiments demonstrate that Dlx2 is critical for cell survival and proliferation during the growth-suppressive phase of TGFβ treatment.

Dlx2 inhibits canonical TGFβ signalling

An attenuation of the canonical pro-apoptotic TGFβ signalling pathway is frequently found responsible for TGFβ-resistant growth (Massague, 2008). Hence, we determined the expression levels and activities of different molecules known to play critical roles in canonical TGFβ signalling. Notably, the protein levels of TGFβRII were found decreased in Dlx2-expressing NMuMG cells, whereas Smad4 protein levels were unchanged (Figure 3A). Reduced TGFβRII mRNA levels pointed to a Dlx2-mediated transcriptional repression of TGFβRII expression in NMuMG cells (Figure 3B). That Dlx2 is indeed a transcriptional repressor of the *TGFβRII* gene was further underlined by the observation that ablation of Dlx2 function counteracted the TGFβ-induced repression of the *TGFβRII* gene (Supplementary Figure S2A). Furthermore, forced expression of Dlx2 in HEK293 and NMuMG cells resulted in reduced *TGFβRII* promoter activity (Supplementary Figure S2B and C). Chromatin immunoprecipitation (ChIP) experiments with NMuMG cells either stably expressing HA-tagged Dlx2 or treated with TGFβ for 6 days demonstrated that Dlx2 directly bound to the *TGFβRII* gene promoter (Figure 3C). The specific binding of endogenous Dlx2 to the *TGFβRII* promoter was also observed in B16 melanoma cells (Supplementary Figure S2D) and in Py2T murine breast cancer cells (data not shown). Changes in the expression of inhibitory Smads, such as Smad7, or of the Smad-specific E3 ubiquitin protein ligase 1 (Smurf1) were not detected (data not shown), both of which have been shown to inhibit TGFβ receptor signalling (Di Guglielmo *et al*, 2003; Zhang *et al*, 2007).

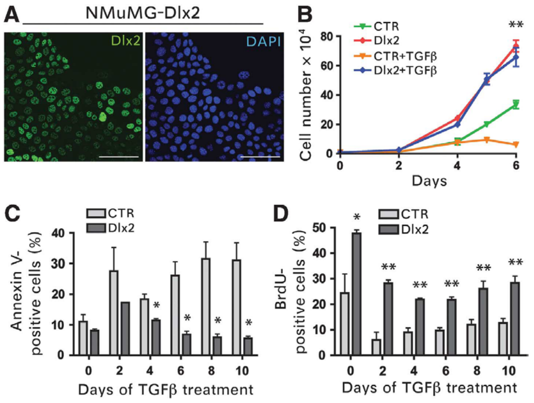

Figure 2 Dlx2 protects from TGFβ-induced cell-cycle arrest and apoptosis. (**A**) Confocal laser scanning microscopy of NMuMG cells stably expressing N-terminal HA-tagged Dlx2. Dlx2 was detected by anti-HA immunofluorescence staining (green). Blue DAPI staining visualizes nuclei. Scale bar = 100 μm. (**B**) Dlx2-expressing (Dlx2) and control (CTR) NMuMG cells were treated with or without TGFβ for the days indicated and counted by trypan blue exclusion using a Neubauer cell counting chamber. The time point day 6 was used to determine statistical significance between Dlx2-expressing and control cells. (**C**) Dlx2-expressing and control NMuMG cells were treated with TGFβ for the days indicated. Apoptosis was measured by Annexin V staining and flow cytometry. (**D**) Dlx2-expressing and control NMuMG cells were treated with TGFβ for the days indicated, and proliferation rates were determined by BrdU incorporation and flow cytometry. Data are shown as mean values ± s.d. and are representative of three independent experiments. Statistical values are calculated by using an unpaired, two-tailed *t*-test. *$P \leqslant 0.05$; **$P \leqslant 0.01$.

As a consequence of the Dlx2-mediated decrease in TGFβRII protein levels, canonical TGFβ signal transduction was found attenuated. The levels of phosphorylated Smad2 were reduced in clones and pools of Dlx2-expressing NMuMG cells (Figure 3D). Concomitantly, the transcriptional activity of the common mediator Smad4 was diminished in Dlx2-expressing cells, as revealed by Smad4-specific luciferase-reporter (CAGA box reporter) analysis (Dennler *et al*, 1998; Figure 3E). This decrease in TGFβ signalling lead to changes in the expression of *bona fide* TGFβ target genes, exemplified by the reduced expression of p21^{CIP1} and the increased expression of c-Myc (Figures 3F and 4A).

In summary, expression of Dlx2 attenuates apoptotic TGFβ signalling via direct transcriptional repression of the *TGFβRII* gene, resulting in reduced TGFβ signalling and Smad4 transcriptional activity and, thus, diminished expression of the cell-cycle inhibitor p21^{CIP1} and increased expression of mitogenic c-Myc.

Dlx2 engages EGFR to promote cell survival and proliferation

Inhibition of apoptotic, canonical TGFβ signalling explains why Dlx2 confers resistance towards TGFβ-mediated growth inhibition. However, it does not explain why Dlx2 expression increases cell proliferation and survival in the presence and in the absence of TGFβ. Recently, several reports have demonstrated that the MAPK and PI3K pathways are interactively engaged to ensure cell survival and proliferation in the presence of tumour-suppressive TGFβ (Janda *et al*, 2002; Lee *et al*, 2007b). Hence, we investigated whether these pathways were activated in TGFβ-resistant Dlx2-expressing NMuMG cells.

To investigate whether the MAPK and PI3K pathways were involved in TGFβ-resistant growth, we treated control and Dlx2-expressing NMuMG cells with chemical inhibitors for the MAPK kinase MEK1/2 (PD98059) or for PI3K (ZSTK474). Treatment with either inhibitor significantly reduced cell growth of Dlx2-expressing NMuMG cells as compared with control cells, and these effects were markedly increased upon combined treatment with TGFβ (Figure 4A and B). Thus,

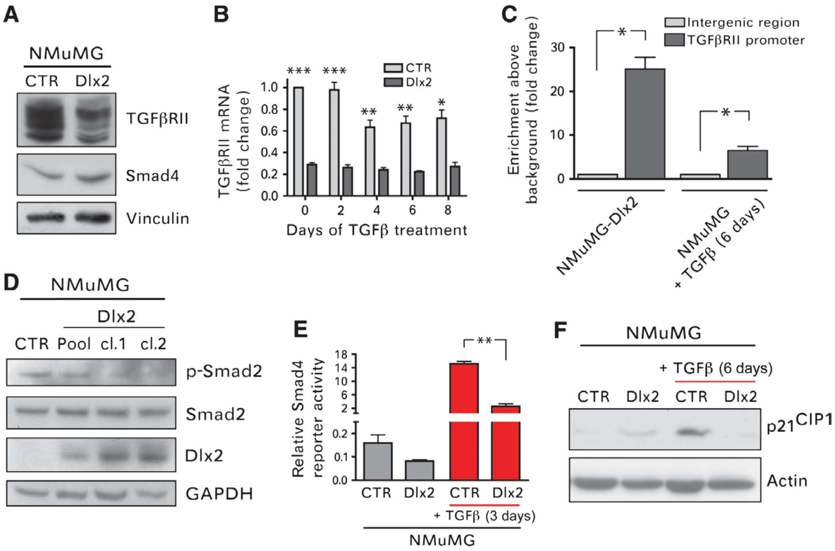

Figure 3 Dlx2 expression attenuates Smad-dependent, canonical TGFβ signalling. (**A**) Immunoblotting analysis of TGFβRII and Smad4 protein levels in Dlx2-expressing and control NMuMG cells is shown. Immunoblotting against vinculin was used as loading control. (**B**) TGFβRII mRNA levels in Dlx2-expressing and control NMuMG cells were determined by quantitative RT–PCR at different days of TGFβ treatment as indicated. Values were normalized to endogenous RPL19 levels. (**C**) Dlx2 binds directly the *TGFβRII* promoter. ChIP of Dlx2 was performed either on Dlx2-expressing NMuMG cells or on NMuMG cells treated for 6 days with TGFβ. Immunoprecipitated DNA fragments were quantified by quantitative PCR using primers covering basepairs −386 to −204 of the *TGFβRII* promoter region and primers covering an intergenic region as negative control. (**D**) Lysates of Dlx2-expressing cell pools or cell clones and control (CTR) NMuMG cells were analysed by immunoblotting analysis with antibodies against p-Smad2, total Smad2, HA to determine Dlx2 expression, and GAPDH as a loading control. (**E**) Dlx2-expressing and control NMuMG cells were transfected with a reporter plasmid where repetitive Smad4-binding motifs control the expression of *firefly* luciferase and then treated with or without TGFβ for 3 days. Luciferase activity values were normalized to co-transfected *Renilla* luciferase activities. (**F**) Immunoblotting analysis of Dlx2-expressing and control NMuMG cells in the absence or presence of TGFβ for 6 days with antibodies against p21^{CIP1} and against actin as loading control. Data are shown as mean ± s.d. and are representative of three independent experiments. Statistical values are calculated by using an unpaired, two-tailed *t*-test. *$P \leqslant 0.05$; **$P \leqslant 0.01$; ***$P \leqslant 0.001$.

Dlx2-mediated proliferation as well as TGFβ-resistant growth substantially relies on the activity of the MAPK and PI3K signalling pathways. Immunoblotting analysis revealed that the levels of the activated (phosphorylated) forms of the MAPK Erk1/2 but not of the PI3K effector protein kinase B (PKB) were higher in Dlx2-expressing NMuMG cells as compared with control cells, in the absence as well as in the presence of TGFβ (Figure 4C and D). Yet, depletion of Dlx2 in NMuMG cells did not affect the overall activation of PKB or Erk1/2 (Supplementary Figure S3).

Various growth factor receptors are known to induce MAPK and PI3K activities upon TGFβ treatment to promote survival and proliferation, including platelet-derived growth factor receptor (PDGFR), vascular endothelial growth factor receptor (VEGFR), and EGFR/ErbB family members (Fabregat *et al*, 1996, 2000; Murillo *et al*, 2005; Del Castillo *et al*, 2006). Hence, we utilized chemical inhibitors against these growth factor receptors to identify a potential upstream activator of MAPK and PI3K signalling. Among the inhibitors tested (VEGFR, PDGFR, IGFR, EGFR), exclusively inhibition of EGFR by the chemical inhibitor Tyrphostin AG1478 significantly repressed Dlx2-mediated, TGFβ-resistant proliferation of NMuMG cells (Figure 4E, data not shown). Dlx2-dependent, elevated activity of EGFR was confirmed by immunoblotting analysis using an antibody against phosphorylated EGFR (tyrosine 1173; Figure 4F).

Since total EGFR protein levels were not changed in Dlx2-expressing NMuMG cells (Figure 4E), we assessed whether the expression of members of the EGF family was upregulated by the expression of Dlx2. Gene expression analysis revealed that the EGFR-ligand betacellulin was significantly upregulated in Dlx2-expressing NMuMG cells as compared with control cells. Quantitative RT–PCR and ELISA analysis confirmed the Dlx2-dependent increased expression of betacellulin at the mRNA and protein levels, respectively (Figure 5A and B). To assess whether betacellulin was responsible for the stimulation of EGFR and increased cell survival and proliferation, control and Dlx2-expressing NMuMG cells were transfected with siRNAs against betacellulin and concomitantly treated with TGFβ. The extent of the ablation of betacellulin expression was determined by ELISA and by quantitative RT–PCR (Figure 5B; Supplementary Figure S4A). Reduced betacellulin levels significantly reduced cell numbers of Dlx2-expressing NMuMG cells but not in control cells and thus abrogated a major part of Dlx2-mediated cell proliferation during TGFβ treatment (Figure 5C). Notably, siRNA-mediated ablation of EGFR expression comparably repressed Dlx2-mediated cell proliferation, suggesting that betacellulin was the only inducer of EGFR in Dlx2-expressing cells (Figure 5C; Supplementary Figure S4B). Indeed, addition of recombinant betacellulin to Dlx2-expressing NMuMG cells that had been ablated for

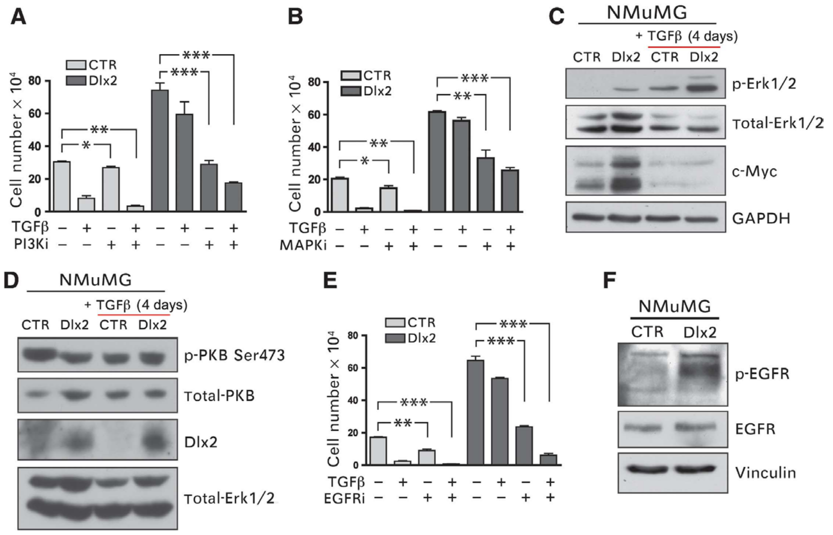

Figure 4 Dlx2 promotes resistance against TGFβ-mediated growth inhibition via activation of EGFR signalling. (**A**) Dlx2-expressing and control NMuMG cells were treated with TGFβ for 4 days in combination with the PI3K inhibitor ZSTK474 (0.239 μM) or DMSO (solvent control) and counted using a Neubauer chamber. (**B**) Dlx2-expressing and control NMuMG cells were treated with TGFβ for 4 days in combination with the MEK1/2 inhibitor PD98059 (9.35 μM) or DMSO (solvent control), and cell numbers were determined using a Neubauer cell counting chamber. (**C**) Dlx2 expression increases phosphorylation of the MAPK Erk1/2 as well as c-Myc total protein levels. Immunoblotting analysis of cell lysates from Dlx2-expressing and control NMuMG cells treated with or without TGFβ for 4 days. Immunoblotting against total Erk1/2 and GAPDH was used as loading control. (**D**) Dlx2 expression has no effect on the phosphorylation of PKB at Ser473, as determined by immunoblotting with an antibody specific for PKB phosphorylated at serine 473. Immunoblotting against total PKB and total-Erk1/2 was used as loading control. (**E**) Dlx2-expressing and control NMuMG cells were treated with TGFβ for 4 days in combination with the EGFR inhibitor AG1478 (3 μM) or DMSO (solvent control) and cell numbers were determined using a Neubauer chamber. (**F**) Dlx2 expression leads to increased phosphorylation of the EGFR at its activating tyrosine 1173. Immunoblotting analysis of cell lysates from Dlx2-expressing and control NMuMG cells with antibodies against pY1173-EGFR and total EGFR. Immunoblotting against vinculin was used as a loading control. Data are shown as mean ± s.d. and are representative of at least three independent experiments. Statistical values are calculated by using an unpaired, two-tailed t-test $^{**}P \leqslant 0.01$; $^{***}P \leqslant 0.001$.

betacellulin expression by siRNA transfection restored cell proliferation in the presence of TGFβ (Figure 5D). As expected by their expression of EGFR (Figure 4F), recombinant betacellulin also exerted a proliferative effect on control cells, yet failed to promote cell proliferation to numbers comparable to Dlx2-expressing cells (Figure 5D), indicating that betacellulin by itself was not sufficient to overcome TGFβ-induced growth arrest and apoptosis. Conversely, siRNA-mediated ablation of betacellulin expression in Dlx2-expressing NMuMG cells significantly increased apoptosis upon TGFβ treatment, underscoring its importance for Dlx2-mediated TGFβ resistance (Figure 5E). Finally, ChIP experiments revealed that Dlx2 directly bound to the *betacellulin* gene promoter in NMuMG cells (Figure 5F), in B16 melanoma cells (Supplementary Figure S4C) and Py2T murine breast cancer cells (not shown), suggesting that it directly induced its expression.

In conclusion, Dlx2-mediated TGFβ resistance appears to rely on two mechanisms, the inhibition of apoptotic, canonical TGFβ signalling via direct transcriptional repression of the *TGFβRII* gene and the activation of mitogenic and pro-survival EGFR signalling via the direct transcriptional induction of *betacellulin* gene expression.

Dlx2 promotes tumour growth and metastasis

Next, we investigated whether increased expression of Dlx2 correlated with human cancer progression and metastasis by surveying gene expression profiles of human cancer biopsies for Dlx2 expression using the NextBio database (nextbio.com). Significant correlations of increased Dlx2 expression with the potential of melanoma and lung cancers to metastasize and with advanced tumour stages in prostate and lung cancers were detected (Table I). Moreover, treatment of human glioma cells with a specific inhibitor for TGFβRI has reduced Dlx2 expression, indicating that Dlx2 is also a target of TGFβ signalling in glioma cells (Table I). Finally, Dlx2 has been found highly expressed in human breast cancer and in breast cancer-initiating cells (Zhang *et al*, 2008; Rhodes *et al*, 2009). These results support the hypothesis that Dlx2 also plays a critical role for cell survival and proliferation during tumour progression and metastasis formation in patients.

The findings that various cancer types, including melanoma, develop resistance against TGFβ-mediated growth inhibition during malignant progression (reviewed in Teicher, 2001) and that Dlx2 expression correlates with melanoma malignancy (Table I) motivated us to investigate whether Dlx2 expression played a significant role in melanoma growth and metastasis formation. Cultured B16 melanoma cells, when treated with TGFβ for 4 days, exhibited increased Dlx2 mRNA levels, revealing that Dlx2 expression is upregulated by TGFβ signalling also in these cells (Figure 6A). Next, we investigated whether ablation of Dlx2 expression impaired the ability of B16 melanoma cells to form tumours and to metastasize to the lungs upon subcutaneous implantation into syngeneic C57Bl/6 mice. Three cell pools of B16

©2011 European Molecular Biology Organization

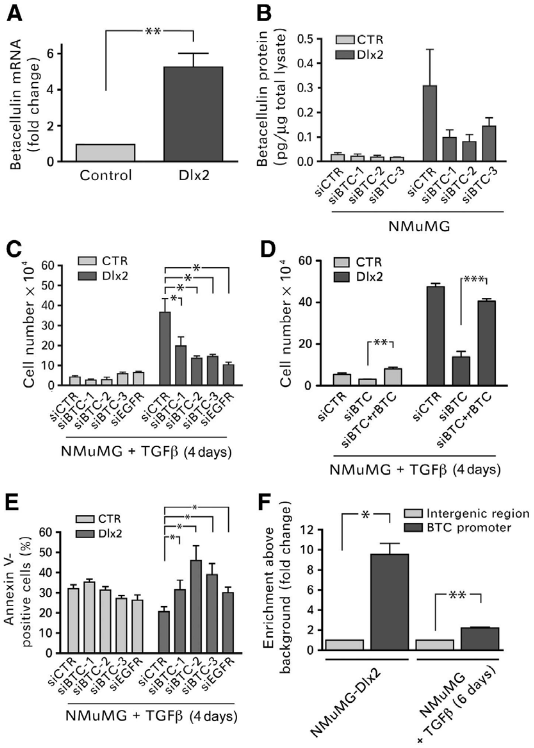

Figure 5 Betacellulin expression is induced by Dlx2 and provides cell survival and proliferation by stimulating EGFR. (**A**) Betacellulin mRNA levels were determined by quantitative RT–PCR in NMuMG cells stably expressing either GFP (Control) or Dlx2. (**B**) The protein levels of betacellulin are increased in Dlx2-expressing NMuMG cells, as determined in cell lysates of GFP and Dlx2-expressing NMuMG cells by ELISA. The high levels of betacellulin induced by Dlx2 expression in NMuMG cells are efficiently reduced by siRNA-mediated knockdown of betacellulin expression (siBTC), as determined by ELISA. (**C**) Betacellulin (BTC) and its receptor EGFR are required for TGFβ-resistant growth of Dlx2-expressing NMuMG cells. siRNA-mediated ablation of either betacellulin or EGFR expression reduces TGFβ-resistant growth of Dlx2-expressing NMuMG cells with comparable efficacies. Viable cells were counted by trypan blue exclusion using a Neubauer cell counting chamber. (**D**) siRNA-mediated ablation of betacellulin expression (mixture of the three siRNAs used in (**B**, **C**)) in Dlx2-expressing cells results in TGFβ-mediated growth arrest and apoptosis, which can be rescued by addition of recombinant betacellulin (rBTC; 10 ng/ml). Viable cells were counted by trypan blue exclusion using a Neubauer cell counting chamber. (**E**) TGFβ-resistant growth of Dlx2-expressing NMuMG cells requires betacellulin. The rates of apoptosis in siCTR, siBTC, and siEGFR transfected control or Dlx2-expressing cells were measured by Annexin V staining and flow cytometry. (**F**) Betacellulin is a direct transcriptional target of Dlx2. ChIP of Dlx2 was performed on either Dlx2-expressing cells or NMuMG cells treated for 6 days with TGFβ. Immunoprecipitated DNA fragments were quantified by quantitative RT–PCR using primers amplifying the promoter region of the *betacellulin* gene and primers covering an intergenic region as negative control. Data are shown as mean ± s.d. and are representative of at least three independent experiments. Statistical values are calculated by using an unpaired, two-tailed *t*-test. $^{*}P \leqslant 0.05$; $^{**}P \leqslant 0.01$; $^{***}P \leqslant 0.001$.

melanoma cells stably transfected with independent shRNA constructs against Dlx2 (shDlx2-B16 I–III) and one control shRNA (shCTR) cell pool (Supplementary Figure S5A) were implanted into the flanks of mice (five mice per cell pool). Primary tumour volumes and the incidence of lung metastasis were quantified 2 weeks after implantation. shRNA-mediated knockdown of Dlx2 resulted in a significant reduction in primary tumour growth (Figure 6B) and in micrometastatic lesions in the lungs (Figure 6C and D) in comparison to shCTR cells. Dlx2 was found expressed at high levels in the nuclei of control B16 cells and at reduced levels in Dlx2-depleted cells (Supplementary Figure S5B). Moreover, the rate of tumour cell apoptosis, as determined by immunohistochemical staining for cleaved caspase 3, was markedly, yet not significantly increased in Dlx2-depleted B16 tumours as compared with control tumours (Figure 6E), while the proliferation rate, as determined by staining for Ki67, was unaffected (Supplementary Figure S5C). Consistent with our findings that Dlx2 promotes cell survival and proliferation, these results demonstrate that Dlx2 expression is also required for primary tumour growth and metastatic outgrowth of B16 melanoma cells.

Discussion

The TGFβ signalling pathway exerts a dual function during tumour development and progression. At early stages of tumourigenesis, TGFβ functions as a tumour suppressor by inducing cell-cycle arrest and apoptosis. During late stage tumourigenesis, TGFβ promotes tumour cell invasion and metastasis by inducing an EMT, immunosuppression, and angiogenesis (Thiery and Sleeman, 2006; Massague, 2008; Yang and Weinberg, 2008). Hence, the breakdown of TGFβ-mediated growth restrains plays an important role during tumour formation and progression. Cancer cells evade this TGFβ-mediated tumour-suppressive barrier via downregulation of the TGFβ receptors by a yet poorly understood mechanism (Kang *et al*, 1999; Kim *et al*, 2000; Lee *et al*, 2007a). Hence, the delineation of the molecular pathways enabling cancer cells to overcome TGFβ-mediated growth inhibition and to convert it into a tumour-promoting factor is a critical milestone for the design and development of adequate therapeutic interventions.

Here, we have identified the transcription factor Dlx2 to enable non-transformed, non-tumourigenic NMuMG cells and B16 melanoma cells to overcome TGFβ-mediated growth inhibition *in vitro* and *in vivo*, respectively. This Dlx2-mediated TGFβ-resistant growth is achieved by two major regulatory modifications (i) the inhibition of the pro-apoptotic TGFβ signalling pathway and (ii) the simultaneous activation of the pro-survival and mitogenic EGF receptor signalling pathway by the direct transcriptional induction of betacellulin expression (Figure 7).

The molecular and cellular analysis presented in this study reveals that Dlx2-mediated attenuation of the canonical TGFβ signalling pathway is a consequence of a direct transcriptional repression of the *TGFβRII* gene and leads to changes in the expression of TGFβ target genes, such as decreased expression of the cell-cycle inhibitor $p21^{CIP1}$ and increased expression of the mitogenic transcription factor c-Myc. Furthermore, we show that Dlx2 itself is a target of canonical TGFβ signalling and, thus, is exerting its function in a negative feedback loop. In summary, we identify Dlx2 as a novel TGFβ-inducible transcriptional repressor that attenu-

©2011 European Molecular Biology Organization

Table I Dlx2 expression in human cancers

Cancer type	Bioset name	*P*-value	Fold upregulation	NCBI-GEO accession number
Melanoma tumours	Intermediate metastatic potential melanoma versus foreskin melanocyte normal	0.0451	4.19	GSE4845
	High metastatic potential melanoma versus foreskin melanocyte normal	0.0361	4.93	GSE4845
	Intermediate metastatic potential melanoma versus low metastatic potential melanoma	0.0196	2.52	GSE4845
	High metastatic potential melanoma versus low metastatic potential melanoma	0.0028	3.03	GSE4845
	High metastatic potential melanoma versus low metastatic potential melanoma	0.0067	2.96	GSE4845
	Metastatic melanoma versus normal melanocytes	0.0021	18.8	GSE4570
Lung cancer	Stage 4 versus stage 1	0.0123	3.847	GSE2109
	Distant metastasis versus no metastasis	0.0064	3.045	GSE2109
	Stage 4 versus stage 1	0.012	3.087	GSE2109
	Stage 2A versus stage 1b	0.0351	3.29	GSE3141
Breast cancer	T2 versus T1	0.0227	2.32	GSE10810_19
	T2 versus normal tissue	0.0269	2.6	GSE10810_3
	ER-positive versus normal	0.0102	2.34	GSE10810_15
	Breast tumour versus normal	0.007	1.91	GSE10810_1
	Lobular versus ductal	0.021	3.39	GSE5460_7
	ER-3 versus ER-0	0.0001	2.8	GSE3143_1
	Mouse mammary tumour initiating cells	0.0095	3.63	GSE8863_11
	Metastasis versus primary breast cancer	0.0086	3.9	GSE8863_7
		0.0242	1.62	GSE3521_GPL885_7
	Lobular versus normal	2.5E−5	1.73	GSE3971_2
		2.5E−5	1.63	GSE3971_1
Prostate cancer	Stage 4 versus stage 2	0.0039	3.27	GSE6919
Glioma	TGFβ inhibition leads to Dlx2 downregulation	0.0037	−21.9	Bruna *et al* (2007)

Expression of Dlx2 correlates significantly with advanced tumour progression and the metastatic potential of melanoma, glioma, lung, and prostate cancers. Microarray data are accessible at the NCBI Gene Expression Omnibus (GEO) database.

ates Smad-dependent TGFβ signalling and thereby promotes cell-cycle arrest and apoptosis (Figure 7).

This mechanistic model of Dlx2-mediated *TGFβRII* gene repression is consistent with previous reports on autocrine negative feedback loops of TGFβ signalling downregulating TGFβRII expression (Gazit *et al*, 1993; Woodward *et al*, 1995; Nishikawa *et al*, 1998; Truty *et al*, 2009). The model also resembles the recently described function of KLF14 in human pancreatic epithelial cancer (PANC1) cells, in which KLF14 has been shown to be a TGFβ-inducible repressor of the *TGFβRII* gene (Truty *et al*, 2009). Notably, in a recent comprehensive genome analysis of cancer cell lines, the *TGFβRII* gene was found to be one of the prominent recessive cancer genes suffering from homozygous deletion during carcinogenesis (Bignell *et al*, 2010).

The capability of Dlx-family transcription factors to interfere with TGFβ signalling is further supported by observations showing that Dlx1 inhibits activin-mediated signalling by blocking Smad4 activity in haematopoietic cells (Chiba *et al*, 2003), and that Dlx2 expression correlates with decreased TGFβRI and Smad4 levels in a thoracic aortic aneurysm model (Jones *et al*, 2008). Interestingly, a recent report shows that Dlx4 blocks the growth-suppressive effects of TGFβ by binding to Smad4 and thus preventing canonical TGFβ signalling and the expression of the cell-cycle inhibitors $p15^{INK4B}$ and $p21^{CIP1}$ (Trinh *et al*, 2011). Moreover, Dlx4 can activate the expression of c-Myc in a Smad-independent manner. Finally, Dlx2 has also been shown to interact with Smad proteins to control the expression of various target genes (Maira *et al*, 2010), indicating that Dlx-family members are not only an autonomous transcriptional regulators but also Smad interaction partners.

Besides directly repressing transcription of the *TGFβRII* gene and inhibiting the canonical TGFβ signalling pathway, we here demonstrate that Dlx2 binds the promoter region and induces transcription of the *betacellulin* gene, an EGF-family member and specific ligand of EGFR and ErbB4. Betacellulin is well known for its roles in cell differentiation and cancer (Shing *et al*, 1993; Dunbar and Goddard, 2000). Increased expression and synthesis of betacellulin leads to the stimulation of EGFR and to the activation of its effector signalling pathways, which are essential for Dlx2-mediated TGFβ-resistant growth, notably the MAPK and PI3K pathways. However, it should be noted that the pharmacological inhibition of the MAPK and the PI3K pathways not only represses Dlx2-mediated signalling but also signalling mediated by other inducers activated during TGFβ treatment of NMuMG cells and thus, their effects are much stronger than the ablation of Dlx2. In fact, depletion of Dlx2 does not have a major effect on the overall activation of PKB or Erk1/2 (Supplementary Figure S3). Other pathways may include FGF receptor signalling, and with it MAPK signalling, induced by neuronal cell adhesion molecule in TGFβ-treated NMuMG cells (and other cells undergoing EMT) (Lehembre *et al*, 2008). From these insights, we conclude that other pathways are also stimulating MAPK and PI3K signalling and that the loss of Dlx2 cannot replicate the complete repression of PI3K or MEK signalling by pharmacological inhibitors. Along these lines, while inhibition of EGFR signalling clearly induces apoptosis and growth arrest of the cells, it does not comple-

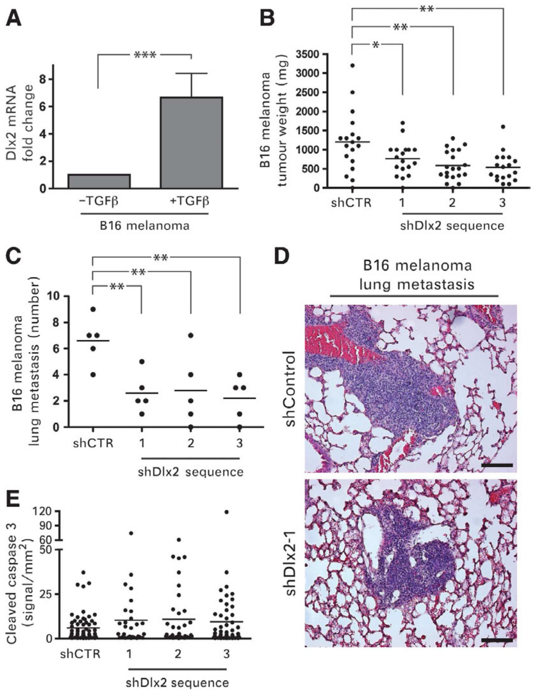

Figure 6 Dlx2 is required for B16 melanoma primary tumour growth and lung metastasis. (**A**) Dlx2 expression is induced by TGFβ in melanoma cells. B16 melanoma cells were treated with TGFβ for 6 days and Dlx2 mRNA levels were determined by quantitative RT–PCR. Values were normalized to endogenous RPL19 mRNA levels. (**B**) Reduced primary tumour growth in B16 melanoma cells transfected to stably express shRNA against Dlx2. Three independent Dlx2-specific shRNA sequences (shDlx2 1–3) and one control shRNA sequence (shCTR) were used to establish stable cell pools. Cells were injected into both flanks of 9–10 C57Bl/6 mice per cell pool and tumour weights were measured 2 weeks after implantation. (**C**) Reduced metastatic outgrowth of B16 melanoma cells depleted for Dlx2 expression. Micrometastatic lesions were counted on histological sections (shown in **D**) of the lungs of the mice described in (**B**) (five lungs per cell pool were analysed). (**D**) Serial histological sections of lungs from C57/Bl6 injected subcutaneously with shDlx2-1 and shCTR B16 melanomas cells were stained with haematoxylin/eosin. Scale bar = 100 μm. (**E**) Tumour sections were stained against cleaved caspase 3 to quantify the rate of apoptosis. The moderate increase in apoptosis observed in Dlx2-depleted tumours was not statistically significant. Data are shown as mean ± s.d. Statistical values are calculated by using an unpaired, two-tailed *t*-test. $^{*}P \leqslant 0.05$; $^{**}P \leqslant 0.01$; $^{***}P \leqslant 0.001$.

tely abrogate their growth, again arguing for additional signalling pathways being active.

A comparable functional interaction between Dlx2 and EGF signalling has been previously shown in neuronal transit amplifying cells, where loss of Dlx2 function dramatically reduces their responsiveness towards EGF (Doetsch *et al*, 2002; Suh *et al*, 2009). Consistent with the regulation of Dlx2 expression and its activation of EGFR signalling, EGFR and TGFβ signalling pathways have been previously reported to influence each other's activities in both positive and negative ways; however, the molecular details of such interactions have not been delineated (Assoian *et al*, 1984; Kizaka-Kondoh *et al*, 2000; Song *et al*, 2006; Semlali *et al*, 2008).

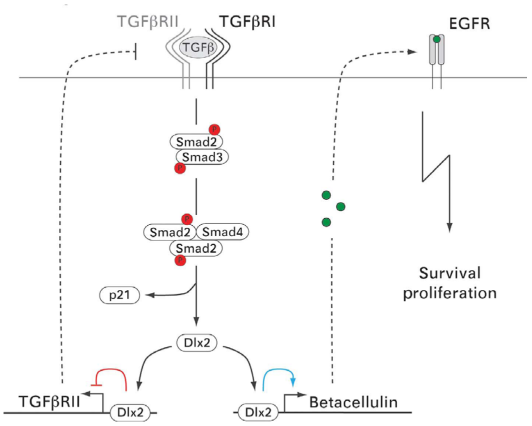

Figure 7 A working model of the molecular mechanisms underlying Dlx2-mediated resistance to TGFβ-induced cell-cycle arrest and apoptosis. Binding of TGFβ to TGFβ receptors induces phosphorylation and activation of the receptor-associated signal transducers Smad2/3. Activated Smad2/3 form a trimeric complex with Smad4 and enter the nucleus to induce expression of TGFβ target genes, such as Dlx2 and the cell-cycle inhibitor $p21^{CIP1}$. Subsequently, Dlx2 directly binds and represses transcription of the *TGFβRII* gene (red line) and directly binds and activates expression of the gene for the EGFR-ligand betacellulin (blue line). Reduced TGFβRII expression results into diminished Smad2/3 activation, reduced Smad4 transcriptional activity and, finally, into an attenuation of cytostatic TGFβ signalling. On the other hand, increased expression of betacellulin leads to the activation of EGFR-mediated signal transduction and to cell proliferation and survival.

Together the data presented here identify Dlx2 as a novel TGFβ-inducible transcription factor, which plays a critical role in balancing cell survival over cell death during TGFβ treatment of NMuMG cells. We demonstrate that Dlx2, by repressing TGFβRII expression and by inducing betacellulin expression, attenuates canonical TGFβ signalling, and activates the EGFR signalling pathway, thus shifting TGFβ's tumour-suppressive functions to tumour progressive functions and favouring cell survival and proliferation. The finding that the loss of Dlx2 function in mouse retina cells results in increased apoptosis is consistent with its anti-apoptotic activity in another cellular context (de Melo *et al*, 2005). The protective function of Dlx2 is also utilized by cancer cells, since we show that ablation of Dlx2 expression in B16 melanoma cells significantly decreases their growth as primary tumours and as metastasis upon transplantation into syngeneic C57/Bl6 mice. The fact that Dlx2 expression shows a significant and positive correlation with increased invasiveness of human melanomas and several other cancer types underscores its relevance in human disease (Table I; Javelaud *et al*, 2008; Boone *et al*, 2009). The finding that Dlx2 exerts a critical switch function during TGFβ treatment and tumour progression makes it an attractive subject matter for further investigations.

Materials and methods

Reagents and antibodies

Human TGFβ and mouse betacellulin include R&D Systems (Abingdon, UK, R&D, #240-B and #1025-CE-025, respectively).

©2011 European Molecular Biology Organization

Antibodies include Vinculin (#V9131, Sigma-Aldrich), GAPDH (#ab9485, Abcam), TGFβRII (#sc-220, Santa Cruz), Smad4 (#sc-7154, Santa Cruz), Smad2 (#3103, Cell Signaling), pSmad2 (#3101, Cell Signaling), p21^{CIP1}(#556430, Pharmingen), c-myc (#06-340, Upstate Biotechnology), total-PKB (gift from E Hirsch, Torino), p-PKB Serine (#9271, Cell Signaling), p-Erk (#M-8159, Sigma-Aldrich), total-Erk (#M7927, Sigma-Aldrich), EGFR (#2232 Cell Signaling), p-Tyr1173EGFR (#sc-12351, Santa Cruz), HA (ab9110, Abcam), BrdU-FITC (#347583, Becton&Dickinson), Dlx2 (AB5726, Millipore for immunostainings, sc-18140x, Santa Cruz for immunoblotting), Ki-67 (clone Tec3, DAKO), cleaved Caspase 3 Asp175 (5A1, Cell Signaling) . Inhibitors include MEK1/2 Inhibitor PD98059 (#ALX-385-023, Alexis Biochemicals), TGFβRI inhibitor SB431542 hydrate (#S4317, Sigma-Aldrich), PI3K inhibitor ZSTK474 (#ALX-270-454, Alexis Biochemicals), EGFR Inhibitor AG1478 (#ALX-270-036, Alexis Biochemicals), PDGFR inhibitor Tyrphostin AG1296 (#ALX-270-037, Alexis Biochemicals), VEGFR inhibitor PTK787 (provided by Novartis Pharma), IGF1R inhibitor AEW541 (provided by Novartis Pharma).

Primers

For quantitative RT–PCR, the following primers were used: murine Dlx2 fwd: 5′-GGCCTCACCCAAACTCAGGT-3′, rev: 5′-GTATCTCGCCGCTTTTCCAC-3′; murine TGFβRII fwd: 5′-GGCTCTGGTACTCTGGGAAA-3′, rev: 5′-AATGGGGGCTCGTAATCCT-3′; murine betacellulin: fwd: 5′-ACC AATGGCTCTCTTTGTGG-3′, rev: 5′-CCGAGAGAAGTGGGTTTTCA-3′; murine EGFR fwd: 5′- GCCACGCCAACTGTACCTAT-3′, rev: 5′-GCCACACTTCACATC CTTGA-3′; murine RPL19 fwd: 5′-ATCCGCAAGCCTGTGACTGT-3′, rev: 5′-TCGGGCCAGGGTGTTTTT-3′. For ChIP, ChIP-quantitative PCR was performed by using the following primers: murine TGFβR2 promoter fwd: 5′-GCCCCTGGGAGTAATGCC-3′, rev: 5′-CTTTTAGCTGCCCACTCC-3′; murine betacellulin promoter fwd: 5′-CTGCGTCAACTGTCAAATGC-3′, rev: 5′-AAGAGGACCTGGTCATGTGG-3′; murine intergenic region: fwd: 5′-GCTCCGGGTCCTATTCTTGT-3′, rev: 5′-TCTTGGTTTCCAGGAGATGC-3′.

Cells and cell lines

A subclone of NMuMG cells (NMuMG/E9; hereafter NMuMG and B16-F1 melanoma cells have been previously described (Fidler, 1975; Maeda *et al*, 2005; Lehembre *et al*, 2008). Cells were cultured in DMEM supplemented with glutamine, penicillin, streptomycin, and 10% FCS (Sigma). NMuMG-shSmad4 and NMuMG-shControl were obtained from P ten Dijke (Leiden University Medical Center, The Netherlands) (Deckers *et al*, 2006). NMuMG cells were treated with TGFβ in normal growth medium every 2 days (2 ng/ml). Murine Dlx2 siRNA was purchased from Dharmacon (ON-TARGET plus, SmartPool, L-043273-01-005), murine EGFR siRNA was from Sigma (SASI_Mm02_01_00101666 and SASI_Mm02_01_00101666_AS), and murine betacellulin siRNA was from Sigma (SASI_Mm02_00311942, 44, 45, and SASI_Mm02_00311942_AS, 44_AS, 45_AS). Transfections with LipofectAMINE RNAiMAX (Invitrogen) were performed according to the manufacturer's instructions.

To determine growth curves, 1×10^4 cells were seeded in each well of 24-well plate and cell numbers were assessed every second day by using a Neubauer counting chamber.

Stable, tetracyclin-inducible HEK293 cells expressing either GFP or N-terminal HA-tagged murine Dlx2 were generated via site-directed recombination into the Flp-In T-Rex HEK293 cell system (Invitrogen, #K6500-01, #R750-07). Subsequently, cells were selected using hygromycin and individual clones were used for further experiments. Protein expression was induced upon treatment with 1 μg/ml doxycycline.

Total cell lysates, immunoblots, and immunofluorescence experiments were performed as previously described (Lehembre *et al*, 2008). Proteins of interest were either visualized by chemoluminescence sequentially or on multiple membranes, and Adobe Photoshop was used to crop the relevant portions of the original scans of X-ray films, as indicated by black frames.

Generation of lentivirus

Murine Dlx2 shRNAs (shDlx2 #1–3, TRCN0000070598-600) and control shRNA (shCTR, SHC002, Mission Non-Target shRNA Control Vector) were purchased from Sigma-Aldrich. A cDNA encoding Dlx2 (kindly provided by P Farlie, University of Melbourne) was tagged N-terminally with HA-tag and cloned into the lentiviral expression vector pWPXL. Lentiviral particles were produced by transfecting HEK293T cells with the lentiviral expression vectors in combination with the packing vector pR8.91 and the envelope encoding vector pVSV using Fugene HD. After 2 days of virus production, lentivirus-containing supernatants were harvested, filtered (0.45 μm), and added to target cells in the presence of polybrene (8 ng/ml). Infections were performed twice a day for 2 consecutive days.

Quantitative RT–PCR

Total RNA was prepared using Trizol (Invitrogen), reverse transcribed with M-MLV reverse transcriptase RNAse (H-) (Promega, Wallisellen, Switzerland), and transcripts were quantified by PCR using SYBR-green PCR MasterMix (Applied Biosystems, Rotkreuz, Switzerland). Human or mouse riboprotein L19 primers were used for normalization (see Supplementary data for primer sequences). PCR assays were performed in triplicates, and fold induction was calculated against control-treated cell lines using the comparative Ct method ($\Delta\Delta C_t$).

Reporter assays

NMuMG and HEK293 FlpIN-Dlx2 and FlpIN-GFP cells were transfected with 200 ng reporter and 5 ng Renilla encoding plasmids using Lipofectamine 2000. After 2 days of transfection, cells were analysed using the Dual-Luciferase Reporter Assay System (#E1960, Promega) and a Berthold Luminometer LB960. HEK cells were induced for 1 day with 1 μg/ml doxycycline to express Dlx2 or GFP and then assayed for reporter activity. Measured luciferase values were normalized to internal Renilla control. Smad4 promoter-reporter, TGFβRII promoter-reporter, and E-cadherin promoter-reporter constructs were kindly provided by P ten Dijke (Leiden University) (Dennler *et al*, 1998), SJ Kim (National Cancer Institute, Bethesda) (Hahm *et al*, 1999), and K Verschueren (VIB and University of Leuven; van Grunsven *et al*, 2003).

Chromatin immunoprecipitation

ChIP experiments were performed as previously described (Weber *et al*, 2007). In brief, crosslinked chromatin was sonicated to achieve an average fragment size of 500 bp. Starting with 100 μg of chromatin and 5 μg of anti-Dlx2 antibody (Abcam-ab18188), 1 μl of ChIP material and 1 μl of input material were used for quantitative real-time PCR using specific primers covering the *TGFβRII* gene promoter region from basepair −386 to −204, covering the *betacellulin* gene promoter region from basepair −450 to −253, and primers covering an intergenic region as control. The efficiencies of PCR amplification were normalized for between the primer pairs.

Proliferation assay

Cells were incubated with BrdU (10 μM) for 2 h at 37°C. Fixed in 70% ice-cold ethanol, permeabilized in 2 N HCL/0.5% Triton X-100 solution for 30 min at RT, resuspended in 0.1 M $Na_2B_4O_7$ pH 8.5 for 2 min at RT, washed twice with 0.5% Tween-20/1% BSA/PBS, and then incubated with FITC labelled anti-BrdU antibody (#347583, BD) for 30 min at RT. After washing twice with 0.5% Tween-20/1% BSA/PBS and resuspending in PBS with 5 μg/ml PI for at least 1 h at RT, the stained cells were analysed on a FACSCanto II using DIVA software (BD).

Apoptosis assay

Cells were washed twice with cold PBS and resuspended in 1× binding buffer at a concentration of 1×10^5 cells/ml. In all, 5 μl of Cy5 Annexin V was added to the cells and incubated for 15 min at RT (25°C) in the dark. After incubation, cells were analysed on a FACSCanto II using DIVA software.

ELISA

Cell lysates were prepared using RIPA buffer complemented with a protease inhibitor cocktail. The amount of betacellulin in 100 μl of undiluted lysate was analysed in triplicates with the mouse Betacellulin DuoSet ELISA Kit from R&D (DY1025) as suggested by the manufacturer's instructions. Total protein concentrations were determined by Pierce BCA Protein Assay Kit from Thermo Scientific (23225).

B16 melanoma syngeneic transplantation

In all, 6 week-old female C57/Bl6 mice were injected subcutaneously with 4×10^5 B16-F1 melanomas cells in PBS into both flanks (9–10 mice per individual cell pool). After 2 weeks incubation, mice were sacrificed and tumour and lungs were isolated and weighed. Metastatic nodules in lungs were counted by histological sectioning of the entire lungs (five lungs per individual cell pool). Immunohistochemical and immunofluorescence analysis was performed as described previously (Lehembre *et al*, 2008). Paraffin sections were deparaffinized and antigen retrieval was performed by autoclaving the samples in 10 mM citrate buffer pH 6.0. Sections were stained with 10 μg/ml anti-Dlx2 antibody (Ab 5726, Millipore) using the Perkin-Elmer TSA amplification system according to the manufacturer's instructions. Stainings were evaluated on an AxioVert microscope and on a LSM 510 META confocal microscope (Zeiss, Oberkochen, Germany).

Statistical analysis

Statistical analysis and graphs were generated using the GraphPad Prism software (GraphPad Software Inc., San Diego, CA). All statistical analysis was performed by unpaired, two-sided *t*-test. Normality testing was performed using the Kolmogorov–Smirnov test with Dallal–Wilkinson–Lillie for *P*-values.

Supplementary data

Supplementary data are available at *The EMBO Journal* Online (http://www.embojournal.org).

Acknowledgements

We thank P ten Dijke, P Farlie, K Verschueren, SJ Kim, E Hirsch, and U Cavallaro for sharing cell lines and important reagents. We are grateful to K Strittmatter, H Antoniadis, and R Jost for technical support and M Wymann and EF Wagner for helpful scientific discussions. This work was supported by EU-FP6 BRECOSM LSHC-CT-2004-503224, EU-FP7 TuMIC HEALTH-F2-2008-201662, the Swiss Bridge Award, Oncosuisse, and the Krebsliga Beider Basel.

Conflict of interest

The authors declare that they have no conflict of interest.

References

Assoian RK, Frolik CA, Roberts AB, Miller DM, Sporn MB (1984) Transforming growth factor-beta controls receptor levels for epidermal growth factor in NRK fibroblasts. *Cell* **36:** 35–41

Bignell GR, Greenman CD, Davies H, Butler AP, Edkins S, Andrews JM, Buck G, Chen L, Beare D, Latimer C, Widaa S, Hinton J, Fahey C, Fu B, Swamy S, Dalgliesh GL, Teh BT, Deloukas P, Yang F, Campbell PJ *et al* (2010) Signatures of mutation and selection in the cancer genome. *Nature* **463:** 893–898

Boone B, Haspeslagh M, Brochez L (2009) Clinical significance of the expression of c-Ski and SnoN, possible mediators in TGF-beta resistance, in primary cutaneous melanoma. *J Dermatol Sci* **53:** 26–33

Bruna A, Darken RS, Rojo F, Ocana A, Penuelas S, Arias A, Paris R, Tortosa A, Mora J, Baselga J, Seoane J (2007) High TGFbeta-Smad activity confers poor prognosis in glioma patients and promotes cell proliferation depending on the methylation of the PDGF-B gene. *Cancer Cell* **11:** 147–160

Chiba S, Takeshita K, Imai Y, Kumano K, Kurokawa M, Masuda S, Shimizu K, Nakamura S, Ruddle FH, Hirai H (2003) Homeoprotein DLX-1 interacts with Smad4 and blocks a signaling pathway from activin A in hematopoietic cells. *Proc Natl Acad Sci USA* **100:** 15577–15582

Cui W, Fowlis DJ, Bryson S, Duffie E, Ireland H, Balmain A, Akhurst RJ (1996) TGFbeta1 inhibits the formation of benign skin tumors, but enhances progression to invasive spindle carcinomas in transgenic mice. *Cell* **86:** 531–542

de Melo J, Du G, Fonseca M, Gillespie LA, Turk WJ, Rubenstein JL, Eisenstat DD (2005) Dlx1 and Dlx2 function is necessary for terminal differentiation and survival of late-born retinal ganglion cells in the developing mouse retina. *Development* **132:** 311–322

Deckers M, van Dinther M, Buijs J, Que I, Lowik C, van der Pluijm G, ten Dijke P (2006) The tumor suppressor Smad4 is required for transforming growth factor beta-induced epithelial to mesenchymal transition and bone metastasis of breast cancer cells. *Cancer Res* **66:** 2202–2209

Del Castillo G, Murillo MM, Alvarez-Barrientos A, Bertran E, Fernandez M, Sanchez A, Fabregat I (2006) Autocrine production of TGF-beta confers resistance to apoptosis after an epithelial-mesenchymal transition process in hepatocytes: role of EGF receptor ligands. *Exp Cell Res* **312:** 2860–2871

Dennler S, Itoh S, Vivien D, ten Dijke P, Huet S, Gauthier JM (1998) Direct binding of Smad3 and Smad4 to critical TGF beta-inducible elements in the promoter of human plasminogen activator inhibitor-type 1 gene. *EMBO J* **17:** 3091–3100

Di Guglielmo GM, Le Roy C, Goodfellow AF, Wrana JL (2003) Distinct endocytic pathways regulate TGF-beta receptor signalling and turnover. *Nat Cell Biol* **5:** 410–421

Doetsch F, Petreanu L, Caille I, Garcia-Verdugo JM, Alvarez-Buylla A (2002) EGF converts transit-amplifying neurogenic precursors in the adult brain into multipotent stem cells. *Neuron* **36:** 1021–1034

Dunbar AJ, Goddard C (2000) Structure-function and biological role of betacellulin. *Int J Biochem Cell Biol* **32:** 805–815

Fabregat I, Herrera B, Fernandez M, Alvarez AM, Sanchez A, Roncero C, Ventura JJ, Valverde AM, Benito M (2000) Epidermal growth factor impairs the cytochrome C/caspase-3 apoptotic pathway induced by transforming growth factor beta in rat fetal hepatocytes via a phosphoinositide 3-kinase-dependent pathway. *Hepatology* **32:** 528–535

Fabregat I, Sanchez A, Alvarez AM, Nakamura T, Benito M (1996) Epidermal growth factor, but not hepatocyte growth factor, suppresses the apoptosis induced by transforming growth factor-beta in fetal hepatocytes in primary culture. *FEBS Lett* **384:** 14–18

Fidler IJ (1975) Biological behavior of malignant melanoma cells correlated to their survival *in vivo*. *Cancer Res* **35:** 218–224

Gal A, Sjoblom T, Fedorova L, Imreh S, Beug H, Moustakas A (2008) Sustained TGFbeta exposure suppresses Smad and non-Smad signalling in mammary epithelial cells, leading to EMT and inhibition of growth arrest and apoptosis. *Oncogene* **27:** 1218–1230

Gazit D, Ebner R, Kahn AJ, Derynck R (1993) Modulation of expression and cell surface binding of members of the transforming growth factor-beta superfamily during retinoic acid-induced osteoblastic differentiation of multipotential mesenchymal cells. *Mol Endocrinol* **7:** 189–198

Gotzmann J, Huber H, Thallinger C, Wolschek M, Jansen B, Schulte-Hermann R, Beug H, Mikulits W (2002) Hepatocytes convert to a fibroblastoid phenotype through the cooperation of TGF-beta1 and Ha-Ras: steps towards invasiveness. *J Cell Sci* **115:** 1189–1202

Hahm KB, Cho K, Lee C, Im YH, Chang J, Choi SG, Sorensen PH, Thiele CJ, Kim SJ (1999) Repression of the gene encoding the TGF-beta type II receptor is a major target of the EWS-FLI1 oncoprotein. *Nat Genet* **23:** 222–227

Huber MA, Kraut N, Beug H (2005) Molecular requirements for epithelial-mesenchymal transition during tumor progression. *Curr Opin Cell Biol* **17:** 548–558

Janda E, Lehmann K, Killisch I, Jechlinger M, Herzig M, Downward J, Beug H, Grunert S (2002) Ras and TGF[beta] cooperatively regulate epithelial cell plasticity and metastasis: dissection of Ras signaling pathways. *J Cell Biol* **156:** 299–313

Javelaud D, Alexaki VI, Mauviel A (2008) Transforming growth factor-beta in cutaneous melanoma. *Pigment Cell Melanoma Res* **21:** 123–132

Jones JA, Barbour JR, Stroud RE, Bouges S, Stephens SL, Spinale FG, Ikonomidis JS (2008) Altered transforming growth factor-beta signaling in a murine model of thoracic aortic aneurysm. *J Vasc Res* **45:** 457–468

Kang SH, Bang YJ, Im YH, Yang HK, Lee DA, Lee HY, Lee HS, Kim NK, Kim SJ (1999) Transcriptional repression of the transforming growth factor-beta type I receptor gene by DNA methylation results in the development of TGF-beta resistance in human gastric cancer. *Oncogene* **18:** 7280–7286

Kim SJ, Im YH, Markowitz SD, Bang YJ (2000) Molecular mechanisms of inactivation of TGF-beta receptors during carcinogenesis. *Cytokine Growth Factor Rev* **11:** 159–168

Kizaka-Kondoh S, Akiyama N, Okayama H (2000) Role of TGF-beta in EGF-induced transformation of NRK cells is sustaining high-level EGF-signaling. *FEBS Lett* **466:** 160–164

Lee EK, Lee YS, Han IO, Park SH (2007a) Expression of Caveolin-1 reduces cellular responses to TGF-beta1 through down-regulating the expression of TGF-beta type II receptor gene in NIH3T3 fibroblast cells. *Biochem Biophys Res Commun* **359:** 385–390

Lee MK, Pardoux C, Hall MC, Lee PS, Warburton D, Qing J, Smith SM, Derynck R (2007b) TGF-beta activates Erk MAP kinase signalling through direct phosphorylation of ShcA. *EMBO J* **26:** 3957–3967

Lehembre F, Yilmaz M, Wicki A, Schomber T, Strittmatter K, Ziegler D, Kren A, Went P, Derksen PW, Berns A, Jonkers J, Christofori G (2008) NCAM-induced focal adhesion assembly: a functional switch upon loss of E-cadherin. *EMBO J* **27:** 2603–2615

Maeda M, Johnson KR, Wheelock MJ (2005) Cadherin switching: essential for behavioral but not morphological changes during an epithelium-to-mesenchyme transition. *J Cell Sci* **118:** 873–887

Maira M, Long JE, Lee AY, Rubenstein JL, Stifani S (2010) Role for TGF-beta superfamily signaling in telencephalic GABAergic neuron development. *J Neurodev Disord* **2:** 48–60

Massague J (2004) G1 cell-cycle control and cancer. *Nature* **432:** 298–306

Massague J (2008) TGFbeta in cancer. *Cell* **134:** 215–230

Moustakas A, Heldin CH (2005) Non-Smad TGF-beta signals. *J Cell Sci* **118**(Part 16): 3573–3584

Murillo MM, del Castillo G, Sanchez A, Fernandez M, Fabregat I (2005) Involvement of EGF receptor and c-Src in the survival signals induced by TGF-beta1 in hepatocytes. *Oncogene* **24:** 4580–4587

Nishikawa Y, Wang M, Carr BI (1998) Changes in TGF-beta receptors of rat hepatocytes during primary culture and liver regeneration: increased expression of TGF-beta receptors associated with increased sensitivity to TGF-beta-mediated growth inhibition. *J Cell Physiol* **176:** 612–623

Oft M, Heider KH, Beug H (1998) TGFbeta signaling is necessary for carcinoma cell invasiveness and metastasis. *Curr Biol* **8:** 1243–1252

Pardali K, Moustakas A (2007) Actions of TGF-beta as tumor suppressor and pro-metastatic factor in human cancer. *Biochim Biophys Acta* **1775:** 21–62

Rhodes DR, Ateeq B, Cao Q, Tomlins SA, Mehra R, Laxman B, Kalyana-Sundaram S, Lonigro RJ, Helgeson BE, Bhojani MS, Rehemtulla A, Kleer CG, Hayes DF, Lucas PC, Varambally S, Chinnaiyan AM (2009) AGTR1 overexpression defines a subset of breast cancer and confers sensitivity to losartan, an AGTR1 antagonist. *Proc Natl Acad Sci USA* **106:** 10284–10289

Semlali A, Jacques E, Plante S, Biardel S, Milot J, Laviolette M, Boulet LP, Chakir J (2008) TGF-beta suppresses EGF-induced MAPK signaling and proliferation in asthmatic epithelial cells. *Am J Respir Cell Mol Biol* **38:** 202–208

Shing Y, Christofori G, Hanahan D, Ono Y, Sasada R, Igarashi K, Folkman J (1993) Betacellulin: a mitogen from pancreatic beta cell tumors. *Science* **259:** 1604–1607

Siegel PM, Massagué J (2003) Cytostatic and apoptotic actions of TGF-beta in homeostasis and cancer. *Nat Rev Cancer* **3:** 807–821

Song K, Krebs TL, Danielpour D (2006) Novel permissive role of epidermal growth factor in transforming growth factor beta (TGF-beta) signaling and growth suppression. Mediation by stabilization of TGF-beta receptor type II. *J Biol Chem* **281:** 7765–7774

Suh Y, Obernier K, Holzl-Wenig G, Mandl C, Herrmann A, Worner K, Eckstein V, Ciccolini F (2009) Interaction between DLX2 and EGFR in the regulation of proliferation and neurogenesis of SVZ precursors. *Mol Cell Neurosci* **42:** 308–314

Teicher BA (2001) Malignant cells, directors of the malignant process: role of transforming growth factor-beta. *Cancer Metastasis Rev* **20:** 133–143

Thiery JP, Sleeman JP (2006) Complex networks orchestrate epithelial-mesenchymal transitions. *Nat Rev Mol Cell Biol* **7:** 131–142

Trinh BQ, Barengo N, Naora H (2011) Homeodomain protein DLX4 counteracts key transcriptional control mechanisms of the TGF-beta cytostatic program and blocks the antiproliferative effect of TGF-beta. *Oncogene* **30:** 2718–2729

Truty MJ, Lomberk G, Fernandez-Zapico ME, Urrutia R (2009) Silencing of the transforming growth factor-beta (TGFbeta) receptor II by Kruppel-like factor 14 underscores the importance of a negative feedback mechanism in TGFbeta signaling. *J Biol Chem* **284:** 6291–6300

van Grunsven LA, Michiels C, Van de Putte T, Nelles L, Wuytens G, Verschueren K, Huylebroeck D (2003) Interaction between Smad-interacting protein-1 and the corepressor C-terminal binding protein is dispensable for transcriptional repression of E-cadherin. *J Biol Chem* **278:** 26135–26145

Wakefield LM, Roberts AB (2002) TGF-beta signaling: positive and negative effects on tumorigenesis. *Curr Opin Genet Dev* **12:** 22–29

Weber M, Hellmann I, Stadler MB, Ramos L, Pääbo S, Rebhan M, Schübeler D (2007) Distribution, silencing potential and evolutionary impact of promoter DNA methylation in the human genome. *Nat Genet* **39:** 457–466

Woodward TL, Dumont N, O'Connor-McCourt M, Turner JD, Philip A (1995) Characterization of transforming growth factor-beta growth regulatory effects and receptors on bovine mammary cells. *J Cell Physiol* **165:** 339–348

Yang J, Weinberg RA (2008) Epithelial-mesenchymal transition: at the crossroads of development and tumor metastasis. *Dev Cell* **14:** 818–829

Zhang M, Behbod F, Atkinson RL, Landis MD, Kittrell F, Edwards D, Medina D, Tsimelzon A, Hilsenbeck S, Green JE, Michalowska AM, Rosen JM (2008) Identification of tumor-initiating cells in a p53-null mouse model of breast cancer. *Cancer Res* **68:** 4674–4682

Zhang S, Fei T, Zhang L, Zhang R, Chen F, Ning Y, Han Y, Feng XH, Meng A, Chen YG (2007) Smad7 antagonizes transforming growth factor beta signaling in the nucleus by interfering with functional Smad-DNA complex formation. *Mol Cell Biol* **27:** 4488–4499

©2011 European Molecular Biology Organization

Yilmaz et al.,
Supplemental Figure S1

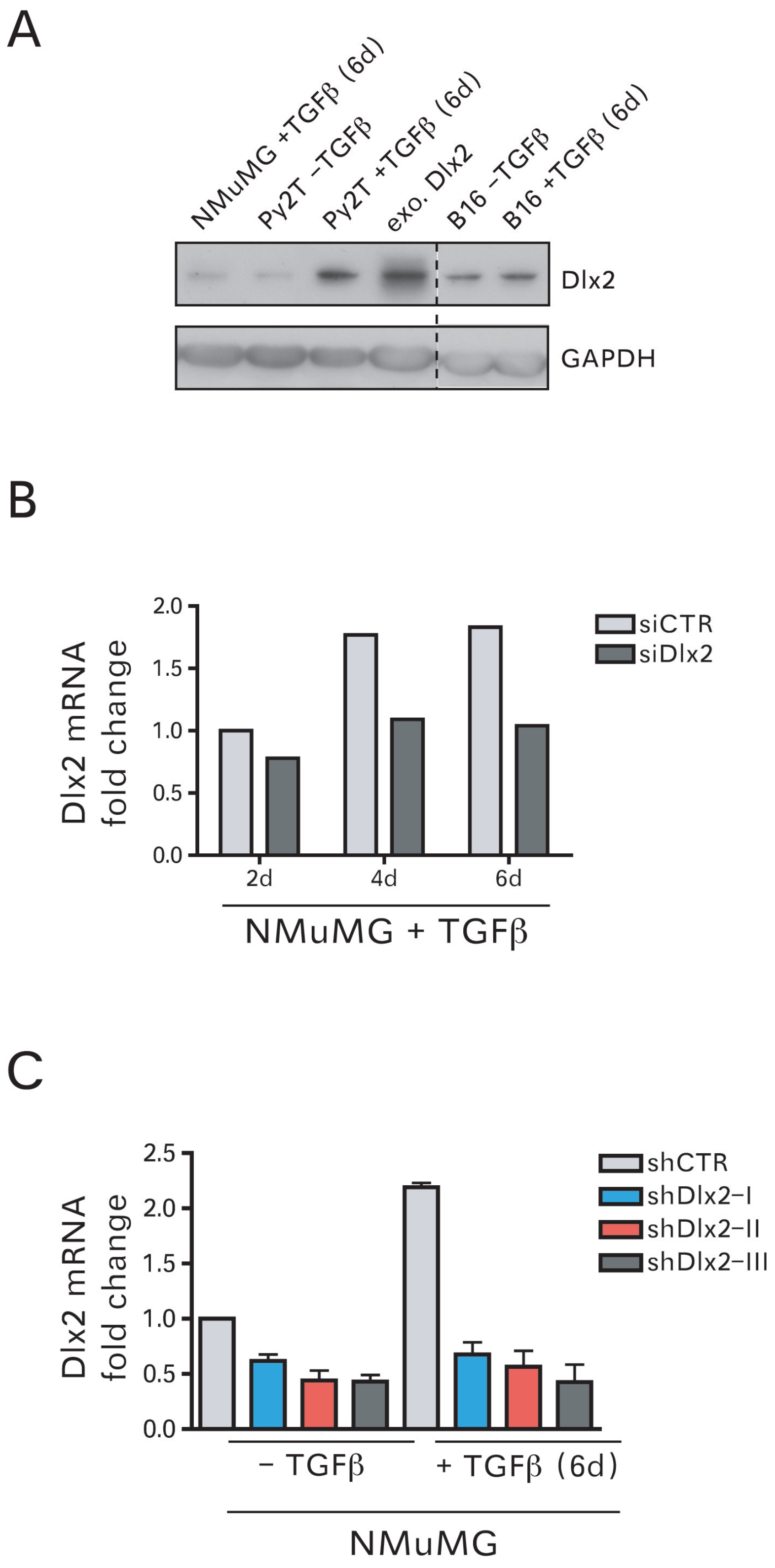

Yilmaz et al.,
Supplemental Figure S2

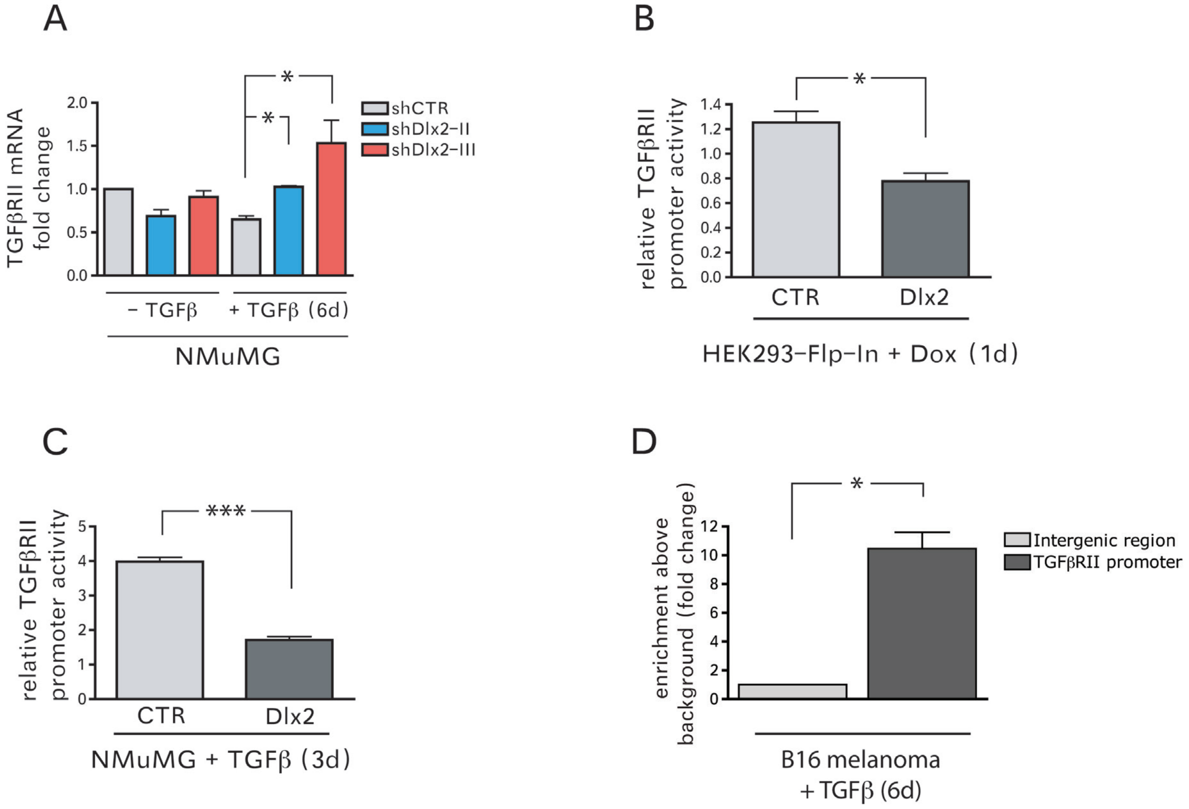

Yilmaz et al.,
Supplemental Figure S3

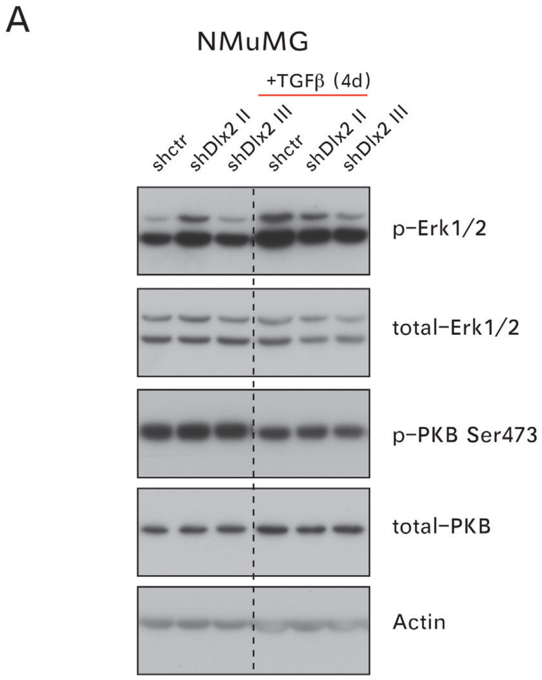
A
NMuMG
+TGFβ (4d)
shctr
shDlx2 II
shDlx2 III
shctr
shDlx2 II
shDlx2 III
p-Erk1/2
total-Erk1/2
p-PKB Ser473
total-PKB
Actin

Yilmaz et al.,
Supplemental Figure S4

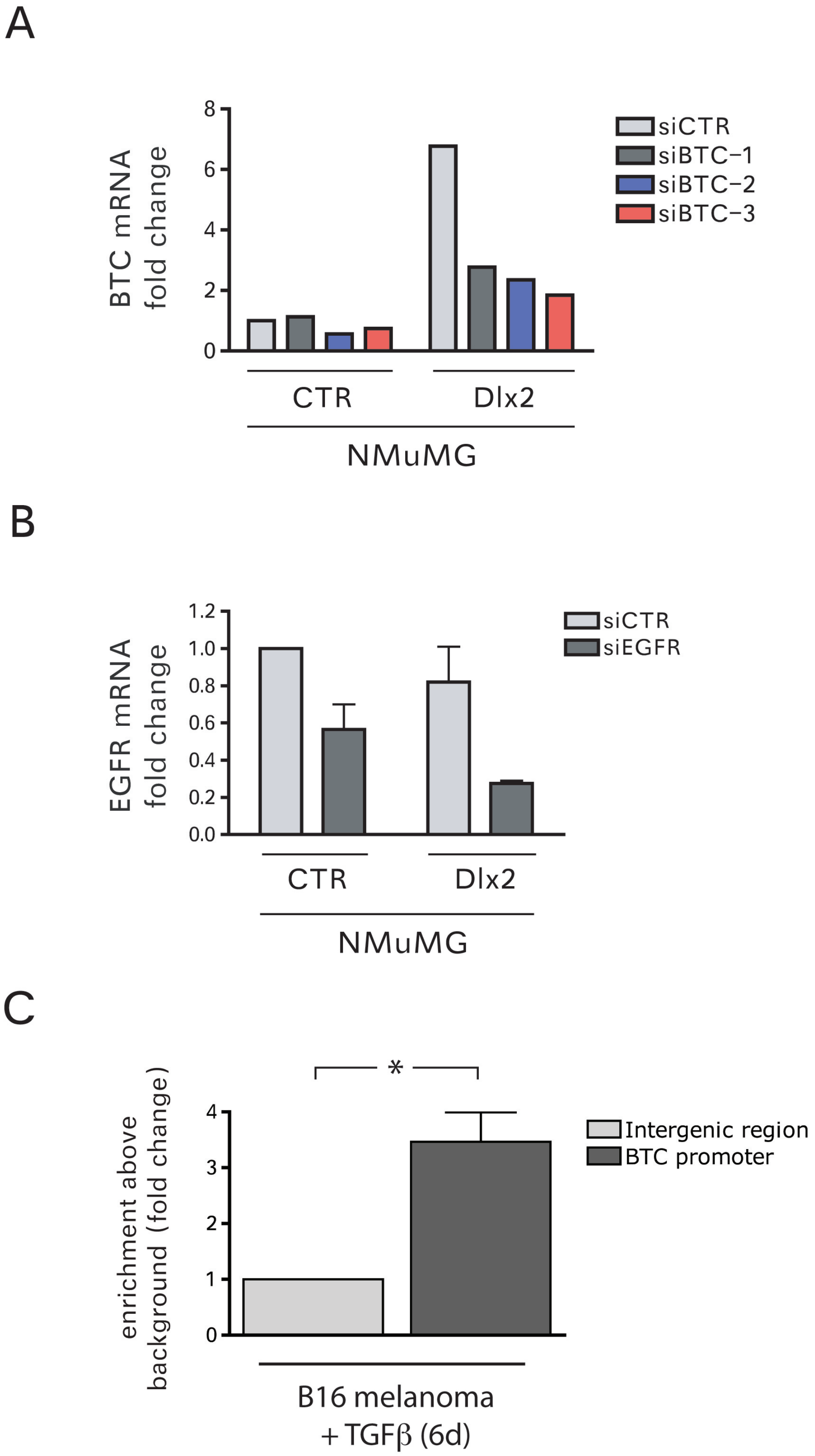

Yilmaz et al.,
Supplemental Figure S5

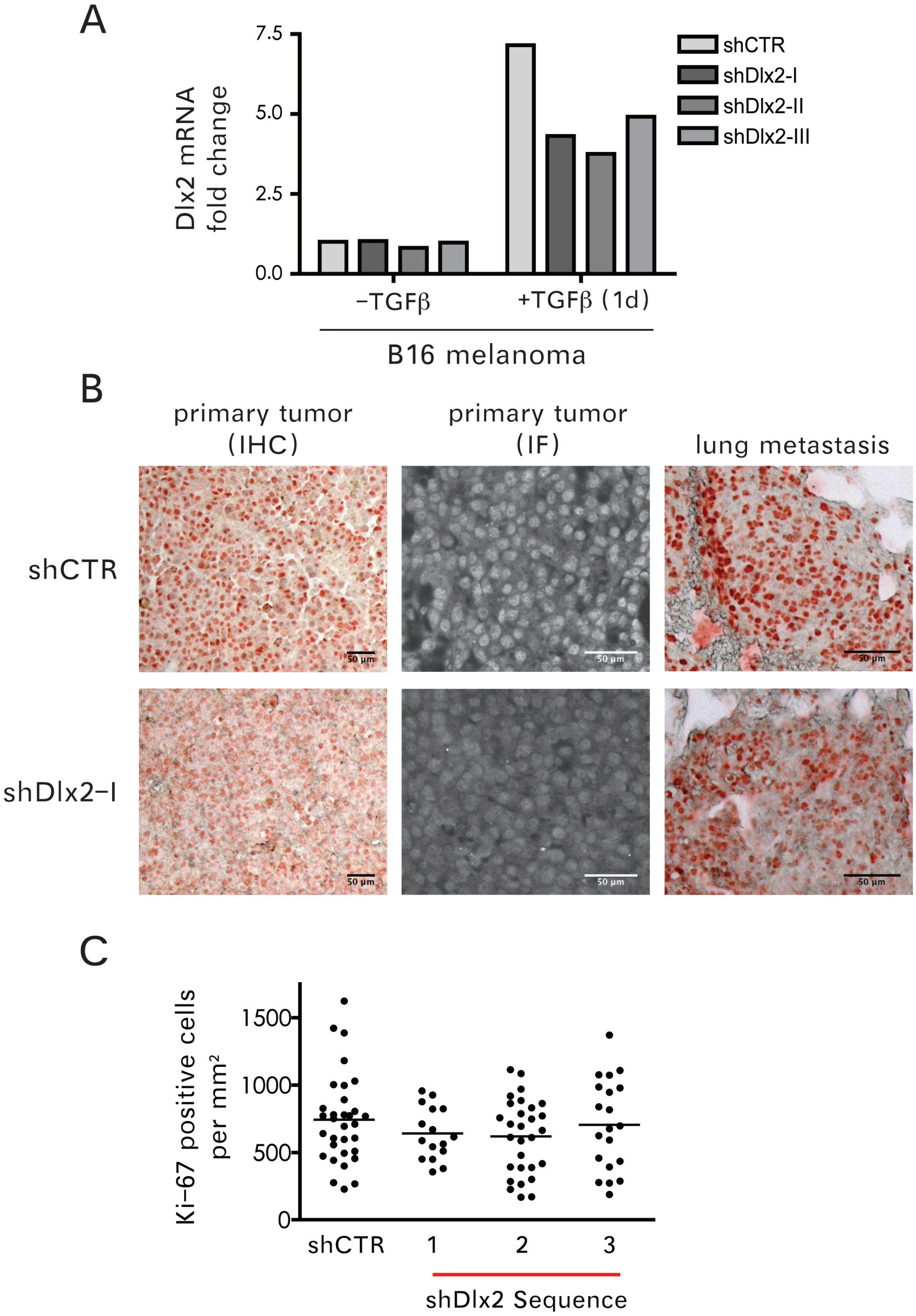

SUPPLEMENTAL INFORMATION

Supplemental Figure Legends

Supplemental Figure S1. TGFβ induces Dlx2 expression in several cellular systems.

(A) NMuMG, Py2T and B16 cells were treated for 6 days with TGFβ. Dlx2 protein levels compared to untreated and Dlx2-overexpressing cells were determined by immunoblotting analysis.

(B) Transient transfection of NMuMG cells with siRNA against Dlx2 (siDlx2) or control siRNA (siCTR) during TGFβ treatment for the days indicated. Expression of Dlx2 mRNA was determined by quantitative RT-PCR and presented as fold changes compared to control (siCTR).

(C) Stable lentiviral expression of three independent shRNAs against Dlx2 (shDLx2-I, II and III) and one control shRNA (shCTR) in NMUMG cells. Expression of Dlx2 mRNA was determined by quantitative RT-PCR and presented as fold changes compared to control (shCTR).

Supplemental Figure S2. Dlx2 regulates *TGFβRII* gene expression.

(A) Quantitative RT-PCR analysis of TGFβRII mRNA expression in shDlx2 cells and shCTR cells treated with TGFβ for 0 or 6 days. TGFβ treatment provokes an increase in TGFβRII mRNA expression in Dlx2-depleted cells as compared to shCTR cells.

(B) Doxycyclin-inducible expression of Dlx2 in HEK293 cells represses TGFβRII promoter activity. Doxycycline-inducible Flp-In T-Rex HEK293 cells expressing either GFP or N-terminal HA-tagged murine Dlx2 were transfected with a *firefly* luciferase-reporter plasmid containing 255 bp of the TGFβRII promoter sequence and treated for 1 day with doxycycline. Luciferase activity values were normalized to co-transfected *Renilla* luciferase activities.

(C) Dlx2-expressing NMuMG cells show a reduced TGFβRII promoter-reporter activity compared to control cells when treated for 3 days with TGFβ. Luciferase activities were quantified as described in panel B.

(D) Dlx2 binds directly to the *TGFβRII* gene promoter in B16 melanoma cells. Chromatin immunoprecipitation of Dlx2 was performed on B16 melanoma cells treated with TGFβ for 6 days. Immunoprecipitated DNA fragments were quantified

by quantitative PCR using primers covering basepairs -386 to -204 of the *TGFβRII* promoter region and primers covering an intergenic region as negative control.
Data are shown as mean ± SD and are representative of at least two independent experiments. Statistical values are calculated by using an unpaired, two-tailed t-test. *, $p \leq 0.05$; **, $p \leq 0.01$; ***, $p \leq 0.001$.

Supplemental Figure S3. Knockdown of Dlx2 expression does not inhibit Erk1/2 and PKB phosphorylation. Immunoblotting analysis of phosphorylated Erk1/2 and PKB comparing shControl and shDlx2 cells. Immunoblotting for actin was used as a loading control.

Supplemental Figure S4. Quantification of siRNA-mediated ablation of **(A)** betacellulin (BTC) and **(B)** EGFR expression in NMuMG cells transfected to express Dlx2 or transfected with a control vector (CTR). NMuMG cells were transfected with siRNA against betacellulin (siBTC-1 to 3), EGFR (siEGFR) or control siRNA (siCTR), and the mRNA levels of betacellulin and EGFR were determined by quantitative RT-PCR. Results are presented as fold changes compared to control (siCTR).
(C) Dlx2 binds directly to the betacellulin promoter in B16 melanoma cells. Chromatin immunoprecipitation of Dlx2 was performed on B16 melanoma cells treated for 6 days with TGFβ. Immunoprecipitated DNA fragments were quantified by quantitative RT-PCR using primers amplifying the promoter region of the *betacellulin* gene and primers covering an intergenic region as negative control.
Data are shown as mean ± SD and are representative of at least two independent experiments. Statistical values are calculated by using an unpaired, two-tailed t-test. *, $p \leq 0.05$.

Supplemental Figure S5. Dlx2 expression in B16 melanoma cells, tumors and metastases.
(A) Dlx2 expression is induced by TGFβ in B16 melanoma cells and reduced in expression by stable lentiviral expression of three independent shRNAs against Dlx2 (shDlx2-I, II, III) but not in cells expressing a control shRNA (shRNA). Dlx2 mRNA levels were determined by quantitative RT-PCR and are presented as fold changes

compared to control (shCTR, no TGFβ).

(B) Histological sections of primary tumors and lung metastasis, formed after subcutaneous injection of shCTR or shDlx2 (shDlx2-I) B16 melanoma cells, were stained for Dlx2, and Dlx2 was visualized by immunofluorescence or immunohistochemical stainings as indicated. Representative microphotographs of shControl and shDlx2-I samples are displayed. Scale bar = 50 μm

(C) Primary tumors formed by B16 melanoma cells either expressing shCTR or shDlx2 were analyzed for proliferation by counting Ki67-positive cells per mm^2.

Supplemental Material and Methods

Cell lines

The murine breast cancer cell line Py2T was established from a primary breast tumor of a MMTV-PyMT transgenic mouse. Py2T cells exhibit epithelial morphology under normal growth conditions. Upon treatment with TGFβ, these cells undergo full EMT within 10 days (Waldmeier et al., unpublished results).

4 General conclusions and outlook

The understanding of cancer progression in all its facets is essential to treat cancer patients effectively always with the ultimate goal in vision to not only prolong the lifespan of patients but to ultimately cure the disease.

My work has focused on various stages of tumor progression. Cells, that have undergone EMT, establish a tumor or metastasis in an accelerated and more efficient way than epithelial cells. EMT cells do so, by inducing angiogenesis via increased VEGF-A production and secretion. Thereby, tumor-initiating cells prepare the needed microenvironment to grow out as a tumor or, at the end, to be able to establish metastases. *De novo* tumor formation is not only a cell autonomous event but requires multiple hits upon which one is the induction of angiogenesis. Cancer cells that are about to leave the primary site by undergoing EMT are exposed to signals that not only help them to progress but are also potentially harmful to them. TGFβ is such a signal that can induce EMT in cancer cells leading to tumor progression. On the other hand, TGFβ is also able to force cells into apoptosis. The transcription factor Dlx2 prevents apoptosis in a negative feedback loop by repressing TGFβRI expression and by elevating survival signals via betacellulin-EGFR. In this way, cancer cells benefit from TGFβ's tumor-promotive signaling. Cells that have undergone EMT also acquire the capacity to move efficiently, and I have described ephrinB2's important role in cell motility. EphrinB2 seems to be needed to orchestrate the cellular movement of mesenchymal cells by regulating focal adhesion dynamics.

The specific proteins in the described pathways could serve as therapeutic targets, although further validation of their effects during tumor progression has to be performed. As an example, an inhibitor targeting Dlx2 could restore sensitization to TGFβ's apoptotic function in a cancer cell that is about to become more aggressive by undergoing EMT. However, Dlx2, as a transcription factor, is difficult to target. A prerequisite for the functionality of Dlx2 inhibition would be that the treated cancer is genetically able to execute TGFβ-induced apoptosis. Additionally, TGFβ signaling would have to be powerful enough to induce apoptosis not being overruled by strong survival signals.

Another example of therapeutic targeting could involve ephrinB2. The migration and invasion capability of cells, that have undergone EMT, could be reduced by interfering with ephrinB2 signaling. ephrinB2's role in cancer cells is still not well characterized compared to its function in endothelial or neuronal cells. The mechanism how ephrinB2 changes focal adhesion dynamics has to be further investigated. Also, the reduced migration ability observed in cells with a knockdown for ephrinB2 has to be validated *in vivo*. Unfortunately, this could not be achieved yet due to experimental limitations within the chosen breast cancer model. However, since other groups have established ephrinB2's role during tumor angiogenesis (*106,114*), targeting ephrinB2 would have dual effects: angiogenesis inhibition and less tumor cell migration.

I made the most important observation, when I compared the tumorigenicity of EMT cells with their epithelial counterparts in mice. EMT cells initiate tumors with an increased efficiency and generate highly vascularized tumors. I have discovered that VEGF-A, the main driver of angiogenesis, plays a role already at very early stages of tumorigenicity and during metastasis. The reduction of VEGF-A secretion by cancer cells has a striking impact on how fast and efficiently cancer cells establish a tumor. Targeted therapy against VEGF-A is already used in the clinics and has proven to be effective for various cancer types, mostly in the late stages of tumor progression. My study suggests that treating cancer patients already at early stages with such a drug would help to reduce cancerous outgrowth at secondary sites. Also, treating patients after therapy with anti-angiogenic drugs could keep residual CSCs and cancer relapse in check. Inhibition of tumor angiogenesis would prevent CSCs from building up the microenvironment they need to reestablish a tumor. To evaluate the relevance of VEGF-A in patients' CSCs, clinical trials specifically looking at metastasis formation and relapse are of importance.

5 References

1. World Health Organization. Cancer: key facts. www.who.int/mediacentre/factsheets/fs297/en. Retrieved 20th August 2012.
2. Hanahan, D. & Weinberg, R. A. Hallmarks of cancer: the next generation. *Cell* **144**, 646-674 (2011).
3. NOWELL, P. C. & HUNGERFORD, D. A. Chromosome studies on normal and leukemic human leukocytes. *J Natl Cancer Inst* **25**, 85-109 (1960).
4. Erickson, P., Gao, J. et al.Drabkin, H. Identification of breakpoints in t(8;21) acute myelogenous leukemia and isolation of a fusion transcript, AML1/ETO, with similarity to Drosophila segmentation gene, runt. *Blood* **80**, 1825-1831 (1992).
5. Visvader, J. E. Keeping abreast of the mammary epithelial hierarchy and breast tumorigenesis. *Genes Dev* **23**, 2563-2577 (2009).
6. Bertos, N. R. & Park, M. Breast cancer - one term, many entities? *J Clin Invest* **121**, 3789-3796 (2011).
7. Perou, C. M., Sorlie, T. et al.Botstein, D. Molecular portraits of human breast tumours. *Nature* **406**, 747-752 (2000).
8. Herschkowitz, J. I., Simin, K. et al.Perou, C. M. Identification of conserved gene expression features between murine mammary carcinoma models and human breast tumors. *Genome Biol* **8**, R76 (2007).
9. Mani, S. A., Guo, W. et al.Weinberg, R. A. The epithelial-mesenchymal transition generates cells with properties of stem cells. *Cell* **133**, 704-715 (2008).
10. Fantozzi, A. & Christofori, G. Mouse models of breast cancer metastasis. *Breast Cancer Res* **8**, 212 (2006).
11. Muller, W. J., Sinn, E. et al.Leder, P. Single-step induction of mammary adenocarcinoma in transgenic mice bearing the activated c-neu oncogene. *Cell* **54**, 105-115 (1988).
12. Folkman, J. & Hanahan, D. Switch to the angiogenic phenotype during tumorigenesis. *Princess Takamatsu Symp* **22**, 339-347 (1991).
13. Holash, J., Maisonpierre, P. C. et al.Wiegand, S. J. Vessel cooption, regression, and growth in tumors mediated by angiopoietins and VEGF. *Science* **284**, 1994-1998 (1999).
14. Baeriswyl, V. & Christofori, G. The angiogenic switch in carcinogenesis. *Semin Cancer Biol* **19**, 329-337 (2009).
15. Weis, S. M. & Cheresh, D. A. Tumor angiogenesis: molecular pathways and therapeutic targets. *Nat Med* **17**, 1359-1370 (2011).
16. Wang, R., Chadalavada, K. et al.Tabar, V. Glioblastoma stem-like cells give rise to tumour endothelium. *Nature* **468**, 829-833 (2010).
17. Sanchez-Elsner, T., Botella, L. M. et al.Bernabeu, C. Synergistic cooperation between hypoxia and transforming growth factor-beta pathways on human vascular endothelial growth factor gene expression. *J Biol Chem* **276**, 38527-38535 (2001).
18. Du, R., Lu, K. V. et al.Bergers, G. HIF1alpha induces the recruitment of bone marrow-derived vascular modulatory cells to regulate tumor angiogenesis and invasion. *Cancer Cell* **13**, 206-220 (2008).
19. Carmeliet, P. & Jain, R. K. Molecular mechanisms and clinical applications of angiogenesis. *Nature* **473**, 298-307 (2011).
20. Hellberg, C., Ostman, A. & Heldin, C. H. PDGF and vessel maturation. *Recent Results Cancer Res* **180**, 103-114 (2010).
21. Folkman, J. Tumor angiogenesis: therapeutic implications. *N Engl J Med* **285**, 1182-1186 (1971).
22. Folkman, J., Watson, K., Ingber, D. & Hanahan, D. Induction of angiogenesis during the transition from hyperplasia to neoplasia. *Nature* **339**, 58-61 (1989).
23. Inai, T., Mancuso, M. et al.McDonald, D. M. Inhibition of vascular endothelial

growth factor (VEGF) signaling in cancer causes loss of endothelial fenestrations, regression of tumor vessels, and appearance of basement membrane ghosts. *Am J Pathol* **165**, 35-52 (2004).

24. Casanovas, O., Hicklin, D. J., Bergers, G. & Hanahan, D. Drug resistance by evasion of antiangiogenic targeting of VEGF signaling in late-stage pancreatic islet tumors. *Cancer Cell* **8**, 299-309 (2005).

25. Compagni, A., Wilgenbus, P. et al.Christofori, G. Fibroblast growth factors are required for efficient tumor angiogenesis. *Cancer Res* **60**, 7163-7169 (2000).

26. Hurwitz, H., Fehrenbacher, L. et al.Kabbinavar, F. Bevacizumab plus irinotecan, fluorouracil, and leucovorin for metastatic colorectal cancer. *N Engl J Med* **350**, 2335-2342 (2004).

27. Allegra, C. J., Yothers, G. et al.Wolmark, N. Phase III trial assessing bevacizumab in stages II and III carcinoma of the colon: results of NSABP protocol C-08. *J Clin Oncol* **29**, 11-16 (2011).

28. Miller, K., Wang, M. et al.Davidson, N. E. Paclitaxel plus bevacizumab versus paclitaxel alone for metastatic breast cancer. *N Engl J Med* **357**, 2666-2676 (2007).

29. Ocana, A., Amir, E. et al.Tannock, I. F. Addition of bevacizumab to chemotherapy for treatment of solid tumors: similar results but different conclusions. *J Clin Oncol* **29**, 254-256 (2011).

30. Bergers, G. & Hanahan, D. Modes of resistance to anti-angiogenic therapy. *Nat Rev Cancer* **8**, 592-603 (2008).

31. Motzer, R. J., Hutson, T. E. et al.Figlin, R. A. Sunitinib versus interferon alfa in metastatic renal-cell carcinoma. *N Engl J Med* **356**, 115-124 (2007).

32. Kalluri, R. & Weinberg, R. A. The basics of epithelial-mesenchymal transition. *J Clin Invest* **119**, 1420-1428 (2009).

33. Drasin, D. J., Robin, T. P. & Ford, H. L. Breast cancer epithelial-to-mesenchymal transition: examining the functional consequences of plasticity. *Breast Cancer Res* **13**, 226 (2011).

34. Thiery, J. P. & Sleeman, J. P. Complex networks orchestrate epithelial-mesenchymal transitions. *Nat Rev Mol Cell Biol* **7**, 131-142 (2006).

35. Yilmaz, M. & Christofori, G. Mechanisms of motility in metastasizing cells. *Mol Cancer Res* **8**, 629-642 (2010).

36. Vleminckx, K., Vakaet, L. J. et al.van Roy, F. Genetic manipulation of E-cadherin expression by epithelial tumor cells reveals an invasion suppressor role. *Cell* **66**, 107-119 (1991).

37. Perl, A. K., Wilgenbus, P. et al.Christofori, G. A causal role for E-cadherin in the transition from adenoma to carcinoma. *Nature* **392**, 190-193 (1998).

38. Thiery, J. P., Acloque, H., Huang, R. Y. & Nieto, M. A. Epithelial-mesenchymal transitions in development and disease. *Cell* **139**, 871-890 (2009).

39. van Roy, F. & Berx, G. The cell-cell adhesion molecule E-cadherin. *Cell Mol Life Sci* **65**, 3756-3788 (2008).

40. Scheel, C. & Weinberg, R. A. Cancer stem cells and epithelial-mesenchymal transition: Concepts and molecular links. *Semin Cancer Biol* (2012).

41. Frisch, S. M. & Francis, H. Disruption of epithelial cell-matrix interactions induces apoptosis. *J Cell Biol* **124**, 619-626 (1994).

42. Valastyan, S. & Weinberg, R. A. Tumor metastasis: molecular insights and evolving paradigms. *Cell* **147**, 275-292 (2011).

43. Kessenbrock, K., Plaks, V. & Werb, Z. Matrix metalloproteinases: regulators of the tumor microenvironment. *Cell* **141**, 52-67 (2010).

44. Friedl, P. & Wolf, K. Proteolytic interstitial cell migration: a five-step process. *Cancer Metastasis Rev* **28**, 129-135 (2009).

45. Tiwari, N., Gheldof, A., Tatari, M. & Christofori, G. EMT as the ultimate survival mechanism of cancer cells. *Semin Cancer Biol* **22**, 194-207 (2012).

46. Sleeman, J. & Steeg, P. S. Cancer metastasis as a therapeutic target. *Eur J Cancer* **46**, 1177-1180 (2010).

47. Klein, C. A. Parallel progression of primary tumours and metastases. *Nat Rev Cancer* **9**, 302-312 (2009).

48. Fidler, I. J. The pathogenesis of cancer metastasis: the 'seed and soil' hypothesis revisited. *Nat Rev Cancer* **3**, 453-458 (2003).

49. Chambers, A. F., Groom, A. C. & MacDonald, I. C. Dissemination and growth of cancer cells in metastatic sites. *Nat Rev Cancer* **2**, 563-572 (2002).

50. Friedl, P. & Wolf, K. Tumour-cell invasion and migration: diversity and escape mechanisms. *Nat Rev Cancer* **3**, 362-374 (2003).

51. Bissell, M. J. & Hines, W. C. Why don't we get more cancer? A proposed role of the microenvironment in restraining cancer progression. *Nat Med* **17**, 320-329 (2011).

52. Nguyen, D. X., Bos, P. D. & Massague, J. Metastasis: from dissemination to organ-specific colonization. *Nat Rev Cancer* **9**, 274-284 (2009).

53. Psaila, B. & Lyden, D. The metastatic niche: adapting the foreign soil. *Nat Rev Cancer* **9**, 285-293 (2009).

54. Peinado, H., Aleckovic, M. et al.Lyden, D. Melanoma exosomes educate bone marrow progenitor cells toward a pro-metastatic phenotype through MET. *Nat Med* **18**, 883-891 (2012).

55. Brabletz, T. To differentiate or not - routes towards metastasis. *Nat Rev Cancer* (2012).

56. Baccelli, I. & Trumpp, A. The evolving concept of cancer and metastasis stem cells. *J Cell Biol* **198**, 281-293 (2012).

57. Nowell, P. C. The clonal evolution of tumor cell populations. *Science* **194**, 23-28 (1976).

58. Barabe, F., Kennedy, J. A., Hope, K. J. & Dick, J. E. Modeling the initiation and progression of human acute leukemia in mice. *Science* **316**, 600-604 (2007).

59. Bonnet, D. & Dick, J. E. Human acute myeloid leukemia is organized as a hierarchy that originates from a primitive hematopoietic cell. *Nat Med* **3**, 730-737 (1997).

60. Lapidot, T., Sirard, C. et al.Dick, J. E. A cell initiating human acute myeloid leukaemia after transplantation into SCID mice. *Nature* **367**, 645-648 (1994).

61. Dontu, G., Abdallah, W. M. et al.Wicha, M. S. In vitro propagation and transcriptional profiling of human mammary stem/progenitor cells. *Genes Dev* **17**, 1253-1270 (2003).

62. Gupta, P. B., Onder, T. T. et al.Lander, E. S. Identification of selective inhibitors of cancer stem cells by high-throughput screening. *Cell* **138**, 645-659 (2009).

63. Lu, D., Choi, M. Y. et al.Carson, D. A. Salinomycin inhibits Wnt signaling and selectively induces apoptosis in chronic lymphocytic leukemia cells. *Proc Natl Acad Sci U S A* **108**, 13253-13257 (2011).

64. Magee, J. A., Piskounova, E. & Morrison, S. J. Cancer stem cells: impact, heterogeneity, and uncertainty. *Cancer Cell* **21**, 283-296 (2012).

65. Visvader, J. E. & Lindeman, G. J. Cancer stem cells: current status and evolving complexities. *Cell Stem Cell* **10**, 717-728 (2012).

66. Quintana, E., Shackleton, M. et al.Morrison, S. J. Efficient tumour formation by single human melanoma cells. *Nature* **456**, 593-598 (2008).

67. Al-Hajj, M., Wicha, M. S. et al.Clarke, M. F. Prospective identification of tumorigenic breast cancer cells. *Proc Natl Acad Sci U S A* **100**, 3983-3988 (2003).

68. Chaffer, C. L., Brueckmann, I. et al.Weinberg, R. A. Normal and neoplastic nonstem cells can spontaneously convert to a stem-like state. *Proc Natl Acad Sci U S A* **108**, 7950-7955 (2011).

69. Beltran, A. S., Rivenbark, A. G. et al.Blancafort, P. Generation of tumor-initiating cells by exogenous delivery of OCT4 transcription factor. *Breast Cancer Res* **13**, R94 (2011).

70. Calabrese, C., Poppleton, H. et al.Gilbertson, R. J. A perivascular niche for brain tumor stem cells. *Cancer Cell* **11**, 69-82 (2007).

71. Sleeman, J. P., Christofori, G. et al.Ruegg, C. Concepts of metastasis in flux: the stromal progression model. *Semin Cancer Biol* **22**, 174-186 (2012).

72. Taube, J. H., Herschkowitz, J. I. et al.Mani, S. A. Core epithelial-to-mesenchymal transition interactome gene-expression signature is associated with claudin-low and metaplastic breast cancer subtypes. *Proc Natl Acad Sci U S A* **107**, 15449-15454 (2010).

73. Creighton, C. J., Li, X. et al.Chang, J. C. Residual breast cancers after conventional therapy display mesenchymal as well as tumor-initiating features. *Proc Natl Acad Sci U S A* **106**, 13820-13825 (2009).

74. May, C. D., Sphyris, N. et al.Mani, S. A. Epithelial-mesenchymal transition and cancer stem cells: a dangerously dynamic duo in breast cancer progression. *Breast Cancer Res* **13**, 202 (2011).

75. Floor, S., van Staveren, W. C. et al.Maenhaut, C. Cancer cells in epithelial-to-mesenchymal transition and tumor-propagating-cancer stem cells: distinct, overlapping or same populations. *Oncogene* **30**, 4609-4621 (2011).

76. Lehembre, F., Yilmaz, M. et al.Christofori, G. NCAM-induced focal adhesion assembly: a functional switch upon loss of E-cadherin. *EMBO J* **27**, 2603-2615 (2008).

77. Sheridan, C., Kishimoto, H. et al.Nakshatri, H. CD44+/CD24- breast cancer cells exhibit enhanced invasive properties: an early step necessary for metastasis. *Breast Cancer Res* **8**, R59 (2006).

78. Stingl, J., Eirew, P. et al.Eaves, C. J. Purification and unique properties of mammary epithelial stem cells. *Nature* **439**, 993-997 (2006).

79. Shackleton, M., Vaillant, F. et al.Visvader, J. E. Generation of a functional mammary gland from a single stem cell. *Nature* **439**, 84-88 (2006).

80. Shafee, N., Smith, C. R. et al.Lee, E. Y. Cancer stem cells contribute to cisplatin resistance in Brca1/p53-mediated mouse mammary tumors. *Cancer Res* **68**, 3243-3250 (2008).

81. Phillips, T. M., McBride, W. H. & Pajonk, F. The response of CD24(-/low)/CD44+ breast cancer-initiating cells to radiation. *J Natl Cancer Inst* **98**, 1777-1785 (2006).

82. Vassilopoulos, A., Wang, R. H. et al.Deng, C. X. Identification and characterization of cancer initiating cells from BRCA1 related mammary tumors using markers for normal mammary stem cells. *Int J Biol Sci* **4**, 133-142 (2008).

83. Wright, M. H., Calcagno, A. M. et al.Varticovski, L. Brca1 breast tumors contain distinct CD44+/CD24- and CD133+ cells with cancer stem cell characteristics. *Breast Cancer Res* **10**, R10 (2008).

84. Thijssen, V. L., Postel, R. et al.Griffioen, A. W. Galectin-1 is essential in tumor angiogenesis and is a target for antiangiogenesis therapy. *Proc Natl Acad Sci U S A* **103**, 15975-15980 (2006).

85. Thijssen, V. L., Barkan, B. et al.Griffioen, A. W. Tumor cells secrete galectin-1 to enhance endothelial cell activity. *Cancer Res* **70**, 6216-6224 (2010).

86. Jelly, N. D., Hussain, I. I. et al.El-Sheemy, M. The stem cell factor antibody enhances the chemotherapeutic effect of adriamycin on chemoresistant breast cancer cells. *Cancer Cell Int* **12**, 21 (2012).

87. Caine, G. J., Lip, G. Y. & Blann, A. D. Platelet-derived VEGF, Flt-1, angiopoietin-1 and P-selectin in breast and prostate cancer: further evidence for a role of platelets in tumour angiogenesis. *Ann Med* **36**, 273-277 (2004).

88. Beck, B., Driessens, G. et al.Blanpain, C. A vascular niche and a VEGF-Nrp1 loop regulate the initiation and stemness of skin tumours. *Nature* **478**, 399-403 (2011).

89. Hamerlik, P., Lathia, J. D. et al.Bartek, J. Autocrine VEGF-VEGFR2-Neuropilin-1 signaling promotes glioma stem-like cell viability and tumor growth. *J Exp Med* **209**, 507-520 (2012).

90. Bao, S., Wu, Q. et al.Rich, J. N. Stem cell-like glioma cells promote tumor

angiogenesis through vascular endothelial growth factor. *Cancer Res* **66**, 7843-7848 (2006).

91. Lee, J., Lee, J. et al.Choi, C. Differential dependency of human cancer cells on vascular endothelial growth factor-mediated autocrine growth and survival. *Cancer Lett* **309**, 145-150 (2011).

92. Lee, J., Ku, T. et al.Choi, C. Blockade of VEGF-A suppresses tumor growth via inhibition of autocrine signaling through FAK and AKT. *Cancer Lett* **318**, 221-225 (2012).

93. Salva, E., Kabasakal, L. et al.Akbuga, J. Local delivery of chitosan/VEGF siRNA nanoplexes reduces angiogenesis and growth of breast cancer in vivo. *Nucleic Acid Ther* **22**, 40-48 (2012).

94. Mercurio, A. M., Lipscomb, E. A. & Bachelder, R. E. Non-angiogenic functions of VEGF in breast cancer. *J Mammary Gland Biol Neoplasia* **10**, 283-290 (2005).

95. Bachelder, R. E., Crago, A. et al.Mercurio, A. M. Vascular endothelial growth factor is an autocrine survival factor for neuropilin-expressing breast carcinoma cells. *Cancer Res* **61**, 5736-5740 (2001).

96. Bachelder, R. E., Lipscomb, E. A. et al.Mercurio, A. M. Competing autocrine pathways involving alternative neuropilin-1 ligands regulate chemotaxis of carcinoma cells. *Cancer Res* **63**, 5230-5233 (2003).

97. Ponti, D., Costa, A. et al.Daidone, M. G. Isolation and in vitro propagation of tumorigenic breast cancer cells with stem/progenitor cell properties. *Cancer Res* **65**, 5506-5511 (2005).

98. Bonnefoix, T., Bonnefoix, P., Verdiel, P. & Sotto, J. J. Fitting limiting dilution experiments with generalized linear models results in a test of the single-hit Poisson assumption. *J Immunol Methods* **194**, 113-119 (1996).

99. Maeda, M., Johnson, K. R. & Wheelock, M. J. Cadherin switching: essential for behavioral but not morphological changes during an epithelium-to-mesenchyme transition. *J Cell Sci* **118**, 873-887 (2005).

100. Waldmeier, L., Meyer-Schaller, N., Diepenbruck, M. & Christofori, G. Py2T murine breast cancer cells, a versatile model of TGFβ-induced EMT *in vitro* and *in vivo*. *PLoS One, submitted*

101. Egea, J. & Klein, R. Bidirectional Eph-ephrin signaling during axon guidance. *Trends Cell Biol* **17**, 230-238 (2007).

102. Pasquale, E. B. Eph-ephrin bidirectional signaling in physiology and disease. *Cell* **133**, 38-52 (2008).

103. Batlle, E., Bacani, J. et al.Clevers, H. EphB receptor activity suppresses colorectal cancer progression. *Nature* **435**, 1126-1130 (2005).

104. Wu, J. & Luo, H. Recent advances on T-cell regulation by receptor tyrosine kinases. *Curr Opin Hematol* **12**, 292-297 (2005).

105. Makinen, T., Adams, R. H. et al.Wilkinson, G. A. PDZ interaction site in ephrinB2 is required for the remodeling of lymphatic vasculature. *Genes Dev* **19**, 397-410 (2005).

106. Sawamiphak, S., Seidel, S. et al.Acker-Palmer, A. Ephrin-B2 regulates VEGFR2 function in developmental and tumour angiogenesis. *Nature* **465**, 487-491 (2010).

107. Kandouz, M. The Eph/Ephrin family in cancer metastasis: communication at the service of invasion. *Cancer Metastasis Rev* **31**, 353-373 (2012).

108. Janes, P. W., Nievergall, E. & Lackmann, M. Concepts and consequences of Eph receptor clustering. *Semin Cell Dev Biol* **23**, 43-50 (2012).

109. Pasquale, E. B. Eph receptors and ephrins in cancer: bidirectional signalling and beyond. *Nat Rev Cancer* **10**, 165-180 (2010).

110. Surawska, H., Ma, P. C. & Salgia, R. The role of ephrins and Eph receptors in cancer. *Cytokine Growth Factor Rev* **15**, 419-433 (2004).

111. Himanen, J. P., Rajashankar, K. R. et al.Nikolov, D. B. Crystal structure of an Eph receptor-ephrin complex. *Nature* **414**, 933-938 (2001).

112. Wang, H. U., Chen, Z. F. & Anderson, D. J. Molecular distinction and angiogenic interaction between embryonic arteries and veins revealed by ephrin-B2 and its receptor Eph-B4. *Cell* **93**, 741-753 (1998).

113. Adams, R. H., Wilkinson, G. A. et al.Klein, R. Roles of ephrinB ligands and EphB receptors in cardiovascular development: demarcation of arterial/venous domains, vascular morphogenesis, and sprouting angiogenesis. *Genes Dev* **13**, 295-306 (1999).

114. Wang, Y., Nakayama, M. et al.Adams, R. H. Ephrin-B2 controls VEGF-induced angiogenesis and lymphangiogenesis. *Nature* **465**, 483-486 (2010).

115. Abengozar, M. A., de Frutos, S. et al.Martinez-Torrecuadrada, J. L. Blocking ephrinB2 with highly specific antibodies inhibits angiogenesis, lymphangiogenesis, and tumor growth. *Blood* **119**, 4565-4576 (2012).

116. Bochenek, M. L., Dickinson, S. et al.Nobes, C. D. Ephrin-B2 regulates endothelial cell morphology and motility independently of Eph-receptor binding. *J Cell Sci* **123**, 1235-1246 (2010).

117. Foo, S. S., Turner, C. J. et al.Adams, R. H. Ephrin-B2 controls cell motility and adhesion during blood-vessel-wall assembly. *Cell* **124**, 161-173 (2006).

118. Nikolova, Z., Djonov, V. et al.Ziemiecki, A. Cell-type specific and estrogen dependent expression of the receptor tyrosine kinase EphB4 and its ligand ephrin-B2 during mammary gland morphogenesis. *J Cell Sci* **111**, 2741-2751 (1998).

119. Haldimann, M., Custer, D. et al.Andres, A. C. Deregulated ephrin-B2 expression in the mammary gland interferes with the development of both the glandular epithelium and vasculature and promotes metastasis formation. *Int J Oncol* **35**, 525-536 (2009).

120. Grunwald, I. C., Korte, M. et al.Klein, R. Hippocampal plasticity requires postsynaptic ephrinBs. *Nat Neurosci* **7**, 33-40 (2004).

121. Weiler, S., Rohrbach, V. et al.Andres, A. C. Mammary epithelial-specific knockout of the ephrin-B2 gene leads to precocious epithelial cell death at lactation. *Dev Growth Differ* **51**, 809-819 (2009).

122. Orsulic, S. & Kemler, R. Expression of Eph receptors and ephrins is differentially regulated by E-cadherin. *J Cell Sci* **113**, 1793-1802 (2000).

123. Yang, N. Y., Pasquale, E. B., Owen, L. B. & Ethell, I. M. The EphB4 receptor-tyrosine kinase promotes the migration of melanoma cells through Rho-mediated actin cytoskeleton reorganization. *J Biol Chem* **281**, 32574-32586 (2006).

124. Meyer, S., Hafner, C. et al.Vogt, T. Ephrin-B2 overexpression enhances integrin-mediated ECM-attachment and migration of B16 melanoma cells. *Int J Oncol* **27**, 1197-1206 (2005).

125. Nakada, M., Anderson, E. M. et al.Berens, M. E. The phosphorylation of ephrin-B2 ligand promotes glioma cell migration and invasion. *Int J Cancer* **126**, 1155-1165 (2010).

126. Noren, N. K., Foos, G., Hauser, C. A. & Pasquale, E. B. The EphB4 receptor suppresses breast cancer cell tumorigenicity through an Abl-Crk pathway. *Nat Cell Biol* **8**, 815-825 (2006).

127. Wehrle-Haller, B. Structure and function of focal adhesions. *Curr Opin Cell Biol* **24**, 116-124 (2012).

128. Riedl, J., Crevenna, A. H. et al.Wedlich-Soldner, R. Lifeact: a versatile marker to visualize F-actin. *Nat Methods* **5**, 605-607 (2008).

129. Guy, C. T., Cardiff, R. D. & Muller, W. J. Induction of mammary tumors by expression of polyomavirus middle T oncogene: a transgenic mouse model for metastatic disease. *Mol Cell Biol* **12**, 954-961 (1992).

130. Wagner, K. U., Wall, R. J. et al.Hennighausen, L. Cre-mediated gene deletion in the mammary gland. *Nucleic Acids Res* **25**, 4323-4330 (1997).

131. Ursini-Siegel, J., Hardy, W. R. et al.Muller, W. J. ShcA signalling is essential for tumour progression in mouse models of human breast cancer. *EMBO J* **27**, 910-920 (2008).

132. Oft, M., Heider, K. H. & Beug, H. TGFbeta signaling is necessary for carcinoma cell invasiveness and metastasis. *Curr Biol* **8**, 1243-1252 (1998).

133. Morita, S., Kojima, T. & Kitamura, T. Plat-E: an efficient and stable system for

transient packaging of retroviruses. *Gene Ther* **7**, 1063-1066 (2000).

134. Heldin, C. H. & Moustakas, A. Role of Smads in TGFbeta signaling. *Cell Tissue Res* (2011).

135. Parvani, J. G., Taylor, M. A. & Schiemann, W. P. Noncanonical TGF-beta signaling during mammary tumorigenesis. *J Mammary Gland Biol Neoplasia* **16**, 127-146 (2011).

136. Hocevar, B. A., Brown, T. L. & Howe, P. H. TGF-beta induces fibronectin synthesis through a c-Jun N-terminal kinase-dependent, Smad4-independent pathway. *EMBO J* **18**, 1345-1356 (1999).

137. Galliher, A. J. & Schiemann, W. P. Beta3 integrin and Src facilitate transforming growth factor-beta mediated induction of epithelial-mesenchymal transition in mammary epithelial cells. *Breast Cancer Res* **8**, R42 (2006).

138. Galliher-Beckley, A. J. & Schiemann, W. P. Grb2 binding to Tyr284 in TbetaR-II is essential for mammary tumor growth and metastasis stimulated by TGF-beta. *Carcinogenesis* **29**, 244-251 (2008).

139. Wendt, M. K. & Schiemann, W. P. Therapeutic targeting of the focal adhesion complex prevents oncogenic TGF-beta signaling and metastasis. *Breast Cancer Res* **11**, R68 (2009).

140. Yamashita, M., Fatyol, K. et al.Zhang, Y. E. TRAF6 mediates Smad-independent activation of JNK and p38 by TGF-beta. *Mol Cell* **31**, 918-924 (2008).

141. Yu, L., Hebert, M. C. & Zhang, Y. E. TGF-beta receptor-activated p38 MAP kinase mediates Smad-independent TGF-beta responses. *EMBO J* **21**, 3749-3759 (2002).

142. Engel, M. E., McDonnell, M. A., Law, B. K. & Moses, H. L. Interdependent SMAD and JNK signaling in transforming growth factor-beta-mediated transcription. *J Biol Chem* **274**, 37413-37420 (1999).

143. Kamaraju, A. K. & Roberts, A. B. Role of Rho/ROCK and p38 MAP kinase pathways in transforming growth factor-beta-mediated Smad-dependent growth inhibition of human breast carcinoma cells in vivo. *J Biol Chem* **280**, 1024-1036 (2005).

144. Lamouille, S. & Derynck, R. Cell size and invasion in TGF-beta-induced epithelial to mesenchymal transition is regulated by activation of the mTOR pathway. *J Cell Biol* **178**, 437-451 (2007).

145. Petritsch, C., Beug, H., Balmain, A. & Oft, M. TGF-beta inhibits p70 S6 kinase via protein phosphatase 2A to induce G(1) arrest. *Genes Dev* **14**, 3093-3101 (2000).

146. Lee, M. K., Pardoux, C. et al.Derynck, R. TGF-beta activates Erk MAP kinase signalling through direct phosphorylation of ShcA. *EMBO J* **26**, 3957-3967 (2007).

147. Ozdamar, B., Bose, R. et al.Wrana, J. L. Regulation of the polarity protein Par6 by TGFbeta receptors controls epithelial cell plasticity. *Science* **307**, 1603-1609 (2005).

148. Bhowmick, N. A., Ghiassi, M. et al.Moses, H. L. TGF-beta-induced RhoA and p160ROCK activation is involved in the inhibition of Cdc25A with resultant cell-cycle arrest. *Proc Natl Acad Sci U S A* **100**, 15548-15553 (2003).

149. Nagarajan, R. P., Zhang, J., Li, W. & Chen, Y. Regulation of Smad7 promoter by direct association with Smad3 and Smad4. *J Biol Chem* **274**, 33412-33418 (1999).

150. Ebisawa, T., Fukuchi, M. et al.Miyazono, K. Smurf1 interacts with transforming growth factor-beta type I receptor through Smad7 and induces receptor degradation. *J Biol Chem* **276**, 12477-12480 (2001).

151. Kavsak, P., Rasmussen, R. K. et al.Wrana, J. L. Smad7 binds to Smurf2 to form an E3 ubiquitin ligase that targets the TGF beta receptor for degradation. *Mol Cell* **6**, 1365-1375 (2000).

152. Shi, W., Sun, C. et al.Cao, X. GADD34-PP1c recruited by Smad7 dephosphorylates TGFbeta type I receptor. *J Cell Biol* **164**, 291-300 (2004).

153. Hayashi, H., Abdollah, S. et al.Falb, D. The MAD-related protein Smad7 associates with the TGFbeta receptor

and functions as an antagonist of TGFbeta signaling. *Cell* **89**, 1165-1173 (1997).

154. Yilmaz, M., Maass, D. et al.Christofori, G. Transcription factor Dlx2 protects from TGFbeta-induced cell-cycle arrest and apoptosis. *EMBO J* (2011).

155. Kang, J. S., Saunier, E. F., Akhurst, R. J. & Derynck, R. The type I TGF-beta receptor is covalently modified and regulated by sumoylation. *Nat Cell Biol* **10**, 654-664 (2008).

156. Di Guglielmo, G. M., Le Roy, C., Goodfellow, A. F. & Wrana, J. L. Distinct endocytic pathways regulate TGF-beta receptor signalling and turnover. *Nat Cell Biol* **5**, 410-421 (2003).

157. Tsukazaki, T., Chiang, T. A. et al.Wrana, J. L. SARA, a FYVE domain protein that recruits Smad2 to the TGFbeta receptor. *Cell* **95**, 779-791 (1998).

158. Lin, H. K., Bergmann, S. & Pandolfi, P. P. Cytoplasmic PML function in TGF-beta signalling. *Nature* **431**, 205-211 (2004).

159. Tang, Y., Katuri, V. et al.Mishra, L. Disruption of transforming growth factor-beta signaling in ELF beta-spectrin-deficient mice. *Science* **299**, 574-577 (2003).

160. Varelas, X., Sakuma, R. et al.Wrana, J. L. TAZ controls Smad nucleocytoplasmic shuttling and regulates human embryonic stem-cell self-renewal. *Nat Cell Biol* **10**, 837-848 (2008).

161. Kim, W., Seok Kang, Y. et al.Song, W. K. The integrin-coupled signaling adaptor p130Cas suppresses Smad3 function in transforming growth factor-beta signaling. *Mol Biol Cell* **19**, 2135-2146 (2008).

162. Lin, X., Duan, X. et al.Feng, X. H. PPM1A functions as a Smad phosphatase to terminate TGFbeta signaling. *Cell* **125**, 915-928 (2006).

163. Dai, F., Shen, T. et al.Feng, X. H. PPM1A dephosphorylates RanBP3 to enable efficient nuclear export of Smad2 and Smad3. *EMBO Rep* (2011).

164. Dupont, S., Mamidi, A. et al.Piccolo, S. FAM/USP9x, a deubiquitinating enzyme essential for TGFbeta signaling, controls Smad4 monoubiquitination. *Cell* **136**, 123-135 (2009).

165. Guo, X., Ramirez, A. et al.Wang, X. F. Axin and GSK3- control Smad3 protein stability and modulate TGF- signaling. *Genes Dev* **22**, 106-120 (2008).

166. Massague, J., Blain, S. W. & Lo, R. S. TGFbeta signaling in growth control, cancer, and heritable disorders. *Cell* **103**, 295-309 (2000).

167. Chen, C. R., Kang, Y., Siegel, P. M. & Massague, J. E2F4/5 and p107 as Smad cofactors linking the TGFbeta receptor to c-myc repression. *Cell* **110**, 19-32 (2002).

168. Gomis, R. R., Alarcon, C. et al.Massague, J. C/EBPbeta at the core of the TGFbeta cytostatic response and its evasion in metastatic breast cancer cells. *Cancer Cell* **10**, 203-214 (2006).

169. Descargues, P., Sil, A. K. et al.Karin, M. IKKalpha is a critical coregulator of a Smad4-independent TGFbeta-Smad2/3 signaling pathway that controls keratinocyte differentiation. *Proc Natl Acad Sci U S A* **105**, 2487-2492 (2008).

170. Gomis, R. R., Alarcon, C. et al.Massague, J. A FoxO-Smad synexpression group in human keratinocytes. *Proc Natl Acad Sci U S A* **103**, 12747-12752 (2006).

171. Seoane, J., Le, H. V. et al.Massague, J. Integration of Smad and forkhead pathways in the control of neuroepithelial and glioblastoma cell proliferation. *Cell* **117**, 211-223 (2004).

172. Seoane, J., Pouponnot, C. et al.Massague, J. TGFbeta influences Myc, Miz-1 and Smad to control the CDK inhibitor p15INK4b. *Nat Cell Biol* **3**, 400-408 (2001).

173. Zheng, Y., Zhao, Y. D. et al.Skapek, S. X. Tgfbeta signaling directly induces Arf promoter remodeling by a mechanism involving Smads 2/3 and p38 MAPK. *J Biol Chem* **285**, 35654-35664 (2010).

174. Kortlever, R. M., Nijwening, J. H. & Bernards, R. Transforming growth factor-beta requires its target plasminogen activator inhibitor-1 for cytostatic activity. *J Biol Chem* **283**, 24308-24313 (2008).

175. Azar, R., Alard, A. et al.Pyronnet, S. 4E-BP1 is a target of Smad4 essential for TGFbeta-mediated inhibition of cell proliferation. *EMBO J* **28**, 3514-3522 (2009).

176. Kang, Y., Chen, C. R. & Massague, J. A self-enabling TGFbeta response coupled to stress signaling: Smad engages stress response factor ATF3 for Id1 repression in epithelial cells. *Mol Cell* **11**, 915-926 (2003).

177. Kowanetz, M., Valcourt, U. et al.Moustakas, A. Id2 and Id3 define the potency of cell proliferation and differentiation responses to transforming growth factor beta and bone morphogenetic protein. *Mol Cell Biol* **24**, 4241-4254 (2004).

178. Siegel, P. M. & Massague, J. Cytostatic and apoptotic actions of TGF-beta in homeostasis and cancer. *Nat Rev Cancer* **3**, 807-821 (2003).

179. Ohgushi, M., Kuroki, S. et al.Yonehara, S. Transforming growth factor beta-dependent sequential activation of Smad, Bim, and caspase-9 mediates physiological apoptosis in gastric epithelial cells. *Mol Cell Biol* **25**, 10017-10028 (2005).

180. Jang, C. W., Chen, C. H. et al.Chen, R. H. TGF-beta induces apoptosis through Smad-mediated expression of DAP-kinase. *Nat Cell Biol* **4**, 51-58 (2002).

181. Valderrama-Carvajal, H., Cocolakis, E. et al.Lebrun, J. J. Activin/TGF-beta induce apoptosis through Smad-dependent expression of the lipid phosphatase SHIP. *Nat Cell Biol* **4**, 963-969 (2002).

182. Moustakas, A. & Heldin, C. H. Non-Smad TGF-beta signals. *J Cell Sci* **118**, 3573-3584 (2005).

183. Yoo, J., Ghiassi, M. et al.Roberts, A. B. Transforming growth factor-beta-induced apoptosis is mediated by Smad-dependent expression of GADD45b through p38 activation. *J Biol Chem* **278**, 43001-43007 (2003).

184. Zhang, S., Ekman, M. et al.Landstrom, M. TGFbeta1-induced activation of ATM and p53 mediates apoptosis in a Smad7-dependent manner. *Cell Cycle* **5**, 2787-2795 (2006).

185. Perlman, R., Schiemann, W. P. et al.Weinberg, R. A. TGF-beta-induced apoptosis is mediated by the adapter protein Daxx that facilitates JNK activation. *Nat Cell Biol* **3**, 708-714 (2001).

186. Larisch, S., Yi, Y. et al.Roberts, A. B. A novel mitochondrial septin-like protein, ARTS, mediates apoptosis dependent on its P-loop motif. *Nat Cell Biol* **2**, 915-921 (2000).

187. Huang, Y., Hutter, D. et al.Holbrook, N. J. Transforming growth factor-beta 1 suppresses serum deprivation-induced death of A549 cells through differential effects on c-Jun and JNK activities. *J Biol Chem* **275**, 18234-18242 (2000).

188. Murillo, M. M., del Castillo, G. et al.Fabregat, I. Involvement of EGF receptor and c-Src in the survival signals induced by TGF-beta1 in hepatocytes. *Oncogene* **24**, 4580-4587 (2005).

189. Thiery, J. P. Epithelial-mesenchymal transitions in development and pathologies. *Curr Opin Cell Biol* **15**, 740-746 (2003).

190. Moustakas, A. & Heldin, C. H. Signaling networks guiding epithelial-mesenchymal transitions during embryogenesis and cancer progression. *Cancer Sci* **98**, 1512-1520 (2007).

191. Yang, Y., Pan, X. et al.Song, J. Transforming growth factor-beta1 induces epithelial-to-mesenchymal transition and apoptosis via a cell cycle-dependent mechanism. *Oncogene* **25**, 7235-7244 (2006).

192. Thuault, S., Tan, E. J. et al.Moustakas, A. HMGA2 and Smads co-regulate SNAIL1 expression during induction of epithelial-to-mesenchymal transition. *J Biol Chem* **283**, 33437-33446 (2008).

193. Papageorgis, P., Lambert, A. W. et al.Thiagalingam, S. Smad signaling is required to maintain epigenetic silencing during breast cancer progression. *Cancer Res* **70**, 968-978 (2010).

194. Levy, L. & Hill, C. S. Alterations in components of the TGF-beta superfamily signaling pathways in human cancer. *Cytokine Growth Factor Rev* **17**, 41-58 (2006).

195. Massague, J. TGFbeta in Cancer. *Cell* **134**, 215-230 (2008).

196. Markowitz, S., Wang, J. et al.et, a. Inactivation of the type II TGF-beta receptor in colon cancer cells with microsatellite instability. *Science* **268**, 1336-1338 (1995).

197. Izumoto, S., Arita, N. et al.Hayakawa, T. Microsatellite instability and mutated type II transforming growth factor-beta receptor gene in gliomas. *Cancer Lett* **112**, 251-256 (1997).

198. Myeroff, L. L., Parsons, R. et al.et, a. A transforming growth factor beta receptor type II gene mutation common in colon and gastric but rare in endometrial cancers with microsatellite instability. *Cancer Res* **55**, 5545-5547 (1995).

199. Biswas, S., Chytil, A. et al.Grady, W. M. Transforming growth factor beta receptor type II inactivation promotes the establishment and progression of colon cancer. *Cancer Res* **64**, 4687-4692 (2004).

200. Munoz, N. M., Upton, M. et al.Grady, W. M. Transforming growth factor beta receptor type II inactivation induces the malignant transformation of intestinal neoplasms initiated by Apc mutation. *Cancer Res* **66**, 9837-9844 (2006).

201. Ijichi, H., Chytil, A. et al.Moses, H. L. Aggressive pancreatic ductal adenocarcinoma in mice caused by pancreas-specific blockade of transforming growth factor-beta signaling in cooperation with active Kras expression. *Genes Dev* **20**, 3147-3160 (2006).

202. Lu, S. L., Herrington, H. et al.Wang, X. J. Loss of transforming growth factor-beta type II receptor promotes metastatic head-and-neck squamous cell carcinoma. *Genes Dev* **20**, 1331-1342 (2006).

203. Forrester, E., Chytil, A. et al.Moses, H. L. Effect of conditional knockout of the type II TGF-beta receptor gene in mammary epithelia on mammary gland development and polyomavirus middle T antigen induced tumor formation and metastasis. *Cancer Res* **65**, 2296-2302 (2005).

204. Guasch, G., Schober, M. et al.Fuchs, E. Loss of TGFbeta signaling destabilizes homeostasis and promotes squamous cell carcinomas in stratified epithelia. *Cancer Cell* **12**, 313-327 (2007).

205. Pasche, B., Kolachana, P. et al.Offit, K. TbetaR-I(6A) is a candidate tumor susceptibility allele. *Cancer Res* **59**, 5678-5682 (1999).

206. Valle, L., Serena-Acedo, T. et al.de la Chapelle, A. Germline allele-specific expression of TGFBR1 confers an increased risk of colorectal cancer. *Science* **321**, 1361-1365 (2008).

207. Kang, S. H., Bang, Y. J. et al.Kim, S. J. Transcriptional repression of the transforming growth factor-beta type I receptor gene by DNA methylation results in the development of TGF-beta resistance in human gastric cancer. *Oncogene* **18**, 7280-7286 (1999).

208. Zeng, Q., Phukan, S. et al.Pasche, B. Tgfbr1 haploinsufficiency is a potent modifier of colorectal cancer development. *Cancer Res* **69**, 678-686 (2009).

209. Copland, J. A., Luxon, B. A. et al.Wood, C. G. Genomic profiling identifies alterations in TGFbeta signaling through loss of TGFbeta receptor expression in human renal cell carcinogenesis and progression. *Oncogene* **22**, 8053-8062 (2003).

210. Finger, E. C., Turley, R. S. et al.Blobe, G. C. TbetaRIII suppresses non-small cell lung cancer invasiveness and tumorigenicity. *Carcinogenesis* **29**, 528-535 (2008).

211. Hempel, N., How, T. et al.Blobe, G. C. Loss of betaglycan expression in ovarian cancer: role in motility and invasion. *Cancer Res* **67**, 5231-5238 (2007).

212. Turley, R. S., Finger, E. C. et al.Blobe, G. C. The type III transforming growth factor-beta receptor as a novel tumor suppressor gene in prostate cancer. *Cancer Res* **67**, 1090-1098 (2007).

213. Han, S. U., Kim, H. T. et al.Kim, S. J. Loss of the Smad3 expression increases susceptibility to tumorigenicity in human gastric cancer. *Oncogene* **23**, 1333-1341 (2004).

214. Eppert, K., Scherer, S. W. et al.Attisano, L. MADR2 maps to 18q21 and encodes a TGFbeta-regulated MAD-related protein that is functionally mutated in colorectal carcinoma. *Cell* **86**, 543-552 (1996).

215. Sjoblom, T., Jones, S. et al.Velculescu, V. E. The consensus coding sequences of human breast and colorectal cancers. *Science* **314**, 268-274 (2006).

216. Uchida, K., Nagatake, M. et al.Takahashi, T. Somatic in vivo alterations of the JV18-1 gene at 18q21 in human lung cancers. *Cancer Res* **56**, 5583-5585 (1996).

217. Hahn, S. A., Schutte, M. et al.Kern, S. E. DPC4, a candidate tumor suppressor gene at human chromosome 18q21.1. *Science* **271**, 350-353 (1996).

218. Shi, Y., Hata, A. et al.Pavletich, N. P. A structural basis for mutational inactivation of the tumour suppressor Smad4. *Nature* **388**, 87-93 (1997).

219. Li, W., Qiao, W. et al.Deng, C. X. Squamous cell carcinoma and mammary abscess formation through squamous metaplasia in Smad4/Dpc4 conditional knockout mice. *Development* **130**, 6143-6153 (2003).

220. Takaku, K., Oshima, M. et al.Taketo, M. M. Intestinal tumorigenesis in compound mutant mice of both Dpc4 (Smad4) and Apc genes. *Cell* **92**, 645-656 (1998).

221. Cui, W., Fowlis, D. J. et al.Akhurst, R. J. TGFbeta1 inhibits the formation of benign skin tumors, but enhances progression to invasive spindle carcinomas in transgenic mice. *Cell* **86**, 531-542 (1996).

222. Muraoka-Cook, R. S., Kurokawa, H. et al.Arteaga, C. L. Conditional overexpression of active transforming growth factor beta1 in vivo accelerates metastases of transgenic mammary tumors. *Cancer Res* **64**, 9002-9011 (2004).

223. Bandyopadhyay, A., Agyin, J. K. et al.Sun, L. Z. Inhibition of pulmonary and skeletal metastasis by a transforming growth factor-beta type I receptor kinase inhibitor. *Cancer Res* **66**, 6714-6721 (2006).

224. Bandyopadhyay, A., Zhu, Y. et al.Sun, L. A soluble transforming growth factor beta type III receptor suppresses tumorigenicity and metastasis of human breast cancer MDA-MB-231 cells. *Cancer Res* **59**, 5041-5046 (1999).

225. Biswas, S., Guix, M. et al.Arteaga, C. L. Inhibition of TGF-beta with neutralizing antibodies prevents radiation-induced acceleration of metastatic cancer progression. *J Clin Invest* **117**, 1305-1313 (2007).

226. Nam, J. S., Terabe, M. et al.Wakefield, L. M. An anti-transforming growth factor beta antibody suppresses metastasis via cooperative effects on multiple cell compartments. *Cancer Res* **68**, 3835-3843 (2008).

227. Grady, W. M., Rajput, A. et al.Markowitz, S. Mutation of the type II transforming growth factor-beta receptor is coincident with the transformation of human colon adenomas to malignant carcinomas. *Cancer Res* **58**, 3101-3104 (1998).

228. Jones, S., Chen, W. D. et al.Markowitz, S. D. Comparative lesion sequencing provides insights into tumor evolution. *Proc Natl Acad Sci U S A* **105**, 4283-4288 (2008).

229. Miyaki, M., Iijima, T. et al.Mori, T. Higher frequency of Smad4 gene mutation in human colorectal cancer with distant metastasis. *Oncogene* **18**, 3098-3103 (1999).

230. Pardali, K. & Moustakas, A. Actions of TGF-beta as tumor suppressor and pro-metastatic factor in human cancer. *Biochim Biophys Acta* **1775**, 21-62 (2007).

231. Dalal, B. I., Keown, P. A. & Greenberg, A. H. Immunocytochemical localization of secreted transforming growth factor-beta 1 to the advancing edges of primary tumors and to lymph node metastases of human mammary carcinoma. *Am J Pathol* **143**, 381-389 (1993).

232. Li, Q. L., Ito, K. et al.Ito, Y. Causal relationship between the loss of RUNX3 expression and gastric cancer. *Cell* **109**, 113-124 (2002).

233. Birchenall-Roberts, M. C., Fu, T. et al.Ruscetti, F. W. Tuberous sclerosis complex 2 gene product interacts with human SMAD proteins. A molecular link of two tumor suppressor pathways. *J Biol Chem* **279**, 25605-25613 (2004).

234. Levy, L., Howell, M. et al.Hill, C. S. Arkadia activates Smad3/Smad4-dependent transcription by triggering signal-induced SnoN degradation. *Mol Cell Biol* **27**, 6068-6083 (2007).

235. Zhu, Q., Krakowski, A. R. et al.Luo, K. Dual role of SnoN in mammalian tumorigenesis. *Mol Cell Biol* **27**, 324-339 (2007).

236. Brandl, M., Seidler, B. et al.Schneider, G. IKK(alpha) controls canonical TGF(ss)-SMAD signaling to regulate genes expressing SNAIL and SLUG during EMT in panc1 cells. *J Cell Sci* **123**, 4231-4239 (2010).

237. Wendt, M. K., Smith, J. A. & Schiemann, W. P. p130Cas is required for mammary tumor growth and transforming growth factor-beta-mediated metastasis through regulation of Smad2/3 activity. *J Biol Chem* **284**, 34145-34156 (2009).

238. Kretzschmar, M., Doody, J., Timokhina, I. & Massague, J. A mechanism of repression of TGFbeta/ Smad signaling by oncogenic Ras. *Genes Dev* **13**, 804-816 (1999).

239. Lehmann, K., Janda, E. et al.Downward, J. Raf induces TGFbeta production while blocking its apoptotic but not invasive responses: a mechanism leading to increased malignancy in epithelial cells. *Genes Dev* **14**, 2610-2622 (2000).

240. Trinh, B. Q., Barengo, N. & Naora, H. Homeodomain protein DLX4 counteracts key transcriptional control mechanisms of the TGF-beta cytostatic program and blocks the antiproliferative effect of TGF-beta. *Oncogene* **30**, 2718-2729 (2011).

241. Singh, G., Singh, S. K. et al.Ellenrieder, V. Sequential activation of NFAT and c-Myc transcription factors mediates the TGF-beta switch from a suppressor to a promoter of cancer cell proliferation. *J Biol Chem* **285**, 27241-27250 (2010).

242. Conery, A. R., Cao, Y. et al.Luo, K. Akt interacts directly with Smad3 to regulate the sensitivity to TGF-beta induced apoptosis. *Nat Cell Biol* **6**, 366-372 (2004).

243. Hannigan, A., Smith, P. et al.Inman, G. J. Epigenetic downregulation of human disabled homolog 2 switches TGF-beta from a tumor suppressor to a tumor promoter. *J Clin Invest* **120**, 2842-2857 (2010).

244. Hoot, K. E., Lighthall, J. et al.Wang, X. J. Keratinocyte-specific Smad2 ablation results in increased epithelial-mesenchymal transition during skin cancer formation and progression. *J Clin Invest* **118**, 2722-2732 (2008).

245. Petersen, M., Pardali, E. et al.Ten Dijke, P. Smad2 and Smad3 have opposing roles in breast cancer bone metastasis by differentially affecting tumor angiogenesis. *Oncogene* **29**, 1351-1361 (2010).

246. Kretschmer, A., Moepert, K. et al.Klippel, A. Differential regulation of TGF-beta signaling through Smad2, Smad3 and Smad4. *Oncogene* **22**, 6748-6763 (2003).

247. Arsura, M., Wu, M. & Sonenshein, G. E. TGF beta 1 inhibits NF-kappa B/Rel activity inducing apoptosis of B cells: transcriptional activation of I kappa B alpha. *Immunity* **5**, 31-40 (1996).

248. Neil, J. R. & Schiemann, W. P. Altered TAB1:I kappaB kinase interaction promotes transforming growth factor beta-mediated nuclear factor-kappaB activation during breast cancer progression. *Cancer Res* **68**, 1462-1470 (2008).

249. Tian, M., Neil, J. R. & Schiemann, W. P. Transforming growth factor-beta and the hallmarks of cancer. *Cell Signal* **23**, 951-962 (2011).

250. Wendt, M. K., Smith, J. A. & Schiemann, W. P. Transforming growth factor-beta-induced epithelial-mesenchymal transition facilitates epidermal growth factor-dependent breast cancer progression. *Oncogene* **29**, 6485-6498 (2010).

251. Chen, C. R., Kang, Y. & Massague, J. Defective repression of c-myc in breast cancer cells: A loss at the core of the transforming growth factor beta growth arrest program. *Proc Natl Acad Sci U S A* **98**, 992-999 (2001).

252. Sasaki, T., Suzuki, H. et al.Kato, M. Lymphoid enhancer factor 1 makes cells resistant to transforming growth factor beta-induced repression of c-myc. *Cancer Res* **63**, 801-806 (2003).

253. Petrocca, F., Visone, R. et al.Vecchione, A. E2F1-regulated microRNAs impair TGFbeta-dependent cell-cycle arrest and apoptosis in gastric cancer. *Cancer Cell* **13**, 272-286 (2008).

254. Stearns, M. E., Garcia, F. U. et al.Wang, M. Role of interleukin 10 and transforming growth factor beta1 in the angiogenesis and metastasis of human prostate primary tumor lines from orthotopic implants in severe combined immunodeficiency mice. *Clin Cancer Res* **5**, 711-720 (1999).

255. Gohongi, T., Fukumura, D. et al.Jain, R. K. Tumor-host interactions in the gallbladder suppress distal angiogenesis and tumor growth: involvement of transforming growth factor beta1. *Nat Med* **5**, 1203-1208 (1999).

256. Kim, K. Y., Jeong, S. Y. et al.Nam, M. J. Induction of angiogenesis by expression of soluble type II transforming growth factor-beta receptor in mouse hepatoma. *J Biol Chem* **276**, 38781-38786 (2001).

257. Wrzesinski, S. H., Wan, Y. Y. & Flavell, R. A. Transforming growth factor-beta and the immune response: implications for anticancer therapy. *Clin Cancer Res* **13**, 5262-5270 (2007).

258. Arsura, M., FitzGerald, M. J., Fausto, N. & Sonenshein, G. E. Nuclear factor-kappaB/Rel blocks transforming growth factor beta1-induced apoptosis of murine hepatocyte cell lines. *Cell Growth Differ* **8**, 1049-1059 (1997).

259. Kitamura, T., Kometani, K. et al.Taketo, M. M. SMAD4-deficient intestinal tumors recruit CCR1+ myeloid cells that promote invasion. *Nat Genet* **39**, 467-475 (2007).

260. Yang, L., Huang, J. et al.Moses, H. L. Abrogation of TGF beta signaling in mammary carcinomas recruits Gr-1+CD11b+ myeloid cells that promote metastasis. *Cancer Cell* **13**, 23-35 (2008).

261. Bhowmick, N. A., Chytil, A. et al.Moses, H. L. TGF-beta signaling in fibroblasts modulates the oncogenic potential of adjacent epithelia. *Science* **303**, 848-851 (2004).

262. Moustakas, A. & Heldin, C. H. Induction of epithelial-mesenchymal transition by transforming growth factor beta. *Semin Cancer Biol* (2012).

263. Padua, D., Zhang, X. H. et al.Massague, J. TGFbeta primes breast tumors for lung metastasis seeding through angiopoietin-like 4. *Cell* **133**, 66-77 (2008).

264. Kang, Y., Siegel, P. M. et al.Massague, J. A multigenic program mediating breast cancer metastasis to bone. *Cancer Cell* **3**, 537-549 (2003).

265. Yin, J. J., Selander, K. et al.Guise, T. A. TGF-beta signaling blockade inhibits PTHrP secretion by breast cancer cells and bone metastases development. *J Clin Invest* **103**, 197-206 (1999).

266. Mohammad, K. S., Javelaud, D. et al.Guise, T. A. TGF-beta-RI kinase inhibitor SD-208 reduces the development and progression of melanoma bone metastases. *Cancer Res* **71**, 175-184 (2011).

267. Kang, Y., He, W. et al.Massague, J. Breast cancer bone metastasis mediated by the Smad tumor suppressor pathway. *Proc Natl Acad Sci U S A* **102**, 13909-13914 (2005).

268. Boulay, J. L., Mild, G. et al.Rochlitz, C. SMAD4 is a predictive marker for 5-fluorouracil-based chemotherapy in patients with colorectal cancer. *Br J Cancer* **87**, 630-634 (2002).

269. Ding, Z., Wu, C. J. et al.DePinho, R. A. SMAD4-dependent barrier constrains prostate cancer growth and metastatic progression. *Nature* **470**, 269-273 (2011).

270. Muraoka, R. S., Dumont, N. et al.Arteaga, C. L. Blockade of TGF-beta inhibits mammary tumor cell viability, migration, and metastases. *J Clin Invest* **109**, 1551-1559 (2002).

271. Yang, Y. A., Dukhanina, O. et al.Wakefield, L. M. Lifetime exposure to a soluble TGF-beta antagonist protects mice against metastasis without adverse side effects. *J Clin Invest* **109**, 1607-1615 (2002).

272. Uhl, M., Aulwurm, S. et al.Weller, M. SD-208, a novel transforming growth factor beta receptor I kinase inhibitor, inhibits growth and invasiveness and enhances immunogenicity of murine and human glioma cells in vitro and in vivo. *Cancer Res* **64**, 7954-7961 (2004).

273. Gorelik, L. & Flavell, R. A. Immune-mediated eradication of tumors through the blockade of transforming growth factor-beta signaling in T cells. *Nat Med* **7**, 1118-1122 (2001).

6 Curriculum Vitae

Dorothea Cornelia Gruber

Maiden name: Maaß

Personal Details

Date of birth: 14.08.1982
Place of birth: Gießen, Germany
Nationality: German
Status: married

Education and Professional Training

Doctoral studies in tumor biology May 2007 – October 2012
Department of Biomedicine,
Institute of Biochemistry and Genetics,
University of Basel, Switzerland
Lab of Prof. Dr. Gerhard Christofori

Certificate in Advanced Biomicroscopy September 2009
Swiss Society for Optics and Microscopy (SSOM)

Introductory Course in Laboratory Animal Science February 2008
University of Zürich
Institut für Labortierkunde

Humanbiology studies October 2001 – November 2006
Major in molecularbiology/genetics and minor in virology
Philipps-Universität Marburg, Germany
Institute of Molecular Biology and Tumor Research
Degree: Diploma of Human Biology (Dipl. Humanbiologin)
Thesis: "Die biologische Relevanz der Interaktion von c-Myc mit dem Mediatorkomplex via Med24"
Lab of Prof. Dr. Martin Eilers

Grammar school August 1994 – July 2001
Major in mathematics and biology
Liebigschule Gießen, Germany

Work Experience

Summer student supervisor August 2010
During doctoral studies

Assistent scientist November 2006 – April 2007
Philipps-Universität Marburg, Germany
Institute of Molecular Biology and Tumor Research
Lab of Prof. Dr. Eilers

Molecularbiological internship on "Survivin interacting proteins" July– August 2005
University of California, San Francisco, USA
Lab of Prof. Michael Bishop, M.D.

Biochemical internship August– September 2002
Justus-Liebig-Universität Gießen, Germany
Lab of Prof. Dr. Alfred Pingoud

Attended Conferences

European Cancer Center Symposium May 2012
Freiburg, Germany (Oral presentation)

Joint TuMIC meeting March 2012
Fribourg, Switzerland (Oral presentation)

TuMIC – Metastasis Research Society – Champalimaud Foundation Conference: June 2011
"New concepts in cancer metastasis"
Lisbon, Portugal (Poster presentation)

TuMIC meeting February 2011
Ghent, Belgium (Oral presentation)

TuMIC meeting July 2010
Paris, France

EMBO 2010 Molecular Medicine Workshop: May 2010
"Cell Guidance Signals in Caneer."
Camogli-Portefino Vetta, Italy (Poster presentation)

TuMIC meeting September 2009
Rotterdam, The Netherlands

Beatson International Cancer Conference July 2009
"Microenvironment, Motility and Metastasis."
Glasgow, Great Britain (Poster Presentation)

Publications

Yilmaz, M.*, Maass, D.* et al. Christofori, G. Transcription factor Dlx2 protects from TGFbeta-induced cell-cycle arrest and apoptosis. *EMBO J* (2011).

Gruber, D.*, Fantozzi, A.*, et al. Christofori, G. VEGF-mediated angiogenesis links EMT-induced cancer stemness to tumor initiation. (*submitted*)

Gruber, D. & Christofori, G. The two faces of TGFβ: tumor suppressor and metastasis promoter. (*in preparation*)

* equal contribution

7 Acknowledgements

First of all, I would like to thank Gerhard. The work environment he created in his lab, combining high-quality research with a friendly atmosphere, has been the prefect place for me to do my PhD studies. I also want to thank him for being an encouraging leader and always open-minded for my ideas and discussions. With Gerhard's guidance I could develope into a researcher who loves her profession.

Secondly, without all the lab members, former and present, I could not have achieved my PhD. The attitude to support each other, workwise and personally, was exactly what I needed during all the highs and lows. I appreciated the open discussions, the helping hands and good advices. For me, the mixture of hard work peppered with jokes, coffee, stories, laughters, crosswords, beers, songs and dancing made these last 5 years rather feel like pleasure than an obligation.

Special thanks go to Anna, my wing-woman in the LN-ΔLN project. We complemented each other perfectly. Also Pascal was indispensable to translate my wild imaging ideas into experimental reality. Thanks for not hanging up immediately when you heard my voice on the phone ;-). Katrin and Rafael from the Pertz group have spent a lot of their time and nerves to help me proceed with my project. Thank you very much!

Also, my whole family always supported and believed in me. To know that they are always there for me no matter what goes wrong helped me to keep my head high and to look confident into the future.

Last but not least, I want to thank my husband Matthias for his love, support and patience. Your arms where always there when I needed nothing but a hug to find my optimism and happiness back.